PHOSPHOLIPID ALTERATIONS ASSOCIATED WITH DOCETAXEL RESISTANT PROSTATE CANCER

by

Lishann Ingram

(Under the Direction of Brian S. Cummings)

ABSTRACT

The association of circulating lipids with clinical outcomes of drug-resistant castration-resistant prostate cancer (CRPC) is not fully understood. Very few studies suggest links between lipid synthesis and poor prognosis. Such a finding has the potential to significantly enhance treatment strategies. Towards this goal, we utilized a multi-platform lipidomics approach to determine differences in the lipidome in diverse *in vitro* models of prostate cancer. This approach was based on recent clinical studies demonstrating an association between plasma lipids and CRPC patient prognosis [1]. However, it is not known if such changes in patients are recapitulated in *in vitro* models. We addressed this question using non-cancerous, hormone sensitive, CRPC and drug resistant prostate cell lines combined with an untargeted shotgun approach (ESI-MS) and quantitative HPLC-ESI-Orbitrap-MS lipidomic analysis. This approach identified distinct metabolite features that varied significantly across all groups analyzed. The abundance of specific classes and subclasses of specific lipids (namely, SM, PC, PE, plasmalogen, TAG) in prostate

cancer cells, as compared to non-tumorgenic cells reflects the heterogeneous nature of this disease. The overall key findings from this study are the following: (1) identification of a unique lipid signature for drug resistant prostate cancer, and (2) determination aberrant pathways in drug-resistant CRPC progression with an integrated lipidomic/transcriptomic high gene signature score correlated to poor survival. These data demonstrate that the lipidomic profile of Docetaxel resistant prostate cancer cells lines and media significantly differs from non-docetaxel resistant cells as well as non-cancerous prostate cells. The data suggest that the lipidomic profile of prostate cancer cells recapitulate the lipidomic profiles seen in the plasma of prostate cancer patients. As such, these cells will be valuable models for understanding molecular mechanisms that alter lipid synthesis in Docetaxel resistant prostate cancer. These data may also aid in the development of biomarkers for early detection of Docetaxel resistant prostate cancer, giving rise to more personalized treatment options for patients.

INDEX WORDS: lipids, lipidomics, prostate cancer, human prostate cells, drug-resistance

Abbreviations/Acronyms: Androgen deprivation therapy (ADT), androgen receptor (AR), castration-resistant prostate cancer (CRPC), ceramide (Cer), diacylglyceride (DAG), dihydrotestosterone (DHT), digital rectal examination (DRE), Docetaxel resistant DU145 cells (DU145-DR), Docetaxel resistant PC-3 cells (PC3-Rx), electrospray ionization tandem mass spectrometry (ESI-MS/MS), glycerophospholipids (GP), gonadotropin-releasing hormone (GnRH), hematoxylin and eosin (H&E), high-performance liquid chromatography (HPLC), luteinizing hormone (LH), lysophosphatidylcholine (LPC), lysophosphatidylethanolamine (LPE), oxidized lysophosphatidylcholine (OxLPC), oxidized lysophosphatidylethanolamine (OxLPE), oxidized phosphatidylcholine (OxPC), oxidized phosphatidylethanolamine (OxPE), oxidized triglycerides (OxTG), phosphatidic acid (PA), phosphatidylcholine (PC), phosphatidylethanolamine (PE), phosphatidylglycerol (PG), phosphatidylserine (PS), phospholipids (PLs), prostate cancer (PCa), sphingomyelin (SM), triacylglycerides (TAG),

PHOSPHOLIPID ALTERATIONS ASSOCIATED WITH DOCETAXEL RESISTANT PROSTATE CANCER

by

Lishann Ingram

B.S., Clark Atlanta University, 2013

A Dissertation Submitted to the Graduate Faculty of The University of Georgia in Partial Fulfillment of the Requirements for the Degree

DOCTOR OF PHILOSOPHY

ATHENS, GEORGIA

2019

PHOSPHOLIPID ALTERATIONS ASSOCIATED WITH DOCETAXEL RESISTANT PROSTATE CANCER

by

Lishann Ingram

Major Professor: Brian S. Cummings

Committee: Michael G. Bartlett

Arthur Edison

Jonathan Eggenschwiler

Electronic Version Approved:

Ron Walcott

Interim Dean of the Graduate School

The University of Georgia

December 2019

DEDICATION

To my parents, *Professor Conrad and Annette Ingram*

For your everlasting love, encouragement and support

To *Rylie-Gatsby,* for your contagious energy and love throughout this entire experience

ACKNOWLEDGEMENTS

I am eternally grateful for the guidance, support and years of mentorship from my advisor, Professor Brian S. Cummings. His enthusiasm, encouragement, and patience with me while I have worked through my scientific journey will always be appreciated and never forgotten. I applaud him for his ability to help me learn from my weaknesses, while also celebrating my strengths, as an ever-growing and evolving scientist. I thank him for going along with my non-traditional ideas and demanding a high quality of work in all my endeavors. The training and strong scientific background he has given me will be carried on throughout my career. I will always remember the countless words of wisdom that apply to not only scientific research, but life in general. I would not be where I am today without his valuable and continuous mentorship. I am especially grateful to Dr. Sumitra Pati for her guidance, training and immensely helpful discussions. I would like to express my sincerest appreciation to my undergraduate, Maryam Mansoura. Her personal and professional contributions truly made this work possible.

To my girlfriends: Shawna Battle, Dr. Abigail R. Case, Dr. Malorie B. Holmes, Dr. Brittany D. Jenkins, Dr. Kaitlyn Ledwitch and Jessica C. Ramadhin, thank you for your ceaseless encouragement and love throughout this process. I could never put into words how much each of your continued support has meant to me. Finally, I am wholeheartedly indebted to my parents, who deserve endless thanks for their love and prayers. I am extremely grateful for my puppy Rylie-Gatsby, for the most constant source of love and energy, I couldn’t be more thankful.

TABLE OF CONTENTS

Page

LIST OF TABLES

Page

LIST OF FIGURES

Page

CHAPTER 1

PROSTATE CANCER

Approximately 1 in 9 men will experience prostate cancer (PCa) during their lifetime [1-3]. There were an estimated 164,640 cases of PCa in 2018 and 29,430 estimated deaths due to PCa in the United States [4]. Despite the advances in screening and early detection, a significant amount of men continue to present with advanced metastatic disease [5, 6]. These deadly statistics make PCa the second most frequent cancer and the fifth leading cause of cancer death in men [4]. More concerning is that patients with metastatic PCa have only a 28.2% five-year survival rate upon initial diagnosis. This is in contrast to the five-year survival rate of patients with non-metastatic PCa, which is 98.9% (2005-2011) [4]. Furthermore, the survival time after tumor recurrence drastically decreases to 1-2 years [7]. Therefore, knowledge of resistant mechanisms to the available therapeutic agents is an active area of research. A review of prostate anatomy is needed to fully appreciate these treatment mechanisms.

Prostate Anatomy

The prostate gland is an exocrine glandular organ located proximal to the urethra and caudal to the bladder (**Figure 1.1**) [8, 9]. It is divided into four zones—anterior, transition, central and peripheral (**Figure 1.2**) [10]. At the cellular level, the prostate is composed of stromal and epithelial components; it is further subdivided into ducts and acini consisting of secretory cells, a few neuroendocrine cells, and basal cells (**Figure 1.3** [10]). Basal

cells separate the secretory cells from the basement membrane by forming a continuous layer in the normal prostate gland. Luminal cells are a differentiated androgen-dependent cell type that produce and release proteolytic secretory proteins including serine protease into the lumen to improve sperm mobility [11, 12]. Most tumors begin to form in proximity to the outer surfaces of a prostate gland. Aggressive tumors can eventually break the capsule and infiltrate nearby organs [13]. Both benign and malignant growth can put pressure on and destroy the glandular tissue that can lead to an increased leakage of PSA into the bloodstream [14]. Despite our knowledge about the pathology of this disease, there remains no reliable or widely available method to distinguish drug-resistant (high-risk) tumors at any stage.

Prostate Cancer Screening and Diagnosis

An increasing number of prostate cancer patients are being diagnosed at earlier stages due to screening programs implemented using PSA testing. The chosen cut-off value of 4 ng/mL for PSA triggers further analysis such as tissue biopsies [15-17]. Biochemical reoccurrence is typically identified following PSA monitoring after treatment for localized disease.

Prostate cancer diagnosis detection can also initiate from an abnormal digital rectal examination (DRE) [14], which may lead to PSA testing or a trans-rectal ultrasound (TRUS)-guided core needle (standard imaging modality) biopsy. DRE can assess the site of the tumor [31]. Diagnosis is based on histology as assessed in a hematoxylin and eosin (H&E) staining where cellular atypia (abnormal glandular patterns), an absence of basal

cells, or atypical nuclei can distinguish between PCa and atypical benign phenotypes [34, 35]. Specifically, for PCa, the histopathological evaluation includes a description of the tumor's differentiation [36-39]. In biopsies, the Gleason grading system correlates with pathological tumor stage, biochemical reoccurrence, and the development of metastases [15].

Pathologists utilize the aforementioned approaches to characterize the nature of cancer and distinguish abnormal nuclear and cytoplasmic features [4]. Some major drawbacks to this standard approach is its limited ability to predict the pathological tumor stage and lack of specificity [16]. These approaches also do not determine the likelihood of the tumor to be castrate resistant or resistant to chemotherapy. While there are a considerable number of prognostic biomarkers proposed, PSA is the only prognostic biomarker routinely being used in the clinics [19]. Consequently, novel markers most likely will complement rather than replace PSA. Identifying and validating novel predictive biomarkers in pre-treatment and post-treatment biopsies is critical to affective therapeutic decision-making. New prognostic tools would also aid patients and clinicians in achieving personalized therapy [44, 45].

Treatments

Recent advances in high-throughput screening led to massive discoveries of new drug targets for PCa. The current targeted therapies include cytotoxic compounds (*i.e.* Docetaxel and Cabazitaxel), AR-targeted therapies (*i.e.* Enzalutamide and Abiraterone*),* and the radioisotope radium-223 [17-20] **(Table 1.1)**. However, none of these targets

have led to curative therapeutics. As mentioned above, one of the main reasons for this is the development of drug resistance. Herein, current evidence about major mechanisms of resistant to PCa treatments is reviewed and insights on new and future therapeutic approaches are introduced [21].

AR-targeted therapies

Androgen receptor (AR) targeted therapies, termed AR deprivation therapy or ADT (**Figure 1.4**), are one of the first therapies for treatment of prostate cancer [21]. However, a portion of patients receiving treatment for PCa will relapse, despite the use of ADT. Tumor outgrowth during ADT represents a key transition point from hormone-sensitive disease to a more aggressive form, castration-resistant prostate cancer (CRPC) [22, 23]. **Table 1.2** describes the most commonly used ADT strategies [24-26]. For example, gonadotropin-releasing hormone (GnRH) antagonism involves GnRH receptor blockage, preventing release of luteinizing hormone (LH) [27] and follicle-stimulating hormone (FSH) producing testosterone suppression [28]. Despite the availability of AR treatments, most AR therapies are ineffective in the majority of patients [29, 30]. Identified mechanisms mediating AR-resistance development include: AR signaling restoration through upregulated steroidogenesis, AR mutation/amplification, AR cross talk with other signaling pathways, and activation of bypass pathways independent of AR signaling [21, 30-36].

AR signaling reactivation mechanisms include cross talk with other oncogenic signaling pathways via activation of downstream signaling molecules [37-40]. Somatic mutations of AR also can allow for the activation of AR by other ligands [41]. There can also be intratumoral upregulation of androgen biosynthesis, leading to a shift from

paracrine stromal growth support to an autocrine mode [42]. Additionally, there exist altered splice variants of the AR that are devoid of a ligand-binding domain and become constitutively active [43].

The AR can also be altered due to changes in transcriptional activity via changes in AR coregulators [44]. Post-translational alterations, such as such changes in phosphorylation can stabilize the AR and protect it from proteolytic degradation [45]. Knowledge of these mechanisms have driven the development of numerous therapies.

The most recent AR therapies include anti-androgen drugs, such as Abiraterone acetate (CYP17A1 inhibitors) and Enzalutamide (nonsteroidal anti-androgens) that were approved by the FDA in 2011 and 2012, respectively [46]. Both drugs increase the median survival time a little over 3 months, as compared to control [19, 47, 48].

Abiraterone acetate is an androgen synthesis inhibitor whose mechanisms involves CYP17A inhibition [46]. Inhibition of CYP17A results in a decrease in androgen synthesis in peripheral tissues and a reduction in precursors required for androgen production [46]. Unfortunately, nearly 1/3 of patients have primary resistance to Abiraterone acetate [49].

Enzalutamide functions to reduce AR signaling through competitively binding to the testosterone/DHT receptor on the AR, which blocks AR translocation to the nucleus [50]. Instead of blocking production of its ligand, Enzalutamide inhibits co-activator recruitment and binds AR to DNA [51]. Even though Enzalutamide treatment increased survival time by 5-month in patients, as compared to placebo treated patients who failed

Docetaxel treatment, ¼ of patients have primary resistance to Enzalutamide, and all patients progressed by 24 months of initial treatment [52].

Even with the early success of Abiraterone and Enzalutamide, clinicians have already noticed the limitations of these drugs [53]. Approximately 20% of patients have no response to the treatment. Most patients who initially respond to the compounds rapidly develop resistance in less than 2 years [19, 47, 48, 54, 55].

Taxanes: Targeted Therapies

Taxanes represent an important chemotherapeutic class of drugs, which have demonstrated survival benefits in CRPC therapy. Microtubules are composed of a backbone of tubulin dimers and microtubule-associated proteins. Taxanes have the capacity to bind strongly to polymers of tubulin. Antimitotic effects occur by reducing spindle-shaped microtubule formation leading to cell cycle arrest in the mitotic phase (G_2 /M). Until 2010, Docetaxel (*Taxotere*®, Docefrez®) and hormonal manipulation were the only strategies available to metastatic patients with CRPC [56]. Taxane compounds such as Docetaxel and Cabazitaxel (*Jevtana*®) were FDA-approved for CRPC in 2004 and 2017, respectively.

Taxane-based standard chemotherapy is based on two landmark randomized control trials, TAX327 and SWOG 99-16 [57]. The TAX327 trial compared Docetaxel with prednisone or Mitoxantrone with prednisone (MP) [58]. The median overall survival benefit to CRPC patients was 17.5 months vs. 15.6 months as compared to placebo treatment [52]. Docetaxel with prednisone is the indicated chemotherapeutic treatment for chemotherapy-naïve PCa patients [59].

Docetaxel was approved in 2004 by the FDA as a combination drug with prednisone demonstrating a 2.5-month median survival benefit (total 19.2 months post castration resistance) in CRPC patients being treated with MP, the previous standard of care [60]. Docetaxel functions by blocking cell division through microtubule formation inhibition [1, 61]. Docetaxel also has roles in the regulation off anti-apoptotic factors and cell cycle regulators [62]. Thus, Docetaxel affects multiple targets simultaneously. Despite the overall benefit shown in these studies, Docetaxel resistance commonly develops, and disease progression occurs in approximately 7.5 months for a subset of patients [29]. The resistance is due to several contributing factors, such as tubulin alterations, overexpression of multi-drug resistant (MDR), ETS fusion genes family, epithelial and mesenchymal transition (EMT), AR splice variants[63, 64].

Cabazitaxel, a second-line taxane chemotherapy, has a similar mechanism of action as Docetaxel and is indicated for Docetaxel resistant CRPC. The TROPIC Phase-III trial observed a 2.4-month median survival benefit (15.1 months total) when compared to other Docetaxel resistant patients treated with MP [65]. Cabazitaxel has a poor affinity to P-glycoprotein due to presence of extra methyl groups [66]. The extra methyl groups give this compound a unique ability to cross blood-brain barrier, which enables Cabazitaxel to be more effective in Docetaxel resistant tumors [66].

Researchers have intensely studied various mechanisms by which prostate cancer cells become resistant to anticancer drugs. These include the loss of cell surface receptors, changes in drug transporters, alterations in drug metabolism, and drug target mutations [67]. The heterogeneity of various PCa tumors is related to the variability of the oncogenic stages [68]. Epigenetic heterogeneity via potent anticancer therapeutics

results in overgrowth of drug-resistant variants and rapid acquisition of drug resistance [69]. Failure to respond to specific therapies can result from general causes such as specific genetic and/or epigenetic alterations and host factors [70]. Host factors include but are not limited to poor absorption, or drug excretion resulting in low serum levels [71]. Other factors include poor tolerance to compounds, especially in geriatric populations [71]. This can result in the need to reduce doses below optimal levels. In addition, the inability to deliver a drug to the site of a tumor could occur with bulky tumors or with high molecular weight and low tissue penetration biological agents such as monoclonal antibodies and immunotoxins [72, 73]. Drug transit could be affected by various alterations in the host tumor microenvironment [74]. Finally, each cancer cell from a patient has the potential to have an individualized genetic make-up depending on the tissue of origin as well as the pattern of activation of oncogenes, inactivation of tumor suppressors, and random variations in gene expression resulting from mutated cancer phenotypes [75]. As a result, every cancer expresses a different array of drug-resistant cells.

Multidrug Resistance

In some cases, researchers use combination therapies with different targets to circumnavigating resistant mechanisms. However, studies show that cells can express mechanisms of resistance to many different structurally and functionally unrelated drugs. This phenomenon known as multidrug resistance typically results from changes limiting drug accumulation within cells. This occurs by limiting uptake, enhancing efflux, or affecting membrane lipids such as ceramide [76, 77]. These changes block programmed cell death (apoptosis) activated by most anticancer drugs [78]. Activation of general

response mechanisms that detoxify drugs and repair DNA damage alter cell cycle checkpoints, which render cells relatively resistant to cytotoxicity effects and also alter drug accumulation [79-81].

Another major mechanism of multidrug resistant in cancer cells is the expression of an energy-dependent drug efflux pump, known alternatively as P-glycoprotein (P-gp), or the multidrug transporter [82]. P-gp is a member of the ATP-dependent transporters known as ATP-binding cassette (ABC) family that are involved in both efflux of drugs and in moving nutrients and other biological important molecules across the plasma and intracellular membranes in cells [83]. P-gp is widely expressed in many human cancers including those of the gastrointestinal tract (small and large intestine, liver cancer and pancreatic cancer), hematopoietic system (myeloma, lymphoma, leukemia), genitourinary system (kidney, ovary, testicle) and childhood cancers (neuroblastoma, fibroscarcoma) [82, 84].

Summary

Despite significant improvements in PCa diagnosis and treatments over the past decades [85], drug resistance remains a barrier to effective treatment of PCa. There also remains a need for improved biomarkers for disease diagnosis, tumor staging classification and predicting drug efficacy as well as predicting drug resistance [85, 86]. The lack of reliable indicators hinders personalized treatments for PCa patients [87, 88]. Moreover, the clinical success of future strategies stems from a greater understanding of Docetaxel (standard chemotherapeutic) resistance mechanisms. Insights into how these processes work can influence the next generation of cancer therapies.

Numerous studies support the hypothesis that lipidomic reprogramming occurs during cancer development and progression [68, 69, 71-75, 79-81, 89]. Understanding the difference in the lipidomic profile between the clinical stages of PCa represents an avenue to better understand tumor pathogenesis and develop new diagnostic testing [90-92], and better define cancer progression [93]. Finally, it's also possible that changes in lipidomic profiles, either in cancer cells or the plasma, may act as indicators of therapeutic resistance.

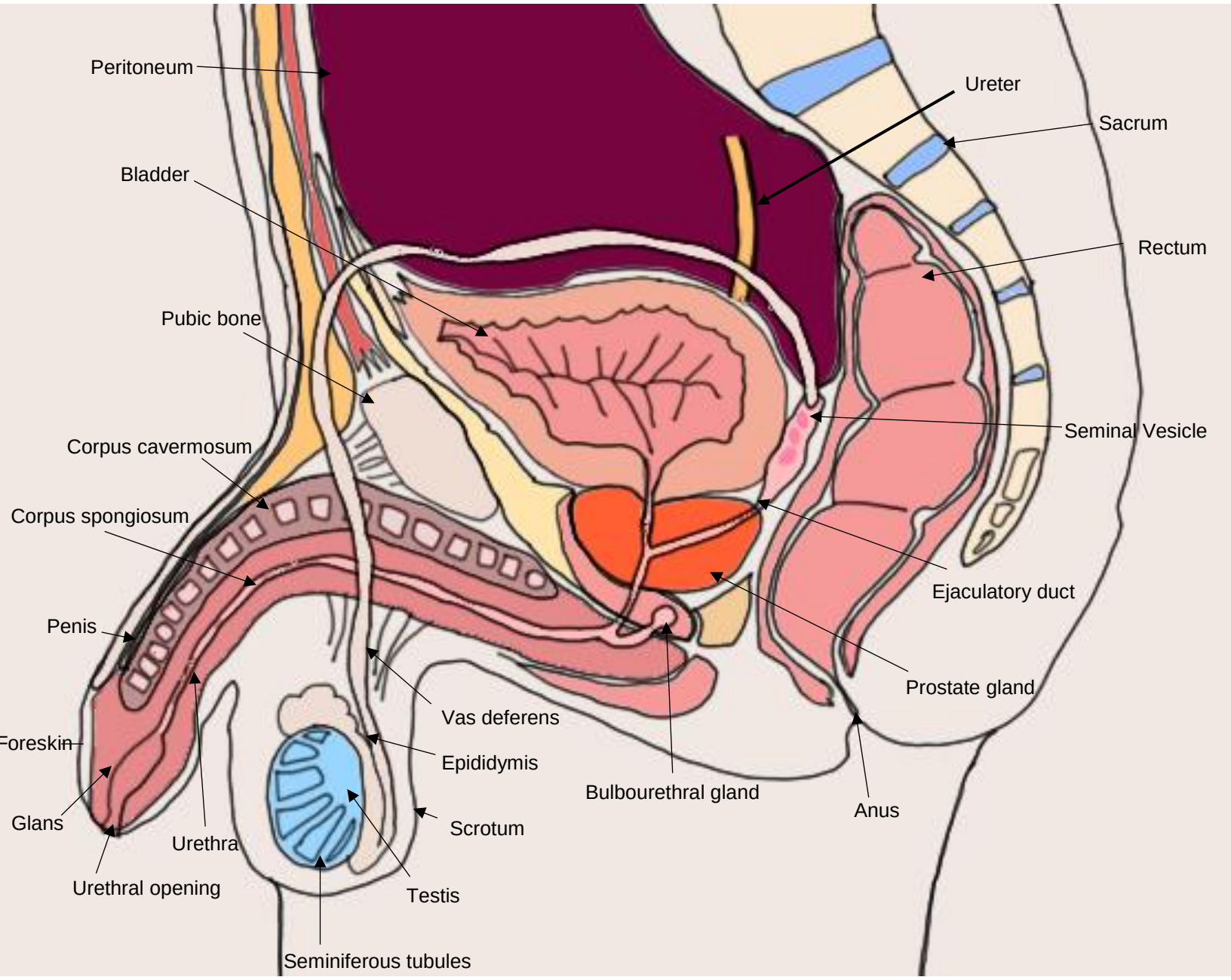

Figure 1.1: Anatomy of the Male Reproductive Systems [94, 95]

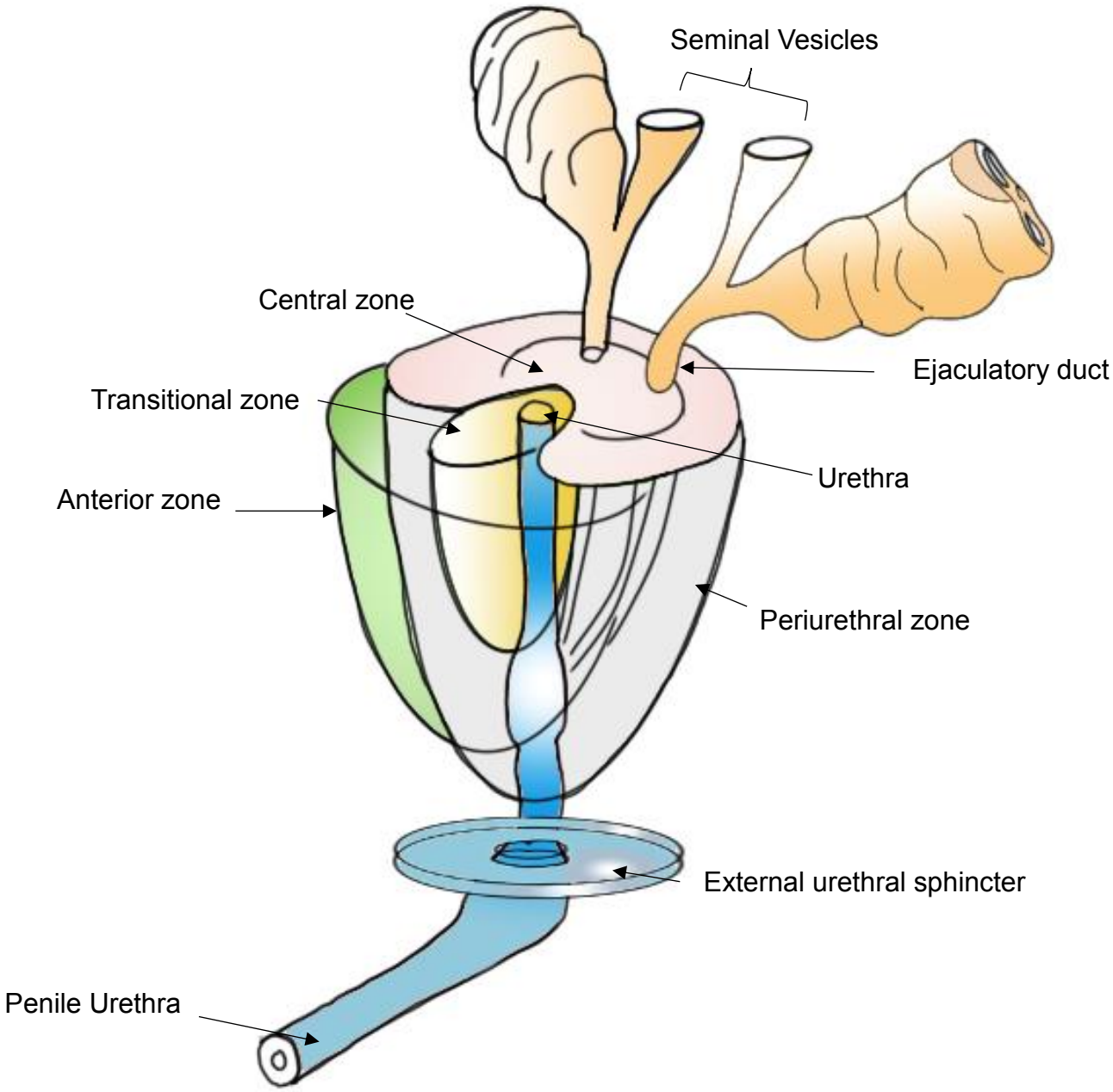

Figure 1.2: Anatomical Zones of the Prostate [96, 97]

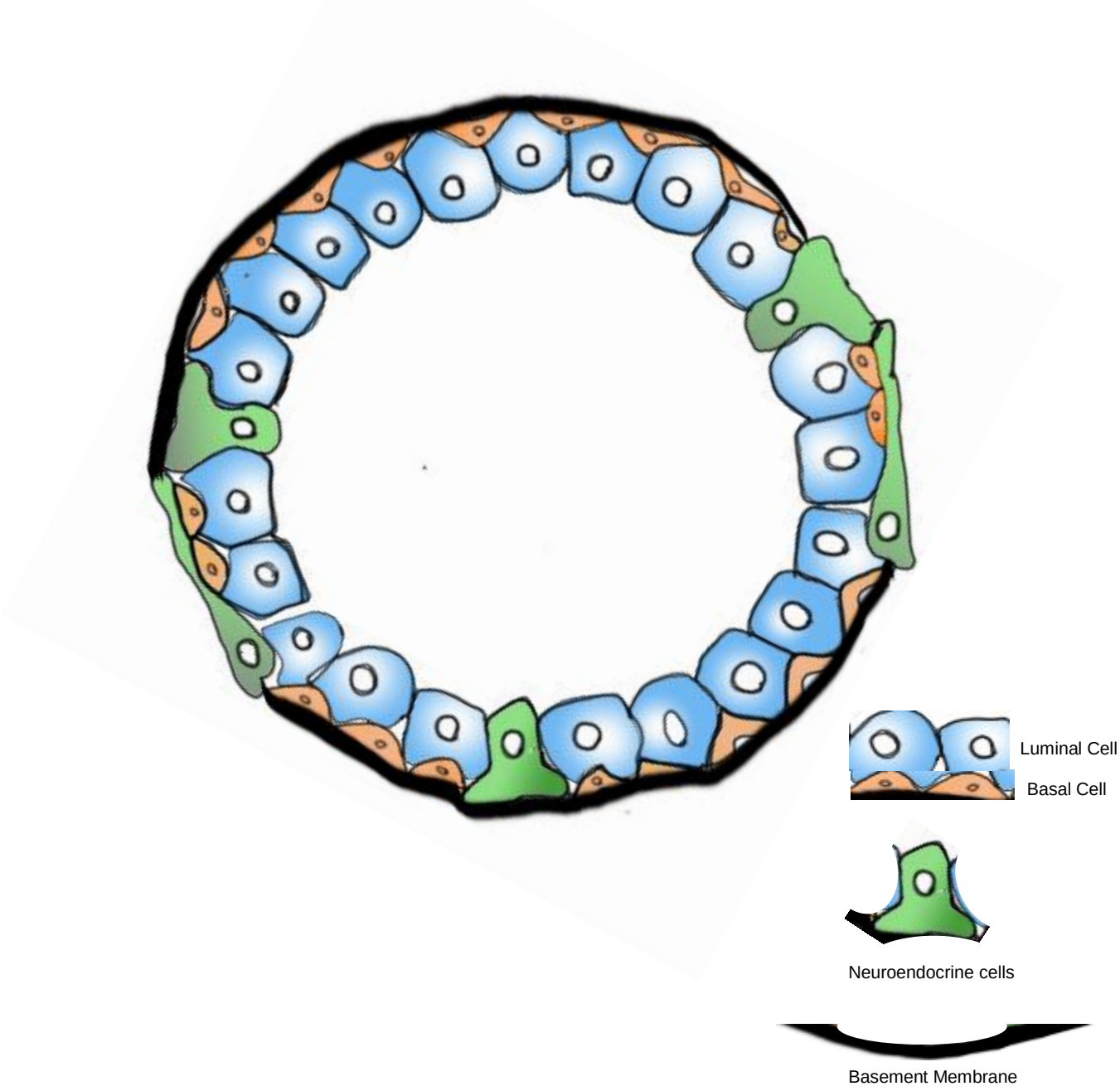

Figure 1.3: Representation of the Cross-section Diagram of the Prostate Gland Duct [98-100]

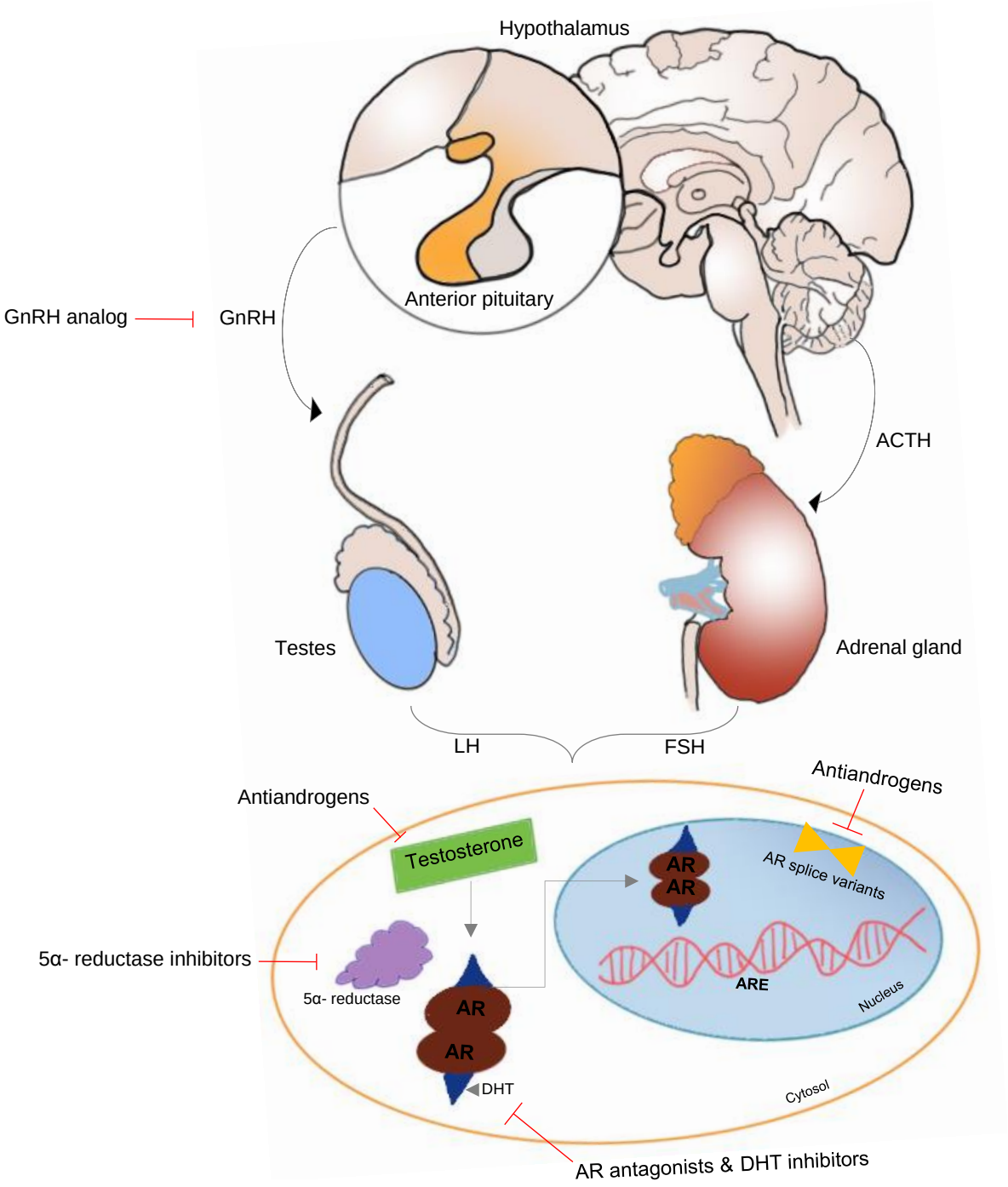

Figure 1.4: Androgen Signaling Mechanisms. Abbreviations: Adrenocorticotropic hormone, ACTH; AR, Androgen receptor; DHT, Dihydrotestosterone; FSH, Follicle-stimulating hormone; GnRH, Gonadotropin-releasing hormone; LH, Luteinizing Hormone [101, 102]

Table 1.1: Current CRPC Therapeutic Agents

Therapeutic Agent	Mechanism of Action	Clinical Trial Status	Mechanism of Resistance	Evidence of Resistance Markers	Reference
Docetaxel (*Taxotere*®, *Docefrez*®)	Binds to β-tubulin & prevents disassembly of the microtubule network Inhibits anti-apoptotic Bcl2	FDA approved May 2004	Stat1, Stat3, HSP, clusterin, NF-κB, IL-6, IL-8, CCL2, TGF-β MIC-1, MDRP	MDR-1, MDR-3 PABP4, Endophilin-A2	Kharaziha, et al. (2014), Gan L, et al. (2011), Domingo-Domenech. et al, (2006), Patterson SG, et al. (2006), Zemskova M, et al. (2008), O'Neill AJ. et al, (2011), Condony-Servant. et al, (2013)
Cabazitaxel (*Jevtana*®)	Stabilization of tubulin, induction of cell cycle arrest and inhibition of cell proliferation Taxane (low affinity to MDRP ABCB1)	FDA approved for men after failure of docetaxel 2.4 month survival benefit over Mitoxantrone June 2010	ERG interaction with to β-tubulin	ERG	Mita AC, et al. (2012) Tsao CK, et al. (2014) Galletti G, et al. (2014)
Abiraterone acetate (Zytiga®)	Irreversible inhibition of CYP17 and subsequent androgen synthesis (Anti-androgen)	FDA approved in the pre- and post-docetaxel settings 3.9- 4.4 month survival benefit with 1/3 patients display resistance April 2011	1.3-4.5 fold increase in Steroidogenesis Pathway Enzymes (CYP17A1, AKR1C3, HSD17B3, SDR5A2) HSD3B1 (1245C) Mutation	Re-activation of androgen synthesis in PC cells (Androgen Precursors)	Mostaghel EA, et al. (2011) Chun JY, et a. (2009) Zhao XY, et al. (2000) Grigoryev DN, et al. (2000) Culig Z, et al. (1993) Attard G, et al. (2012)

			IL-6, HSD3B2, AKR1C3 AR activation by ligands other than Androgen		
Enzalutamide (Xtandi, ENZA, MDV3100)	Irreversible inhibition of CYP17 and subsequent androgen synthesis Reducing AR activity Competitive inhibitor of ligand binding to AR Inhibits AR translocation to the nucleus, co-activator recruitment, AR binding to DNA and activation of AR target genes	FDA approved in the pre- and post-docetaxel settings (Phase III clinical trial in comparison with placebo in chemotherapy naïve) August 2012	Steroidogenesis, Glucose metabolism & Autophagy AKR1C3 10-30% of CRPC patients have AR Mutations (Phe876Leu mutation) Stat3 and IL-6	Cholesterol, DHEA, progesterone,	Watering KK, et al. (2012) Eisermann K, et al. (2012) Korpal M, et al. (2013)
Alpharadin (Radium-223)	An alpha emitter which selectively targets bone metastasis with alpha particles	Phase III clinical trial in med who had received, were not eligible to receive, or declined Docetaxel May 2013			
Sipleucel-T (Provenge)	Cellular Immunotherapy Therapeutic Cancer Vaccine	4.1 month Benefit 3 –year Survival Rate of 34.1% April 2010			

Table 1.2: Current ADT Therapeutic Strategies

Drug Class	Drugs	Site of Action	Strategies
Gonatropin-Releasing Hormone (GnRH) Agonist	Leuprolide	Anterior Pituitary Gland	Decreases release of LH through down regulation of GnRH Receptors
	Goserelin	Anterior Pituitary Gland	
GnRH Antagonist	Abarelix	Anterior Pituitary Gland	Directly inhibits GnRH Receptors
Adrenal Ablating Drugs	Ketoconazole	Adrenal Gland	Decreases androgen synthesis from Steroid Precursors through Inhibition of Cytochrome P450 Enzymes
Androgen Receptor Antagonist	Flutamide	Prostate Gland	Inhibits androgen receptor ligand-binging domain through competitive binding
	Bicalutamide	Prostate Gland	Inhibits androgen receptor ligand-binging domain through competitive binding
	Nilutamide	Prostate Gland	Inhibits androgen receptor ligand-binging domain through competitive binding
5a-Reductase Inhibitors	Finasteride	Prostate Gland	Decreases conversion of testosterone to DHT through inhibition of 5a-Reductase

References

1. Karantanos, T., P.G. Corn, and T.C. Thompson, *Prostate cancer progression after androgen deprivation therapy: mechanisms of castrate resistance and novel therapeutic approaches.* Oncogene, 2013. **32**(49): p. 5501-5511.

2. Jemal, A., et al., *Cancer statistics, 2008.* CA Cancer J Clin, 2008. **58**(2): p. 71-96.

3. Chambers, S.K., et al., *Defining young in the context of prostate cancer.* Am J Mens Health, 2015. **9**(2): p. 103-14.

4. Siegel, R.L., K.D. Miller, and A. Jemal, *Cancer statistics, 2019.* CA: A Cancer Journal for Clinicians, 2019. **69**(1): p. 7-34.

5. Fontenot, P.A., Jr., et al., *Metastatic prostate cancer in the modern era of PSA screening.* Int Braz J Urol, 2017. **43**(3): p. 416-421.

6. Roobol, M.J., *Screening for prostate cancer: are organized screening programs necessary?* Transl Androl Urol, 2018. **7**(1): p. 4-11.

7. Salinas, C.A., et al., *Prostate cancer in young men: an important clinical entity.* Nat Rev Urol, 2014. **11**(6): p. 317-23.

8. Hiraoka, Y. and M. Akimoto, *Anatomy of the prostate from fetus to adult--origin of benign prostatic hyperplasia.* Urol Res, 1987. **15**(3): p. 177-80.

9. Humphrey, P.A., *Histopathology of Prostate Cancer.* Cold Spring Harb Perspect Med, 2017. **7**(10).

10. Bhavsar, A. and S. Verma, *Anatomic imaging of the prostate.* Biomed Res Int, 2014. **2014**: p. 728539.

11. Garraway, L.A., et al., *Intermediate basal cells of the prostate: in vitro and in vivo characterization.* Prostate, 2003. **55**(3): p. 206-18.

12. van Leenders, G.J. and J.A. Schalken, *Epithelial cell differentiation in the human prostate epithelium: implications for the pathogenesis and therapy of prostate cancer.* Crit Rev Oncol Hematol, 2003. **46 Suppl**: p. S3-10.

13. Man, Y.-G., et al., *Tumor-infiltrating immune cells promoting tumor invasion and metastasis: existing theories.* Journal of Cancer, 2013. **4**(1): p. 84-95.

14. Tchetgen, M.B., et al., *Ejaculation increases the serum prostate-specific antigen concentration.* Urology, 1996. **47**(4): p. 511-6.

15. Liu, A.Y. and L.D. True, *Characterization of prostate cell types by CD cell surface molecules.* Am J Pathol, 2002. **160**(1): p. 37-43.

16. Cary, K.C. and M.R. Cooperberg, *Biomarkers in prostate cancer surveillance and screening: past, present, and future.* Therapeutic advances in urology, 2013. **5**(6): p. 318-329.

17. Petrylak, D.P., et al., *Docetaxel and estramustine compared with mitoxantrone and prednisone for advanced refractory prostate cancer.* New England Journal of Medicine, 2004. **351**(15): p. 1513-1520.

18. Tannock, I.F., et al., *Docetaxel plus prednisone or mitoxantrone plus prednisone for advanced prostate cancer.* New England Journal of Medicine, 2004. **351**(15): p. 1502-1512.

19. de Bono, J.S., et al., *Abiraterone and increased survival in metastatic prostate cancer.* N Engl J Med, 2011. **364**(21): p. 1995-2005.

20. Parker, C., et al., *Alpha emitter radium-223 and survival in metastatic prostate cancer.* New England Journal of Medicine, 2013. **369**(3): p. 213-223.

21. Desouki, M., et al., *hZip2 and hZip3 zinc transporters are down regulated in human prostate adenocarcinomatous glands.* Molecular Cancer, 2007. **6**: p. 37.

22. Logothetis, C., et al., *Current perspectives on bone metastases in castrate-resistant prostate cancer.* Cancer Metastasis Rev, 2018. **37**(1): p. 189-196.

23. Merseburger, A.S., A. Alcaraz, and C.A. von Klot, *Androgen deprivation therapy as backbone therapy in the management of prostate cancer.* Onco Targets Ther, 2016. **9**: p. 7263-7274.

24. Boccon-Gibod, L., E. van der Meulen, and B.-E. Persson, *An update on the use of gonadotropin-releasing hormone antagonists in prostate cancer.* Therapeutic advances in urology, 2011. **3**(3): p. 127-140.

25. Wadosky, K.M. and S. Koochekpour, *Molecular mechanisms underlying resistance to androgen deprivation therapy in prostate cancer.* Oncotarget, 2016. **7**(39): p. 64447-64470.

26. Gamat, M. and D.G. McNeel, *Androgen deprivation and immunotherapy for the treatment of prostate cancer.* Endocrine-related cancer, 2017. **24**(12): p. T297-T310.

27. Montgomery, R.B., et al., *Maintenance of intratumoral androgens in metastatic prostate cancer: a mechanism for castration-resistant tumor growth.* Cancer Res, 2008. **68**(11): p. 4447-54.

28. Heidenreich, A., et al., *[EAU guidelines on prostate cancer. Part I: screening, diagnosis, and treatment of clinically localised disease].* Actas Urol Esp, 2011. **35**(9): p. 501-14.

29. Li, Y., et al., *Androgen receptor splice variants mediate enzalutamide resistance in castration-resistant prostate cancer cell lines.* Cancer Res, 2013. **73**(2): p. 483-9.

30. Crona, D.J. and Y.E. Whang, *Androgen Receptor-Dependent and -Independent Mechanisms Involved in Prostate Cancer Therapy Resistance.* Cancers (Basel), 2017. **9**(6).

31. Thoma, C., *AR-Vs not predictive in mCRPC.* Nature Reviews Urology, 2018. **15**: p. 203.

32. Sharp, A., et al., *Androgen receptor splice variant-7 expression emerges with castration resistance in prostate cancer.* The Journal of Clinical Investigation, 2019. **129**(1): p. 192-208.

33. Chandrasekar, T., et al., *Mechanisms of resistance in castration-resistant prostate cancer (CRPC).* Transl Androl Urol, 2015. **4**(3): p. 365-80.

34. Tilki, D., E.M. Schaeffer, and C.P. Evans, *Understanding Mechanisms of Resistance in Metastatic Castration-resistant Prostate Cancer: The Role of the Androgen Receptor.* European Urology Focus, 2016. **2**(5): p. 499-505.

35. Huang, Y., et al., *Molecular and cellular mechanisms of castration resistant prostate cancer.* Oncol Lett, 2018. **15**(5): p. 6063-6076.

36. Kahn, B., J. Collazo, and N. Kyprianou, *Androgen receptor as a driver of therapeutic resistance in advanced prostate cancer.* Int J Biol Sci, 2014. **10**(6): p. 588-95.

37. Yuan, X. and S.P. Balk, *Mechanisms mediating androgen receptor reactivation after castration.* Urologic oncology, 2009. **27**(1): p. 36-41.

38. Sharifi, N., *Mechanisms of androgen receptor activation in castration-resistant prostate cancer.* Endocrinology, 2013. **154**(11): p. 4010-4017.

39. Tan, M.H.E., et al., *Androgen receptor: structure, role in prostate cancer and drug discovery.* Acta Pharmacologica Sinica, 2014. **36**: p. 3.

40. Prins, G.S. and O. Putz, *Molecular signaling pathways that regulate prostate gland development.* Differentiation; research in biological diversity, 2008. **76**(6): p. 641-659.

41. Di Lorenzo, G., et al., *Expression of Epidermal Growth Factor Receptor Correlates with Disease Relapse and Progression to Androgen-independence in Human Prostate Cancer.* Clinical Cancer Research, 2002. **8**(11): p. 3438-3444.

42. Cai, C., et al., *Intratumoral de novo steroid synthesis activates androgen receptor in castration-resistant prostate cancer and is upregulated by treatment with CYP17A1 inhibitors.* Cancer Res, 2011. **71**(20): p. 6503-13.

43. Kallio, H.M.L., et al., *Constitutively active androgen receptor splice variants AR-V3, AR-V7 and AR-V9 are co-expressed in castration-resistant prostate cancer metastases.* British Journal of Cancer, 2018. **119**(3): p. 347-356.

44. Heinlein, C.A. and C. Chang, *Androgen receptor (AR) coregulators: an overview.* Endocr Rev, 2002. **23**(2): p. 175-200.

45. van der Steen, T., D.J. Tindall, and H. Huang, *Posttranslational modification of the androgen receptor in prostate cancer.* International journal of molecular sciences, 2013. **14**(7): p. 14833-14859.

46. Stein, M.N., et al., *Androgen synthesis inhibitors in the treatment of castration-resistant prostate cancer.* Asian journal of andrology, 2014. **16**(3): p. 387-400.

47. Beer, T.M., et al., *Enzalutamide in metastatic prostate cancer before chemotherapy.* N Engl J Med, 2014. **371**(5): p. 424-33.

48. James, N.D., et al., *Abiraterone for Prostate Cancer Not Previously Treated with Hormone Therapy.* N Engl J Med, 2017. **377**(4): p. 338-351.

49. Armstrong, C.M. and A.C. Gao, *Drug resistance in castration resistant prostate cancer: resistance mechanisms and emerging treatment strategies.* American journal of clinical and experimental urology, 2015. **3**(2): p. 64-76.

50. Schalken, J. and J.M. Fitzpatrick, *Enzalutamide: targeting the androgen signalling pathway in metastatic castration-resistant prostate cancer.* BJU international, 2016. **117**(2): p. 215-225.

51. Rodriguez-Vida, A., et al., *Enzalutamide for the treatment of metastatic castration-resistant prostate cancer.* Drug design, development and therapy, 2015. **9**: p. 3325-3339.

52. Petrylak, D.P., et al., *Docetaxel and estramustine compared with mitoxantrone and prednisone for advanced refractory prostate cancer.* N Engl J Med, 2004. **351**(15): p. 1513-20.

53. Fang, M., et al., *Efficacy of Abiraterone and Enzalutamide in Pre- and Postdocetaxel Castration-Resistant Prostate Cancer: A Trial-Level Meta-Analysis.* Prostate cancer, 2017. **2017**: p. 8560827-8560827.

54. Antonarakis, E.S., *Current understanding of resistance to abiraterone and enzalutamide in advanced prostate cancer.* Clin Adv Hematol Oncol, 2016. **14**(5): p. 316-9.

55. Antonarakis, E.S., et al., *AR-V7 and Resistance to Enzalutamide and Abiraterone in Prostate Cancer.* New England Journal of Medicine, 2014. **371**(11): p. 1028-1038.

56. Hotte, S.J. and F. Saad, *Current management of castrate-resistant prostate cancer.* Current oncology (Toronto, Ont.), 2010. **17 Suppl 2**(Suppl 2): p. S72-S79.

57. Mendiratta, P., A.J. Armstrong, and D.J. George, *Current standard and investigational approaches to the management of hormone-refractory prostate cancer.* Reviews in urology, 2007. **9 Suppl 1**(Suppl 1): p. S9-S19.

58. Berthold, D.R., et al., *Docetaxel plus prednisone or mitoxantrone plus prednisone for advanced prostate cancer: updated survival in the TAX 327 study.* J Clin Oncol, 2008. **26**(2): p. 242-5.

59. Lohiya, V., J.B. Aragon-Ching, and G. Sonpavde, *Role of Chemotherapy and Mechanisms of Resistance to Chemotherapy in Metastatic Castration-Resistant Prostate Cancer.* Clinical Medicine Insights. Oncology, 2016. **10**(Suppl 1): p. 57-66.

60. Dagher, R., et al., *Approval summary: Docetaxel in combination with prednisone for the treatment of androgen-independent hormone-refractory prostate cancer.* Clin Cancer Res, 2004. **10**(24): p. 8147-51.

61. Zhu, M.-L., et al., *Tubulin-targeting chemotherapy impairs androgen receptor activity in prostate cancer.* Cancer research, 2010. **70**(20): p. 7992-8002.

62. Fitzpatrick, J.M. and R. de Wit, *Taxane mechanisms of action: potential implications for treatment sequencing in metastatic castration-resistant prostate cancer.* Eur Urol, 2014. **65**(6): p. 1198-204.

63. Terry, S., et al., *Increased expression of class III β-tubulin in castration-resistant human prostate cancer.* British journal of cancer, 2009. **101**(6): p. 951.

64. Ranganathan, S., et al., *Modulation of endogenous β-tubulin isotype expression as a result of human β III cDNA transfection into prostate carcinoma cells.* British journal of cancer, 2001. **85**(5): p. 735.

65. Oudard, S., *TROPIC: Phase III trial of cabazitaxel for the treatment of metastatic castration-resistant prostate cancer.* Future Oncol, 2011. **7**(4): p. 497-506.

66. Kartner, N., J.R. Riordan, and V. Ling, *Cell surface P-glycoprotein associated with multidrug resistance in mammalian cell lines.* Science, 1983. **221**(4617): p. 1285-8.

67. Assaraf, Y.G., *The role of multidrug resistance efflux transporters in antifolate resistance and folate homeostasis.* Drug Resist Updat, 2006. **9**(4-5): p. 227-46.

68. Wyatt, A.W., et al., *The diverse heterogeneity of molecular alterations in prostate cancer identified through next-generation sequencing.* Asian journal of andrology, 2013. **15**(3): p. 301-308.

69. Hoey, T., *Drug resistance, epigenetics, and tumor cell heterogeneity.* Sci Transl Med, 2010. **2**(28): p. 28ps19.

70. Coyle, K.M., J.E. Boudreau, and P. Marcato, *Genetic Mutations and Epigenetic Modifications: Driving Cancer and Informing Precision Medicine.* BioMed research international, 2017. **2017**: p. 9620870-9620870.

71. Fernandez, E., et al., *Factors and Mechanisms for Pharmacokinetic Differences between Pediatric Population and Adults.* Pharmaceutics, 2011. **3**(1): p. 53-72.

72. Li, M., et al., *Clinical targeting recombinant immunotoxins for cancer therapy.* OncoTargets and therapy, 2017. **10**: p. 3645-3665.

73. Thurber, G.M., M.M. Schmidt, and K.D. Wittrup, *Antibody tumor penetration: transport opposed by systemic and antigen-mediated clearance.* Advanced drug delivery reviews, 2008. **60**(12): p. 1421-1434.

74. Corn, P.G., *The tumor microenvironment in prostate cancer: elucidating molecular pathways for therapy development.* Cancer management and research, 2012. **4**: p. 183-193.

75. Pedraza-Fariña, L.G., *Mechanisms of oncogenic cooperation in cancer initiation and metastasis.* The Yale journal of biology and medicine, 2006. **79**(3-4): p. 95-103.

76. Liu, Y.Y., et al., *Ceramide glycosylation potentiates cellular multidrug resistance.* Faseb j, 2001. **15**(3): p. 719-30.

77. Nguyen, K.T., et al., *Transactivation of the human multidrug resistance (MDR1) gene promoter by p53 mutants.* Oncol Res, 1994. **6**(2): p. 71-7.

78. Smets, L.A., *Programmed cell death (apoptosis) and response to anti-cancer drugs.* Anticancer Drugs, 1994. **5**(1): p. 3-9.

79. Xue, X., et al., *Nanoscale drug delivery platforms overcome platinum-based resistance in cancer cells due to abnormal membrane protein trafficking.* ACS nano, 2013. **7**(12): p. 10452-10464.

80. Glavinas, H., et al., *The role of ABC transporters in drug resistance, metabolism and toxicity.* Curr Drug Deliv, 2004. **1**(1): p. 27-42.

81. Kis, O., et al., *The complexities of antiretroviral drug-drug interactions: role of ABC and SLC transporters.* Trends Pharmacol Sci, 2010. **31**(1): p. 22-35.

82. Goldstein, L.J., et al., *Expression of a multidrug resistance gene in human cancers.* J Natl Cancer Inst, 1989. **81**(2): p. 116-24.

83. Wilkens, S., *Structure and mechanism of ABC transporters.* F1000prime reports, 2015. **7**: p. 14-14.

84. Cunha, G.R., A.A. Donjacour, and Y. Sugimura, *Stromal-epithelial interactions and heterogeneity of proliferative activity within the prostate.* Biochem Cell Biol, 1986. **64**(6): p. 608-14.

85. Filella, X., et al., *Emerging biomarkers in the diagnosis of prostate cancer.* Pharmacogenomics and personalized medicine, 2018. **11**: p. 83-94.

86. Velonas, V.M., et al., *Current status of biomarkers for prostate cancer.* International journal of molecular sciences, 2013. **14**(6): p. 11034-11060.

87. Ross, R.K., et al., *Androgen metabolism and prostate cancer: establishing a model of genetic susceptibility.* Cancer Res, 1998. **58**(20): p. 4497-504.

88. Costello, L.C., R.B. Franklin, and P. Feng, *Mitochondrial function, zinc, and intermediary metabolism relationships in normal prostate and prostate cancer.* Mitochondrion, 2005. **5**(3): p. 143-53.

89. Eidelman, E., et al., *The Metabolic Phenotype of Prostate Cancer.* Frontiers in oncology, 2017. **7**: p. 131-131.

90. Carracedo, A., et al., *Cancer metabolism: fatty acid oxidation in the limelight.* Nature Reviews Cancer, 2013. **13**: p. 227-232.

91. Puchades-Carrasco, L. and A. Pineda-Lucena, *Metabolomics Applications in Precision Medicine: An Oncological Perspective.* Current topics in medicinal chemistry, 2017. **17**(24): p. 2740-2751.

92. Gowda, G.A.N., et al., *Metabolomics-based methods for early disease diagnostics.* Expert review of molecular diagnostics, 2008. **8**(5): p. 617-633.

93. Kelly, R.S., et al., *The role of tumor metabolism as a driver of prostate cancer progression and lethal disease: results from a nested case-control study.* Cancer & metabolism, 2016. **4**: p. 22-22.

94. Mann, T., *The biochemistry of semen and of the male reproductive tract.* The biochemistry of semen and of the male reproductive tract., 1964.

95. De Kretser, D., P. Temple-Smith, and J. Kerr, *Anatomical and functional aspects of the male reproductive organs*, in *Disturbances in Male Fertility*. 1982, Springer. p. 1-131.

96. Everaerts, W. and A.J. Costello, *Applied Anatomy of the Male Pelvis*, in *Prostate Ultrasound: Current Practice and Future Directions*, C.R. Porter and E.M. Wolff, Editors. 2015, Springer New York: New York, NY. p. 11-30.

97. Fine, S.W. and R. Mehra, *Anatomy of the Prostate Revisited: Implications for Prostate Biopsy and Zonal Origins of Prostate Cancer*, in *Genitourinary Pathology: Practical Advances*, C. Magi-Galluzzi and C.G. Przybycin, Editors. 2015, Springer New York: New York, NY. p. 3-12.

98. Rybak, A., R. Bristow, and A. Kapoor, *Prostate cancer stem cells: Deciphering the origins and pathways involved in prostate tumorigenesis and aggression.* Oncotarget, 2014. **6**.

99. Barron, D.A. and D.R. Rowley, *The reactive stroma microenvironment and prostate cancer progression.* 2012. **19**(6): p. R187.

100. Toivanen, R. and M.M. Shen, *Prostate organogenesis: tissue induction, hormonal regulation and cell type specification.* Development, 2017. **144**(8): p. 1382-1398.

101. Obinata, D., et al., *Review of novel therapeutic medicines targeting androgen signaling in castration-resistant prostate cancer.* World Journal of Clinical Urology, 2014. **3**(3): p. 264-271.

102. Turner, B. and L. Drudge-Coates, *New pharmacological treatments for prostate cancer.* Nurse Prescribing, 2012. **10**: p. 498-502.

CHAPTER 2

LIPID PHYSIOLOGY and SIGNALING

Lipid Physiology

Lipids are fundamental organic molecules utilized in the human body for a number of essential cellular processes. It is estimated that mammalian biological systems contain more than 10,000 different lipid species [103]. Lipids vary in size, head groups, fatty acid chains and type of linkage formed between two structural domains [59, 104, 105]. These include a number of fatty acids, triglycerides, phospholipids, sterol lipids and sphingolipids [106]. As much as 50% of lipids and their corresponding lipid metabolizing enzymes remain without an assigned function [107].

Lipids constitutes the cell and organelle walls and create a semi-permeable space that allows for cellular function and phase separation. Their primary functions include structural components of the cell, energy storage for long-term use, hormonal roles, insulation, nutrition and protection of internal organs [104]. Lipids also facilitate imperative processes important for the generation of primary and secondary messengers in molecular recognition, intracellular membrane trafficking, cell division, and biological reproduction [104]. However, the potential medical relevance of many lipid synthesis pathways have yet to be fully revealed. This includes the relevance of these pathways in disease such as cancer. A review of lipid physiology is needed to fully understand the possible mechanisms mediating lipid changes in cancer (**Figure 2.1**).

Phospholipid Physiology

Phospholipids are composed of a polar head group (choline, ethanolamine, serine, and inositol) and fatty acyl chains that can differ in both length and saturation (double bonds), leading to thousands of different lipid species [108]. Phospholipids are synthesized by esterification of an alcohol to the phosphate of phosphatidic acid (1,2 diacylglycerol 3-phosphate). Phosphatidic acid serves as a precursor building block for phosphatidylserine (PS), phosphatidylethanolamine (PE), and phosphatidylcholine (PS) synthesis. Most phospholipids have a saturated fatty acid on C-1 and an unsaturated fatty acid on C-2 of the glycerol backbone. The commonly added alcohols (serine, ethanolamine and choline) also contain nitrogen that may be positively charged, whereas, glycerol and inositol are not charged. The major classifications of glycerophospholipids are phosphatidylserine (PS), phosphatidylethanolamine (PE), phosphatidylcholine (PC), phosphatidylinositol (PI), and phosphatidylglycerol (PG).

Phospholipid Synthesis

Phosphatidylcholine, PC

Phosphatidylcholine (PC) accounts for 40-60% of the phospholipids in the eukaryotic membrane and plays a vital role in cellular structure and other biological functions [109]. In humans, PC is primarily synthesized *de novo* through the Kennedy pathway [110]. Choline is first activated by phosphorylation and then coupled to CDP prior to attachment to a 1,2-diacylglycerol. PC fatty acyl composition at the *sn*-2-position is then altered in a remodeling pathway known as the Lands' cycle [111], through which diverse individual PC species differing in carbon chain length and degree of fatty acid

saturation are produced [112-114]. This neutral class of zwitterions typically contains palmitic or steric acid at c1 and primarily oleic acid (18:1); linoleic acid (18:2) or linoleic acid (18:3) at c2.

The PC intermediate glycerophosphatidylcholine is a precursor for signaling molecules such as phosphatidic acid (PA). PA has been shown to directly activate protein-tyrosine phosphatase [115], protein kinases [116], and sphingosine kinase [117]. Furthermore, this bioactive phospholipid modulates critical processes related to the pathogenesis of cancer [118]. PA has been shown to be involved in the development of resistance to the anti-cancer drug rapamycin [104].

Lysophosphatidylcholine (LPC) is a precursor of lysophosphatidic acid, a biogenic lipid involved in prostate cancer initiation and progression [119-121]. LPC levels and fatty acid composition are also affected by *de novo* synthesis and remodeling pathways, such as the Lands' cycle [111]. LPC is produced by PC hydrolysis via phospholipase A_2 (PLA_2). PLA_2 are a group of enzymes that catalyze the hydrolysis of phospholipids at the *sn*-2 position of the glycerol backbone. In addition to producing lysophospholipids like LPC, PLA_2 are responsible for releasing arachidonic acid, a precursor of eicosanoids (prostaglandins and leukotrienes) [122]. Further research is needed to elucidate the association between LPC expression and prostate cancer progression.

Phosphatidylethanolamine, PE

Phosphatidylethanolamines are neutral zwitterionic lipids at physiological pH. This lipid species typically contains palmitic or stearic acid on carbon 1 of the glycerol backbone, and a long chain unsaturated fatty acid on carbon 2. The long chain

unsaturated fatty acid on carbon 2 can include 18:2, 20:4 and 22:6. In humans, PE synthesis occur either in the ER or in the inner mitochondrial membrane. The pathway that occurs in the ER involves ethanolamine phosphorylation. The pathway that occurs in the inner mitochondrial membrane and involves the decarboxylation of PS. A minor PE synthesis pathway is the fatty acylation of a lysophosphatidylserine (LPE) conversion to PE, which is catalyzed by an LPE acyltransferase in the Lands cycle in a variety of tissues [123]. PE can serve as the precursor for PC via methylation reactions. Recent studies targeting PE on endothelial cells in tumor vasculature has inspired investigations to explore PE on the surface of certain cancer cells as a potential target for anticancer (PE-binding peptides and small molecules) therapy [124].

Phosphatidylserine, PS

Phosphatidylserine carries a net charge of -1 at physiological pH. PS are generated from PE and PC via base exchange reactions. PS synthesis involves base exchange reactions of serine for the ethanolamine in PE, or serine for the choline in PC. PS can serve as a source of PE through a decarboxylation reaction. PS is present on the inner leaflet of the cell membrane and is an essential component in all human cells. PS-targeting nanovesicles have been efficacious against pancreatic cancer [125], glioblastoma [126] and lung cancer cells [127]. Therefore, this strategy could be useful as an innovative approach for prostate cancer tumor.

Phosphatidylglycerols, PG

PG exhibits a net charge of -1 at physiological pH. PG is found in high concentration in mitochondrial membranes. PG synthesis occurs in a two-step process.

This process begins with CDP-diacylglycerol and glycerol-3-phosphate. The first reaction yields phosphatidylglycerol phosphate that is then converted to PG via removal of phosphate. Previous reports suggest that specific PG species present in the nucleus may be responsible for stimulation of nuclear protein kinase C (PKC) activity observed in nuclear membranes [128]. PKC is a family of serine/threonine kinases involved in transmission of a wide variety of extracellular signals [129]. The relevant roles of PG species in various cellular processes suggest that PG can be used as a potential therapeutic target.

Oxidized Phospholipids (oxPL)

Oxidized phospholipids (oxPL) are peroxidation products recognized as important bioactive lipid mediators in a variety of signaling events including inflammation [130-134]. OxPL have been identified in biological fluids [135-138], cells [139-144] and tissues [145-148]. They are hypothesized to play key roles in maintenance of cell and tissue health [135, 149, 150] and in the development of numerous diseases, such as cardiovascular disease and atherosclerosis [148, 151].

oxPL are not simply by-products formed during lipid peroxidation reactions, but are key mediators in inflammation [131, 133], infection [152], and immune response [153, 154]. Identification of these lipids and improvement in our ability to detect these lipids in biological matrices gave rise to the field of oxidative lipidomics. Despite advances in our ability to measure oxPL, there is still a gap in knowledge on the basal levels of oxPL with respect to many diseases, including their role in drug resistance in prostate cancer progression. As such, the clinical significance of oxPL has not yet been translated into new biomarkers, or novel drug targets.

As far as oxPL impact in diseases, few studies have been conducted quantifying these lipids in plasma using spectrophotometric methods [135-137, 148, 149, 155-157]. oxPL are suggested to be involved in regulation of hydrolytic enzymatic systems such as PLA_2 [158, 159]. They have also been suggested to activate genes involved in the regulation of growth factors, chemokines, signal transduction, extracellular matrices, chemokines, angiogenesis, autophagy and apoptosis [160, 161].

The biological effects exhibited by oxPL are dependent on their structural features such as the polar head group [162-165], acyl chain length [164], the terminal group at the truncated sn-2 acyl chains [164]; the functional group in the oxygenated sn-2 acyl chain [162] and the ester/ ether linkage of oxidized chains to the glycerol moiety [146]. A comprehensive understanding on the basal levels of oxPL in heath and disease is important to better classify and understand these lipids and their potential as biomarkers and as novel therapeutic targets.

Acylglycerol Physiology

Triacylglycerol (TAG)

TAGs are composed of a glycerol molecule linked to three fatty acids through ester bonds. The position at which the fatty acids are added to the glycerol backbone affects the physical and physiological properties of the TAG molecule [166]. The major roles of TAG include energy and fatty acid storage and precursors for phospholipid biosynthesis. TAG synthesis primarily occurs in adipose tissue and the liver, but is also observed in skeletal muscle, lung, heart, kidney and the brain. TAG syntheses can occur via the glycerol-3-phosphate, or the monoacylglycerol pathway in both the ER and the

mitochondria [166-168]. In the glycerol-3-phosphate pathway, synthesis begins with glucose, which is converted into glycerol-3-phosphate by a multi-step reaction. Glycerol-3-phosphate formation, the rate-limiting step of TAG synthesis, is converted to lysophosphatidic acid by glycerol-3-phosphate acyltransferase (GPAT). Lysophosphatidic acid is then converted into phosphatidic acid by 1-acylglycerol-3-phosphate acyltransferase (AGPAT), phosphatidic acid into 1,2-diacylglycerol by phosphatidic acid phosphatase (PAP) and finally 1,2-diacylglycerol into TAG by diacylglycerol acyltransferase (DGAT).

The synthesis of monoacylglycerol is similar to above; however, instead of starting with glucose, this pathway begins with monoacylglycerol, which is converted into 1,2-diacylglycerol by monoacylglycerol acyltransferase (MGAT). The pathway then continues along that given for glycerol-3-phoshphate. Once synthesized, TAGs are packaged into lipid droplets [169]. Numerous studies have demonstrated significantly higher TAG levels in the plasma from breast cancer patients, as compared to control group [170]. The potential therapeutic implications of this phenomenon are not known.

Sphingolipid Physiology

Sphingolipids are known to be dysregulated in several cancer-related processes such as proliferation, apoptosis, migration and metastasis [171-173]. Sphingolipids are essential for cellular structural integrity and play a role in regulating the fluidity of the lipid bilayer [174]. Dysregulation of sphingolipid metabolism in cancer becomes more complex due to the incredible diversity of sphingolipid species and enzymes involved in the pathway. These include, but are not limited to ceramide and sphingomyelin.

Ceramide

Ceramide is one of the most studied sphingolipids in cancer. Ceramides differ in their long chain sphingoid base, as well as in their fatty acid composition [175]. Endogenous ceramides can be generated by four different mechanisms: *De novo* synthesis condensation of serine and palmitoyl-CoA, by sphingomyelin catabolism via sphingomyelinases, by glycosphingolipids catabolism or by ceramide-1-phosphate dephosphorylation [176].

Ceramide is known to be differentially regulated in many cancers [177]. Endogenous ceramide accumulation in response to chemotherapy treatment has been associated with cell death [178, 179], and many chemotherapeutic agents have been shown to increase the levels of ceramides [180]. Previous reports demonstrate increases in ceramide after radiation therapy in prostate cancer cells lead to cell death [180]. However, early studies also reported a decrease in ceramide content.

Ceramide is also known to be decreased in tumors from several tissues, including ovarian tissue [173]. Both ceramide and sphingomyelin content is reduced in human colon cancer tissue [181]. While these decreases are intriguing, studies suggest that a simple decrease in ceramide may not be key to the formation and growth of a tumor. Rather, the change in the overall ceramide species may be more important. In support, of this hypothesis, lipidomic analysis demonstrated specific ceramide species are elevated in cancer. For example, C16 and C24 ceramides, which are significantly associated with malignant breast cancer tissue compared to benign tissue [182, 183]. However, other studies indicate a decrease of C18 ceramide was significantly associated with a higher incidence lymphovascular invasion and nodal metastasis in head and neck squamous cell carcinoma patients [182]. These data suggest the distinct role of individual ceramide

species in tumor types and exemplifies the complexity of sphingolipids and their dysregulation in cancer.

Sphingomyelin

Sphingomyelin is a major sphingolipid in the membrane and has been shown to be dysregulated in Alzheimer's disease, diabetes, hepatocellular carcinoma [184-186]. It is localized to the outer membrane leaflet where it contributes to formation of lipid rafts [171]. Different acyl chain lengths on this lipid will dictate it's function and membrane biophysical properties [187]. Previous studies demonstrate that addition of exogenous dietary sphingomyelin after gemcitabine treatment increased the levels of ceramide and cell death in pancreatic cancer cells [185]. Furthermore, administration of sphingomyelin also inhibited malignant cancer progression in mice [188]. Similar findings were observed after exogenous ceramide analogous were delivered in human Tu138 head and neck squamous carcinoma cell line [189, 190]. The underlying molecular mechanisms that effect sphingolipid imbalance are unknown. Future investigations delineating between the initiation and transitional events imparted by sphingolipids during cancer progression are needed to understand the therapeutic potential of these lipids, as well as other sphingolipids.

Plasmalogens Physiology

Plasmalogens are a subclass of glycerophospholipids distributed in the biological membrane of animals and certain anaerobic bacteria [191]. Plasmologens appear to have unique functions within the cells that directly correlates to the bond at the *sn*-1 and *sn*-2 position [192]. Structurally, these alkenyls based glycerophospholipids exhibit a vinyl

ether at the *sn*-1 position and an ester bond at the *sn*-2 position of the glycerol backbone [193, 194]. The vinyl ether (R1) are attached to a saturated (C16:0) or monosaturated carbon chains (C18:0 and C18:1, respectively) [192, 194]. The *sn*-2 (R2) position are enriched with polysaturated fatty acid, specifically docosahexaenoic acid (C22:6 n-3) or arachidonic acid (C20:4 ω-6) [195]. Plasmalogens have relatively short-half life: about 30 minutes for plasmenylcholines (PC plasmalogens) and 3 hours for plasmenylethanolamine (PE plasmalogens) [196, 197].

Plasmalogens have several roles in cellular function, primarily in part by the unique biophysical properties that that they impart to the cellular plasma membrane [198]. The presence of plasmalogens directly reduces phospholipid surface tension and viscosity, which can affect synaptic transmission, membrane vesicle formation, the regulation of fusion, fission and fluidity of the cell membrane, alter the activity of membrane proteins, alter ion transport, and mediate platelet activation [199, 200].

Several methods for identifying plasmalogens have been developed to gain knowledge about their role in various disease states [193, 201]. Although the mechanisms of action in some diseases still remains unclear studies suggests association with Down syndrome, Alzheimer's disease, metabolic diseases associated with oxidative stress, and molecular signaling abnormalities in cancer [197]. With regards to cancer, quantitative LC-MS demonstrated elevated concentration of 34:2 PE plasmalogens species in colorectal carcinoma [202], which agrees with several studies consistently reporting higher concentration of plasma plasmalogens in cancer patients [203]. These includes studies showing that changes in plasmalogens levels in biofluids

and tissues of various cancer types compared to controls [203]. This suggest that plasmalogens could be good candidates as indicators for cancer.

Lipid Synthesis in Cancer

Initially, lipids were primarily viewed as passive components of cell membranes and moieties for energy storage. This view has radically changed, and lipids are now known to regulate several critical physiological process, as well as to be primary mediators of several pathological events. This includes, a key role in a variety of carcinogenic processes [204-206]. The Warburg effect is dominant in most cancer cells, where malignant cells shift their dominant ATP producing pathways away from oxidative phosphorylation to aerobic glycolysis resulting in lactic acid fermentation [207, 208]. In contrast to other cells, PCa cells do not show initial increases in glucose uptake, which suggest that the Warburg effect is not consistent during onset of this disease [209]. However, high glucose uptake does occur during late stage PCa resulting from numerous mutation events [209]. PCa cells in part obtain and employ lipids for energy production [210-213]. PCa cells ability to become lipid producers and generate key molecules without androgen regulation is critical to both survival and progression [89, 214]. A variety of lipid alterations occur when a benign cell becomes resistant. There is still a great deal of research to be done, as many of the mechanisms of this process is not well understood.

To understand the role of lipid alterations in the development of drug resistance, we need to first gain insight into defects in lipid classes associated with all stages of prostate cancer *in vitro*. Such knowledge could assist in the investigation of the molecular

mechanisms mediating lipidomic changes during the progression of prostate cancer progression. **Summary**

In summary, lipid dysregulation is a relevant factor in the etiology of many diseases. This includes metabolic disorders [215], respiratory conditions [216, 217], infectious diseases [218] and cancer [219, 220]. Studies integrating clinical information (patient response data, imaging and specimens) have revealed the complexity in certain cancers, such as PCa. For example, previous studies demonstrated changes in lipid features identified in prostate cancer patient samples and were correlated with poor prognosis [221-223]. Current knowledge has not yielded a clear insight into mechanism mediating these lipid changes in patient plasma or development of drug resistance in prostate cancer progression. Such a comparison may be extremely therapeutically useful as they would form the basis for a biomimetic model to non-invasively determine metastatic status. Such data would also aid in understanding the mechanisms mediating aberrant lipid modulation in cell in responses to therapeutic agents and facilitate the finding of new markers for drug resistant cancer progression.

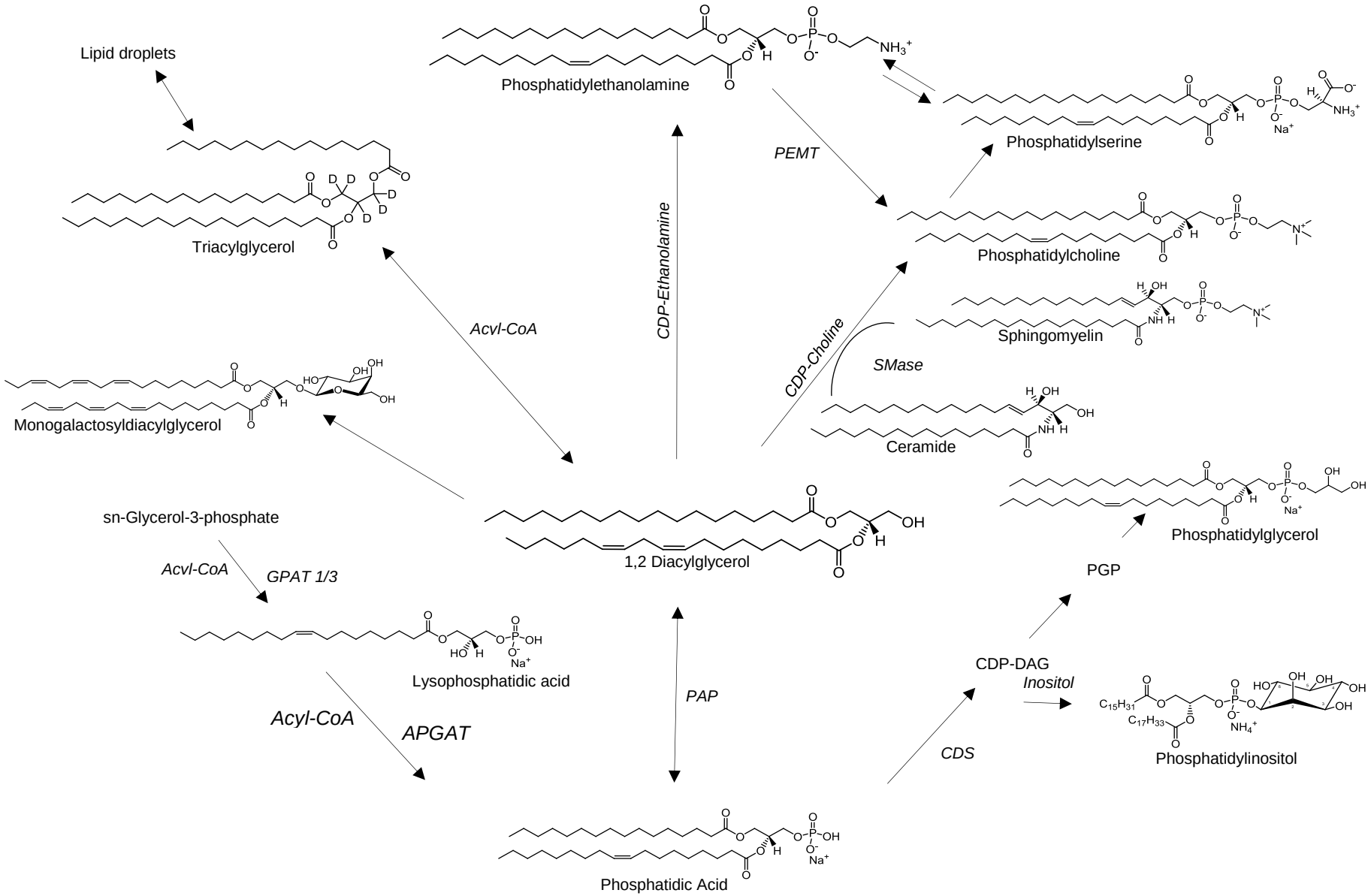

Fig 2.1. Lipid synthesis in prostate cancer cell progression Abbreviations: 1-acylglycerol-3-phosphate-O-acyltransferase, (AGPAT); Glycerol-3-phosphate acyltransferase, (GPAT); Phosphatidate phosphatase (PAP); Phosphatidylethanolamine N-methyltransferase (PEMT), Sphingomyelinase (SMase)

References

1. Wenk, M.R., *The emerging field of lipidomics.* Nature Reviews Drug Discovery, 2005. **4**: p. 594.

2. van Meer, G., D.R. Voelker, and G.W. Feigenson, *Membrane lipids: where they are and how they behave.* Nat Rev Mol Cell Biol, 2008. **9**(2): p. 112-24.

3. Gurr, M. and A. James, *Lipid biochemistry: an introduction.(eds.) Chapman & Hall, London.* 1971.

4. Lohiya, V., J.B. Aragon-Ching, and G. Sonpavde, *Role of Chemotherapy and Mechanisms of Resistance to Chemotherapy in Metastatic Castration-Resistant Prostate Cancer.* Clinical Medicine Insights. Oncology, 2016. **10**(Suppl 1): p. 57-66.

5. Fahy, E., et al., *Update of the LIPID MAPS comprehensive classification system for lipids.* J Lipid Res, 2009. **50 Suppl**: p. S9-14.

6. Kennedy, E.P., *Biosynthesis of complex lipids.* Fed Proc, 1961. **20**: p. 934-40.

7. Rysman, E., et al., *De novo lipogenesis protects cancer cells from free radicals and chemotherapeutics by promoting membrane lipid saturation.* Cancer Research, 2010. **70**: p. 8117-8126.

8. Kent, C., *Regulatory enzymes of phosphatidylcholine biosynthesis: a personal perspective.* Biochim Biophys Acta, 2005. **1733**(1): p. 53-66.

9. Kennedy, E.P. and S.B. Weiss, *The function of cytidine coenzymes in the biosynthesis of phospholipides.* J Biol Chem, 1956. **222**(1): p. 193-214.

10. Lands, W.E., *Metabolism of glycerolipides; a comparison of lecithin and triglyceride synthesis.* J Biol Chem, 1958. **231**(2): p. 883-8.

11. Shimizu, T., T. Ohto, and Y. Kita, *Cytosolic phospholipase A2: biochemical properties and physiological roles.* IUBMB Life, 2006. **58**(5-6): p. 328-33.

12. Schlame, M., D. Rua, and M.L. Greenberg, *The biosynthesis and functional role of cardiolipin.* Prog Lipid Res, 2000. **39**(3): p. 257-88.

13. Lands, W.E., *Stories about acyl chains.* Biochim Biophys Acta, 2000. **1483**(1): p. 1-14.

14. Sergeant, S., et al., *Phosphatidic acid regulates tyrosine phosphorylating activity in human neutrophils enhancement of Fgr activity.* Journal of Biological Chemistry, 2001. **276**(7): p. 4737-4746.

15. Rizzo, M.A., et al., *Phospholipase D and its product, phosphatidic acid, mediate agonist-dependent raf-1 translocation to the plasma membrane and the activation of the mitogen-activated protein kinase pathway.* J Biol Chem, 1999. **274**(2): p. 1131-9.

16. Olivera, A., J. Rosenthal, and S. Spiegel, *Effect of acidic phospholipids on sphingosine kinase.* Journal of cellular biochemistry, 1996. **60**(4): p. 529-537

.

17. Lim, H.-K., et al., *Phosphatidic acid regulates systemic inflammatory responses by modulating the Akt-mammalian target of rapamycin-p70 S6 kinase 1 pathway.* Journal of Biological Chemistry, 2003. **278**(46): p. 45117-45127.

18. Daaka, Y., *Mitogenic action of LPA in prostate.* Biochim Biophys Acta, 2002. **1582**(1-3): p. 265-9.

19. Kulkarni, P. and R.H. Getzenberg, *High-fat diet, obesity and prostate disease: the ATX-LPA axis?* Nat Clin Pract Urol, 2009. **6**(3): p. 128-31.

20. Terada, N., et al., *Cyr61 is regulated by cAMP-dependent protein kinase with serum levels correlating with prostate cancer aggressiveness.* Prostate, 2012. **72**(9): p. 966-76.

21. Yui, K., et al., *Eicosanoids Derived From Arachidonic Acid and Their Family Prostaglandins and Cyclooxygenase in Psychiatric Disorders.* Current neuropharmacology, 2015. **13**(6): p. 776-785.

22. MacDonald, J.I. and H. Sprecher, *Phospholipid fatty acid remodeling in mammalian cells.* Biochimica et Biophysica Acta (BBA)-Lipids and Lipid Metabolism, 1991. **1084**(2): p. 105-121.

23. Patel, D. and S.N. Witt, *Ethanolamine and Phosphatidylethanolamine: Partners in Health and Disease.* Oxidative medicine and cellular longevity, 2017. **2017**: p. 4829180-4829180.

24. Chu, Z., et al., *Targeting and cytotoxicity of SapC-DOPS nanovesicles in pancreatic cancer.* PloS one, 2013. **8**(10): p. e75507.

25. Wojton, J., et al., *Systemic delivery of SapC-DOPS has antiangiogenic and antitumor effects against glioblastoma.* Molecular Therapy, 2013. **21**(8): p. 1517-1525.

26. Zhao, S., et al., *SapC–DOPS nanovesicles as targeted therapy for lung cancer.* Molecular cancer therapeutics, 2015. **14**(2): p. 491-498.

27. Murray, N.R. and A.P. Fields, *Phosphatidylglycerol is a physiologic activator of nuclear protein kinase C.* Journal of Biological Chemistry, 1998. **273**(19): p. 11514-11520.

28. Murray, N., L. Thompson, and A. Fields, *Protein Kinase C Molecular Biology Intelligence Unit*. 1997, The role of protein kinase C in cellular proliferation and cell cycle ….

29. Reis, A., *Oxidative Phospholipidomics in health and disease: Achievements, challenges and hopes.* Free Radical Biology and Medicine, 2017. **111**: p. 25-37.

30. Fu, P. and K.G. Birukov, *Oxidized phospholipids in control of inflammation and endothelial barrier.* Translational Research, 2009. **153**(4): p. 166-176.

31. Ashraf, M.Z., N.S. Kar, and E.A. Podrez, *Oxidized phospholipids: Biomarker for cardiovascular diseases.* The International Journal of Biochemistry & Cell Biology, 2009. **41**(6): p. 1241-1244.

32. Maskrey, B.H., et al., *Mechanisms of Resolution of Inflammation.* Arteriosclerosis, Thrombosis, and Vascular Biology, 2011. **31**(5): p. 1001-1006.

33. Salomon, R.G. and A. Bhatnagar, *Structural Identification and Cardiovascular Activities of Oxidized Phospholipids.* Circulation Research, 2012. **111**(7): p. 930-946.

34. Miyazawa, T., et al., *Age-related change of phosphatidylcholine hydroperoxide and phosphatidylethanolamine hydroperoxide levels in normal human red blood cells.* Mechanisms of Ageing and Development, 1996. **86**(3): p. 145-150.

35. Adachi, J., et al., *Plasma phosphatidylcholine hydroperoxide as a new marker of oxidative stress in alcoholic patients.* Journal of Lipid Research, 2004. **45**(5): p. 967-971.

36. Hui, S.-P., et al., *An improved HPLC assay for phosphatidylcholine hydroperoxides (PCOOH) in human plasma with synthetic PCOOH as internal standard.* Journal of Chromatography B, 2007. **857**(1): p. 158-163.

37. Jónasdóttir, H.S., et al., *Detection and Structural Elucidation of Esterified Oxylipids in Human Synovial Fluid by Electrospray Ionization-Fourier Transform Ion-Cyclotron Mass Spectrometry and Liquid Chromatography-Ion Trap-MS3: Detection of Esterified Hydroxylated Docosapentaenoic Acid Containing Phospholipids.* Analytical Chemistry, 2013. **85**(12): p. 6003-6010.

38. Gruber, F., et al., *Photooxidation generates biologically active phospholipids that induce heme oxygenase-1 in skin cells.* Journal of Biological Chemistry, 2007. **282**(23): p. 16934-16941.
39. Birukova, A.A., et al., *Signaling pathways involved in OxPAPC-induced pulmonary endothelial barrier protection.* Microvascular research, 2007. **73**(3): p. 173-181.

40. Stemmer, U., et al., *Toxicity of oxidized phospholipids in cultured macrophages.* Lipids in health and disease, 2012. **11**(1): p. 110.

41. Thimmulappa, R.K., et al., *Oxidized phospholipids impair pulmonary antibacterial defenses: evidence in mice exposed to cigarette smoke.* Biochemical and biophysical research communications, 2012. **426**(2): p. 253-259.

42. Halasiddappa, L.M., et al., *Oxidized phospholipids induce ceramide accumulation in RAW 264.7 macrophages: role of ceramide synthases.* PLoS One, 2013. **8**(7): p. e70002.

43. Koller, D., et al., *Effects of oxidized phospholipids on gene expression in RAW 264.7 macrophages: a microarray study.* PloS one, 2014. **9**(10): p. e110486.

44. Hoff, H.F., et al., *Phospholipid hydroxyalkenals: biological and chemical properties of specific oxidized lipids present in atherosclerotic lesions.*
Arteriosclerosis, thrombosis, and vascular biology, 2003. **23**(2): p. 275-282.

45. Kamido, H., et al., *Core aldehydes of alkyl glycerophosphocholines in atheroma induce platelet aggregation and inhibit endothelium-dependent arterial relaxation.* Journal of lipid research, 2002. **43**(1): p. 158-166.

46. Ravandi, A., et al., *Phospholipids and oxophospholipids in atherosclerotic plaques at different stages of plaque development.* Lipids, 2004. **39**(2): p. 97-109.

47. Hammad, L.A., et al., *Elevated levels of hydroxylated phosphocholine lipids in the blood serum of breast cancer patients.* Rapid Communications in Mass Spectrometry: An International Journal Devoted to the Rapid Dissemination of Up-to-the-Minute Research in Mass Spectrometry, 2009. **23**(6): p. 863-876.

48. Kinoshita, M., et al., *Age-related increases in plasma phosphatidylcholine hydroperoxide concentrations in control subjects and patients with hyperlipidemia.* Clinical chemistry, 2000. **46**(6): p. 822-828.

49. Akasaka, K., et al., *Automatic determination of hydroperoxides of phosphatidylcholine and phosphatidylethanolamine in human plasma.* Journal of Chromatography B: Biomedical Sciences and Applications, 1995. **665**(1): p. 37-43.

50. Rolla, R., et al., *Antibodies against oxidized phospholipids in laboratory tests exploring lupus anti-coagulant activity.* Clinical & Experimental Immunology, 2007. **149**(1): p. 63-69.

51. Matt, U., et al., *Accumulating evidence for a role of oxidized phospholipids in infectious diseases.* Cellular and molecular life sciences, 2015. **72**(6): p. 1059-1071.

52. Cruz, D., et al., *Host-derived oxidized phospholipids and HDL regulate innate immunity in human leprosy.* The Journal of clinical investigation, 2008. **118**(8): p. 2917-2928.

53. O'Donnell, V.B. and R.C. Murphy, *New families of bioactive oxidized phospholipids generated by immune cells: identification and signaling actions.* Blood, 2012. **120**(10): p. 1985-1992.

54. Stübiger, G., et al., *Targeted profiling of atherogenic phospholipids in human plasma and lipoproteins of hyperlipidemic patients using MALDI-QIT-TOF-MS/MS.* Atherosclerosis, 2012. **224**(1): p. 177-186.

55. Frey, B., et al., *Increase in fragmented phosphatidylcholine in blood plasma by oxidative stress.* Journal of lipid research, 2000. **41**(7): p. 1145-1153.

56. Podrez, E.A., et al., *Platelet CD36 links hyperlipidemia, oxidant stress and a prothrombotic phenotype.* Nature medicine, 2007. **13**(9): p. 1086.

57. Korotaeva, A.A., et al., *Oxidized phosphatidylcholine stimulates activity of secretory phospholipase A2 group IIA and abolishes sphingomyelin-induced inhibition of the enzyme.* Prostaglandins & other lipid mediators, 2010. **91**(1-2): p. 38-41.

58. Ramprecht, C., et al., *Toxicity of oxidized phosphatidylcholines in cultured human melanoma cells.* Chemistry and physics of lipids, 2015. **189**: p. 39-47.

59. Bochkov, V., et al., *Oxidized Phospholipids Stimulate Angiogenesis Via Autocrine Mechanisms, Implicating a Novel Role for Lipid Oxidation in the Evolution of Atherosclerotic Lesions*. Vol. 99. 2006. 900-8.

60. T Reddy, S., et al., *Identification of genes induced by oxidized phospholipids in human aortic endothelial cells*. Vol. 38. 2002. 211-8.

61. Oskolkova, O.V., et al., *ATF4-dependent transcription is a key mechanism in VEGF up-regulation by oxidized phospholipids: critical role of oxidized sn-2 residues in activation of unfolded protein response.* Blood, 2008. **112**(2): p. 330-339.

62. Blüml, S., et al., *The Oxidation State of Phospholipids Controls the Oxidative Burst in Neutrophil Granulocytes.* The Journal of Immunology, 2008. **181**(6): p. 4347-4353.

63. Gao, D., et al., *Structural Basis for the Recognition of Oxidized Phospholipids in Oxidized Low Density Lipoproteins by Class B Scavenger Receptors CD36 and SR-BI.* Journal of Biological Chemistry, 2010. **285**(7): p. 4447-4454.

64. Boullier, A., et al., *The Binding of Oxidized Low Density Lipoprotein to Mouse CD36 Is Mediated in Part by Oxidized Phospholipids That Are Associated with Both the Lipid and Protein Moieties of the Lipoprotein.* Journal of Biological Chemistry, 2000. **275**(13): p. 9163-9169.

65. Karupaiah, T. and K. Sundram, *Effects of stereospecific positioning of fatty acids in triacylglycerol structures in native and randomized fats: a review of their nutritional implications.* Nutrition & metabolism, 2007. **4**(1): p. 16.

66. Dircks, L. and H.S. Sul, *Acyltransferases of de novo glycerophospholipid biosynthesis.* Prog Lipid Res, 1999. **38**(5-6): p. 461-79.

67. Weiss, S.B., E.P. Kennedy, and J.Y. Kiyasu, *The enzymatic synthesis of triglycerides.* Journal of Biological Chemistry, 1960. **235**(1): p. 40-44.

68. Coleman, R.A. and D.P. Lee, *Enzymes of triacylglycerol synthesis and their regulation.* Progress in lipid research, 2004. **43**(2): p. 134-176.

69. Wei, L., et al., *A case-control study on the association between serum lipid level and the risk of breast cancer.* Zhonghua yu fang yi xue za zhi [Chinese journal of preventive medicine], 2016. **50**(12): p. 1091-1095.

70. Ogretmen, B. and Y.A. Hannun, *Biologically active sphingolipids in cancer pathogenesis and treatment.* Nature Reviews Cancer, 2004. **4**(8): p. 604.

71. Ogretmen, B., *Sphingolipids in cancer: regulation of pathogenesis and therapy.* FEBS letters, 2006. **580**(23): p. 5467-5476.

72. Ryland, L.K., et al., *Dysregulation of sphingolipid metabolism in cancer.* Cancer biology & therapy, 2011. **11**(2): p. 138-149.

73. Fyrst, H. and J.D. Saba, *An update on sphingosine-1-phosphate and other sphingolipid mediators.* Nat Chem Biol, 2010. **6**(7): p. 489-97.

74. Maula, T., et al., *Importance of the sphingoid base length for the membrane properties of ceramides.* Biophysical journal, 2012. **103**(9): p. 1870-1879.

76. Ponnusamy, S., et al., *Sphingolipids and cancer: ceramide and sphingosine-1-phosphate in the regulation of cell death and drug resistance.* Future oncology (London, England), 2010. **6**(10): p. 1603-1624.

77. Taha, T.A., T.D. Mullen, and L.M. Obeid, *A house divided: ceramide, sphingosine, and sphingosine-1-phosphate in programmed cell death.* Biochim Biophys Acta, 2006. **1758**(12): p. 2027-36.

78. Ogretmen, B. and Y.A. Hannun, *Biologically active sphingolipids in cancer pathogenesis and treatment.* Nat Rev Cancer, 2004. **4**(8): p. 604-16.

79. Wang, X.-Z., et al., *Aberrant Sphingolipid Signaling Is Involved in the Resistance of Prostate Cancer Cell Lines to Chemotherapy.* Cancer Research, 1999. **59**(22): p. 5842-5848.

80. García-Barros, M., et al., *Sphingolipids in colon cancer.* Biochimica et biophysica acta, 2014. **1841**(5): p. 773-782.

81. Karahatay, S., et al., *Clinical relevance of ceramide metabolism in the pathogenesis of human head and neck squamous cell carcinoma (HNSCC): attenuation of C(18)-ceramide in HNSCC tumors correlates with lymphovascular invasion and nodal metastasis.* Cancer Lett, 2007. **256**(1): p. 101-11.

82. Schiffmann, S., et al., *Ceramide synthases and ceramide levels are increased in breast cancer tissue.* Carcinogenesis, 2009. **30**(5): p. 745-52.

83. Pralhada Rao, R., et al., *Sphingolipid metabolic pathway: an overview of major roles played in human diseases.* Journal of lipids, 2013. **2013**: p. 178910-178910.

84. Modrak, D.E., D.V. Gold, and D.M. Goldenberg, *Sphingolipid targets in cancer therapy.* Molecular Cancer Therapeutics, 2006. **5**(2): p. 200-208.

85. Lemonnier, L.A., et al., *Sphingomyelin in the suppression of colon tumors: prevention versus intervention.* Arch Biochem Biophys, 2003. **419**(2): p. 129-38.

86. Al Sazzad, M.A., et al., *The Long-Chain Sphingoid Base of Ceramides Determines Their Propensity for Lateral Segregation.* Biophysical journal, 2017. **112**(5): p. 976-983.

87. Dillehay, D.L., et al., *Dietary sphingomyelin inhibits 1,2-dimethylhydrazine-induced colon cancer in CF1 mice.* J Nutr, 1994. **124**(5): p. 615-20.

88. Mehta, S., et al., *Combined cytotoxic action of paclitaxel and ceramide against the human Tu138 head and neck squamous carcinoma cell line.* Cancer Chemother Pharmacol, 2000. **46**(2): p. 85-92.

89. Schmelz, E.M., et al., *Colonic cell proliferation and aberrant crypt foci formation are inhibited by dairy glycosphingolipids in 1, 2-dimethylhydrazine-treated CF1 mice.* J Nutr, 2000. **130**(3): p. 522-7.

90. Onodera, T., et al., *Phosphatidylethanolamine plasmalogen enhances the inhibiting effect of phosphatidylethanolamine on γ-secretase activity.* The Journal of Biochemistry, 2014. **157**(5): p. 301-309.

91. Braverman, N.E. and A.B. Moser, *Functions of plasmalogen lipids in health and disease.* Biochim Biophys Acta, 2012. **1822**(9): p. 1442-52.

92. Hu, C., M. Wang, and X. Han, *Shotgun lipidomics in substantiating lipid peroxidation in redox biology: Methods and applications.* Redox Biol, 2017. **12**: p. 946-955.

93. Wallner, S. and G. Schmitz, *Plasmalogens the neglected regulatory and scavenging lipid species.* Chem Phys Lipids, 2011. **164**(6): p. 573-89.

94. Fuchs, B., *Analytical methods for (oxidized) plasmalogens: Methodological aspects and applications.* Free Radic Res, 2015. **49**(5): p. 599-617.

95. Maeba, R., et al., *Chapter Two - Plasma/Serum Plasmalogens: Methods of Analysis and Clinical Significance*, in *Advances in Clinical Chemistry*, G.S. Makowski, Editor. 2015, Elsevier. p. 31-94.

96. Maeba, R., et al., *Plasma/Serum Plasmalogens: Methods of Analysis and Clinical Significance.* Adv Clin Chem, 2015. **70**: p. 31-94.

97. Han, X., *Lipidomics for studying metabolism.* Nat Rev Endocrinol, 2016. **12**(11): p. 668-679.

98. Mankidy, R., et al., *Membrane plasmalogen composition and cellular cholesterol regulation: a structure activity study.* Lipids Health Dis, 2010. **9**: p. 62.

99. Brites, P., H.R. Waterham, and R.J. Wanders, *Functions and biosynthesis of plasmalogens in health and disease.* Biochim Biophys Acta, 2004. **1636**(2-3): p. 219-31.

100. Fhaner, C.J., et al., *Functional group selective derivatization and gas-phase fragmentation reactions of plasmalogen glycerophospholipids.* Mass Spectrometry, 2013. **2**(Special_Issue): p. S0015-S0015.

101. Gerbig, S., et al., *Analysis of colorectal adenocarcinoma tissue by desorption electrospray ionization mass spectrometric imaging.* Analytical and bioanalytical chemistry, 2012. **403**(8): p. 2315-2325.

102. Lv, J., et al., *Plasma Content Variation and Correlation of Plasmalogen and GIS, TC, and TPL in Gastric Carcinoma Patients: A Comparative Study.* Medical science monitor basic research, 2015. **21**: p. 157-160.

103. Kunkel, G.T., et al., *Targeting the sphingosine-1-phosphate axis in cancer, inflammation and beyond.* Nature reviews. Drug discovery, 2013. **12**(9): p. 688-702.

104. Wang, D. and R.N. Dubois, *Eicosanoids and cancer.* Nature reviews. Cancer, 2010. **10**(3): p. 181-193.

105. Nakanishi, M. and D.W. Rosenberg. *Multifaceted roles of PGE 2 in inflammation and cancer*. in *Seminars in immunopathology*. 2013. Springer.

106. Asgari, Y., et al., *Alterations in cancer cell metabolism: the Warburg effect and metabolic adaptation.* Genomics, 2015. **105**(5-6): p. 275-81.

107. Santos, C., et al., *Lipid metabolism in cancer.* FEBS Journal, 2012. **279**: p. 2610-2623.

108. Dueregger, A., et al., *Differential Utilization of Dietary Fatty Acids in Benign and Malignant Cells of the Prostate.* PLoS One, 2015. **10**(8): p. e0135704.

109. Twum-Ampofo, J., et al., *Metabolic targets for potential prostate cancer therapeutics.* Curr Opin Oncol, 2016. **28**(3): p. 241-7.

110. Ngo, D.C., et al., *Introduction to the molecular basis of cancer metabolism and the Warburg effect.* Mol Biol Rep, 2015. **42**(4): p. 819-23.

111. Medes, G., A. Thomas, and S. Weinhouse, *Metabolism of neoplastic tissue. IV. A study of lipid synthesis in neoplastic tissue slices in vitro.* Cancer Res, 1953. **13**(1): p. 27-9.

112. Ookhtens, M., et al., *Liver and adipose tissue contributions to newly formed fatty acids in an ascites tumor.* Am J Physiol, 1984. **247**(1 Pt 2): p. R146-53.

113. Eidelman, E., et al., *The Metabolic Phenotype of Prostate Cancer.* Frontiers in oncology, 2017. **7**: p. 131-131.

114. Srihari, S., et al., *Metabolic deregulation in prostate cancer.* Mol Omics, 2018. **14**(5): p. 320-329.

115. Perona, J.S., *Membrane lipid alterations in the metabolic syndrome and the role of dietary oils*. 2017, Elsevier.

116. Hidalgo, A., A. Cruz, and J. Pérez-Gil, *Pulmonary surfactant and nanocarriers: toxicity versus combined nanomedical applications.* Biochimica et Biophysica Acta (BBA)-Biomembranes, 2017. **1859**(9): p. 1740-1748.

117. Echaide, M., et al., *Restoring pulmonary surfactant membranes and films at the respiratory surface.* Biochimica et Biophysica Acta (BBA)-Biomembranes, 2017. **1859**(9): p. 1725-1739.

118. Dumas, F. and E. Haanappel, *Lipids in infectious diseases–the case of AIDS and tuberculosis.* Biochimica et Biophysica Acta (BBA)-Biomembranes, 2017. **1859**(9): p. 1636-1647.

119. Fuentes, N.R., et al., *Emerging role of chemoprotective agents in the dynamic shaping of plasma membrane organization.* Biochimica et Biophysica Acta (BBA)-Biomembranes, 2017. **1859**(9): p. 1668-1678.

120. Ríos-Marco, P., et al., *Alkylphospholipids: An update on molecular mechanisms and clinical relevance*. 2017, Elsevier.

121. Baker, M.J., et al., *FTIR-based spectroscopic analysis in the identification of clinically aggressive prostate cancer.* Br J Cancer, 2008. **99**(11): p. 1859-66.

122. Zhou, X., et al., *Identification of plasma lipid biomarkers for prostate cancer by lipidomics and bioinformatics.* PLoS One, 2012. **7**(11): p. e48889.

123. Sorvina, A., et al., *Lipid profiles of prostate cancer cells.* Oncotarget, 2018. **9**(85): p. 35541-35552.

CHAPTER 3

LIPID ALTERATIONS ASSOCIATED WITH PROSTATE CANCER CELL TYPES

Lishann M. Ingram, Maryam Mansoura, Chau Chou, Brian S. Cummings. **To be submitted to Oncogene**

Abstract

The association of circulating lipids with clinical outcomes of drug-resistant castration-resistant prostate cancer (CRPC) is not fully understood. While it is known that increases in select lipids correlates to decreased survival, neither the mechanisms mediating these alterations nor the correlation of resistance to treatments are well characterized. We addressed this gap-in-knowledge using *in vitro* models of non-cancerous, hormone-sensitive, CRPC and drug-resistant cell lines combined with quantitative HPLC-ESI-Orbitrap-MS lipidomic analysis. A total of 7,460 features were identified as being dysregulated between the cell lines studied, and 21 lipid species were significantly altered in drug-resistant cell lines as compared to non-resistant cell lines. Docetaxel resistance cells (PC3-Rx and DU145-DR) and media from these cells had higher levels of oxidized lipid species, phosphatidylcholine (PC), phosphatidylethanolamine (PE), and sphingomyelin (SM) as compared to parent control cells (PC-3 and DU-145). Subsequent validation assays using MS/MS fragmentation identified 83 lipids whose levels differed in Docetaxel resistant cells as compared to parent controls cells. Twelve of these lipids, were previously identified as being increased in the plasma of prostate cancer patients or other metastatic tumors. These data suggest that the lipidomic profiles of prostate cancer cell lines recapitulate lipidomic profiles in the plasma of prostate cancer patients. These data also identify novel lipids whose levels may correlate to Docetaxel sensitivity and progression of prostate cancer. Overall, our study highlights the power of using comprehensive lipidomic approaches to identify indicators and underlying mechanisms in Docetaxel resistance cells.

Introduction

Prostate cancer is one of the most prevalent cancers diagnosed among men in the United States. Although reports have shown that taxane-mediated microtubule stabilization differentially affects the androgen receptor, Docetaxel, a first-line chemotherapy for metastatic CRPC, has a known associated mechanism of resistance. While the mechanisms linking the role of lipids and drug-resistant prostate cancer cells is unclear, several studies propose that unbalanced cellular lipid composition and quantity may cause alterations in cellular functions that contribute drug resistance [224]. Despite these studies, there are limited studies demonstrating links between lipid levels and poor prognosis. Even fewer studies exist demonstrating links between lipids and drug resistance. However, recent studies demonstrated an association between plasma lipids and CRPC patient prognosis from a phase I discovery cohort, resulting in a proposed prognostic three-lipid signature of ceramide, sphingomyelin and phosphatidylcholine (PC) [225, 226]. These data are encouraging, but the mechanisms mediating these lipid alterations are not known.

While some studies suggest that links exist between select lipids in plasma and drug resistance in prostate cancer, the molecular mechanisms mediating these changes are not known. One barrier to addressing this gap in knowledge is that it's not known if similar changes in lipids occur in *in vitro* models of prostate cancer. Establishing the lipid changes seen in prostate cancer patients *in vivo* are recapitulated *in vitro* will provide models for not only understanding the molecular mechanism mediating lipid changes in prostate cancer, but also allow for identification of additional indicators of cancer cell progression and/or drug resistance.

Toward the above goal we utilized an *in vitro* panel of diverse prostate cancer cells that included non-cancerous, hormone sensitive, CRPC and drug-resistant cell lines. We used both an untargeted shotgun approach (ESI-MS) and quantitative HPLC- ESI-Orbitrap-MS lipidomic analysis to determine the differential levels of lipids in these cells. To our knowledge, these studies represent the most comprehensive identification of difference in lipid profiles in drug-resistant prostate cancer cell lines, castration-resistant and hormone-sensitive cells and corresponding media.

Materials and Methods

Cell Culture

PC-3, LNCaP, 22RV-1, DU-145, RWPE1 and PNT2 cell lines were purchased from ATCC (Manassas, VA). The Docetaxel resistant human DU145-DR cell line was acquired from Dr. Begona Mellado's laboratory in the Medical Oncology Department, Hospital Clinic de Barcelona, Spain. The Docetaxel resistant human PC3-Rx cell line was acquired from Dr. LG Horvath's laboratory in the Garvan Institute of Medical Research in Darlinghurst, Australia. Cell supplements, including antibiotics and primary cell culture media, were purchased from ATCC (Manassas, VA). Standard cell culture media were purchased from Corning Inc (Corning, NY). Human prostate cancer cells were cultured in 10% FBS (Seradigm, Radnor, PA) and 1% penicillin/streptomycin supplemented RPMI-1640, respectively. All cells were incubated in 95% humidity and 5% CO_2 at 37°C. Docetaxel resistant cell lines maintained resistance by receiving a range of nM concentrations of Docetaxel at every 2^{nd} and 4^{th} passage. Docetaxel dose response curves were consistently generated to check resistant levels using MTT assays **(Supplemental Figure 3.2).**

Bligh-Dyer Lipid extraction

Media from cells were collected followed by centrifugation. Cells were washed twice and harvested in 1x phosphate buffered saline (PBS), followed by centrifugation. Phospholipids from both cells and media were immediately extracted using chloroform and methanol according to the method of Bligh and Dyer [227]. Briefly, cell lines and

media were suspended in 3 ml of methanol and 3 ml of chloroform. Tubes were vortexed for 30 s, allowed to sit for 10 min on ice, centrifuged (300 x *g*; 5 min), and the bottom chloroform layer was transferred to a new test tube and spiked with a commercial mix of SPLASH Lipidomix internal standards (Avanti Polar Lipids, Inc.). SPLASH Lipidomix Mass Spec standards includes all major lipid classes at ratios similar to that found in human plasma. The extraction procedure was repeated three times and the chloroform layers combined. The collected chloroform layers were dried under nitrogen, reconstituted with 50 µl of methanol: chloroform (3:1 v/v), and stored at 80ºC until analysis.

Liquid Phosphorus Assay

Lipid content was quantified by determining the level of inorganic phosphorus using the Bartlett Assay [228].

Sulfuric acid 400 µl (5M) was added to lipid extracts (10 µL) in a glass test tube, and heated at 180-200ºC for 1 h. H_2O_2 (100 µl of 30 % v/v) was then added while vortexing, and heated at 180-200ºC for 1.5 h. Reagent (4.6 ml of 1.1 g ammonium molybdate tetrahydrate in 12.5 ml sulfuric acid in 500 ml ddH_20) was added followed by vortexing, which was followed by addition of 100 µl of 15% ascorbic acid (v/v), and further vortexing. The solution was heated for 7-10 min at 100ºC, and a 150 µl aliquot was used to measure the absorbance at 830 nm.

ESI-MS/MS Analysis of Cells and Media

Lipid extracts (500 pmol/µl) were prepared by reconstitution in chloroform: methanol (2:1, v/v). ESI-MS was performed as previously described [229-231] using a LCQ Deca ion-mass spectrometer (LCQ Finnigan mass spectrometer (Thermo Fisher-Fenning Institute, CA)) with a nitrogen drying gas flow-rate of 81/min at 350 ºC and a nebulizer pressure of 30 psi. The scanning range was from 200 to 1000 *m/z* on 5 µl of the samples scanned in positive and negative mode for 2.5 min with a mobile phase of acetonitrile; methanol; water (2:3:1) in 0.1% ammonium formate. Samples were run in triplicate (n=3) and overlap of confident identifications or most abundant species was defined as the core lipid pool [232].

NanoHRLC-LTQ-Orbitrap MS

Lipid extracts were also analyzed by using a high resolution LC linear ion trap-Orbitrap Hybrid MS" (nanoHRLC-LTQ-Orbitrap MS) (Thermo Scientific, San Jose, CA). Individuals running samples were blinded to sample conditions. Mass spectra were acquired in the positive ion mode. Mass spectrometric parameters for lipid extracts were as follows: spray voltage: 3.5/2.5 kV, sheath gas: 40/35 AU; auxiliary nitrogen pressure: 15 AU; sweep gas: 1/0 AU; ion transfer tube and vaporizer temperatures: 325 and 300/275°C, respectfully. Full scan, data-dependent MS/MS (top10-ddMS2), and data-independent acquisition were collected at *m/z* 150–2000, corresponding to the mass range of most expected cellular lipids. External calibration was applied before each run to allow for LC-HRMS analysis at 120,000 resolution (at *m/z* 200).

Lipids were separated on a nanoC18 column (length, 130 mm; i.d., 100 µm; particle size, 5 µm; pore size, 150 Å; max flow rate, 500 nL/min; packing material, Bruker Micron Magic 18). Mobile phase A was 0.1% formic acid/water; mobile phase B was 0.1% formic acid/acetonitrile. 10 µL of each sample was injected for analysis. A constant flow rate of 500 nL/min was applied to perform a gradient profiling with the following proportional change of solvent A (v/v): 0 to 1.5 min at 98% A, 1.5 to 15.0 min from 98% to 75% A, 15.0 to 20.0 min from 75% to 40% A, 20.0 to 25.0 min from 40% to 5% A, 25.0 to 28.0 min kept at 5% A, and 28.0 to 30.0 min from 5% to 98% A. The washing elution ended with a 4 min re-equilibration. The LTQ-Orbitrap Elite MS was set in the positive full scan mode within range of 50 to 1500 m/z. Settings of the electrospray ionization were: heater temperature of 300°C, sheath gas of 35 arbitrary unit, auxiliary gas of 10 arbitrary unit, capillary temperature of 350°C, and source voltage of +3.0 kV. MS/MS fragmentation was induced using a collision-induced dissociation [233] scan with a Fourier transform resolving power of 120,000 (transient = 192 ms; scan repetition rate = 4 Hz) at 400 m/z over 50–1500 m/z [234]. The autosampler temperature was maintained at 4°C for all experiments. Solvent extraction blanks and samples were jointly analyzed over the course of a batch (10–15 samples).

Data Processing

Full scan raw data files were acquired from Xcalibur™ (Thermo Fisher Scientific), centroided and converted to a useable format (mzXML) using MSConvert. Data processing and peak area integration were performed using MZmine [235], and XCMS [236], resulting in a feature intensity table. Feature tables and MS/MS data were placed

into a directory for each substrate analyzed. Each folder contained each sample type, feature tables end in “pos.csv” for positive mode. LipidMatch developed by Koelmel et al [237] was used to identify features. Peak areas were normalized to a mixture of deuterium labeled internal standards for each sample (SPLASH® LIPIDOMIX® Mass Spec Standard.

Multivariate Statistical Analysis of Cells and Media

Multivariate principal component analysis (PCA) was performed using MetaboAnalyst 3.0 (http://www.metaboanalyst.ca/). Automatic peak detection and spectrum deconvolution was performed using a peak width set to 0.5. Analysis parameters consisted of interquartile range filtering and sum normalization with no removal of outliers from the dataset. Features were selected based on volcano plot analysis and were further identified using MS/MS analysis. Significance for volcano plot analysis was determined based on a fold-change threshold of 2.00 and $p \leq 0.05$. Following identification, total ion count was used to normalize each parent lipid level, and the change in the relative abundance of that phospholipid species as compared to its control was determined. This method is standard for lipidomic analysis as reported in our previous studies [231, 238].

Statistical Analyses

All statistical analyses were compiled using GraphPad Prism for windows version 8.2.1 (GraphPad Software, Inc., La Jolla, CA). For all analysis, the experimental unit was individual samples obtained from a minimum of 4 groups were assessed. One passage

of cells was equivalent to one group of sample (n). We controlled for the effect of multiple testing by measuring the statistical significance of each association using both the *p* value and the *q* value. Using a FDR of $q < 0.05$, the *q* value quantifies significance in terms of the false discovery rate (FDR) rather than the false positive rate and forms a measure of how likely a particular *p* value is to represent a genuine association (**Supplemental Table 3.2-3.4**). For all analyses, significance was set at $p \leq 0.05$ where data are expressed as mean ± SEM based on t-test for pairwise analysis and/or ANOVA analysis (with Kruskal-Wallis *post hoc* test).

Results

Positive ion ESI-MS analysis

LC-ESI-MS/MS was performed on total lipid extracts prepared from a panel of normal (non-malignant) PNT2 and RWPE1 cells and six prostate cancer cell lines, LNCaP, 22RV1, PC-3, DU-145, PC3-Rx and DU145-DR (**Table 3.1**). The positive ion ESI mass spectra exhibited ions in the range of 200-1000 *m/z* (**Figure 3.1**). All samples were analyzed by direct infusion ESI-MS method. Representative ESI-MS spectra showed visual differences in the relative intensities of lipid species among non-cancerous (**Figure 3.1A**), hormone-sensitive (**Figure 3.1B**), CRPC-bone metastasized (**Figure 3.1C**) and CRPC-brain derived (**Figure 3.1D**) cell lines.

Supervised orthogonal projections to latent structures discriminant analysis (OPLS-DA) model was performed on hormone-sensitive and castration-resistant cell-lines and compared to control non-cancerous cells[239, 240]. This analysis separates the X variable into two parts for better interpretation; 1) linear relationship with Y and 2) unrelated to Y[241]. OPLS-DA comparing hormone-sensitive cell-lines to control cells in the positive mode (ESI+) showed distinct separation of each prostate cell line (**Figure 3.2A**). This is further demonstrated in **Figure 3.2B**, which presents a cloud plot demonstrating directional fold changes, significance, retention times and *m/z* values. This analysis identified 84 altered lipidomic features altered between hormone-sensitive cells as compared to normal cells. These lipids were also identified via heat map analysis (**Figure 3.2C**). This analysis demonstrated that phosphatidylcholine (PC, **Figure 3.3A**), PC plasmalogen (**Figure 3.3C**) sphingomyelin (SM, **Figure 3.4A**) and diacylglycerol (DAG, **Figure 3.6A**) were significantly augmented in hormone-sensitive cells relative to

non-cancerous control cells. However, oxidized-PC (**Figure 3.3B**) and ceramide (**Figure 3.4B**) were less abundant relative to non-cancerous control cells.

Lipidomic Profiling of Castration-Resistant Prostate Cancer Cells

OPLS-DA showed clear separation between castration-resistant and non-cancerous prostate cancer cell lines (**Figure 3.6A**), suggesting differential lipidomic profiles with the cell types. This was supported by a cloud plot analysis (**Figure 3.6B**) that identified 45 lipids whose levels differed between castration-resistant cell-lines and non-cancer control cells. The relative abundance of each lipid species levels varied significantly across all samples identified in CRPC cell lines in comparison to normal cells (**Figure 3.6C**). Specific lipids included PC (**Figure 3.7A**) and PC plasmalogen (**Figure 3.7F)**.

Several lipid species were enriched in bone metastatic PC-3 cells, as compared to other cells. Among them were, lysophosphatidylcholine (LPC, **Figure 3.7B),** 20:4 LPC (**Figure 3.7C**), OxPC (**Figure 3.7D**), OxLPC (**Figure 3.7E**), phosphatidic acid (PA, **Figure 3.12A**), and phosphatidylglycerol (PG, **Figure 3.12B)**. In addition, **figure 3.8** depicts the relative abundance of phosphatidylethanolamine (PE). PE (**Figure 3.8A**) and LPE (**Figure 3.8B**) were augmented in both CRPC cell-lines, as compared to non-cancerous cells, as were OxPE (**Figure 3.8D**) and OxLPE (**Figure 3.8E**). Surprisingly, SM (**Figure 3.9A**), DAG (**Figure 3.11A**) and triacylglycerol (TAG, **Figure 3.11B**) all showed significant enrichment in DU-145 cells as compared to non-cancer cells. In contrast, Cer was not significantly altered in CRPC cells in comparison to non-cancer cells (**Figure 3.9B**).

Comprehensive LC-ESI-MS/MS Analysis between PCa Cancer Cells and Media

The above analysis compared changes in lipid species among cells representative of different states of prostate cancer (i.e. hormone sensitive, hormone insensitive, drug resistant, etc.). To validate these data, and to further analyze lipid changes, a comprehensive LC-ESI-MS/MS analysis was conducted comparing changes in lipid levels between hormone-sensitive, castration-resistant and drug resistant human prostate cancer cell lines in comparison to non-cancer cell lines and media isolated from cell culture. This resulted in the identification of 7,460 dysregulated ion features, encompassing 15 different lipid species (**Figure 3.12A**). This was supported by a cloud plot analysis (**Figure 3.12B)** that identified lipids whose levels were altered between all the cell lines and media analyzed. The lipid content in these matrixes were normalized using the peak area of the corresponding internal standard present (**Supplemental Figure 3.26**). Similar to the previous analysis, PC, LPC, OxLPC, PE, LPE, OxPE, SM, plasmalogen, TAG were enriched in PCa cancer cells and the media, as compared to non-cancer cells.

Alterations in PC Lipids

PC lipids were augmented in all six PCa cell lines analyzed, when compared to non-cancerous RWPE1 and PNT2 cells (**Figure 3.13A**). Amongst the PC lipids, 36:1 PC was significantly increased in both Docetaxel resistant cells types analyzed (**Figures 3.13B** and **D**). 12:0-24:1 PC was also identified as a dominant PC species (**Figure 3.15C**) in

these cells. Interestingly, 38:4 PC (**Figure 3.14A**) was significantly enriched in PC3-Rx cells, as compared to its content level in PC-3 parent and non-cancer control cells.

LPC were also augmented in PC-3 cells when compared to non-cancerous and hormone-sensitive cells. More specifically, 16:0 LPC (**Figure 3.15B**), 18:0 LPC (**Figure 3.15C**), and 20:4 LPC (**Figure 3.15D**) were the dominant species, that accounted for the increase in the cells, as compared to non-cancer cells.

Not surprisingly, the levels of oxidized PC (OxPC) showed similar trends in PC-3 as the LPC species. However, there was a significant enrichment of OxPC in the media from drug-resistant cells and hormone-sensitive (LNCaP) cells, when compared to the parent cells (PC-3 and DU-145) and relative to non-cancer control cells. (**Figure 3.16A**). OxLPC was also significantly enriched in LNCaP media, PC-3 cells, PC3-Rx cells and PC3-Rx media as compared to non-cancerous prostate cells (**Figure 3.16B**).

Alteration in PE Lipids

PE was significantly enriched in 22RV1, DU-145 and PC3Rx cells as compared to normal cells (**Figure 3.17**). 38:4 PE, identified as 18:0-20:4 PE, was the most dominant of the PE lipid species in PC3Rx cells, as compared to PC-3 parent control (**Figures 3.18A and B**). 8:0-18:4 PE levels were also increased in both drug-resistant PC3Rx media and PC-3 media as compared to PC3Rx cells and PC-3 cells. Similar trend were observed in DU145-DR media, in relation to corresponding parent control DU-145 media (**Figure 3.18C**). OxPE was significantly enriched in PC-3 and PC3Rx cells, as compared to non-cancerous cells (**Figure 3.19A**). 3:0 (CHO)-3:0 (CHO)+H was the dominant OxPE

identified in both drug-resistant cell lines, as compared to their corresponding parent controls (PC-3 and DU-145) and to non-cancerous cells(**Figure 3.19B**). LPE was significantly enriched in PC-3 cells and LNCaP media as compared to hormone-sensitive and non-cancerous cells (**Figure 3.20A**). 20:4 was a dominant LPE identified in DU145-DR media, in relation to corresponding parent control DU-145 media (**Figure 3.20B**).

Alterations in other Lipids

SM was significantly enriched in PC3-Rx cells as compared to PC-3 parent control and non-cancerous cells (**Figure 3.21A**). d10:0-24:1+H was the dominant SM species identified in PC3-Rx cells (**Figure 3.21B**). Although Cer was not significantly altered in PCa cells, Cer were significantly augmented in both drug-resistant PC3Rx and DU145-DR media as compared to PC3Rx cells and DU-145 cells. Not surprisingly, similar trends were observed in PC-3 media compared to PC-3 cells. Additionally Cer demonstrated significant enrichment in PC3Rx media as compared to PC-3 media (**Figure 3.22**). TAG were augmented in PC3-Rx cells, as compared to parent and non-cancerous cells (**Figure 3.23A**). More specifically, OxTAG was enriched in DU145-DR media as compared to DU145-DR cells (**Figure 3.23B**). Plasmalogen lipids were augmented in the drug-resistant cells, as compared to non-cancerous cells (**Figure 3.23**).

Discussion

Drug resistance in prostate cancer remains an un-solved challenge and is one of the primary drivers of low survivability among prostate cancer patients. Owing to the high complexity and diversity among lipid molecules, only a few attempts have been made to identify individual lipid species as biomarkers and therapeutic agents in various cancers. Further, no few attempts have been made for drug resistance in prostate cancer. Recent evidence suggests elevated plasma levels of phospholipids are associated with an increased risk of PCa [242]. Unfortunately, the mechanism(s) linking changes in lipid composition and drug resistance are not fully understood. A first step toward identifying any such mechanisms is to determine if the lipid changes identified in the plasma of prostate cancer patients can be recapitulated *in vitro*. As such we conducted comprehensive analysis of lipidomic difference in diverse range of prostate cells using both shotgun lipidomics (untargeted) and LC-ES-MS/MS (targeted) approaches.

Data from both untargeted and targeted analysis of the lipidome from human prostate cancer cell lines demonstrated significant differences between prostate cancer cells and non-cancerous control cells. ESI-MS/MS demonstrated the significant enrichment of three lipid classes (namely, PC, SM, Cer) in hormone-sensitive cells **(Supplemental Figure 3.3-3.6**) in comparison to normal control cells. This result is consistent with previous reports in plasma from prostate cancer patients [223, 225, 242]. Elevated concentrations of SM in plasma were previously reported in patients with PCa in comparison to the control group [243]. Other reports have found elevated levels of Cer [176, 177, 244]. These data suggest that sphingolipids have a potential role in regulating prostate cancer cells response to chemotherapy [179].

Data from this study also showed elevated levels of PC plasmalogen and DAG in hormone-sensitive cell lines, as opposed to non-cancerous control cells. To the best of our knowledge, an in increase in PC plasmalogen and DAG in these cells lines has not been previously reported. However, a previous study reported an increase in the levels of PC plasmalogen phospholipids in neoplastic human breast tissue as compared to benign tissue, and correlated this with metastatic properties of human cancer [245]. The significance of these data to prostate cancer progression or drug resistance is not known, but DAG is reported to promote cancer pathogenicity through stimulating protein kinase C pathways [246].

Our study also allowed us to compare change in lipids in media derived from individual cell types. Media derived from hormone-sensitive cell-lines had significantly elevated levels of PE as compared to media from non-cancerous control groups, specifically, elevated levels of 26:4 PE, OxLPE in media derived from hormone-sensitive (LNCaP cells). To our knowledge this is another novel finding, and these lipids may be novel indicators for early-stage prostate cancer.

The targeted analysis employed in our study validated the shotgun analysis. This analysis also added rigor as it used a secondary platform and additional extractions and sample. This comprehensive analysis demonstrated elevated levels of PC, PE, Plasmalogens, SM, Cer, PA, PG, DAG and TAG classes.

The increase in PC levels in PC-3 cells, but not in DU-145 cells mirrored data seen for LPC, OxPC and OxLPC levels in PC-3 cells. Elevated PC in plasma has been associated with prostate cancer progression. For example, a 20:4 LPC was suggested as top biomarker for prostate cancer [22]. LPC has also been shown to be elevated in tissues

exposed to radio/chemotherapy treatments [178, 180, 247]; however, it's not known if chemotherapy increased LPC levels, or if LPC was elevated prior to treatment [248]. Other reports have demonstrated that the LPC is increased in ovarian cancer patients and the fatty acid composition of this LPC is changed [249].

To our knowledge, these data are some of the first to report that OxPC and OxLPC are increased in castration-resistant cell-lines compared to non-cancerous control cells. Previous studies have reported the presence of oxidized-phospholipids in macrophages [141] and skin cells. The increase in oxidized PC and LPC may result from the increase in the parent lipids for these species, or it may reflect changes in the oxidative environment in the cells.

Our data also showed increased in PE. These data agree with the finding of increased in PE in patient plasma samples [222, 225], as well as in prostate cancer cells (LNCaP, 22RV1 and DU-145), as compared to PNT2 [223]. PE has also been detected in high abundance in exosomes derived from PC-3 cells [250]. Unlike previous study that reported no significant differences in LPE from plasma between PCa patients vs. controls [222], our data demonstrated elevated levels of PE plasmalogens in a castration-resistant cell-line (DU-145), as compared to non-cancerous control cells. Previous studies did compare PE plasmalogens in normal, benign and neoplastic samples from human prostate, breast, and lung tissues, and suggested that these are lipid tumor markers for distinguishing between benign vs. neoplastic tissue, and identifying *in-vivo* metastatic progression.

Two sphingolipid classes (PC-3 and DU-145) were significantly increased in the CRPC cell-lines as compared to the normal control prostate epithelial cell-line (RWPE1

or PNT2). Previous studies suggest that SM is increased in plasma from prostate cancer patients, and as such this lipids has investigated for its chemotherapeutic and chemo preventative potential [185, 186]. Another sphingolipid, Cer was reported to accumulate in patient plasma after chemotherapy treatment [179]. These data agree with studies showing that chemotherapeutics resistance may involve sphingolipid defects in apoptotic regulation. For example, etoposide and doxorubicin chemotherapeutics elevated ceramide during indication of cell death in leukemia cells [247]. Further, the combination of paclitaxel and tamoxifen increases ceramide and overcomes drug resistance in ovarian cancer [251]. Inhibition of *de novo* generation of ceramide also decreases the cellular response to cytotoxic agents [179].

Our data also identified several other glycerophospholipids (PA and PG) that were significantly elevated in PC-3, but not in DU-145 cells as compared to control (PNT2 and RWPE1). Although PA is present at low levels in most cell types, increased PA levels have been reported in glioblastoma [252]. The lower-levels of PA in brain-derived DU-145 could alter downstream signaling events. In other studies, PG was present at elevated levels in urinary exosomes of PCa patients compared to healthy controls [253], and also in renal cells and hepatocellular carcinomas [254, 255].

While this study represents one of the most comprehensive analysis of lipid composition in prostate cells to date, it is limited by the facts that the actual concentrations for lipid species were not provided. This was in part intentional and these data are meant to springboard further studies focusing on the specific lipids identified are being altered in these cells. Further, it important to point out that many of these lipids are rather novel

and do not have a suitable internal standard at this time. Future studies will focus on quantifying these specific lipids in these cells as well as validating their existence in human plasma.

These data, as well as previous studies demonstrates that there are fundamental differences between the lipidome of non-cancer and cancer cells [223, 256-258]. Non-cancer cells typically exhibit neutral total membrane charge due to the presence of zwitterionic phospholipids (PC and SM) on the outer leaflet of the membrane and PS and PE located in the inner leaflet of the membrane [259-261].Unlike normal cells, cancer cells typically lose their capacity to maintain asymmetrical distribution leading to abnormal exposure of (PS and PE) to the cells outer membrane and/or PC and SM to cytosolic leaflet causing changes in cell signaling and down-stream gene expression. The changes in the lipidome in our studies may reflect these changes. We performed pathway analysis to help narrow down and identify lipids of specific pathways of specific interest (see **Chapter 4**).

Conclusion

This study demonstrates that the lipidomic profiles of various hormone-sensitive, CRPC and drug-resistant PCa cell differ with regards to select lipids. Further, these data support the conclusion that changes in these lipidomic profiles mirror those reported in patient samples. The abundance of specific classes and subclasses of specific lipids (namely, SM, PC, PE, plasmalogen, TAG) in prostate cancer cells, as compared to non-tumorgenic cells reflects the heterogeneous nature of this disease. As such these cells may be useful tools to further understand mechanisms underlying changes in lipids in prostate cancer during progression and during the development of resistance. These

data also identify several novel lipids whose levels correlated to the stage of cancer and Docetaxel resistance. These data may be used to design screens of plasma from prostate cancer patients to identify novel biomarkers of progression and resistance.

Supplementary Materials

The following are available **Supplemental Table 3.5**: Lipid species in cancer models (Modified from [223]) **and Supplemental Table 3.6** PosID molecular species normalized (data not shown).

Author Contributions

L.M.I. and B.S.C. conceived and designed the experiments; L.M.I. and M.M. performed the experiments; L.M.I. and B.S.C. analyzed the data; B.S.C. contributed reagents/materials/analysis tools; L.M.I. and B.S.C. wrote the paper.

CONFLICT OF INTEREST

The authors declare no conflict of interest.

Acknowledgments: This project was supported in part with funds from the Department of Defense Prostate Cancer Research Program Idea Development Award (PC150431 GRANT11996600) to B.S.C. We gratefully acknowledge the UGA Proteomics and Mass

Spectrometry Core Facility, which was funded in part by NIH grant S10RR028859. We also want to thank Dr. Jun Zhou for guiding me in learning new programs for lipid analysis and Dr. Mandi Murph for the use of SpectraMax® series.

References

1. Karantanos, T., P.G. Corn, and T.C. Thompson, *Prostate cancer progression after androgen deprivation therapy: mechanisms of castrate resistance and novel therapeutic approaches.* Oncogene, 2013. **32**(49): p. 5501-5511.

2. Jemal, A., et al., *Cancer statistics, 2008.* CA Cancer J Clin, 2008. **58**(2): p. 71-96.

3. Chambers, S.K., et al., *Defining young in the context of prostate cancer.* Am J Mens Health, 2015. **9**(2): p. 103-14.

4. Siegel, R.L., K.D. Miller, and A. Jemal, *Cancer statistics, 2019.* CA: A Cancer Journal for Clinicians, 2019. **69**(1): p. 7-34.

5. Fontenot, P.A., Jr., et al., *Metastatic prostate cancer in the modern era of PSA screening.* Int Braz J Urol, 2017. **43**(3): p. 416-421.

6. Roobol, M.J., *Screening for prostate cancer: are organized screening programs necessary?* Transl Androl Urol, 2018. **7**(1): p. 4-11.

7. Salinas, C.A., et al., *Prostate cancer in young men: an important clinical entity.* Nat Rev Urol, 2014. **11**(6): p. 317-23.

8. Hiraoka, Y. and M. Akimoto, *Anatomy of the prostate from fetus to adult--origin of benign prostatic hyperplasia.* Urol Res, 1987. **15**(3): p. 177-80.

9. Humphrey, P.A., *Histopathology of Prostate Cancer.* Cold Spring Harb Perspect Med, 2017. **7**(10).

10. Bhavsar, A. and S. Verma, *Anatomic imaging of the prostate.* Biomed Res Int, 2014. **2014**: p. 728539.

11. Garraway, L.A., et al., *Intermediate basal cells of the prostate: in vitro and in vivo characterization.* Prostate, 2003. **55**(3): p. 206-18.

12. van Leenders, G.J. and J.A. Schalken, *Epithelial cell differentiation in the human prostate epithelium: implications for the pathogenesis and therapy of prostate cancer.* Crit Rev Oncol Hematol, 2003. **46 Suppl**: p. S3-10.

13. Man, Y.-G., et al., *Tumor-infiltrating immune cells promoting tumor invasion and metastasis: existing theories.* Journal of Cancer, 2013. **4**(1): p. 84-95.

14. Tchetgen, M.B., et al., *Ejaculation increases the serum prostate-specific antigen concentration.* Urology, 1996. **47**(4): p. 511-6.

15. Liu, A.Y. and L.D. True, *Characterization of prostate cell types by CD cell surface molecules.* Am J Pathol, 2002. **160**(1): p. 37-43.

16. Cary, K.C. and M.R. Cooperberg, *Biomarkers in prostate cancer surveillance and screening: past, present, and future.* Therapeutic advances in urology, 2013. **5**(6): p. 318-329.

17. Petrylak, D.P., et al., *Docetaxel and estramustine compared with mitoxantrone and prednisone for advanced refractory prostate cancer.* New England Journal of Medicine, 2004. **351**(15): p. 1513-1520.

18. Tannock, I.F., et al., *Docetaxel plus prednisone or mitoxantrone plus prednisone for advanced prostate cancer.* New England Journal of Medicine, 2004. **351**(15): p. 1502-1512.

19. de Bono, J.S., et al., *Abiraterone and increased survival in metastatic prostate cancer.* N Engl J Med, 2011. **364**(21): p. 1995-2005.

20. Parker, C., et al., *Alpha emitter radium-223 and survival in metastatic prostate cancer.* New England Journal of Medicine, 2013. **369**(3): p. 213-223.

21. Desouki, M., et al., *hZip2 and hZip3 zinc transporters are down regulated in human prostate adenocarcinomatous glands.* Molecular Cancer, 2007. **6**: p. 37.

22. Logothetis, C., et al., *Current perspectives on bone metastases in castrate-resistant prostate cancer.* Cancer Metastasis Rev, 2018. **37**(1): p. 189-196.

23. Merseburger, A.S., A. Alcaraz, and C.A. von Klot, *Androgen deprivation therapy as backbone therapy in the management of prostate cancer.* Onco Targets Ther, 2016. **9**: p. 7263-7274.

24. Boccon-Gibod, L., E. van der Meulen, and B.-E. Persson, *An update on the use of gonadotropin-releasing hormone antagonists in prostate cancer.* Therapeutic advances in urology, 2011. **3**(3): p. 127-140.

25. Wadosky, K.M. and S. Koochekpour, *Molecular mechanisms underlying resistance to androgen deprivation therapy in prostate cancer.* Oncotarget, 2016. **7**(39): p. 64447-64470.

26. Gamat, M. and D.G. McNeel, *Androgen deprivation and immunotherapy for the treatment of prostate cancer.* Endocrine-related cancer, 2017. **24**(12): p. T297-T310.

27. Montgomery, R.B., et al., *Maintenance of intratumoral androgens in metastatic prostate cancer: a mechanism for castration-resistant tumor growth.* Cancer Res, 2008. **68**(11): p. 4447-54.

28. Heidenreich, A., et al., *[EAU guidelines on prostate cancer. Part I: screening, diagnosis, and treatment of clinically localised disease].* Actas Urol Esp, 2011. **35**(9): p. 501-14.

29. Li, Y., et al., *Androgen receptor splice variants mediate enzalutamide resistance in castration-resistant prostate cancer cell lines.* Cancer Res, 2013. **73**(2): p. 483-9.

30. Crona, D.J. and Y.E. Whang, *Androgen Receptor-Dependent and -Independent Mechanisms Involved in Prostate Cancer Therapy Resistance.* Cancers (Basel), 2017. **9**(6).

31. Thoma, C., *AR-Vs not predictive in mCRPC.* Nature Reviews Urology, 2018. **15**: p. 203.

32. Sharp, A., et al., *Androgen receptor splice variant-7 expression emerges with castration resistance in prostate cancer.* The Journal of Clinical Investigation, 2019. **129**(1): p. 192-208.

33. Chandrasekar, T., et al., *Mechanisms of resistance in castration-resistant prostate cancer (CRPC).* Transl Androl Urol, 2015. **4**(3): p. 365-80.

34. Tilki, D., E.M. Schaeffer, and C.P. Evans, *Understanding Mechanisms of Resistance in Metastatic Castration-resistant Prostate Cancer: The Role of the Androgen Receptor.* European Urology Focus, 2016. **2**(5): p. 499-505.

35. Huang, Y., et al., *Molecular and cellular mechanisms of castration resistant prostate cancer.* Oncol Lett, 2018. **15**(5): p. 6063-6076.

36. Kahn, B., J. Collazo, and N. Kyprianou, *Androgen receptor as a driver of therapeutic resistance in advanced prostate cancer.* Int J Biol Sci, 2014. **10**(6): p. 588-95.

37. Yuan, X. and S.P. Balk, *Mechanisms mediating androgen receptor reactivation after castration.* Urologic oncology, 2009. **27**(1): p. 36-41.

38. Sharifi, N., *Mechanisms of androgen receptor activation in castration-resistant prostate cancer.* Endocrinology, 2013. **154**(11): p. 4010-4017.

39. Tan, M.H.E., et al., *Androgen receptor: structure, role in prostate cancer and drug discovery.* Acta Pharmacologica Sinica, 2014. **36**: p. 3.

40. Prins, G.S. and O. Putz, *Molecular signaling pathways that regulate prostate gland development.* Differentiation; research in biological diversity, 2008. **76**(6): p. 641-659.

41. Di Lorenzo, G., et al., *Expression of Epidermal Growth Factor Receptor Correlates with Disease Relapse and Progression to Androgen-independence in Human Prostate Cancer.* Clinical Cancer Research, 2002. **8**(11): p. 3438-3444.

42. Cai, C., et al., *Intratumoral de novo steroid synthesis activates androgen receptor in castration-resistant prostate cancer and is upregulated by treatment with CYP17A1 inhibitors.* Cancer Res, 2011. **71**(20): p. 6503-13.

43. Kallio, H.M.L., et al., *Constitutively active androgen receptor splice variants AR-V3, AR-V7 and AR-V9 are co-expressed in castration-resistant prostate cancer metastases.* British Journal of Cancer, 2018. **119**(3): p. 347-356.

44. Heinlein, C.A. and C. Chang, *Androgen receptor (AR) coregulators: an overview.* Endocr Rev, 2002. **23**(2): p. 175-200.

45. van der Steen, T., D.J. Tindall, and H. Huang, *Posttranslational modification of the androgen receptor in prostate cancer.* International journal of molecular sciences, 2013. **14**(7): p. 14833-14859.

46. Stein, M.N., et al., *Androgen synthesis inhibitors in the treatment of castration-resistant prostate cancer.* Asian journal of andrology, 2014. **16**(3): p. 387-400.

47. Beer, T.M., et al., *Enzalutamide in metastatic prostate cancer before chemotherapy.* N Engl J Med, 2014. **371**(5): p. 424-33.

48. James, N.D., et al., *Abiraterone for Prostate Cancer Not Previously Treated with Hormone Therapy.* N Engl J Med, 2017. **377**(4): p. 338-351.

49. Armstrong, C.M. and A.C. Gao, *Drug resistance in castration resistant prostate cancer: resistance mechanisms and emerging treatment strategies.* American journal of clinical and experimental urology, 2015. **3**(2): p. 64-76.

50. Schalken, J. and J.M. Fitzpatrick, *Enzalutamide: targeting the androgen signalling pathway in metastatic castration-resistant prostate cancer.* BJU international, 2016. **117**(2): p. 215-225.

51. Rodriguez-Vida, A., et al., *Enzalutamide for the treatment of metastatic castration-resistant prostate cancer.* Drug design, development and therapy, 2015. **9**: p. 3325-3339.

52. Petrylak, D.P., et al., *Docetaxel and estramustine compared with mitoxantrone and prednisone for advanced refractory prostate cancer.* N Engl J Med, 2004. **351**(15): p. 1513-20.

53. Fang, M., et al., *Efficacy of Abiraterone and Enzalutamide in Pre- and Postdocetaxel Castration-Resistant Prostate Cancer: A Trial-Level Meta-Analysis.* Prostate cancer, 2017. **2017**: p. 8560827-8560827.

54. Antonarakis, E.S., *Current understanding of resistance to abiraterone and enzalutamide in advanced prostate cancer.* Clin Adv Hematol Oncol, 2016. **14**(5): p. 316-9.

55. Antonarakis, E.S., et al., *AR-V7 and Resistance to Enzalutamide and Abiraterone in Prostate Cancer.* New England Journal of Medicine, 2014. **371**(11): p. 1028-1038.

56. Hotte, S.J. and F. Saad, *Current management of castrate-resistant prostate cancer.* Current oncology (Toronto, Ont.), 2010. **17 Suppl 2**(Suppl 2): p. S72-S79.

57. Mendiratta, P., A.J. Armstrong, and D.J. George, *Current standard and investigational approaches to the management of hormone-refractory prostate cancer.* Reviews in urology, 2007. **9 Suppl 1**(Suppl 1): p. S9-S19.

58. Berthold, D.R., et al., *Docetaxel plus prednisone or mitoxantrone plus prednisone for advanced prostate cancer: updated survival in the TAX 327 study.* J Clin Oncol, 2008. **26**(2): p. 242-5.

59. Lohiya, V., J.B. Aragon-Ching, and G. Sonpavde, *Role of Chemotherapy and Mechanisms of Resistance to Chemotherapy in Metastatic Castration-Resistant Prostate Cancer.* Clinical Medicine Insights. Oncology, 2016. **10**(Suppl 1): p. 57-66.

60. Dagher, R., et al., *Approval summary: Docetaxel in combination with prednisone for the treatment of androgen-independent hormone-refractory prostate cancer.* Clin Cancer Res, 2004. **10**(24): p. 8147-51.

61. Zhu, M.-L., et al., *Tubulin-targeting chemotherapy impairs androgen receptor activity in prostate cancer.* Cancer research, 2010. **70**(20): p. 7992-8002.

62. Fitzpatrick, J.M. and R. de Wit, *Taxane mechanisms of action: potential implications for treatment sequencing in metastatic castration-resistant prostate cancer.* Eur Urol, 2014. **65**(6): p. 1198-204.

63. Terry, S., et al., *Increased expression of class III β-tubulin in castration-resistant human prostate cancer.* British journal of cancer, 2009. **101**(6): p. 951.

64. Ranganathan, S., et al., *Modulation of endogenous β-tubulin isotype expression as a result of human β III cDNA transfection into prostate carcinoma cells.* British journal of cancer, 2001. **85**(5): p. 735.

65. Oudard, S., *TROPIC: Phase III trial of cabazitaxel for the treatment of metastatic castration-resistant prostate cancer.* Future Oncol, 2011. **7**(4): p. 497-506.

66. Kartner, N., J.R. Riordan, and V. Ling, *Cell surface P-glycoprotein associated with multidrug resistance in mammalian cell lines.* Science, 1983. **221**(4617): p. 1285-8.

67. Assaraf, Y.G., *The role of multidrug resistance efflux transporters in antifolate resistance and folate homeostasis.* Drug Resist Updat, 2006. **9**(4-5): p. 227-46.

68. Wyatt, A.W., et al., *The diverse heterogeneity of molecular alterations in prostate cancer identified through next-generation sequencing.* Asian journal of andrology, 2013. **15**(3): p. 301-308.

69. Hoey, T., *Drug resistance, epigenetics, and tumor cell heterogeneity.* Sci Transl Med, 2010. **2**(28): p. 28ps19.

70. Coyle, K.M., J.E. Boudreau, and P. Marcato, *Genetic Mutations and Epigenetic Modifications: Driving Cancer and Informing Precision Medicine.* BioMed research international, 2017. **2017**: p. 9620870-9620870.

71. Fernandez, E., et al., *Factors and Mechanisms for Pharmacokinetic Differences between Pediatric Population and Adults.* Pharmaceutics, 2011. **3**(1): p. 53-72.

72. Li, M., et al., *Clinical targeting recombinant immunotoxins for cancer therapy.* OncoTargets and therapy, 2017. **10**: p. 3645-3665.

73. Thurber, G.M., M.M. Schmidt, and K.D. Wittrup, *Antibody tumor penetration: transport opposed by systemic and antigen-mediated clearance.* Advanced drug delivery reviews, 2008. **60**(12): p. 1421-1434.

74. Corn, P.G., *The tumor microenvironment in prostate cancer: elucidating molecular pathways for therapy development.* Cancer management and research, 2012. **4**: p. 183-193.

75. Pedraza-Fariña, L.G., *Mechanisms of oncogenic cooperation in cancer initiation and metastasis.* The Yale journal of biology and medicine, 2006. **79**(3-4): p. 95-103.

76. Liu, Y.Y., et al., *Ceramide glycosylation potentiates cellular multidrug resistance.* Faseb j, 2001. **15**(3): p. 719-30.

77. Nguyen, K.T., et al., *Transactivation of the human multidrug resistance (MDR1) gene promoter by p53 mutants.* Oncol Res, 1994. **6**(2): p. 71-7.

78. Smets, L.A., *Programmed cell death (apoptosis) and response to anti-cancer drugs.* Anticancer Drugs, 1994. **5**(1): p. 3-9.

79. Xue, X., et al., *Nanoscale drug delivery platforms overcome platinum-based resistance in cancer cells due to abnormal membrane protein trafficking.* ACS nano, 2013. **7**(12): p. 10452-10464.

80. Glavinas, H., et al., *The role of ABC transporters in drug resistance, metabolism and toxicity.* Curr Drug Deliv, 2004. **1**(1): p. 27-42.

81. Kis, O., et al., *The complexities of antiretroviral drug-drug interactions: role of ABC and SLC transporters.* Trends Pharmacol Sci, 2010. **31**(1): p. 22-35.

82. Goldstein, L.J., et al., *Expression of a multidrug resistance gene in human cancers.* J Natl Cancer Inst, 1989. **81**(2): p. 116-24.

83. Wilkens, S., *Structure and mechanism of ABC transporters.* F1000prime reports, 2015. **7**: p. 14-14.

84. Cunha, G.R., A.A. Donjacour, and Y. Sugimura, *Stromal-epithelial interactions and heterogeneity of proliferative activity within the prostate.* Biochem Cell Biol, 1986. **64**(6): p. 608-14.

85. Filella, X., et al., *Emerging biomarkers in the diagnosis of prostate cancer.* Pharmacogenomics and personalized medicine, 2018. **11**: p. 83-94.

86. Velonas, V.M., et al., *Current status of biomarkers for prostate cancer.* International journal of molecular sciences, 2013. **14**(6): p. 11034-11060.

87. Ross, R.K., et al., *Androgen metabolism and prostate cancer: establishing a model of genetic susceptibility.* Cancer Res, 1998. **58**(20): p. 4497-504.

88. Costello, L.C., R.B. Franklin, and P. Feng, *Mitochondrial function, zinc, and intermediary metabolism relationships in normal prostate and prostate cancer.* Mitochondrion, 2005. **5**(3): p. 143-53.

89. Eidelman, E., et al., *The Metabolic Phenotype of Prostate Cancer.* Frontiers in oncology, 2017. **7**: p. 131-131.

90. Carracedo, A., et al., *Cancer metabolism: fatty acid oxidation in the limelight.* Nature Reviews Cancer, 2013. **13**: p. 227-232.

91. Puchades-Carrasco, L. and A. Pineda-Lucena, *Metabolomics Applications in Precision Medicine: An Oncological Perspective.* Current topics in medicinal chemistry, 2017. **17**(24): p. 2740-2751.

92. Gowda, G.A.N., et al., *Metabolomics-based methods for early disease diagnostics.* Expert review of molecular diagnostics, 2008. **8**(5): p. 617-633.

93. Kelly, R.S., et al., *The role of tumor metabolism as a driver of prostate cancer progression and lethal disease: results from a nested case-control study.* Cancer & metabolism, 2016. **4**: p. 22-22.

94. Mann, T., *The biochemistry of semen and of the male reproductive tract.* The biochemistry of semen and of the male reproductive tract., 1964.

95. De Kretser, D., P. Temple-Smith, and J. Kerr, *Anatomical and functional aspects of the male reproductive organs*, in *Disturbances in Male Fertility*. 1982, Springer. p. 1-131.

96. Everaerts, W. and A.J. Costello, *Applied Anatomy of the Male Pelvis*, in *Prostate Ultrasound: Current Practice and Future Directions*, C.R. Porter and E.M. Wolff, Editors. 2015, Springer New York: New York, NY. p. 11-30.

97. Fine, S.W. and R. Mehra, *Anatomy of the Prostate Revisited: Implications for Prostate Biopsy and Zonal Origins of Prostate Cancer*, in *Genitourinary Pathology: Practical Advances*, C. Magi-Galluzzi and C.G. Przybycin, Editors. 2015, Springer New York: New York, NY. p. 3-12.

98. Rybak, A., R. Bristow, and A. Kapoor, *Prostate cancer stem cells: Deciphering the origins and pathways involved in prostate tumorigenesis and aggression.* Oncotarget, 2014. **6**.

99. Barron, D.A. and D.R. Rowley, *The reactive stroma microenvironment and prostate cancer progression.* 2012. **19**(6): p. R187.

100. Toivanen, R. and M.M. Shen, *Prostate organogenesis: tissue induction, hormonal regulation and cell type specification.* Development, 2017. **144**(8): p. 1382-1398.

101. Obinata, D., et al., *Review of novel therapeutic medicines targeting androgen signaling in castration-resistant prostate cancer.* World Journal of Clinical Urology, 2014. **3**(3): p. 264-271.

102. Turner, B. and L. Drudge-Coates, *New pharmacological treatments for prostate cancer.* Nurse Prescribing, 2012. **10**: p. 498-502.

103. Wenk, M.R., *The emerging field of lipidomics.* Nature Reviews Drug Discovery, 2005. **4**: p. 594.

104. van Meer, G., D.R. Voelker, and G.W. Feigenson, *Membrane lipids: where they are and how they behave.* Nat Rev Mol Cell Biol, 2008. **9**(2): p. 112-24.

105. Gurr, M. and A. James, *Lipid biochemistry: an introduction.(eds.) Chapman & Hall, London.* 1971.

106. Fahy, E., et al., *Update of the LIPID MAPS comprehensive classification system for lipids.* J Lipid Res, 2009. **50 Suppl**: p. S9-14.

107. Kennedy, E.P., *Biosynthesis of complex lipids.* Fed Proc, 1961. **20**: p. 934-40.

108. Rysman, E., et al., *De novo lipogenesis protects cancer cells from free radicals and chemotherapeutics by promoting membrane lipid saturation.* Cancer Research, 2010. **70**: p. 8117-8126.

109. Kent, C., *Regulatory enzymes of phosphatidylcholine biosynthesis: a personal perspective.* Biochim Biophys Acta, 2005. **1733**(1): p. 53-66.

110. Kennedy, E.P. and S.B. Weiss, *The function of cytidine coenzymes in the biosynthesis of phospholipides.* J Biol Chem, 1956. **222**(1): p. 193-214.

111. Lands, W.E., *Metabolism of glycerolipides; a comparison of lecithin and triglyceride synthesis.* J Biol Chem, 1958. **231**(2): p. 883-8.

112. Shimizu, T., T. Ohto, and Y. Kita, *Cytosolic phospholipase A2: biochemical properties and physiological roles.* IUBMB Life, 2006. **58**(5-6): p. 328-33.

113. Schlame, M., D. Rua, and M.L. Greenberg, *The biosynthesis and functional role of cardiolipin.* Prog Lipid Res, 2000. **39**(3): p. 257-88.

114. Lands, W.E., *Stories about acyl chains.* Biochim Biophys Acta, 2000. **1483**(1): p. 1-14.

115. Sergeant, S., et al., *Phosphatidic acid regulates tyrosine phosphorylating activity in human neutrophils enhancement of Fgr activity.* Journal of Biological Chemistry, 2001. **276**(7): p. 4737-4746.

116. Rizzo, M.A., et al., *Phospholipase D and its product, phosphatidic acid, mediate agonist-dependent raf-1 translocation to the plasma membrane and the activation of the mitogen-activated protein kinase pathway.* J Biol Chem, 1999. **274**(2): p. 1131-9.

117. Olivera, A., J. Rosenthal, and S. Spiegel, *Effect of acidic phospholipids on sphingosine kinase.* Journal of cellular biochemistry, 1996. **60**(4): p. 529-537.

118. Lim, H.-K., et al., *Phosphatidic acid regulates systemic inflammatory responses by modulating the Akt-mammalian target of rapamycin-p70 S6 kinase 1 pathway.* Journal of Biological Chemistry, 2003. **278**(46): p. 45117-45127.

119. Daaka, Y., *Mitogenic action of LPA in prostate.* Biochim Biophys Acta, 2002. **1582**(1-3): p. 265-9.

120. Kulkarni, P. and R.H. Getzenberg, *High-fat diet, obesity and prostate disease: the ATX-LPA axis?* Nat Clin Pract Urol, 2009. **6**(3): p. 128-31.

121. Terada, N., et al., *Cyr61 is regulated by cAMP-dependent protein kinase with serum levels correlating with prostate cancer aggressiveness.* Prostate, 2012. **72**(9): p. 966-76.

122. Yui, K., et al., *Eicosanoids Derived From Arachidonic Acid and Their Family Prostaglandins and Cyclooxygenase in Psychiatric Disorders.* Current neuropharmacology, 2015. **13**(6): p. 776-785.

123. MacDonald, J.I. and H. Sprecher, *Phospholipid fatty acid remodeling in mammalian cells.* Biochimica et Biophysica Acta (BBA)-Lipids and Lipid Metabolism, 1991. **1084**(2): p. 105-121.

124. Patel, D. and S.N. Witt, *Ethanolamine and Phosphatidylethanolamine: Partners in Health and Disease.* Oxidative medicine and cellular longevity, 2017. **2017**: p. 4829180-4829180.

125. Chu, Z., et al., *Targeting and cytotoxicity of SapC-DOPS nanovesicles in pancreatic cancer.* PloS one, 2013. **8**(10): p. e75507.

126. Wojton, J., et al., *Systemic delivery of SapC-DOPS has antiangiogenic and antitumor effects against glioblastoma.* Molecular Therapy, 2013. **21**(8): p. 1517-1525.

127. Zhao, S., et al., *SapC–DOPS nanovesicles as targeted therapy for lung cancer.* Molecular cancer therapeutics, 2015. **14**(2): p. 491-498.

128. Murray, N.R. and A.P. Fields, *Phosphatidylglycerol is a physiologic activator of nuclear protein kinase C.* Journal of Biological Chemistry, 1998. **273**(19): p. 11514-11520.

129. Murray, N., L. Thompson, and A. Fields, *Protein Kinase C Molecular Biology Intelligence Unit*. 1997, The role of protein kinase C in cellular proliferation and cell cycle ….

130. Reis, A., *Oxidative Phospholipidomics in health and disease: Achievements, challenges and hopes.* Free Radical Biology and Medicine, 2017. **111**: p. 25-37.

131. Fu, P. and K.G. Birukov, *Oxidized phospholipids in control of inflammation and endothelial barrier.* Translational Research, 2009. **153**(4): p. 166-176.

132. Ashraf, M.Z., N.S. Kar, and E.A. Podrez, *Oxidized phospholipids: Biomarker for cardiovascular diseases.* The International Journal of Biochemistry & Cell Biology, 2009. **41**(6): p. 1241-1244.

133. Maskrey, B.H., et al., *Mechanisms of Resolution of Inflammation.* Arteriosclerosis, Thrombosis, and Vascular Biology, 2011. **31**(5): p. 1001-1006.

134. Salomon, R.G. and A. Bhatnagar, *Structural Identification and Cardiovascular Activities of Oxidized Phospholipids.* Circulation Research, 2012. **111**(7): p. 930-946.

135. Miyazawa, T., et al., *Age-related change of phosphatidylcholine hydroperoxide and phosphatidylethanolamine hydroperoxide levels in normal human red blood cells.* Mechanisms of Ageing and Development, 1996. **86**(3): p. 145-150.

136. Adachi, J., et al., *Plasma phosphatidylcholine hydroperoxide as a new marker of oxidative stress in alcoholic patients.* Journal of Lipid Research, 2004. **45**(5): p. 967-971.

137. Hui, S.-P., et al., *An improved HPLC assay for phosphatidylcholine hydroperoxides (PCOOH) in human plasma with synthetic PCOOH as internal standard.* Journal of Chromatography B, 2007. **857**(1): p. 158-163.

138. Jónasdóttir, H.S., et al., *Detection and Structural Elucidation of Esterified Oxylipids in Human Synovial Fluid by Electrospray Ionization-Fourier Transform Ion-Cyclotron Mass Spectrometry and Liquid Chromatography-Ion Trap-MS3: Detection of Esterified Hydroxylated Docosapentaenoic Acid Containing Phospholipids.* Analytical Chemistry, 2013. **85**(12): p. 6003-6010.

139. Gruber, F., et al., *Photooxidation generates biologically active phospholipids that induce heme oxygenase-1 in skin cells.* Journal of Biological Chemistry, 2007. **282**(23): p. 16934-16941.

140. Birukova, A.A., et al., *Signaling pathways involved in OxPAPC-induced pulmonary endothelial barrier protection.* Microvascular research, 2007. **73**(3): p. 173-181.

141. Stemmer, U., et al., *Toxicity of oxidized phospholipids in cultured macrophages.* Lipids in health and disease, 2012. **11**(1): p. 110.

142. Thimmulappa, R.K., et al., *Oxidized phospholipids impair pulmonary antibacterial defenses: evidence in mice exposed to cigarette smoke.* Biochemical and biophysical research communications, 2012. **426**(2): p. 253-259.

143. Halasiddappa, L.M., et al., *Oxidized phospholipids induce ceramide accumulation in RAW 264.7 macrophages: role of ceramide synthases.* PLoS One, 2013. **8**(7): p. e70002.

144. Koller, D., et al., *Effects of oxidized phospholipids on gene expression in RAW 264.7 macrophages: a microarray study.* PloS one, 2014. **9**(10): p. e110486.

145. Hoff, H.F., et al., *Phospholipid hydroxyalkenals: biological and chemical properties of specific oxidized lipids present in atherosclerotic lesions.* Arteriosclerosis, thrombosis, and vascular biology, 2003. **23**(2): p. 275-282.

146. Kamido, H., et al., *Core aldehydes of alkyl glycerophosphocholines in atheroma induce platelet aggregation and inhibit endothelium-dependent arterial relaxation.* Journal of lipid research, 2002. **43**(1): p. 158-166.

147. Ravandi, A., et al., *Phospholipids and oxophospholipids in atherosclerotic plaques at different stages of plaque development.* Lipids, 2004. **39**(2): p. 97-109.

148. Hammad, L.A., et al., *Elevated levels of hydroxylated phosphocholine lipids in the blood serum of breast cancer patients.* Rapid Communications in Mass

Spectrometry: An International Journal Devoted to the Rapid Dissemination of Up‐to‐the‐Minute Research in Mass Spectrometry, 2009. **23**(6): p. 863-876.

149. Kinoshita, M., et al., *Age-related increases in plasma phosphatidylcholine hydroperoxide concentrations in control subjects and patients with hyperlipidemia.* Clinical chemistry, 2000. **46**(6): p. 822-828.

150. Akasaka, K., et al., *Automatic determination of hydroperoxides of phosphatidylcholine and phosphatidylethanolamine in human plasma.* Journal of Chromatography B: Biomedical Sciences and Applications, 1995. **665**(1): p. 37-43.

151. Rolla, R., et al., *Antibodies against oxidized phospholipids in laboratory tests exploring lupus anti‐coagulant activity.* Clinical & Experimental Immunology, 2007. **149**(1): p. 63-69.

152. Matt, U., et al., *Accumulating evidence for a role of oxidized phospholipids in infectious diseases.* Cellular and molecular life sciences, 2015. **72**(6): p. 1059-1071.

153. Cruz, D., et al., *Host-derived oxidized phospholipids and HDL regulate innate immunity in human leprosy.* The Journal of clinical investigation, 2008. **118**(8): p. 2917-2928.

154. O'Donnell, V.B. and R.C. Murphy, *New families of bioactive oxidized phospholipids generated by immune cells: identification and signaling actions.* Blood, 2012. **120**(10): p. 1985-1992.

155. Stübiger, G., et al., *Targeted profiling of atherogenic phospholipids in human plasma and lipoproteins of hyperlipidemic patients using MALDI-QIT-TOF-MS/MS.* Atherosclerosis, 2012. **224**(1): p. 177-186.

156. Frey, B., et al., *Increase in fragmented phosphatidylcholine in blood plasma by oxidative stress.* Journal of lipid research, 2000. **41**(7): p. 1145-1153.

157. Podrez, E.A., et al., *Platelet CD36 links hyperlipidemia, oxidant stress and a prothrombotic phenotype.* Nature medicine, 2007. **13**(9): p. 1086.

158. Korotaeva, A.A., et al., *Oxidized phosphatidylcholine stimulates activity of secretory phospholipase A2 group IIA and abolishes sphingomyelin-induced inhibition of the enzyme.* Prostaglandins & other lipid mediators, 2010. **91**(1-2): p. 38-41.

159. Ramprecht, C., et al., *Toxicity of oxidized phosphatidylcholines in cultured human melanoma cells.* Chemistry and physics of lipids, 2015. **189**: p. 39-47.

160. Bochkov, V., et al., *Oxidized Phospholipids Stimulate Angiogenesis Via Autocrine Mechanisms, Implicating a Novel Role for Lipid Oxidation in the Evolution of Atherosclerotic Lesions*. Vol. 99. 2006. 900-8.

161. T Reddy, S., et al., *Identification of genes induced by oxidized phospholipids in human aortic endothelial cells*. Vol. 38. 2002. 211-8.

162. Oskolkova, O.V., et al., *ATF4-dependent transcription is a key mechanism in VEGF up-regulation by oxidized phospholipids: critical role of oxidized sn-2 residues in activation of unfolded protein response.* Blood, 2008. **112**(2): p. 330-339.

163. Blüml, S., et al., *The Oxidation State of Phospholipids Controls the Oxidative Burst in Neutrophil Granulocytes.* The Journal of Immunology, 2008. **181**(6): p. 4347-4353.

164. Gao, D., et al., *Structural Basis for the Recognition of Oxidized Phospholipids in Oxidized Low Density Lipoproteins by Class B Scavenger Receptors CD36 and SR-BI.* Journal of Biological Chemistry, 2010. **285**(7): p. 4447-4454.

165. Boullier, A., et al., *The Binding of Oxidized Low Density Lipoprotein to Mouse CD36 Is Mediated in Part by Oxidized Phospholipids That Are Associated with Both the Lipid and Protein Moieties of the Lipoprotein.* Journal of Biological Chemistry, 2000. **275**(13): p. 9163-9169.

166. Karupaiah, T. and K. Sundram, *Effects of stereospecific positioning of fatty acids in triacylglycerol structures in native and randomized fats: a review of their nutritional implications.* Nutrition & metabolism, 2007. **4**(1): p. 16.

167. Dircks, L. and H.S. Sul, *Acyltransferases of de novo glycerophospholipid biosynthesis.* Prog Lipid Res, 1999. **38**(5-6): p. 461-79.

168. Weiss, S.B., E.P. Kennedy, and J.Y. Kiyasu, *The enzymatic synthesis of triglycerides.* Journal of Biological Chemistry, 1960. **235**(1): p. 40-44.

169. Coleman, R.A. and D.P. Lee, *Enzymes of triacylglycerol synthesis and their regulation.* Progress in lipid research, 2004. **43**(2): p. 134-176.

170. Wei, L., et al., *A case-control study on the association between serum lipid level and the risk of breast cancer.* Zhonghua yu fang yi xue za zhi [Chinese journal of preventive medicine], 2016. **50**(12): p. 1091-1095.

171. Ogretmen, B. and Y.A. Hannun, *Biologically active sphingolipids in cancer pathogenesis and treatment.* Nature Reviews Cancer, 2004. **4**(8): p. 604.

172. Ogretmen, B., *Sphingolipids in cancer: regulation of pathogenesis and therapy.* FEBS letters, 2006. **580**(23): p. 5467-5476.

173. Ryland, L.K., et al., *Dysregulation of sphingolipid metabolism in cancer.* Cancer biology & therapy, 2011. **11**(2): p. 138-149.

174. Fyrst, H. and J.D. Saba, *An update on sphingosine-1-phosphate and other sphingolipid mediators.* Nat Chem Biol, 2010. **6**(7): p. 489-97.

175. Maula, T., et al., *Importance of the sphingoid base length for the membrane properties of ceramides.* Biophysical journal, 2012. **103**(9): p. 1870-1879.

176. Saddoughi, S.A., P. Song, and B. Ogretmen, *Roles of bioactive sphingolipids in cancer biology and therapeutics.* Sub-cellular biochemistry, 2008. **49**: p. 413-440.

177. Ponnusamy, S., et al., *Sphingolipids and cancer: ceramide and sphingosine-1-phosphate in the regulation of cell death and drug resistance.* Future oncology (London, England), 2010. **6**(10): p. 1603-1624.

178. Taha, T.A., T.D. Mullen, and L.M. Obeid, *A house divided: ceramide, sphingosine, and sphingosine-1-phosphate in programmed cell death.* Biochim Biophys Acta, 2006. **1758**(12): p. 2027-36.

179. Ogretmen, B. and Y.A. Hannun, *Biologically active sphingolipids in cancer pathogenesis and treatment.* Nat Rev Cancer, 2004. **4**(8): p. 604-16.

180. Wang, X.-Z., et al., *Aberrant Sphingolipid Signaling Is Involved in the Resistance of Prostate Cancer Cell Lines to Chemotherapy.* Cancer Research, 1999. **59**(22): p. 5842-5848.

181. García-Barros, M., et al., *Sphingolipids in colon cancer.* Biochimica et biophysica acta, 2014. **1841**(5): p. 773-782.

182. Karahatay, S., et al., *Clinical relevance of ceramide metabolism in the pathogenesis of human head and neck squamous cell carcinoma (HNSCC): attenuation of C(18)-ceramide in HNSCC tumors correlates with lymphovascular invasion and nodal metastasis.* Cancer Lett, 2007. **256**(1): p. 101-11.

183. Schiffmann, S., et al., *Ceramide synthases and ceramide levels are increased in breast cancer tissue.* Carcinogenesis, 2009. **30**(5): p. 745-52.

184. Pralhada Rao, R., et al., *Sphingolipid metabolic pathway: an overview of major roles played in human diseases.* Journal of lipids, 2013. **2013**: p. 178910-178910.

185. Modrak, D.E., D.V. Gold, and D.M. Goldenberg, *Sphingolipid targets in cancer therapy.* Molecular Cancer Therapeutics, 2006. **5**(2): p. 200-208.

186. Lemonnier, L.A., et al., *Sphingomyelin in the suppression of colon tumors: prevention versus intervention.* Arch Biochem Biophys, 2003. **419**(2): p. 129-38.

187. Al Sazzad, M.A., et al., *The Long-Chain Sphingoid Base of Ceramides Determines Their Propensity for Lateral Segregation.* Biophysical journal, 2017. **112**(5): p. 976-983.

188. Dillehay, D.L., et al., *Dietary sphingomyelin inhibits 1,2-dimethylhydrazine-induced colon cancer in CF1 mice.* J Nutr, 1994. **124**(5): p. 615-20.

189. Mehta, S., et al., *Combined cytotoxic action of paclitaxel and ceramide against the human Tu138 head and neck squamous carcinoma cell line.* Cancer Chemother Pharmacol, 2000. **46**(2): p. 85-92.

190. Schmelz, E.M., et al., *Colonic cell proliferation and aberrant crypt foci formation are inhibited by dairy glycosphingolipids in 1, 2-dimethylhydrazine-treated CF1 mice.* J Nutr, 2000. **130**(3): p. 522-7.

191. Onodera, T., et al., *Phosphatidylethanolamine plasmalogen enhances the inhibiting effect of phosphatidylethanolamine on γ-secretase activity.* The Journal of Biochemistry, 2014. **157**(5): p. 301-309.

192. Braverman, N.E. and A.B. Moser, *Functions of plasmalogen lipids in health and disease.* Biochim Biophys Acta, 2012. **1822**(9): p. 1442-52.

193. Hu, C., M. Wang, and X. Han, *Shotgun lipidomics in substantiating lipid peroxidation in redox biology: Methods and applications.* Redox Biol, 2017. **12**: p. 946-955.

194. Wallner, S. and G. Schmitz, *Plasmalogens the neglected regulatory and scavenging lipid species.* Chem Phys Lipids, 2011. **164**(6): p. 573-89.

195. Fuchs, B., *Analytical methods for (oxidized) plasmalogens: Methodological aspects and applications.* Free Radic Res, 2015. **49**(5): p. 599-617.

196. Maeba, R., et al., *Chapter Two - Plasma/Serum Plasmalogens: Methods of Analysis and Clinical Significance*, in *Advances in Clinical Chemistry*, G.S. Makowski, Editor. 2015, Elsevier. p. 31-94.

197. Maeba, R., et al., *Plasma/Serum Plasmalogens: Methods of Analysis and Clinical Significance.* Adv Clin Chem, 2015. **70**: p. 31-94.

198. Han, X., *Lipidomics for studying metabolism.* Nat Rev Endocrinol, 2016. **12**(11): p. 668-679.

199. Mankidy, R., et al., *Membrane plasmalogen composition and cellular cholesterol regulation: a structure activity study.* Lipids Health Dis, 2010. **9**: p. 62.

200. Brites, P., H.R. Waterham, and R.J. Wanders, *Functions and biosynthesis of plasmalogens in health and disease.* Biochim Biophys Acta, 2004. **1636**(2-3): p. 219-31.

201. Fhaner, C.J., et al., *Functional group selective derivatization and gas-phase fragmentation reactions of plasmalogen glycerophospholipids.* Mass Spectrometry, 2013. **2**(Special_Issue): p. S0015-S0015.

202. Gerbig, S., et al., *Analysis of colorectal adenocarcinoma tissue by desorption electrospray ionization mass spectrometric imaging.* Analytical and bioanalytical chemistry, 2012. **403**(8): p. 2315-2325.

203. Lv, J., et al., *Plasma Content Variation and Correlation of Plasmalogen and GIS, TC, and TPL in Gastric Carcinoma Patients: A Comparative Study.* Medical science monitor basic research, 2015. **21**: p. 157-160.

204. Kunkel, G.T., et al., *Targeting the sphingosine-1-phosphate axis in cancer, inflammation and beyond.* Nature reviews. Drug discovery, 2013. **12**(9): p. 688-702.

205. Wang, D. and R.N. Dubois, *Eicosanoids and cancer.* Nature reviews. Cancer, 2010. **10**(3): p. 181-193.

206. Nakanishi, M. and D.W. Rosenberg. *Multifaceted roles of PGE 2 in inflammation and cancer*. in *Seminars in immunopathology*. 2013. Springer.

207. Asgari, Y., et al., *Alterations in cancer cell metabolism: the Warburg effect and metabolic adaptation.* Genomics, 2015. **105**(5-6): p. 275-81.

208. Santos, C., et al., *Lipid metabolism in cancer.* FEBS Journal, 2012. **279**: p. 2610-2623.

209. Dueregger, A., et al., *Differential Utilization of Dietary Fatty Acids in Benign and Malignant Cells of the Prostate.* PLoS One, 2015. **10**(8): p. e0135704.

210. Twum-Ampofo, J., et al., *Metabolic targets for potential prostate cancer therapeutics.* Curr Opin Oncol, 2016. **28**(3): p. 241-7.

211. Ngo, D.C., et al., *Introduction to the molecular basis of cancer metabolism and the Warburg effect.* Mol Biol Rep, 2015. **42**(4): p. 819-23.

212. Medes, G., A. Thomas, and S. Weinhouse, *Metabolism of neoplastic tissue. IV. A study of lipid synthesis in neoplastic tissue slices in vitro.* Cancer Res, 1953. **13**(1): p. 27-9.

213. Ookhtens, M., et al., *Liver and adipose tissue contributions to newly formed fatty acids in an ascites tumor.* Am J Physiol, 1984. **247**(1 Pt 2): p. R146-53.

214. Srihari, S., et al., *Metabolic deregulation in prostate cancer.* Mol Omics, 2018. **14**(5): p. 320-329.

215. Perona, J.S., *Membrane lipid alterations in the metabolic syndrome and the role of dietary oils*. 2017, Elsevier.

216. Hidalgo, A., A. Cruz, and J. Pérez-Gil, *Pulmonary surfactant and nanocarriers: toxicity versus combined nanomedical applications.* Biochimica et Biophysica Acta (BBA)-Biomembranes, 2017. **1859**(9): p. 1740-1748.

217. Echaide, M., et al., *Restoring pulmonary surfactant membranes and films at the respiratory surface.* Biochimica et Biophysica Acta (BBA)-Biomembranes, 2017. **1859**(9): p. 1725-1739.

218. Dumas, F. and E. Haanappel, *Lipids in infectious diseases–the case of AIDS and tuberculosis.* Biochimica et Biophysica Acta (BBA)-Biomembranes, 2017. **1859**(9): p. 1636-1647.

219. Fuentes, N.R., et al., *Emerging role of chemoprotective agents in the dynamic shaping of plasma membrane organization.* Biochimica et Biophysica Acta (BBA)-Biomembranes, 2017. **1859**(9): p. 1668-1678.

220. Ríos-Marco, P., et al., *Alkylphospholipids: An update on molecular mechanisms and clinical relevance*. 2017, Elsevier.

221. Baker, M.J., et al., *FTIR-based spectroscopic analysis in the identification of clinically aggressive prostate cancer.* Br J Cancer, 2008. **99**(11): p. 1859-66.

222. Zhou, X., et al., *Identification of plasma lipid biomarkers for prostate cancer by lipidomics and bioinformatics.* PLoS One, 2012. **7**(11): p. e48889.

223. Sorvina, A., et al., *Lipid profiles of prostate cancer cells.* Oncotarget, 2018. **9**(85): p. 35541-35552.

224. Hultsch, S., et al., *Association of tamoxifen resistance and lipid reprogramming in breast cancer.* BMC Cancer, 2018. **18**(1): p. 850.

225. Lin, H.-M., et al., *A distinct plasma lipid signature associated with poor prognosis in castration-resistant prostate cancer.* International Journal of Cancer, 2017. **141**(10): p. 2112-2120.

226. Horvath, L., et al., *The plasma lipidome in castration-resistant prostate cancer.* Journal of Clinical Oncology, 2017. **35**(15_suppl): p. 5055-5055.

227. Bligh, E.G. and W.J. Dyer, *A rapid method of total lipid extraction and purification.* Canadian journal of biochemistry and physiology, 1959. **37**(8): p. 911-917.

228. Bartlett, G.R., *Phosphorus assay in column chromatography.* J biol chem, 1959. **234**(3): p. 466-468.

229. Kinsey, G.R., et al., *Decreased iPLA2γ expression induces lipid peroxidation and cell death and sensitizes cells to oxidant-induced apoptosis.* Journal of lipid research, 2008. **49**(7): p. 1477-1487.

230. Zhang, L., B.L. Peterson, and B.S. Cummings, *The effect of inhibition of Ca2+-independent phospholipase A2 on chemotherapeutic-induced death and phospholipid profiles in renal cells.* Biochemical pharmacology, 2005. **70**(11): p. 1697-1706.

231. Peterson, B., et al., *Alterations in phospholipid and fatty acid lipid profiles in primary neocortical cells during oxidant-induced cell injury.* Chem Biol Interact, 2008. **174**(3): p. 163-76.

232. Maes, E., et al., *Determination of Variation Parameters as a Crucial Step in Designing TMT-Based Clinical Proteomics Experiments.* PLOS ONE, 2015. **10**(3): p. e0120115.

233. Schaaf, M.J. and J.A. Cidlowski, *Molecular mechanisms of glucocorticoid action and resistance.* J Steroid Biochem Mol Biol, 2002. **83**(1-5): p. 37-48.

234. Kalli, A., et al., *Evaluation and optimization of mass spectrometric settings during data-dependent acquisition mode: focus on LTQ-Orbitrap mass analyzers.* Journal of proteome research, 2013. **12**(7): p. 3071-3086.

235. Pluskal, T., et al., *MZmine 2: modular framework for processing, visualizing, and analyzing mass spectrometry-based molecular profile data.* BMC Bioinformatics, 2010. **11**: p. 395.

236. Tautenhahn, R., et al., *XCMS Online: a web-based platform to process untargeted metabolomic data.* Anal Chem, 2012. **84**(11): p. 5035-9.

237. Koelmel, J.P., et al., *LipidMatch: an automated workflow for rule-based lipid identification using untargeted high-resolution tandem mass spectrometry data.* BMC Bioinformatics, 2017. **18**(1): p. 331.

238. Kinsey, G.R., et al., *Decreased iPLA2gamma expression induces lipid peroxidation and cell death and sensitizes cells to oxidant-induced apoptosis.* J Lipid Res, 2008. **49**(7): p. 1477-87.

239. Trygg, J. and S. Wold, *Orthogonal Projections to Latent Structures (O-PLS).* Journal of Chemometrics, 2002. **16**: p. 119-128.

240. Trygg, J., E. Holmes, and T. Lundstedt, *Chemometrics in Metabonomics.* Journal of proteome research, 2007. **6**: p. 469-79.

241. Worley, B. and R. Powers, *Multivariate Analysis in Metabolomics.* Current Metabolomics, 2013. **1**(1): p. 92-107.

242. Richman, E.L., et al., *Choline intake and risk of lethal prostate cancer: incidence and survival.* The American journal of clinical nutrition, 2012. **96**(4): p. 855-863.

243. Zhou, Y., E.C. Bolton, and J.O. Jones, *Androgens and androgen receptor signaling in prostate tumorigenesis.* 2015. **54**(1): p. R15.

244. Cheng, J.C., et al., *Radiation-induced acid ceramidase confers prostate cancer resistance and tumor relapse.* The Journal of Clinical Investigation, 2013. **123**(10): p. 4344-4358.

245. Merchant, T.E., et al., *Phospholipid profiles of human colon cancer using 31P magnetic resonance spectroscopy.* Int J Colorectal Dis, 1991. **6**(2): p. 121-6.

246. Griner, E.M. and M.G. Kazanietz, *Protein kinase C and other diacylglycerol effectors in cancer.* Nat Rev Cancer, 2007. **7**(4): p. 281-94.

247. Perry, D.K. and Y.A. Hannun, *The role of ceramide in cell signaling.* Biochim Biophys Acta, 1998. **1436**(1-2): p. 233-43.

248. Schneider, G., et al., *Bioactive lipids, LPC and LPA, are novel prometastatic factors and their tissue levels increase in response to radio/chemotherapy.* Molecular cancer research : MCR, 2014. **12**(11): p. 1560-1573.

249. Okita, M., et al., *Elevated levels and altered fatty acid composition of plasma lysophosphatidlycholine (lysoPC) in ovarian cancer patients.* International journal of cancer, 1997. **71**(1): p. 31-34.

250. Phuyal, S., et al., *The ether lipid precursor hexadecylglycerol stimulates the release and changes the composition of exosomes derived from PC-3 cells.* J Biol Chem, 2015. **290**(7): p. 4225-37.

251. Devalapally, H., et al., *Modulation of drug resistance in ovarian adenocarcinoma by enhancing intracellular ceramide using tamoxifen-loaded biodegradable polymeric nanoparticles.* Clin Cancer Res, 2008. **14**(10): p. 3193-203.

252. Park, M.H., et al., *Overexpression of phospholipase D enhances matrix metalloproteinase-2 expression and glioma cell invasion via protein kinase C and protein kinase A/NF-kappaB/Sp1-mediated signaling pathways.* Carcinogenesis, 2009. **30**(2): p. 356-65.

253. Yang, J.S., et al., *Size Dependent Lipidomic Analysis of Urinary Exosomes from Patients with Prostate Cancer by Flow Field-Flow Fractionation and Nanoflow Liquid Chromatography-Tandem Mass Spectrometry.* Analytical Chemistry, 2017. **89**(4): p. 2488-2496.

254. Perry, R.H., et al., *Characterization of MYC-induced tumorigenesis by in situ lipid profiling.* Analytical chemistry, 2013. **85**(9): p. 4259-4262.

255. Shroff, E.H., et al., *MYC oncogene overexpression drives renal cell carcinoma in a mouse model through glutamine metabolism.* Proceedings of the National Academy of Sciences, 2015. **112**(21): p. 6539-6544.

256. Lisec, J., et al., *Cancer cell lipid class homeostasis is altered under nutrient-deprivation but stable under hypoxia.* BMC Cancer, 2019. **19**(1): p. 501.

257. Burch, T.C., et al., *Comparative metabolomic and lipidomic analysis of phenotype stratified prostate cells.* PLoS One, 2015. **10**(8): p. e0134206.

258. Jung, J.H., et al., *Phospholipids of tumor extracellular vesicles stratify gefitinib-resistant nonsmall cell lung cancer cells from gefitinib-sensitive cells.* Proteomics, 2015. **15**(4): p. 824-835.

259. Bevers, E.M., P. Comfurius, and R.F. Zwaal, *Regulatory mechanisms in maintenance and modulation of transmembrane lipid asymmetry: pathophysiological implications.* Lupus, 1996. **5**(5): p. 480-7.

260. Escriba, P.V., et al., *Membranes: a meeting point for lipids, proteins and therapies.* J Cell Mol Med, 2008. **12**(3): p. 829-75.

261. Escriba, P.V., *Membrane-lipid therapy: a new approach in molecular medicine.* Trends Mol Med, 2006. **12**(1): p. 34-43.

262. Thadani-Mulero, M., et al., *Androgen receptor splice variants determine taxane sensitivity in prostate cancer.* Cancer research, 2014. **74**(8): p. 2270-2282.

263. Ploussard, G., et al., *Class III β-tubulin expression predicts prostate tumor aggressiveness and patient response to docetaxel-based chemotherapy.* Cancer research, 2010. **70**(22): p. 9253-9264.

264. Zhu, Y., et al., *Inhibition of ABCB1 expression overcomes acquired docetaxel resistance in prostate cancer.* Molecular cancer therapeutics, 2013. **12**(9): p. 1829-1836.

265. Chen, H., H. Li, and Q. Chen, *INPP4B reverses docetaxel resistance and epithelial-to-mesenchymal transition via the PI3K/Akt signaling pathway in prostate cancer.* Biochemical and biophysical research communications, 2016. **477**(3): p. 467-472.

266. de Bessa Garcia, S.A., et al., *Prostate apoptosis response 4 (PAR4) expression modulates WNT signaling pathways in MCF7 breast cancer cells: A possible mechanism underlying PAR4-mediated docetaxel chemosensitivity.* International journal of molecular medicine, 2017. **39**(4): p. 809-818.

267. Codony‐Servat, J., et al., *Nuclear factor‐kappa B and interleukin‐6 related docetaxel resistance in castration‐resistant prostate cancer.* The Prostate, 2013. **73**(5): p. 512-521.

268. Marín-Aguilera, M., et al., *Epithelial-to-mesenchymal transition mediates docetaxel resistance and high risk of relapse in prostate cancer.* Molecular cancer therapeutics, 2014. **13**(5): p. 1270-1284.

269. Baenke, F., et al., *Hooked on fat: the role of lipid synthesis in cancer metabolism and tumour development.* Disease models & mechanisms, 2013. **6**(6): p. 1353-1363.

270. Ackerman, D. and M.C. Simon, *Hypoxia, lipids, and cancer: surviving the harsh tumor microenvironment.* Trends in cell biology, 2014. **24**(8): p. 472-478.

271. Cruz, P.M., et al., *The role of cholesterol metabolism and cholesterol transport in carcinogenesis: a review of scientific findings, relevant to future cancer therapeutics.* Frontiers in pharmacology, 2013. **4**: p. 119.

272. Cheng, C., et al., *Glucose-mediated N-glycosylation of SCAP is essential for SREBP-1 activation and tumor growth.* Cancer cell, 2015. **28**(5): p. 569-581.

273. Guo, D., et al., *EGFR signaling through an Akt-SREBP-1–dependent, rapamycin-resistant pathway sensitizes glioblastomas to antilipogenic therapy.* Sci. Signal., 2009. **2**(101): p. ra82-ra82.

274. Guo, D., et al., *An LXR agonist promotes glioblastoma cell death through inhibition of an EGFR/AKT/SREBP-1/LDLR–dependent pathway.* Cancer discovery, 2011. **1**(5): p. 442-456.

275. Acevedo, A., et al., *LIPEA: Lipid Pathway Enrichment Analysis.* bioRxiv, 2018: p. 274969.

276. Li, S., et al., *Predicting network activity from high throughput metabolomics.* PLoS computational biology, 2013. **9**(7): p. e1003123.

277. Chong, J., et al., *MetaboAnalyst 4.0: towards more transparent and integrative metabolomics analysis.* Nucleic Acids Res, 2018. **46**(W1): p. W486-w494.

278. Dolce, V., et al., *Glycerophospholipid synthesis as a novel drug target against cancer.* Curr Mol Pharmacol, 2011. **4**(3): p. 167-75.

279. Tappia, P.S. and T. Singal, *Phospholipid-mediated signaling and heart disease.* Subcell Biochem, 2008. **49**: p. 299-324.

280. Oude Weernink, P.A., et al., *Dynamic phospholipid signaling by G protein-coupled receptors.* Biochim Biophys Acta, 2007. **1768**(4): p. 888-900.

281. Fernandis, A.Z. and M.R. Wenk, *Membrane lipids as signaling molecules.* Curr Opin Lipidol, 2007. **18**(2): p. 121-8.

282. Brzozowski, J.S., et al., *Lipidomic profiling of extracellular vesicles derived from prostate and prostate cancer cell lines.* Lipids Health Dis, 2018. **17**(1): p. 211.

283. Dixon, S.J., et al., *Ferroptosis: an iron-dependent form of nonapoptotic cell death.* Cell, 2012. **149**(5): p. 1060-1072.

284. Latunde-Dada, G.O., *Ferroptosis: Role of lipid peroxidation, iron and ferritinophagy.* Biochim Biophys Acta Gen Subj, 2017. **1861**(8): p. 1893-1900.

285. Agmon, E., et al., *Modeling the effects of lipid peroxidation during ferroptosis on membrane properties.* Sci Rep, 2018. **8**(1): p. 5155.

286. Agmon, E. and B.R. Stockwell, *Lipid homeostasis and regulated cell death.* Curr Opin Chem Biol, 2017. **39**: p. 83-89.

287. Stockwell, B.R., et al., *Ferroptosis: a regulated cell death nexus linking metabolism, redox biology, and disease.* Cell, 2017. **171**(2): p. 273-285.

288. Beloribi-Djefaflia, S., S. Vasseur, and F. Guillaumond, *Lipid metabolic reprogramming in cancer cells.* Oncogenesis, 2016. **5**(1): p. e189.

289. DeBerardinis, R.J. and N.S. Chandel, *Fundamentals of cancer metabolism.* Sci Adv, 2016. **2**(5): p. e1600200.

290. DeBerardinis, R.J., et al., *The Biology of Cancer: Metabolic Reprogramming Fuels Cell Growth and Proliferation.* Cell Metabolism, 2008. **7**(1): p. 11-20.

291. Pietilainen, K.H., et al., *Acquired obesity is associated with changes in the serum lipidomic profile independent of genetic effects--a monozygotic twin study.* PLoS One, 2007. **2**(2): p. e218.

292. Ekroos, K., et al., *Lipidomics: a tool for studies of atherosclerosis.* Curr Atheroscler Rep, 2010. **12**(4): p. 273-81.

293. Lankinen, M., et al., *Fatty fish intake decreases lipids related to inflammation and insulin signaling--a lipidomics approach.* PLoS One, 2009. **4**(4): p. e5258.

294. de Mello, V.D., et al., *Link between plasma ceramides, inflammation and insulin resistance: association with serum IL-6 concentration in patients with coronary heart disease.* Diabetologia, 2009. **52**(12): p. 2612-5.

295. Graessler, J., et al., *Top-down lipidomics reveals ether lipid deficiency in blood plasma of hypertensive patients.* PLoS One, 2009. **4**(7): p. e6261.

296. Han, X., et al., *Alterations in myocardial cardiolipin content and composition occur at the very earliest stages of diabetes: a shotgun lipidomics study.* Biochemistry, 2007. **46**(21): p. 6417-28.

297. Ollero, M., et al., *Plasma lipidomics reveals potential prognostic signatures within a cohort of cystic fibrosis patients.* J Lipid Res, 2011. **52**(5): p. 1011-22.

298. Gorke, R., et al., *Determining and interpreting correlations in lipidomic networks found in glioblastoma cells.* BMC Syst Biol, 2010. **4**: p. 126.

299. Balogh, G., et al., *Lipidomics reveals membrane lipid remodelling and release of potential lipid mediators during early stress responses in a murine melanoma cell line.* Biochim Biophys Acta, 2010. **1801**(9): p. 1036-47.

300. Kolak, M., et al., *Adipose tissue inflammation and increased ceramide content characterize subjects with high liver fat content independent of obesity.* Diabetes, 2007. **56**(8): p. 1960-8.

301. Zhao, Y.Y., X.L. Cheng, and R.C. Lin, *Lipidomics applications for discovering biomarkers of diseases in clinical chemistry.* Int Rev Cell Mol Biol, 2014. **313**: p. 1-26.

302. Lydic, T.A. and Y.-H. Goo, *Lipidomics unveils the complexity of the lipidome in metabolic diseases.* Clinical and translational medicine, 2018. **7**(1): p. 4-4.

303. Wu, Q., et al., *Cancer-associated adipocytes: key players in breast cancer progression.* Journal of hematology & oncology, 2019. **12**(1): p. 95-95.

304. Balaban, S., et al., *Obesity and cancer progression: is there a role of fatty acid metabolism?* BioMed research international, 2015. **2015**: p. 274585-274585.

305. Zhou, J. and P. Giannakakou, *Targeting microtubules for cancer chemotherapy.* Curr Med Chem Anticancer Agents, 2005. **5**(1): p. 65-71.

306. Luo, X., et al., *The implications of signaling lipids in cancer metastasis.* Experimental & molecular medicine, 2018. **50**(9): p. 127-127.

307. Zhang, T.Y., et al., *Management of castrate resistant prostate cancer-recent advances and optimal sequence of treatments.* Curr Urol Rep, 2013. **14**(3): p. 174-83.

308. Pascual, F. and G.M. Carman, *Phosphatidate phosphatase, a key regulator of lipid homeostasis.* Biochimica et biophysica acta, 2013. **1831**(3): p. 514-522.

309. Brohée, L., et al., *Lipin-1 regulates cancer cell phenotype and is a potential target to potentiate rapamycin treatment.* Oncotarget, 2015. **6**(13): p. 11264-11280.

310. Montoya, A., et al., *The beta adrenergic receptor antagonist propranolol alters mitogenic and apoptotic signaling in late stage breast cancer.* Biomedical Journal, 2019. **42**(3): p. 155-165.

311. Wang, F., et al., *Propranolol suppresses the proliferation and induces the apoptosis of liver cancer cells.* Molecular medicine reports, 2018. **17**(4): p. 5213-5221.

312. Pantziarka, P., et al., *Repurposing Drugs in Oncology (ReDO)-Propranolol as an anti-cancer agent.* Ecancermedicalscience, 2016. **10**: p. 680-680.

313. Hessvik, N.P. and A. Llorente, *Current knowledge on exosome biogenesis and release.* Cellular and molecular life sciences : CMLS, 2018. **75**(2): p. 193-208.

314. Co-operation, O.f.E. and Development, *Toward a New Comprehensive Global Database of Per-and Polyfluoroalkyl Substances (PFASs): Summary Report on Updating the OECD 2007 List of per-and Polyfluoroalkyl Substances (PFASs).* 2018.

315. Banks, R.E., B.E. Smart, and J. Tatlow, *Organofluorine chemistry: principles and commercial applications*. 2013: Springer Science & Business Media.

316. Buck, R.C., *Toxicology data for alternative "short-chain" fluorinated substances*, in *Toxicological Effects of Perfluoroalkyl and Polyfluoroalkyl Substances*. 2015, Springer. p. 451-477.

317. Domingo, J.L., *Health risks of dietary exposure to perfluorinated compounds.* Environment international, 2012. **40**: p. 187-195.

318. Suja, F., B.K. Pramanik, and S.M. Zain, *Contamination, bioaccumulation and toxic effects of perfluorinated chemicals (PFCs) in the water environment: a review paper.* Water Science and Technology, 2009. **60**(6): p. 1533-1544.

319. Sunderland, E.M., et al., *A review of the pathways of human exposure to poly- and perfluoroalkyl substances (PFASs) and present understanding of health effects.* J Expo Sci Environ Epidemiol, 2019. **29**(2): p. 131-147.

320. Winkens, K., et al., *Early life exposure to per- and polyfluoroalkyl substances (PFASs): A critical review.* Emerging Contaminants, 2017. **3**(2): p. 55-68.

321. D'Hollander, W., et al., *Perfluorinated substances in human food and other sources of human exposure.* Rev Environ Contam Toxicol, 2010. **208**: p. 179-215.

322. Post, G.B., et al., *Occurrence and potential significance of perfluorooctanoic acid (PFOA) detected in New Jersey public drinking water systems.* Environmental science & technology, 2009. **43**(12): p. 4547-4554.

323. Barbarossa, A., et al., *Assessment of Perfluorooctane Sulfonate and Perfluorooctanoic Acid Exposure Through Fish Consumption in Italy.* Italian journal of food safety, 2016. **5**(4): p. 6055-6055.

324. Shi, Y., et al., *Tissue distribution of perfluorinated compounds in farmed freshwater fish and human exposure by consumption.* Environ Toxicol Chem, 2012. **31**(4): p. 717-23.

325. Eriksson, U., et al., *Perfluoroalkyl substances (PFASs) in food and water from Faroe Islands.* Environ Sci Pollut Res Int, 2013. **20**(11): p. 7940-8.

326. Hlouskova, V., et al., *Occurrence of brominated flame retardants and perfluoroalkyl substances in fish from the Czech aquatic ecosystem.* Sci Total Environ, 2013. **461-462**: p. 88-98.

327. Chain, E.Panel o.C.i.t.F., et al., *Risk to human health related to the presence of perfluorooctane sulfonic acid and perfluorooctanoic acid in food.* EFSA Journal, 2018. **16**(12): p. e05194.

328. Lewis, R.C., L.E. Johns, and J.D. Meeker, *Serum Biomarkers of Exposure to Perfluoroalkyl Substances in Relation to Serum Testosterone and Measures of Thyroid Function among Adults and Adolescents from NHANES 2011-2012.* Int J Environ Res Public Health, 2015. **12**(6): p. 6098-114.

329. Crinnion, W.J., *The CDC fourth national report on human exposure to environmental chemicals: what it tells us about our toxic burden and how it assists environmental medicine physicians.* Alternative medicine review, 2010. **15**(2): p. 101-109.

330. Calafat, A.M., et al., *Polyfluoroalkyl chemicals in the US population: data from the National Health and Nutrition Examination Survey (NHANES) 2003–2004 and comparisons with NHANES 1999–2000.* Environmental health perspectives, 2007. **115**(11): p. 1596-1602.

331. Graber, J.M., et al., *Per and polyfluoroalkyl substances (PFAS) blood levels after contamination of a community water supply and comparison with 2013-2014 NHANES.* Journal of exposure science & environmental epidemiology, 2019. **29**(2): p. 172-182.

332. Borg, D., et al., *Cumulative health risk assessment of 17 perfluoroalkylated and polyfluoroalkylated substances (PFASs) in the Swedish population.* Environment International, 2013. **59**: p. 112-123.

333. Lieder, P.H., et al., *A two-generation oral gavage reproduction study with potassium perfluorobutanesulfonate (K+ PFBS) in Sprague Dawley rats.* Toxicology, 2009. **259**(1-2): p. 33-45.

334. Lieder, P.H., et al., *Toxicological evaluation of potassium perfluorobutanesulfonate in a 90-day oral gavage study with Sprague–Dawley rats.* Toxicology, 2009. **255**(1-2): p. 45-52.

335. Domingo, J.L. and M. Nadal, *Per- and Polyfluoroalkyl Substances (PFASs) in Food and Human Dietary Intake: A Review of the Recent Scientific Literature.* Journal of Agricultural and Food Chemistry, 2017. **65**(3): p. 533-543.

336. Gorrochategui, E., et al., *Perfluoroalkylated Substance Effects in Xenopus laevis A6 Kidney Epithelial Cells Determined by ATR-FTIR Spectroscopy and Chemometric Analysis.* Chemical research in toxicology, 2016. **29**(5): p. 924-932.

337. Gorrochategui, E., et al., *Chemometric strategy for untargeted lipidomics: biomarker detection and identification in stressed human placental cells.* Analytica chimica acta, 2015. **854**: p. 20-33.

338. Lin, P.-I.D., et al., *Per- and polyfluoroalkyl substances and blood lipid levels in pre-diabetic adults—longitudinal analysis of the diabetes prevention program outcomes study.* Environment International, 2019. **129**: p. 343-353.

339. Liu, J., et al., *[Development and evaluation of a high-fat/high-fructose diet-induced nonalcoholic steatohepatitis mouse model].* Zhonghua Gan Zang Bing Za Zhi, 2014. **22**(6): p. 445-50.

340. EPA, U., *Drinking Water Health Advisory for Perfluorooctanoic Acid (PFOA).* EPA Document Number: 822-R-16-005, 2016.

341. PFOS, P.S., *ENVIRONMENTAL CRITERIA PERFLUORINATED ALKYL COMPOUNDS.*

342. Tiwari-Heckler, S., et al., *Circulating Phospholipid Patterns in NAFLD Patients Associated with a Combination of Metabolic Risk Factors.* Nutrients, 2018. **10**(5): p. 649.

343. Ipsen, D.H., J. Lykkesfeldt, and P. Tveden-Nyborg, *Molecular mechanisms of hepatic lipid accumulation in non-alcoholic fatty liver disease.* Cellular and molecular life sciences : CMLS, 2018. **75**(18): p. 3313-3327.

344. Gorden, D.L., et al., *Increased diacylglycerols characterize hepatic lipid changes in progression of human nonalcoholic fatty liver disease; comparison to a murine model.* PloS one, 2011. **6**(8): p. e22775-e22775.

345. Barr, J., et al., *Obesity-dependent metabolic signatures associated with nonalcoholic fatty liver disease progression.* Journal of proteome research, 2012. **11**(4): p. 2521-2532.

346. Vance, J.E., *Lipoproteins secreted by cultured rat hepatocytes contain the antioxidant 1-alk-1-enyl-2-acylglycerophosphoethanolamine.* Biochimica et Biophysica Acta (BBA)-Lipids and Lipid Metabolism, 1990. **1045**(2): p. 128-134.

347. Puri, P., et al., *The plasma lipidomic signature of nonalcoholic steatohepatitis.* Hepatology, 2009. **50**(6): p. 1827-1838.

348. Nelson, J.W., E.E. Hatch, and T.F. Webster, *Exposure to polyfluoroalkyl chemicals and cholesterol, body weight, and insulin resistance in the general US population.* Environmental health perspectives, 2009. **118**(2): p. 197-202.

349. Gorden, D.L., et al., *Biomarkers of NAFLD progression: a lipidomics approach to an epidemic.* Journal of lipid research, 2015. **56**(3): p. 722-736.

350. Fu, Y., et al., *Associations between serum concentrations of perfluoroalkyl acids and serum lipid levels in a Chinese population.* Ecotoxicology and environmental safety, 2014. **106**: p. 246-252.

351. Starling, A.P., et al., *Perfluoroalkyl substances and lipid concentrations in plasma during pregnancy among women in the Norwegian Mother and Child Cohort Study.* Environment international, 2014. **62**: p. 104-112.

352. Liew, Z., H. Goudarzi, and Y. Oulhote, *Developmental Exposures to Perfluoroalkyl Substances (PFASs): An Update of Associated Health Outcomes.* Current environmental health reports, 2018. **5**(1): p. 1-19.

353. Huang, M.C., et al., *Toxicokinetics of perfluorobutane sulfonate (PFBS), perfluorohexane-1-sulphonic acid (PFHxS), and perfluorooctane sulfonic acid (PFOS) in male and female Hsd:Sprague Dawley SD rats after intravenous and gavage administration.* Toxicology reports, 2019. **6**: p. 645-655.

354. Hayward, S.W., et al., *Malignant transformation in a nontumorigenic human prostatic epithelial cell line.* Cancer research, 2001. **61**(22): p. 8135-8142.

355. Katoh, M. and H. Nakagama, *FGF receptors: cancer biology and therapeutics.* Medicinal research reviews, 2014. **34**(2): p. 280-300.

356. Feng, S., et al., *FGF23 promotes prostate cancer progression.* Oncotarget, 2015. **6**(19): p. 17291.

357. Corn, P.G., et al., *Targeting fibroblast growth factor pathways in prostate cancer.* Clinical cancer research, 2013. **19**(21): p. 5856-5866.

358. Nagamatsu, H., et al., *FGF19 promotes progression of prostate cancer.* The Prostate, 2015. **75**(10): p. 1092-1101.

359. Dieci, M.V., et al., *Fibroblast growth factor receptor inhibitors as a cancer treatment: from a biologic rationale to medical perspectives.* Cancer discovery, 2013. **3**(3): p. 264-279.

360. Acevedo, V.D., et al., *Inducible FGFR-1 activation leads to irreversible prostate adenocarcinoma and an epithelial-to-mesenchymal transition.* Cancer cell, 2007. **12**(6): p. 559-571.

361. Wan, X., et al., *Prostate cancer cell-stromal cell crosstalk via FGFR1 mediates antitumor activity of dovitinib in bone metastases.* Sci Transl Med, 2014. **6**(252): p. 252ra122.

362. Guo, Z., et al., *Regulation of androgen receptor activity by tyrosine phosphorylation.* Cancer cell, 2006. **10**(4): p. 309-319.

363. Wu, Y.-M., et al., *Identification of targetable FGFR gene fusions in diverse cancers.* Cancer discovery, 2013. **3**(6): p. 636-647.

364. Kwabi-Addo, B., M. Ozen, and M. Ittmann, *The role of fibroblast growth factors and their receptors in prostate cancer.* Endocrine-related cancer, 2004. **11**(4): p. 709-724.

365. Bova, G.S., et al., *Integrated clinical, whole-genome, and transcriptome analysis of multisampled lethal metastatic prostate cancer.* Molecular Case Studies, 2016. **2**(3): p. a000752.

366. Mehta, P., et al., *Fibroblast growth factor receptor‐2 mutation analysis in human prostate cancer.* BJU international, 2000. **86**(6): p. 681-685.

367. Freeman, K.W., et al., *Inducible prostate intraepithelial neoplasia with reversible hyperplasia in conditional FGFR1-expressing mice.* Cancer research, 2003. **63**(23): p. 8256-8263.

368. Xin, L., et al., *In vivo regeneration of murine prostate from dissociated cell populations of postnatal epithelia and urogenital sinus mesenchyme.* Proceedings of the National Academy of Sciences, 2003. **100**(suppl 1): p. 11896-11903.

369. Memarzadeh, S., et al., *Enhanced paracrine FGF10 expression promotes formation of multifocal prostate adenocarcinoma and an increase in epithelial androgen receptor.* Cancer cell, 2007. **12**(6): p. 572-585.

370. Memarzadeh, S., et al., *Role of autonomous androgen receptor signaling in prostate cancer initiation is dichotomous and depends on the oncogenic signal.* Proceedings of the National Academy of Sciences, 2011. **108**(19): p. 7962-7967.

371. Tomlins, S.A., et al., *Role of the TMPRSS2-ERG gene fusion in prostate cancer.* Neoplasia (New York, NY), 2008. **10**(2): p. 177.

372. Sadar, M.D., *Small molecule inhibitors targeting the "achilles' heel" of androgen receptor activity.* Cancer research, 2011. **71**(4): p. 1208-1213.

373. Taylor, B.S., et al., *Integrative genomic profiling of human prostate cancer.* Cancer cell, 2010. **18**(1): p. 11-22.

374. Xin, L., et al., *Progression of prostate cancer by synergy of AKT with genotropic and nongenotropic actions of the androgen receptor.* Proceedings of the National Academy of Sciences, 2006. **103**(20): p. 7789-7794.

375. Zong, Y., et al., *ETS family transcription factors collaborate with alternative signaling pathways to induce carcinoma from adult murine prostate cells.* Proc Natl Acad Sci U S A, 2009. **106**(30): p. 12465-70.

376. Cai, H., et al., *Collaboration of Kras and androgen receptor signaling stimulates EZH2 expression and tumor-propagating cells in prostate cancer.* Cancer Res, 2012. **72**(18): p. 4672-81.

377. Cai, H., et al., *Invasive prostate carcinoma driven by c-Src and androgen receptor synergy.* Cancer research, 2011. **71**(3): p. 862-872.

378. Cai, H., et al., *Differential transformation capacity of Src family kinases during the initiation of prostate cancer.* Proceedings of the National Academy of Sciences, 2011. **108**(16): p. 6579-6584.

379. Lacal, P., C. Pennington, and J. Lacal, *Transforming activity of ras proteins translocated to the plasma membrane by a myristoylation sequence from the src gene product.* Oncogene, 1988. **2**(6): p. 533-537.

380. Patwardhan, P. and M.D. Resh, *Myristoylation and membrane binding regulate c-Src stability and kinase activity.* Molecular and cellular biology, 2010. **30**(17): p. 4094-4107.

381. Kim, S., et al., *Blocking myristoylation of Src inhibits its kinase activity and suppresses prostate cancer progression.* Cancer research, 2017. **77**(24): p. 6950-6962.

382. Bluemn, E.G., et al., *Androgen receptor pathway-independent prostate cancer is sustained through FGF signaling.* Cancer cell, 2017. **32**(4): p. 474-489. e6.

383. Katoh, Y. and M. Katoh, *FGFR2-related pathogenesis and FGFR2-targeted therapeutics.* International journal of molecular medicine, 2009. **23**(3): p. 307-311.

384. Ranieri, D., et al., *Expression of the FGFR2 mesenchymal splicing variant in epithelial cells drives epithelial-mesenchymal transition.* Oncotarget, 2016. **7**(5): p. 5440.

385. Savagner, P., et al., *Alternative splicing in fibroblast growth factor receptor 2 is associated with induced epithelial-mesenchymal transition in rat bladder carcinoma cells.* Molecular biology of the cell, 1994. **5**(8): p. 851-862.

386. Zhu, D.-Y., et al., *Twist1 correlates with poor differentiation and progression in gastric adenocarcinoma via elevation of FGFR2 expression.* World Journal of Gastroenterology: WJG, 2014. **20**(48): p. 18306.

387. Qian, X., et al., *N-cadherin/FGFR promotes metastasis through epithelial-to-mesenchymal transition and stem/progenitor cell-like properties.* Oncogene, 2014. **33**(26): p. 3411.

388. Sandilands, E., et al., *Src kinase modulates the activation, transport and signalling dynamics of fibroblast growth factor receptors.* EMBO reports, 2007. **8**(12): p. 1162-1169.

389. Brooks, A.N., E. Kilgour, and P.D. Smith, *Molecular pathways: fibroblast growth factor signaling: a new therapeutic opportunity in cancer.* Clinical cancer research, 2012. **18**(7): p. 1855-1862.

390. Ridyard, M.S. and S.M. Robbins, *Fibroblast growth factor-2-induced signaling through lipid raft-associated fibroblast growth factor receptor substrate 2 (FRS2).* J Biol Chem, 2003. **278**(16): p. 13803-9.

391. Su, N., M. Jin, and L. Chen, *Role of FGF/FGFR signaling in skeletal development and homeostasis: learning from mouse models.* Bone Res, 2014. **2**: p. 14003.

392. Kim, S., et al., *Myristoylation of Src kinase mediates Src-induced and high-fat diet–accelerated prostate tumor progression in mice.* Journal of Biological Chemistry, 2017. **292**(45): p. 18422-18433.

393. Felsted, R.L., C.J. Glover, and K. Hartman, *Protein N-myristoylation as a chemotherapeutic target for cancer.* J Natl Cancer Inst, 1995. **87**(21): p. 1571-3.

394. Ducker, C.E., et al., *Two N-myristoyltransferase isozymes play unique roles in protein myristoylation, proliferation, and apoptosis.* Mol Cancer Res, 2005. **3**(8): p. 463-76.

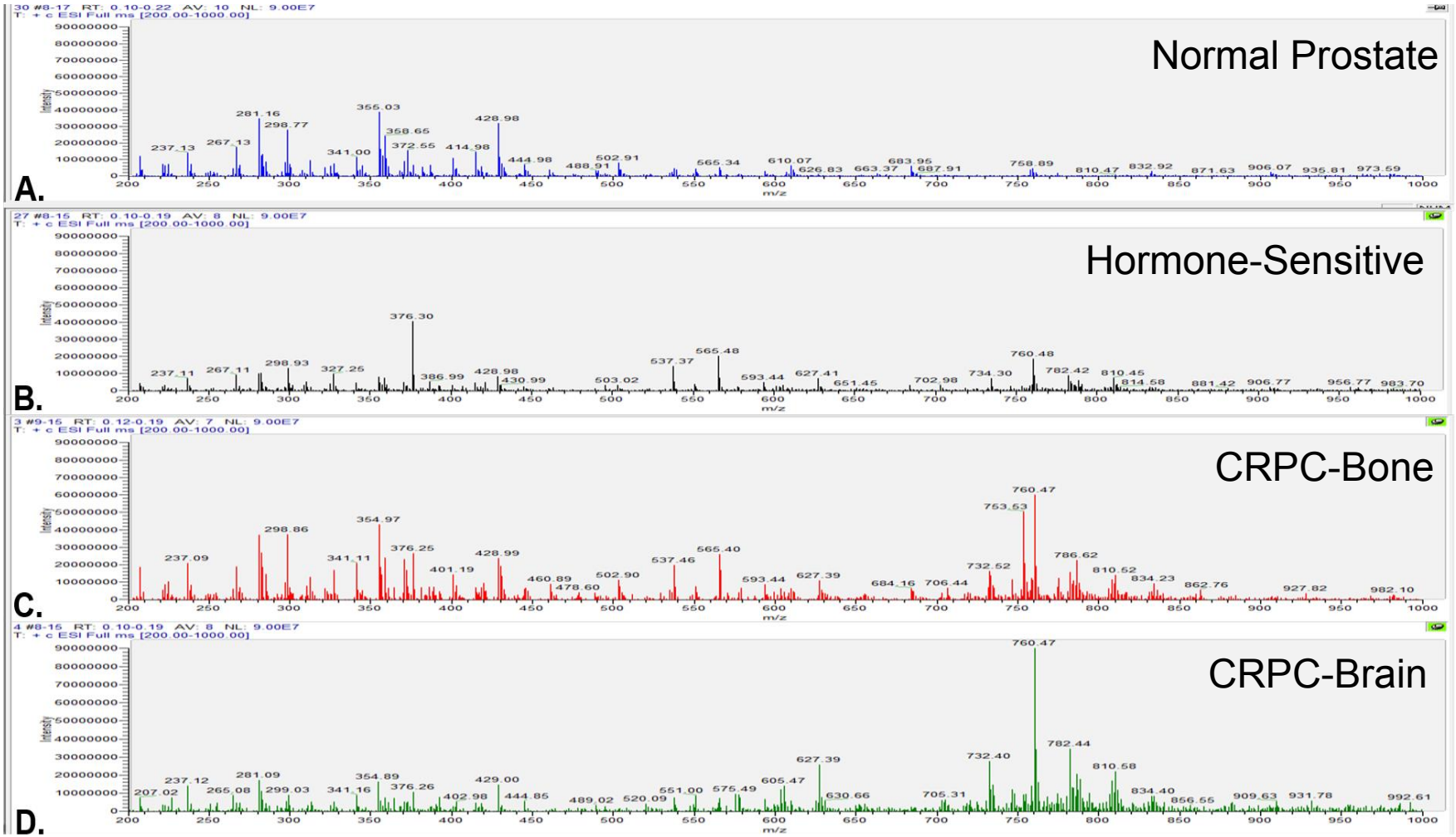

Figure 3.1. ESI mass spectrum of non-cancerous PNT2 **(A)**, hormone sensitive LNCaP **(B)**, CRPC PC-3-bone metastasized **(C)** and CRPC-brain DU-145 metastasized **(D)** lipid extract, as recorded in the positive ion mode. Spectra were derived using a LCQ Deca ion-trap mass spectrometer. Spectra are representative of at least 4 (n = 4) separate experiment

A.

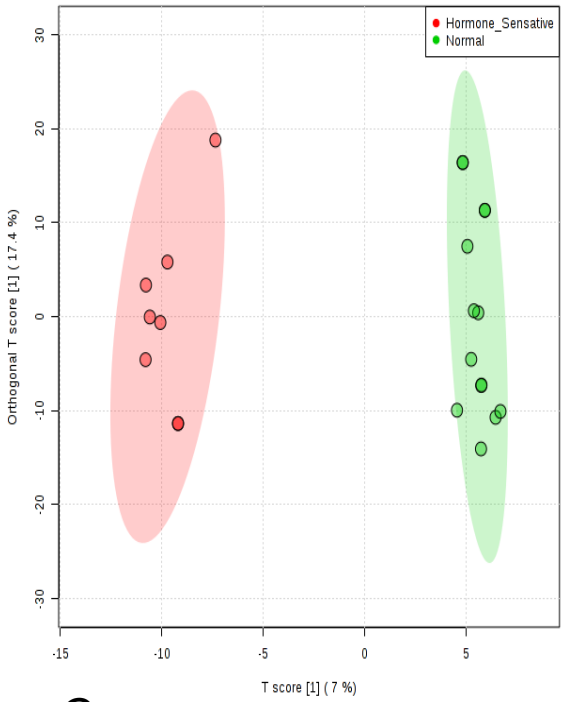
Scores Plot
Hormone_Sensative
Normal
Orthogonal T score [1] (17.4 %)
T score [1] (7 %)

B.

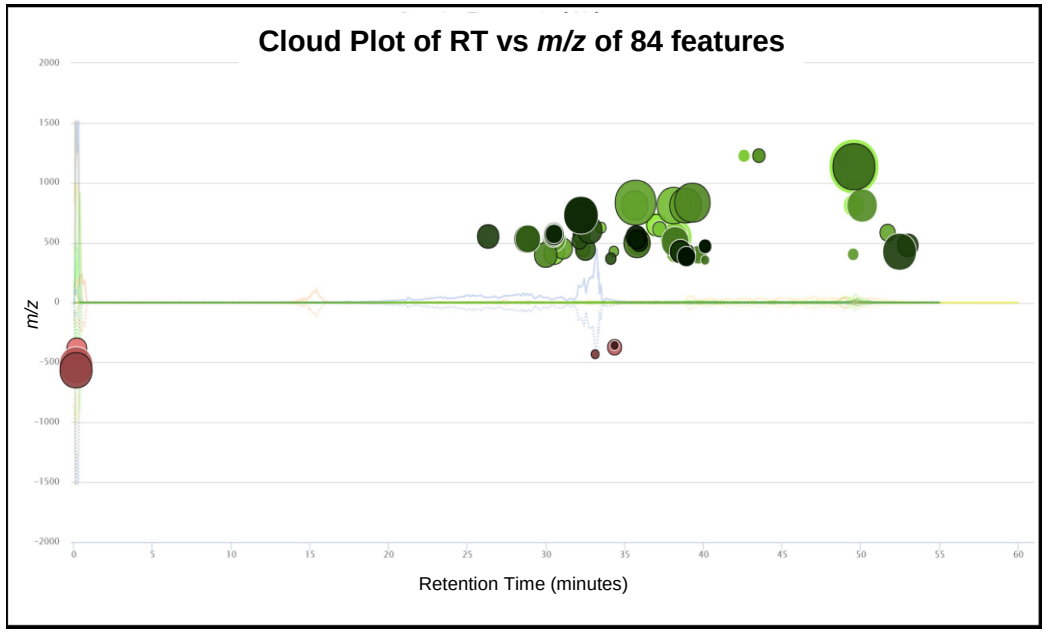
Cloud Plot of RT vs m/z of 84 features
m/z
Retention Time (minutes)

C.

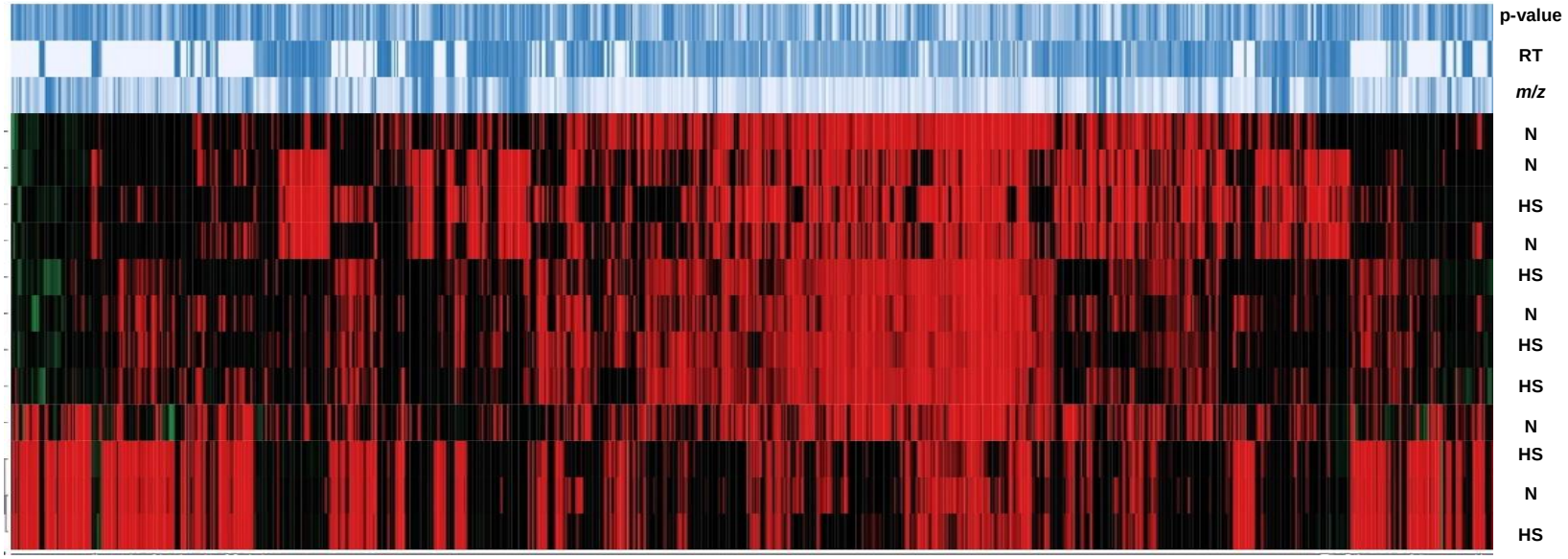
p-value
RT
m/z
N
N
HS
N
HS
N
HS
HS
N
HS
N
HS

Figure 3.2. A) Multiple variable analysis (MVA) of lipid features isolated from hormone sensitive LNCaP and 22RV1 cells. **B)** Differential cloud plot demonstrating dysregulated features between hormone-sensitive cells and non-cancerous cells PNT2 and RWPE1 (*p-value* <= 0.05 threshold, fold change >= 1.5 threshold). Up-regulated features (features that have a positive fold change) are graphed above the x-axis shown in green while down-regulated features (features that have a negative fold change) shown in red are graphed below the x-axis. **C**) Differential expression of lipid features in non-cancerous prostate cells (N) as compared to hormone-sensitive (HS) prostate cancer cells. Only those features who levels varied significantly ($p < 0.05$) are projected on the heat map. Rows represents a metabolite feature and each column represents a sample.

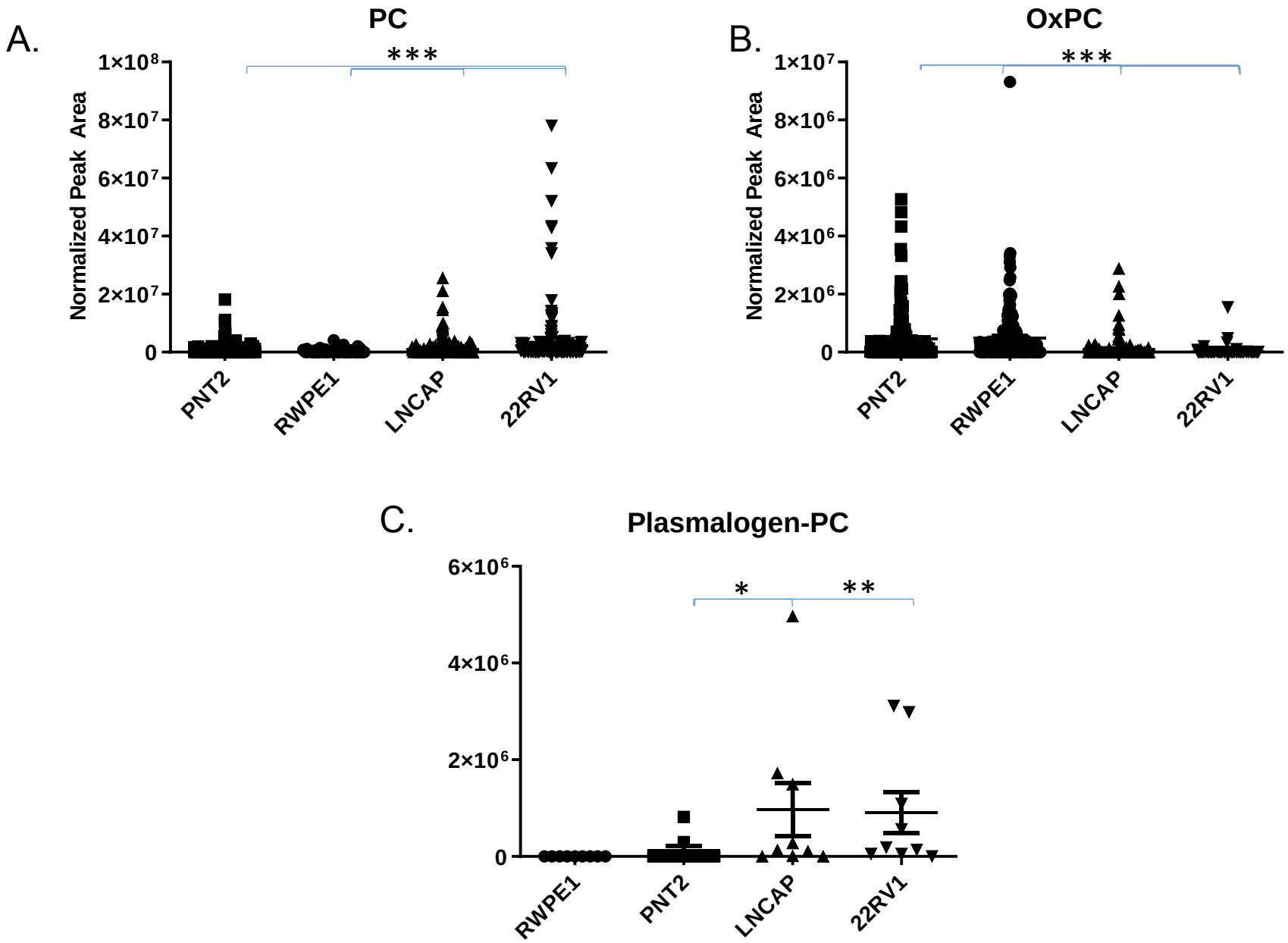
A.
PC
***
Normalized Peak Area
1×10^8
8×10^7
6×10^7
4×10^7
2×10^7
0
PNT2
RWPE1
LNCAP
22RV1
B.
OxPC
***
Normalized Peak Area
1×10^7
8×10^6
6×10^6
4×10^6
2×10^6
0
PNT2
RWPE1
LNCAP
22RV1
C.
Plasmalogen-PC
*
**
6×10^6
4×10^6
2×10^6
0
RWPE1
PNT2
LNCAP
22RV1

Figure 3.3. Comparison of phosphatidylcholine (PC) levels in non-cancerous (PNT2 and RWPE1) prostate and hormone-sensitive (LNCaP and 22RV1) prostate cancer cell lines. Data are indicative of 6 samples per group and are expressed as mean ± the SEM (*$p < 0.05$ **$p < 0.01$*** $p < 0.001$). Each symbol represents an individual lipid feature as identified by MS/MS. Difference in normalized peak areas between hormone-sensitive and non-cancerous prostate cells are shown for (**A**) phosphatidylcholine (PC), **B**) oxidized-PC and **C)** plasmalogen PC.

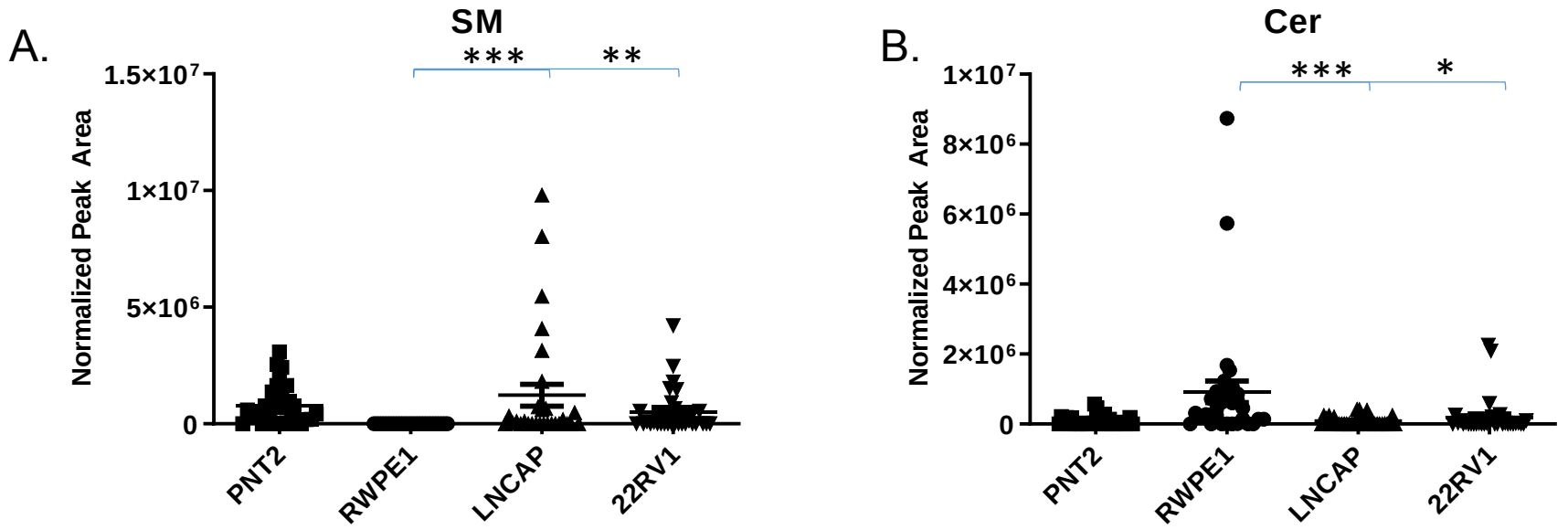

Figure 3.4. Comparison of sphingolipid levels in non-cancerous (PNT2 and RWPE1) and hormone-sensitive (LNCaP and 22RV1) prostate cell lines. Data are indicative of 6 samples per group and are expressed as mean ± the SEM (*$p < 0.05$ **$p < 0.01$*** $p < 0.001$). Each symbol represents an individual lipid feature as identified by MS/MS. Normalized peak areas between hormone-sensitive and control cells shown for **A)** sphingomyelin (SM) and **b)** ceramide (Cer) species.

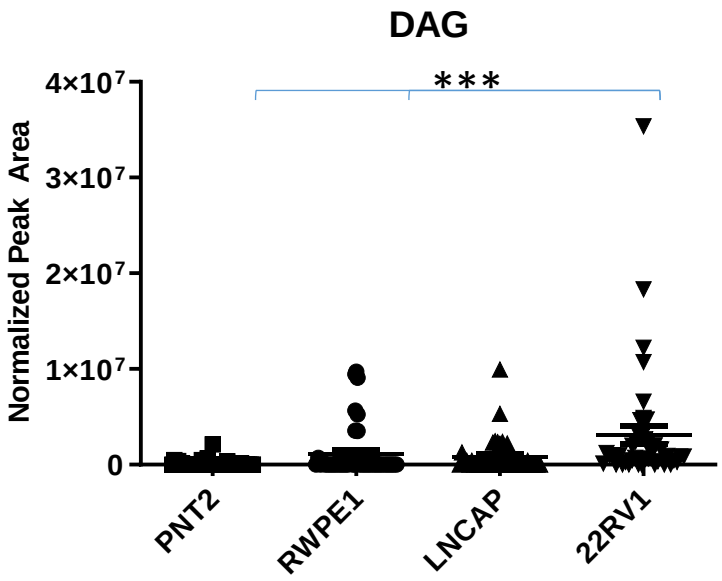

Figure 3.5. Comparison of diacylglycerol (DAG) levels in non-cancerous (PNT2 and RWPE1) and hormone-sensitive (LNCaP and 22RV1) prostate cell lines. Data are indicative of 6 samples per group and are expressed as mean ± the SEM (*$p < 0.05$ **$p < 0.01$*** $p < 0.001$). Each symbol represents an individual lipid feature as identified by MS/MS. Normalized peak areas between hormone-sensitive and control cells shown above.

A.

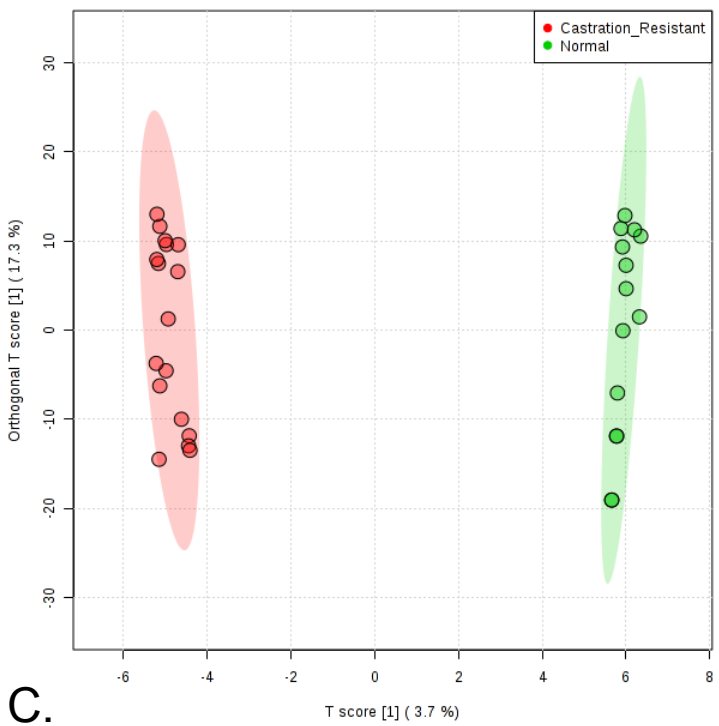
Scores Plot
Castration_Resistant
Normal
Orthogonal T score [1] (17.3 %)
T score [1] (3.7 %)

B.

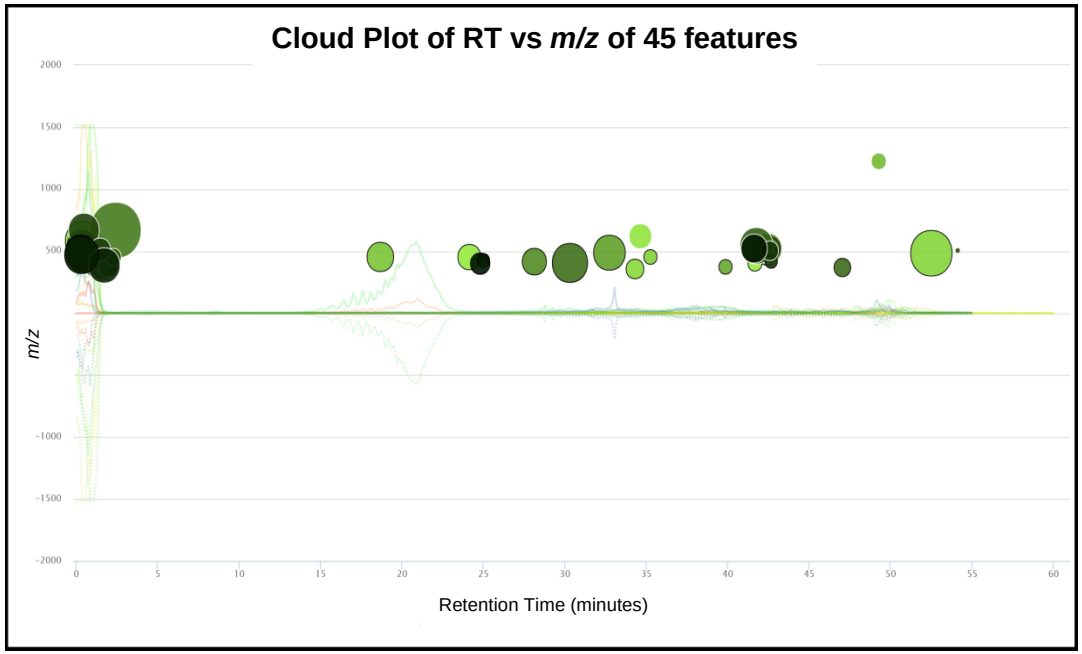
Cloud Plot of RT vs m/z of 45 features
m/z
Retention Time (minutes)

C.

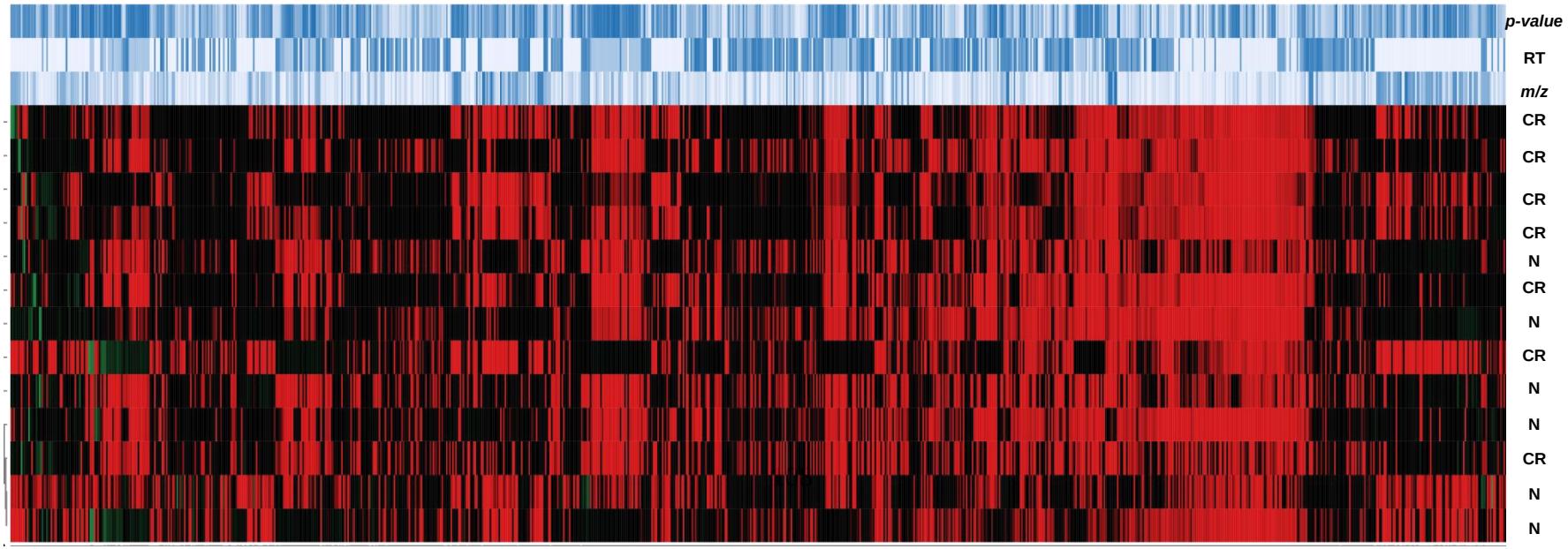
p-value
RT
m/z
CR
CR
CR
CR
N
CR
N
CR
N
N
CR
N
N

Figure 3.6. A) Multiple variable analysis (MVA) of lipid features isolated from castration-resistant PC-3 and DU-145 cells. **B**) Differential cloud plot demonstrating dysregulated features between hormone-sensitive cells and non-cancerous cells (PNT2 and RWPE1) (*p*-value <= 0.05 threshold, fold change >= 1.5 threshold). Up-regulated features (features that have a positive fold change) are graphed above the x-axis shown in green while down-regulated features (features that have a negative fold change), shown in red, are graphed below the x-axis. **C**) Differential expression of lipid features in non-cancerous prostate cells (N) as compared to castration-resistant (CR) prostate cancer cells. Only those features who levels that vary significantly ($p < 0.05$) are projected on the heat map. Each row in **C**. represents a metabolite feature and each column represents a sample.

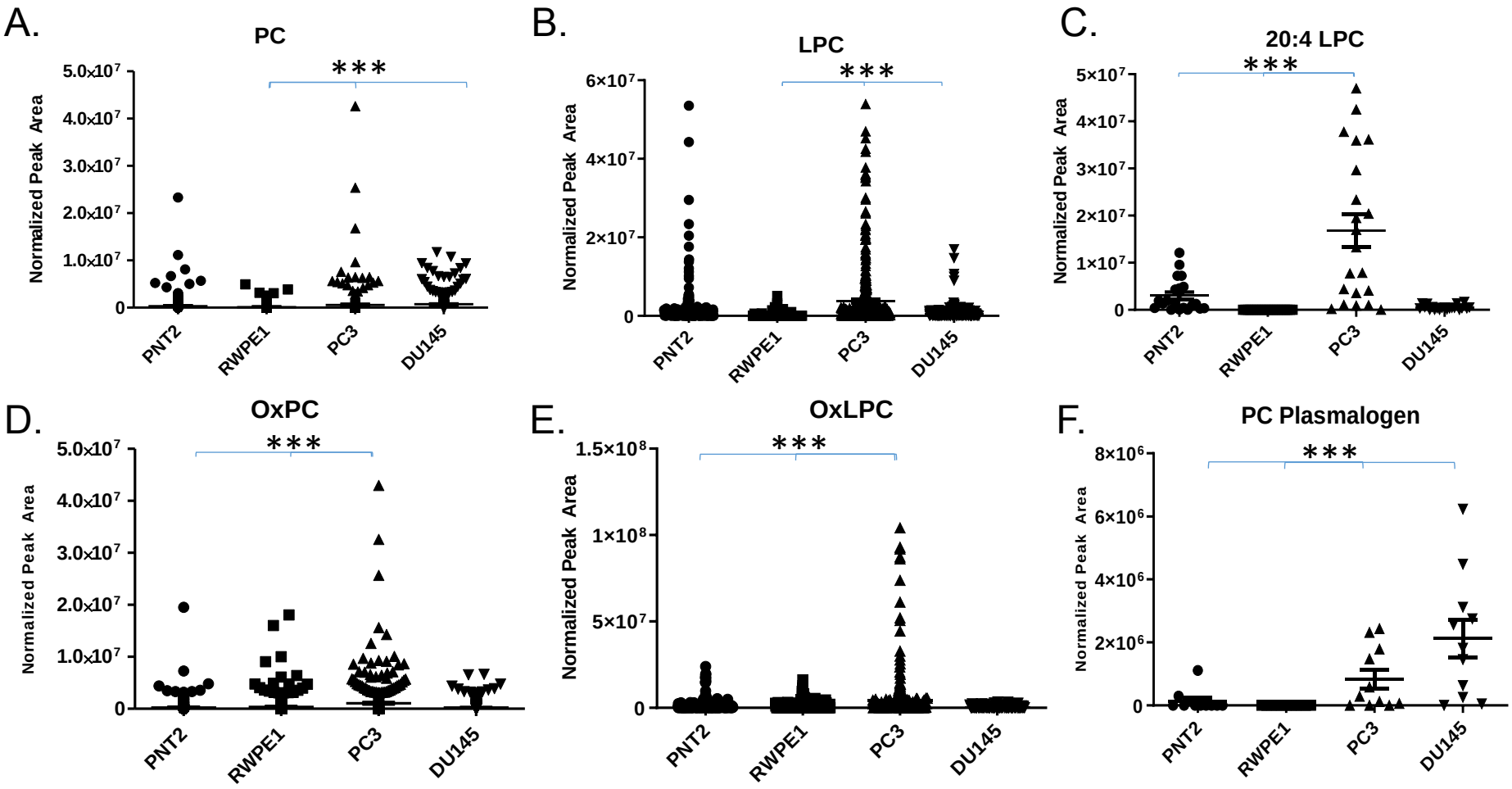
A.
PC
***
Normalized Peak Area
5.0x10^7
4.0x10^7
3.0x10^7
2.0x10^7
1.0x10^7
0
PNT2
RWPE1
PC3
DU145
B.
LPC
***
Normalized Peak Area
6×10^7
4×10^7
2×10^7
0
PNT2
RWPE1
PC3
DU145
C.
20:4 LPC
***
Normalized Peak Area
5×10^7
4×10^7
3×10^7
2×10^7
1×10^7
0
PNT2
RWPE1
PC3
DU145
D.
OxPC
***
Normalized Peak Area
5.0x10^7
4.0x10^7
3.0x10^7
2.0x10^7
1.0x10^7
0
PNT2
RWPE1
PC3
DU145
E.
OxLPC
***
Normalized Peak Area
1.5×10^8
1×10^8
5×10^7
0
PNT2
RWPE1
PC3
DU145
F.
PC Plasmalogen
***
Normalized Peak Area
8×10^6
6×10^6
4×10^6
2×10^6
0
PNT2
RWPE1
PC3
DU145

Figure 3.7. Comparison of phosphatidylcholine (PC) levels in non-cancerous (PNT2 and RWPE1) and castration-resistant (PC-3 and DU-145) prostate cell lines. Data are indicative of 6 samples per group and are expressed as mean ± the SEM (*$p < 0.05$ **$p < 0.01$*** $p < 0.001$). Each symbol represents an individual lipid feature as identified by MS/MS. Normalized peak areas between castration-resistant and control cells shown for **A)** phosphatidylcholine (PC), **B)** lysophosphatidylcholine (LPC), **C)** 20:4 LPC,**D)** oxidized-PC(OxPC), **E)** oxidized LPC (OxLPC) and **F)** PC plasmalogen.

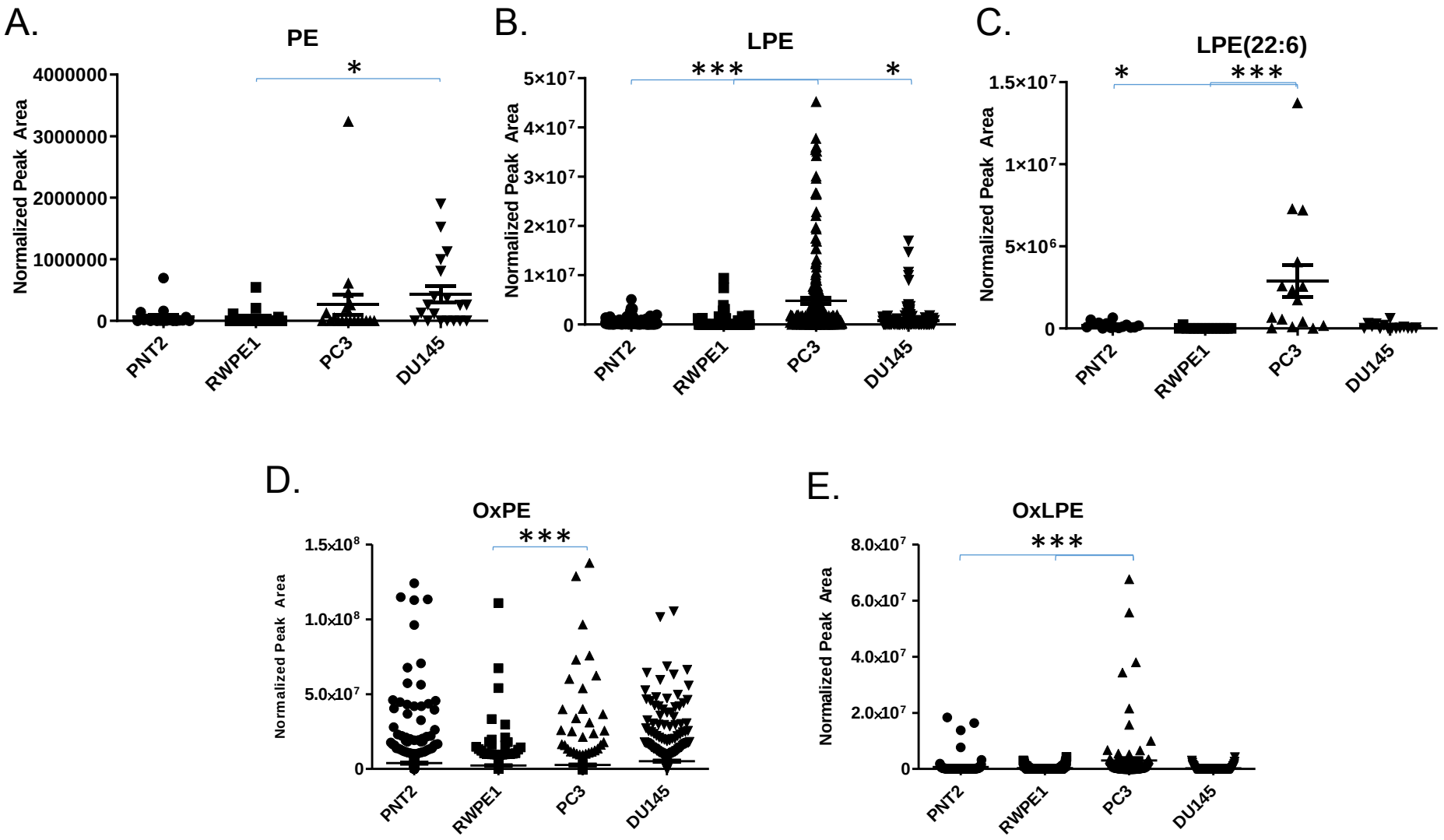
A.
PE
Normalized Peak Area
4000000
3000000
2000000
1000000
0
*
PNT2
RWPE1
PC3
DU145
B.
LPE
Normalized Peak Area
5×10^7
4×10^7
3×10^7
2×10^7
1×10^7
0
***
*
PNT2
RWPE1
PC3
DU145
C.
LPE(22:6)
Normalized Peak Area
1.5×10^7
1×10^7
5×10^6
0
*
***
PNT2
RWPE1
PC3
DU145
D.
OxPE
Normalized Peak Area
1.5x10^8
1.0x10^8
5.0x10^7
0
***
PNT2
RWPE1
PC3
DU145
E.
OxLPE
Normalized Peak Area
8.0x10^7
6.0x10^7
4.0x10^7
2.0x10^7
0
***
PNT2
RWPE1
PC3
DU145

Figure 3.8. Comparison of phosphatidylethanolamine (PE) levels in non-cancerous (PNT2 and RWPE1) and castration-resistant (PC-3 and DU-145) prostate cell lines. Data are indicative of 6 samples per group and are expressed as mean ± the SEM (*$p < 0.05$ **$p < 0.01$*** $p < 0.001$). Each symbol represents an individual lipid feature as identified by MS/MS. Normalized peak areas between castration-resistant and control cells are shown for **A)** phosphatidylethanolamine (PE), **B)** lysophosphatidylethanolamine (LPE), **C)** lysophosphatidylethanolamine (22:6 LPC), **D)** oxidized PE (OxPE) and **E)** oxidized lysophosphatidylethanolamine (OxLPE).

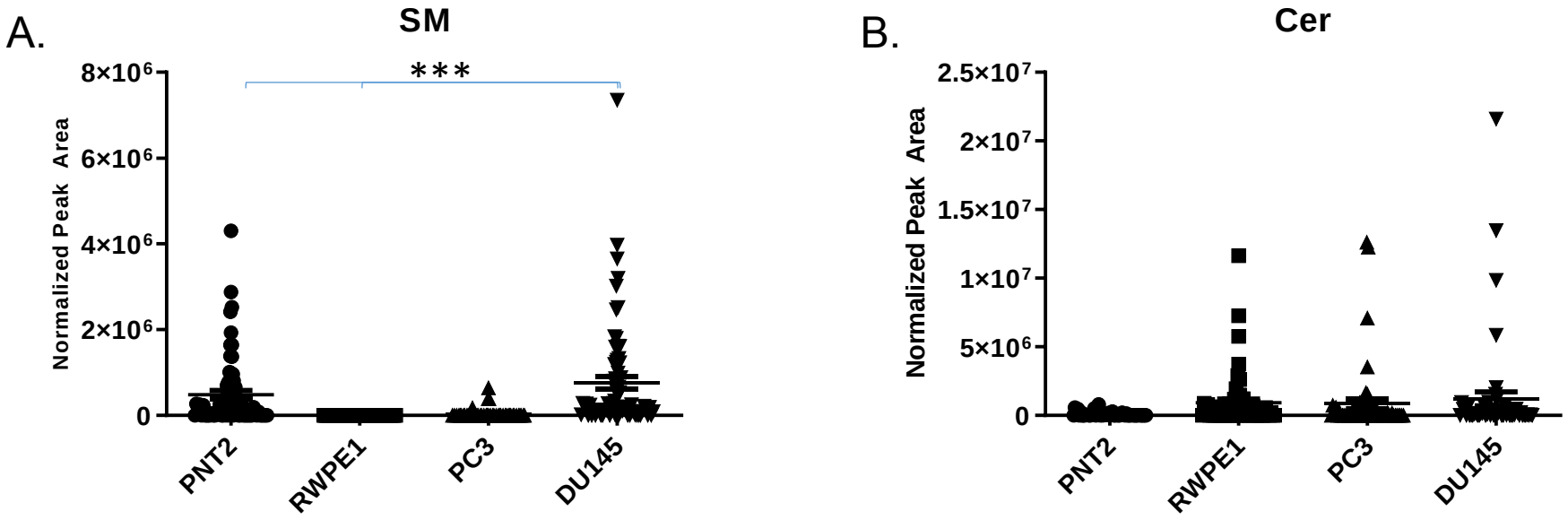

Figure 3.9. Comparison of sphingolipid levels in non-cancerous (PNT2 and RWPE1) and castration-resistant (PC-3 and DU-145) prostate cell lines. Data are indicative of 6 samples per group and are expressed as mean ± the SEM (*$p < 0.05$ **$p < 0.01$*** $p < 0.001$). Each symbol represents an individual lipid feature as identified by MS/MS. Normalized peak areas between castration-resistant and control cells are shown for **A)** sphingomyelin (SM) and **B)** ceramide (Cer).

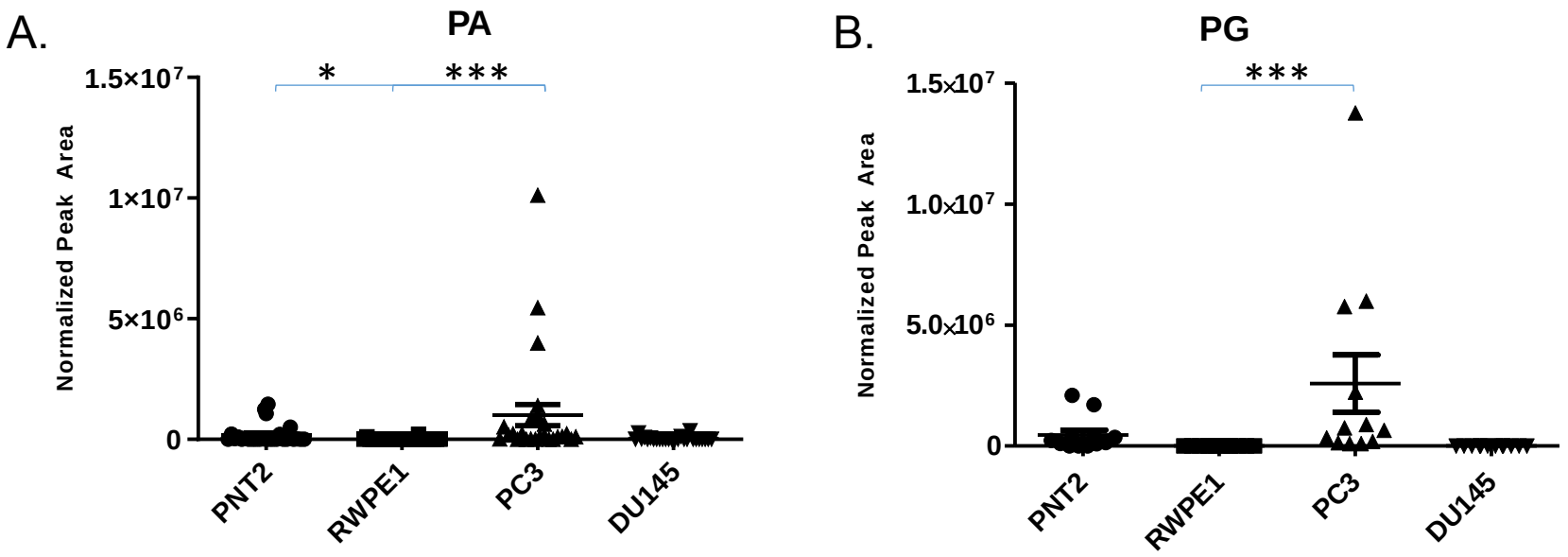

Figure 3.10. Comparison of additional glycerophospholipids in non-cancerous (PNT2 and RWPE1) and castration-resistant (PC-3 and DU-145) prostate cell lines. Data are indicative of 6 samples per group and are expressed as mean ± the SEM (*$p < 0.05$ **$p < 0.01$*** $p < 0.001$). Each symbol represents an individual lipid feature as identified by MS/MS. Normalized peak areas between castration-resistant and control cells are shown for **A)** phosphatidic acid (PA) and **B)** phosphatidylglycerol (PG).

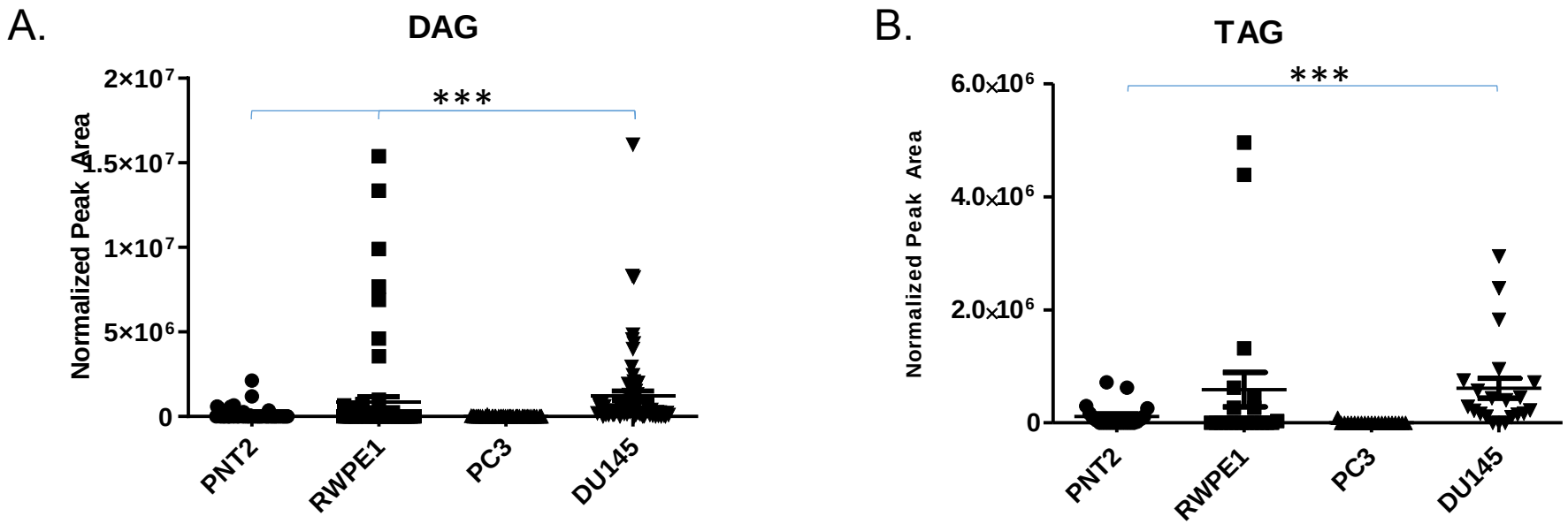

Figure 3.11. Comparison of acylglycerides in non-cancerous (PNT2 and RWPE1) and castration-resistant (PC-3 and DU-145) prostate cell lines. Data are indicative of 6 samples per group and are expressed as mean ± the SEM (*$p < 0.05$ **$p < 0.01$*** $p < 0.001$). Each symbol represents an individual lipid feature as identified by MS/MS. Normalized peak areas between castration-resistant and control cells are shown for **A)** diacylglycerol (DAG) and **B)** triacylglycerol (TAG).

A.

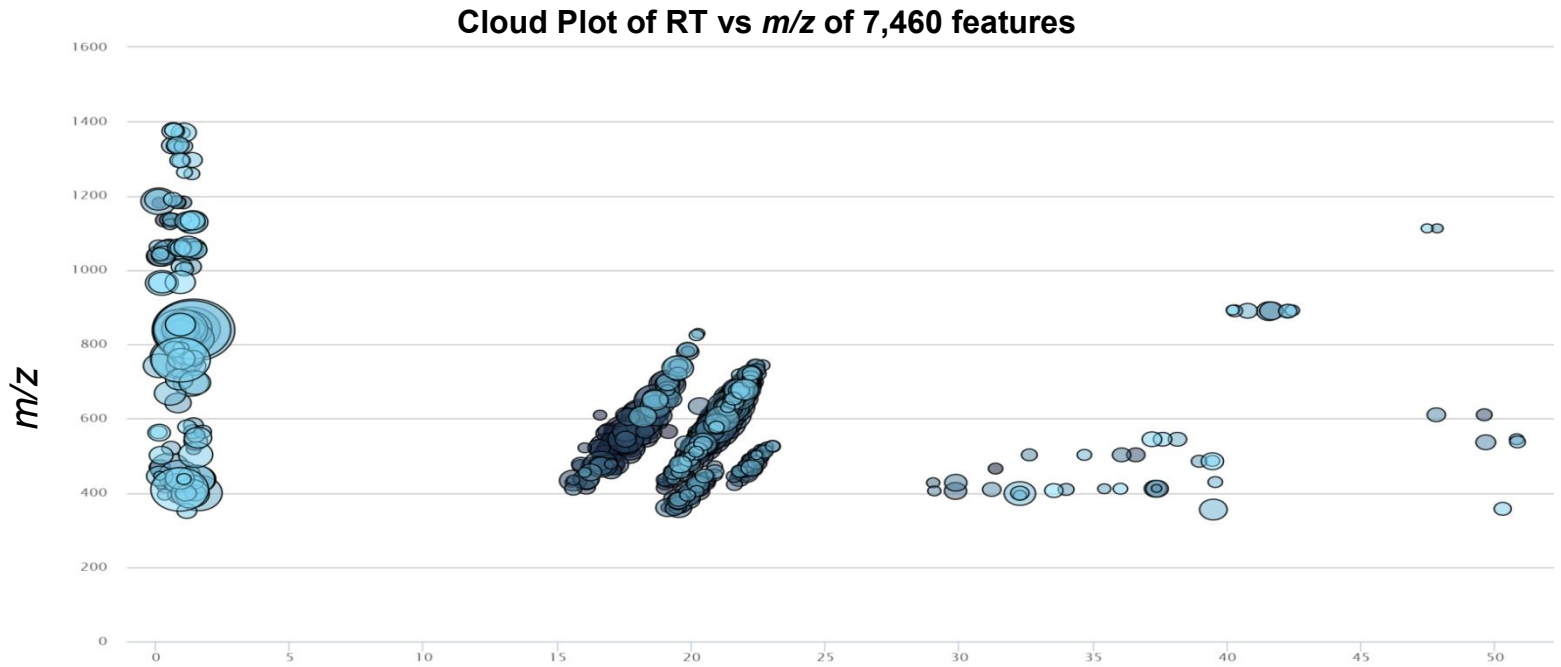
Cloud Plot of RT vs *m/z* of 7,460 features
m/z
1600
1400
1200
1000
800
600
400
200
0
0
5
10
15
20
25
30
35
40
45
50
Retention Time (minutes)

B.

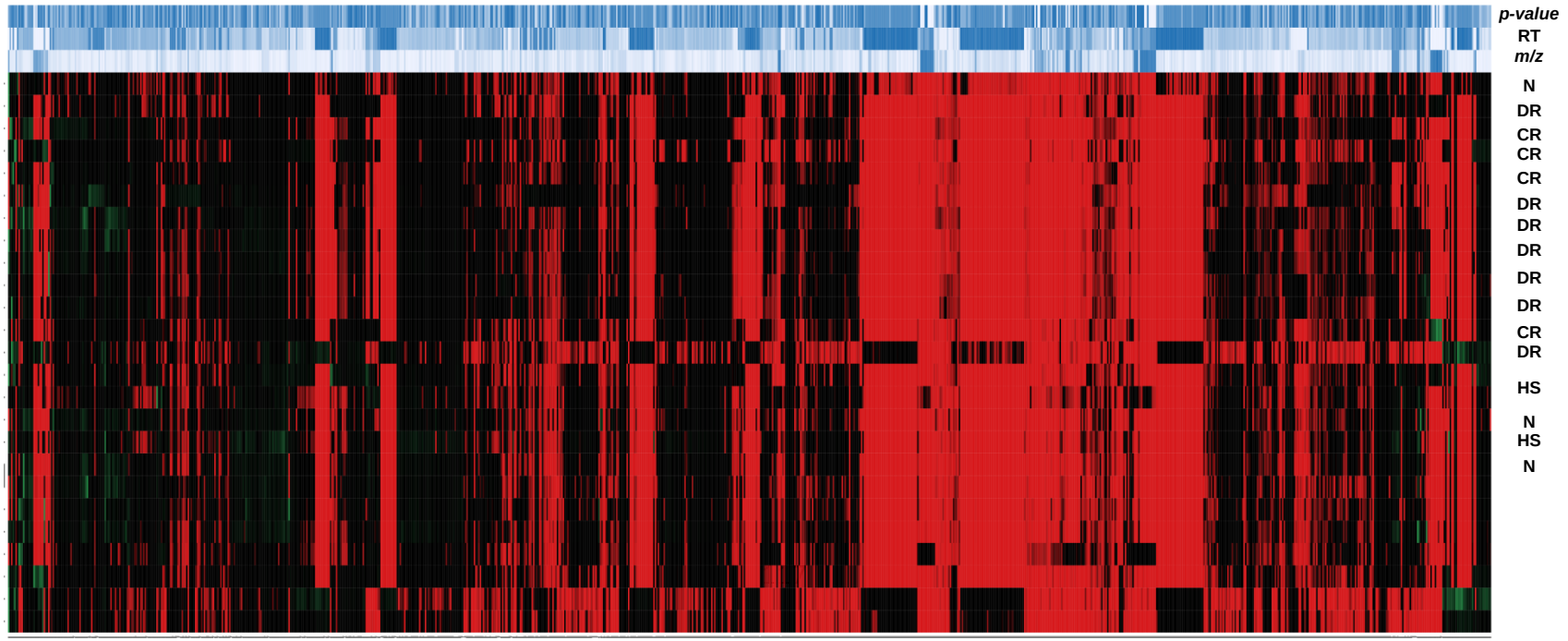
p-value
RT
m/z
N
DR
CR
CR
CR
DR
DR
DR
DR
DR
CR
DR
HS
N
HS
N

Figure 3.12. A) Multiple variable analysis (MVA) of lipid features isolated from hormone sensitive (LNCaP and 22RV1), castration-resistant (PC-3 and DU-145) and Docetaxel resistant (PC3-Rx and DU145-DR) cells. **B**) Differential cloud plot demonstrating dysregulated features between hormone-sensitive, castration-resistant, Docetaxel resistant cells and non-cancerous cells (PNT2 and RWPE1) (*p*-value < 0.05 threshold, fold change > 1.5 threshold). Up-regulated features (features that have a positive fold change) are graphed above the x-axis shown in green while down-regulated features, (features that have a negative fold change), shown in red, are graphed below the x-axis. **C**) Differential expression of lipid features in non-cancerous prostate cells (N) as compared to hormone-sensitive (HS), castration-resistant (CR) and Docetaxel resistant (DR) prostate cancer cells. Only those features who levels that vary significantly ($p < 0.05$) are projected on the heat map. Each row represents a metabolite feature and each column represents a sample.

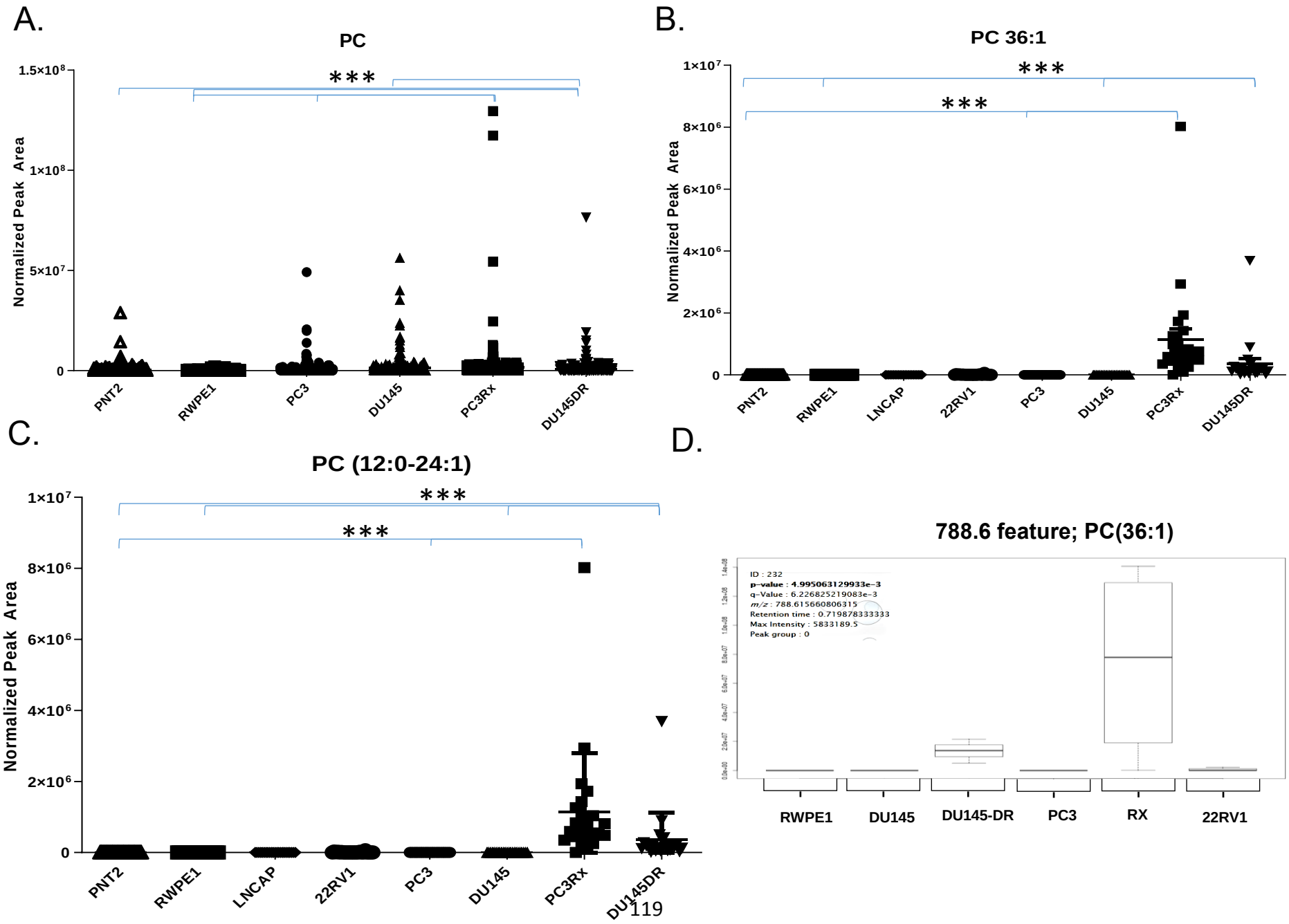
A.
PC
***
1.5×10⁸
1×10⁸
5×10⁷
0
Normalized Peak Area
PNT2
RWPE1
PC3
DU145
PC3Rx
DU145DR
B.
PC 36:1
***
***
1×10⁷
8×10⁶
6×10⁶
4×10⁶
2×10⁶
0
Normalized Peak Area
PNT2
RWPE1
LNCAP
22RV1
PC3
DU145
PC3Rx
DU145DR
C.
PC (12:0-24:1)
***
***
1×10⁷
8×10⁶
6×10⁶
4×10⁶
2×10⁶
0
Normalized Peak Area
PNT2
RWPE1
LNCAP
22RV1
PC3
DU145
PC3Rx
DU145DR
D.
788.6 feature; PC(36:1)
ID : 232
p-value : 4.995063129933e-3
q-Value : 6.226825219083e-3
m/z : 788.615660806315
Retention time : 0.719878333333
Max Intensity : 5833189.5
Peak group : 0
RWPE1
DU145
DU145-DR
PC3
RX
22RV1

Figure 3.13. Comparison of phosphatidylcholine (PC) in non-cancerous (PNT2 and RWPE1) and hormone-sensitive (LNCaP and 22RV1), castration-resistant (PC-3 and DU-145) and Docetaxel resistant (PC3-Rx and DU145-DR) prostate cell lines. Data are indicative of 6 samples per group and are expressed as mean ± the SEM (*$p < 0.05$ **$p < 0.01$*** $p < 0.001$). Each symbol represents an individual lipid feature as identified by MS/MS. Normalized peak areas between all cells are shown for **A)** 36:1 phosphatidylcholine (PC), **C)** 12:0-24:1 PC and **D)** Box-whisker plot of 36:1 PC

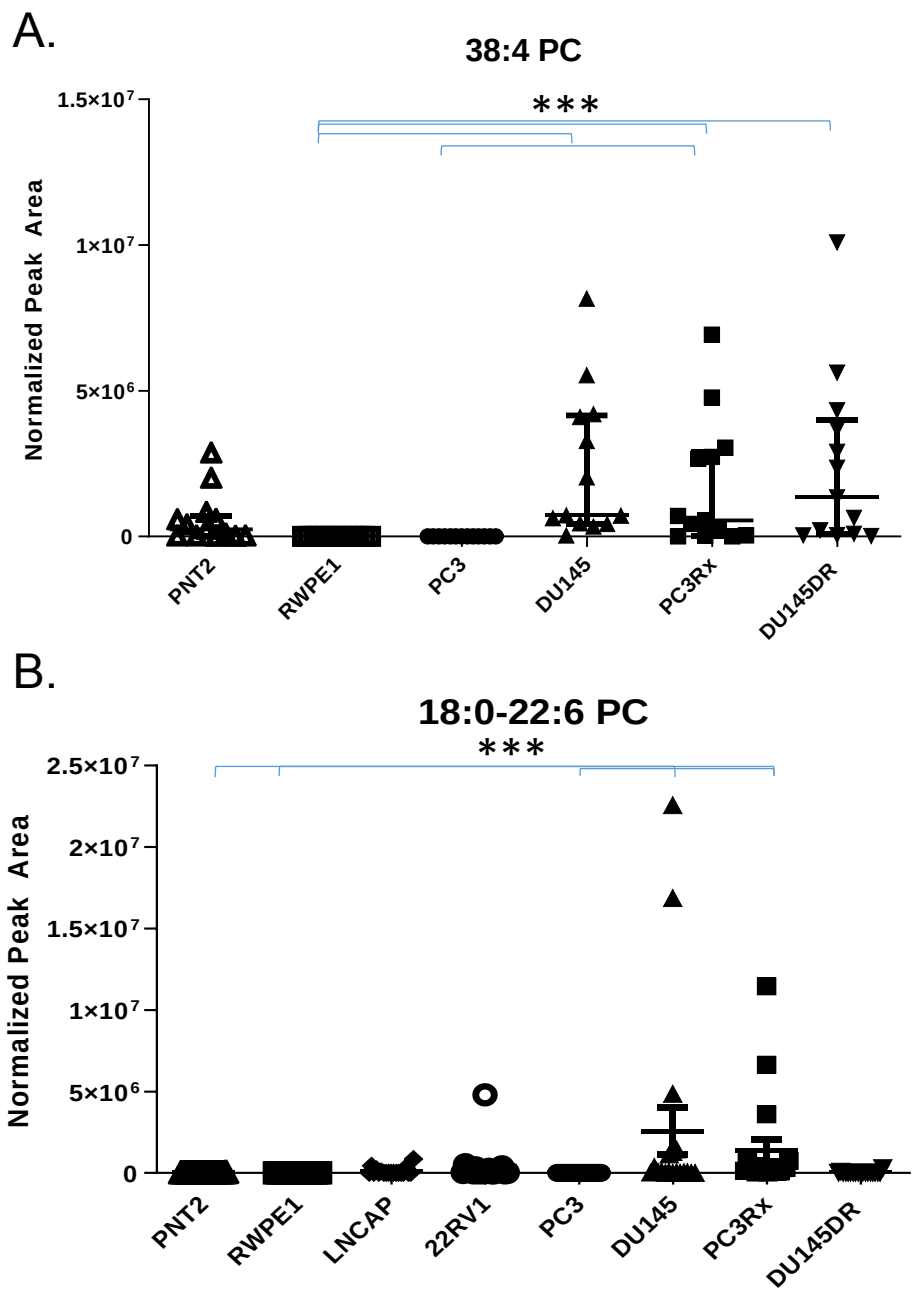

Figure 3.14. Comparison of phosphatidylcholine (PC) levels in non-cancerous (PNT2 and RWPE1), hormone-sensitive (LNCaP and 22RV1), castration-resistant (PC-3 and DU-145) and Docetaxel resistant (PC3-Rx and DU145-DR) prostate cell lines. Data are indicative of 6 samples per group and are expressed as mean ± the SEM (*$p < 0.05$ **$p < 0.01$*** $p < 0.001$). Each symbol represents an individual lipid feature as identified by MS/MS. Normalized peak areas between all cells and media are shown for **A)** 38:4 PC, and **B)** 18:0-22:6 PC.

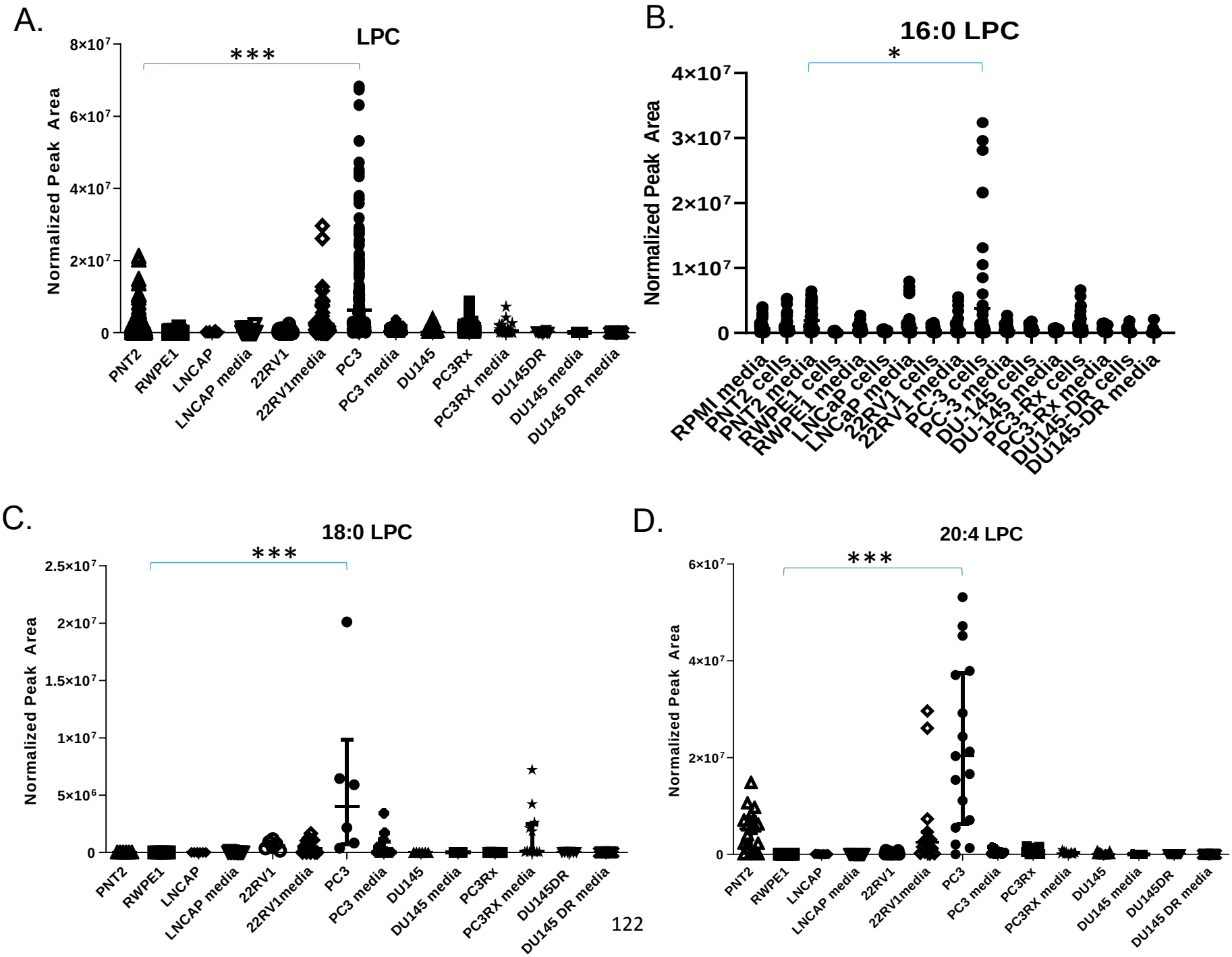
A.
LPC
***
Normalized Peak Area
8×10^7
6×10^7
4×10^7
2×10^7
0
PNT2
RWPE1
LNCAP
LNCAP media
22RV1
22RV1media
PC3
PC3 media
DU145
PC3Rx
PC3RX media
DU145DR
DU145 media
DU145 DR media
B.
16:0 LPC
*
Normalized Peak Area
4×10^7
3×10^7
2×10^7
1×10^7
0
RPMI media
PNT2 cells
PNT2 media
RWPE1 cells
RWPE1 media
LNCaP cells
LNCaP media
22RV1 cells
22RV1 media
PC-3 cells
PC-3 media
DU-145 cells
DU-145 media
PC3-Rx cells
PC3-Rx media
DU145-DR cells
DU145-DR media
C.
18:0 LPC
***
Normalized Peak Area
2.5×10^7
2×10^7
1.5×10^7
1×10^7
5×10^6
0
PNT2
RWPE1
LNCAP
LNCAP media
22RV1
22RV1media
PC3
PC3 media
DU145
DU145 media
PC3Rx
PC3RX media
DU145DR
DU145 DR media
D.
20:4 LPC
***
Normalized Peak Area
6×10^7
4×10^7
2×10^7
0
PNT2
RWPE1
LNCAP
LNCAP media
22RV1
22RV1media
PC3
PC3 media
PC3Rx
PC3RX media
DU145
DU145 media
DU145DR
DU145 DR media

Figure 3.15. Comparison of lysophosphatidylcholine (LPC) levels in non-cancerous (PNT2 and RWPE1), hormone-sensitive (LNCaP and 22RV1), castration-resistant (PC-3 and DU-145) and Docetaxel resistant (PC3-Rx and DU145-DR) prostate cell lines and media. Data are indicative of 6 samples per group and are expressed as mean ± the SEM (*$p < 0.05$ **$p < 0.01$*** $p < 0.001$). Each symbol represents an individual lipid feature as identified by MS/MS. Normalized peak areas between all cells are shown for **A)** lysophosphatidylcholine (LPC), **B)** 16:0 LPC,**C)** 18:0 LPC, and **D)** 20:4 LPC.

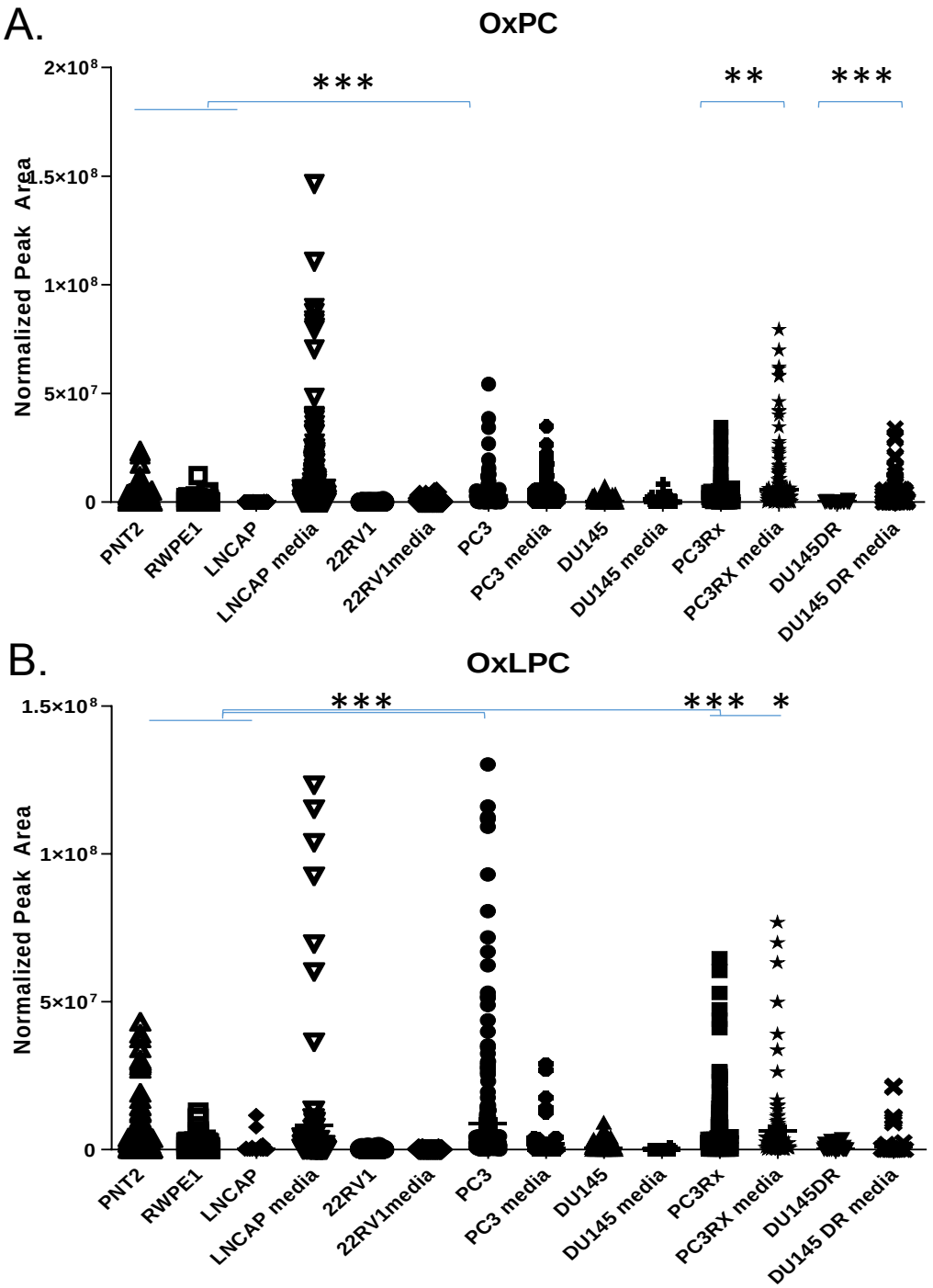
A.
OxPC
Normalized Peak Area
2×10^8
1.5×10^8
1×10^8
5×10^7
0
***
**
***
PNT2
RWPE1
LNCAP
LNCAP media
22RV1
22RV1media
PC3
PC3 media
DU145
DU145 media
PC3Rx
PC3RX media
DU145DR
DU145 DR media
B.
OxLPC
Normalized Peak Area
1.5×10^8
1×10^8
5×10^7
0
***
***
*
PNT2
RWPE1
LNCAP
LNCAP media
22RV1
22RV1media
PC3
PC3 media
DU145
DU145 media
PC3Rx
PC3RX media
DU145DR
DU145 DR media

Figure 3.16. Comparison of oxidized phosphatidylcholines (OxPC) levels in non-cancerous (PNT2 and RWPE1), hormone-sensitive (LNCaP and 22RV1), castration-resistant (PC-3 and DU-145) and Docetaxel resistant (PC3-Rx and DU145-DR) prostate cell lines and media. Data are indicative of 6 samples per group and are expressed as mean ± the SEM (*$p < 0.05$ **$p < 0.01$*** $p < 0.001$). Each symbol represents an individual lipid feature as identified by MS/MS. Normalized peak areas between all cells are shown for **A)** oxidized phosphatidylcholine (OxPC), **B)** oxidized lysophosphatidylcholine (OxLPC).

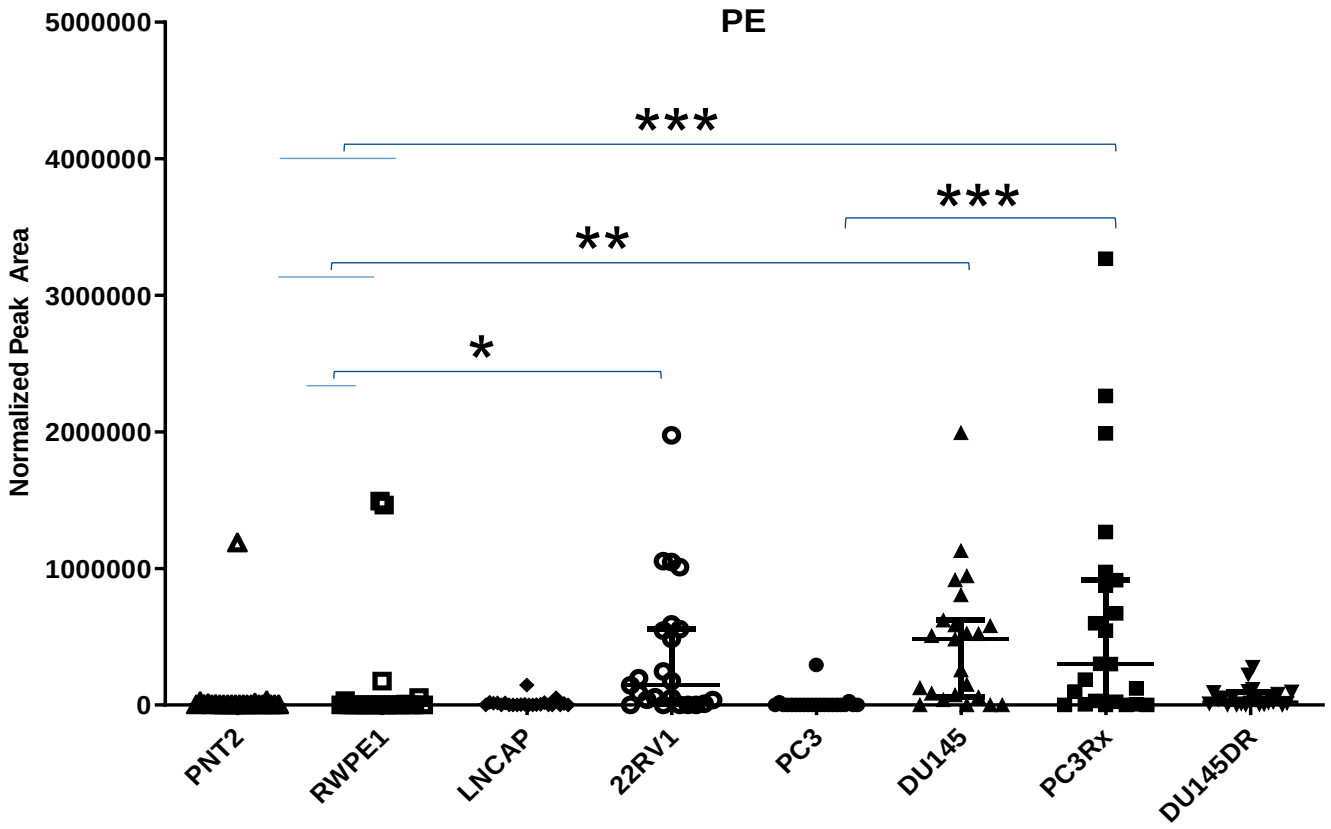

Figure 3.17. Comparison of phosphatidylethanolamine (PE) levels in non-cancerous (PNT2 and RWPE1), hormone-sensitive (LNCaP and 22RV1), castration-resistant (PC-3 and DU-145) and Docetaxel resistant (PC3-Rx and DU145-DR) prostate cell lines and media. Data are indicative of 6 samples per group and are expressed as mean ± the SEM (*$p < 0.05$ **$p < 0.01$*** $p < 0.001$). Each symbol represents an individual lipid feature as identified by MS/MS. Normalized peak areas between all cells are shown for phosphatidylethanolamine (PE), **B)** 38:4 PE and **C)** 18:0-20:4 PE.

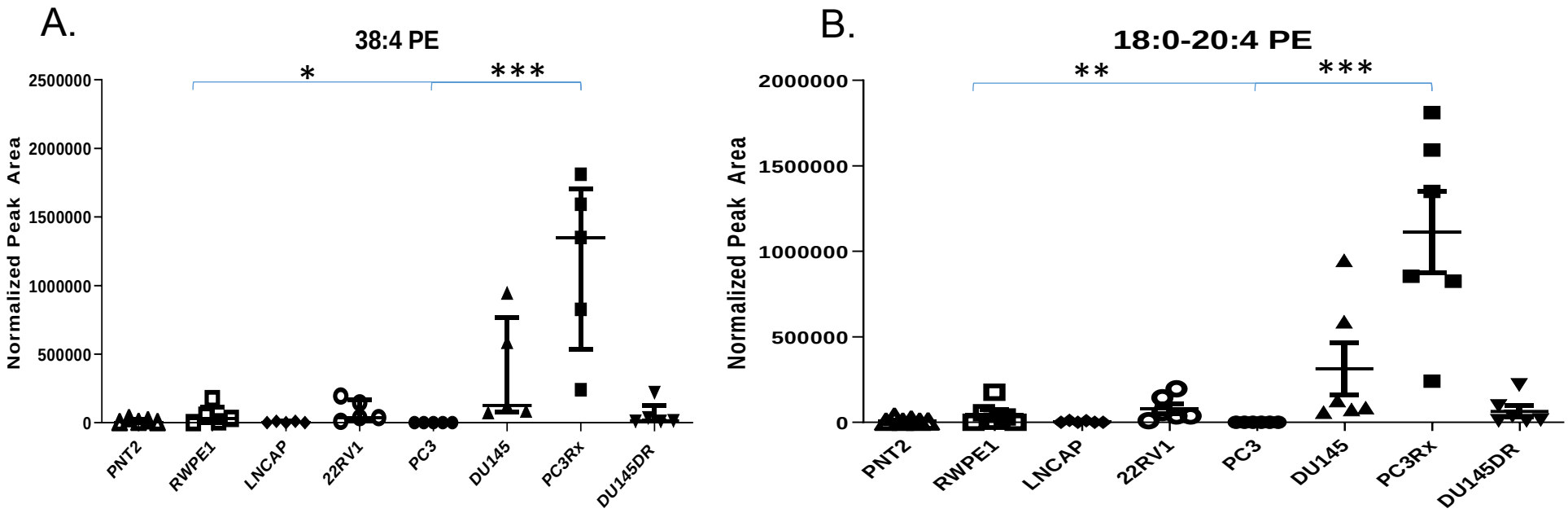
A.
38:4 PE
*
***
Normalized Peak Area
2500000
2000000
1500000
1000000
500000
0
PNT2
RWPE1
LNCAP
22RV1
PC3
DU145
PC3Rx
DU145DR
B.
18:0-20:4 PE
**
***
Normalized Peak Area
2000000
1500000
1000000
500000
0
PNT2
RWPE1
LNCAP
22RV1
PC3
DU145
PC3Rx
DU145DR

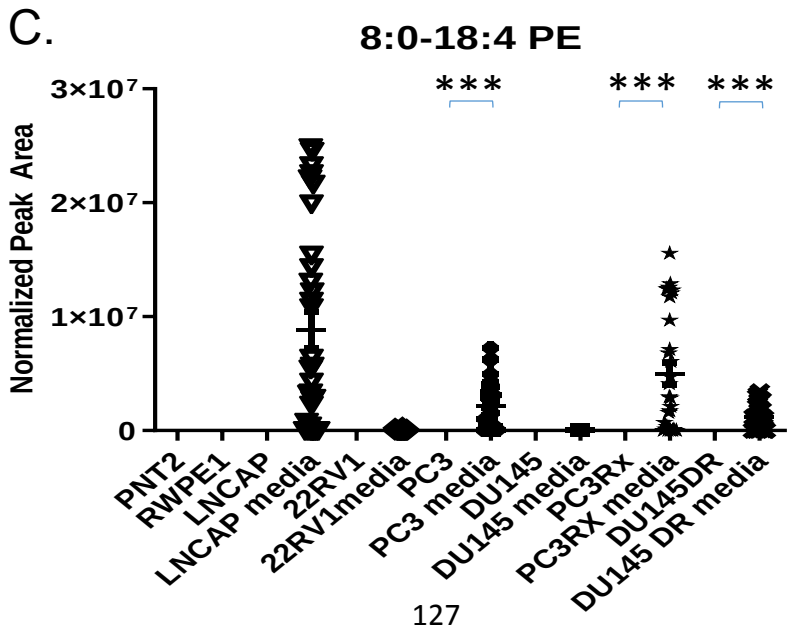
C.
8:0-18:4 PE
***
***
***
Normalized Peak Area
3×10⁷
2×10⁷
1×10⁷
0
PNT2
RWPE1
LNCAP
LNCAP media
22RV1
22RV1media
PC3
PC3 media
DU145
DU145 media
PC3Rx
PC3RX media
DU145DR
DU145 DR media

Figure 3.18. Comparison of phosphatidylethanolamine (PE) levels in non-cancerous (PNT2 and RWPE1), hormone-sensitive (LNCaP and 22RV1), castration-resistant (PC-3 and DU-145) and Docetaxel resistant (PC3-Rx and DU145-DR) prostate cell lines and media. Data are indicative of 6 samples per group and are expressed as mean ± the SEM (*$p < 0.05$ **$p < 0.01$*** $p < 0.001$). Each symbol represents an individual lipid feature as identified by MS/MS. Normalized peak areas between all cells are shown for **A)** 38:4 PE, **B)** 18:0-20:4 PE and **C)** 8:0-18:4 PE.

A.

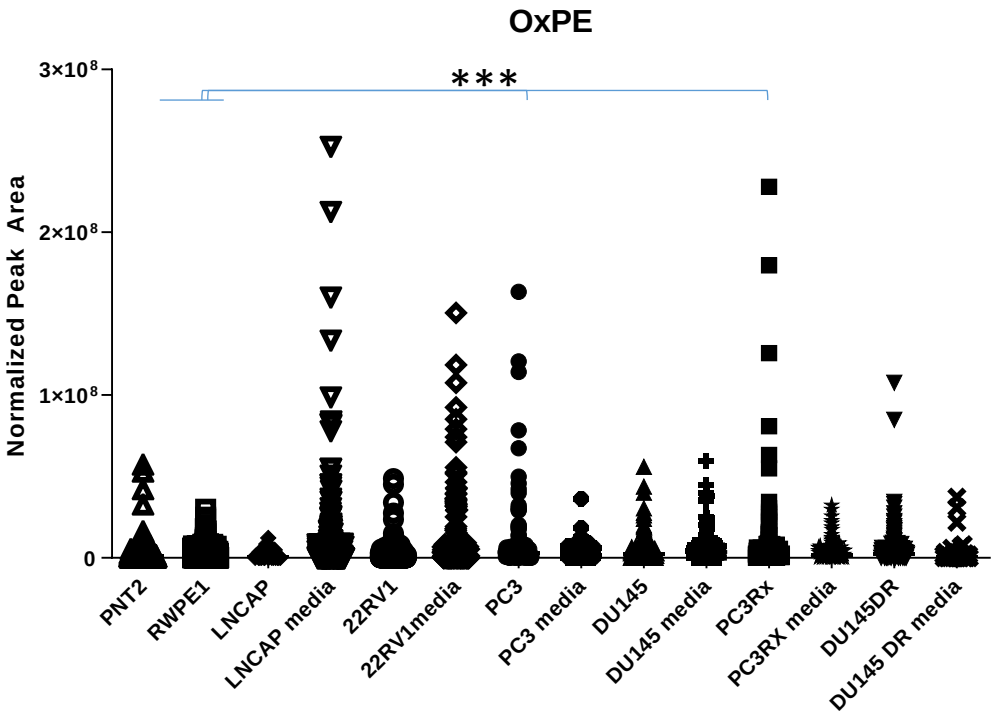
OxPE
***
Normalized Peak Area
3×10⁸
2×10⁸
1×10⁸
0
PNT2
RWPE1
LNCAP
LNCAP media
22RV1
22RV1media
PC3
PC3 media
DU145
DU145 media
PC3Rx
PC3RX media
DU145DR
DU145 DR media

B.

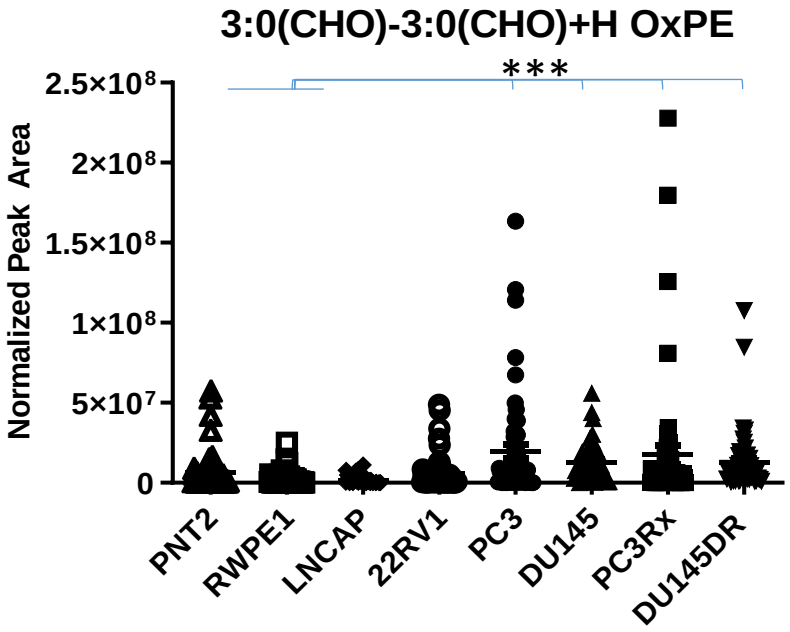
3:0(CHO)-3:0(CHO)+H OxPE
***
Normalized Peak Area
2.5×10⁸
2×10⁸
1.5×10⁸
1×10⁸
5×10⁷
0
PNT2
RWPE1
LNCAP
22RV1
PC3
DU145
PC3Rx
DU145DR

Figure 3.19. Comparison of oxidized phosphatidylethanolamine (OxPE) levels in non-cancerous (PNT2 and RWPE1), hormone-sensitive (LNCaP and 22RV1), castration-resistant (PC-3 and DU-145) and Docetaxel resistant (PC3-Rx and DU145-DR) prostate cell lines and media. Data are indicative of 6 samples per group and are expressed as mean ± SEM (*$p < 0.05$ **$p < 0.01$*** $p < 0.001$). Each symbol represents an individual lipid feature as identified by MS/MS. Normalized peak areas between all cells are shown for **A)** oxidized phosphatidylethanolamine (OxPE) and **B)** 3:0(CHO-3:0(CHO)+H OxPE.

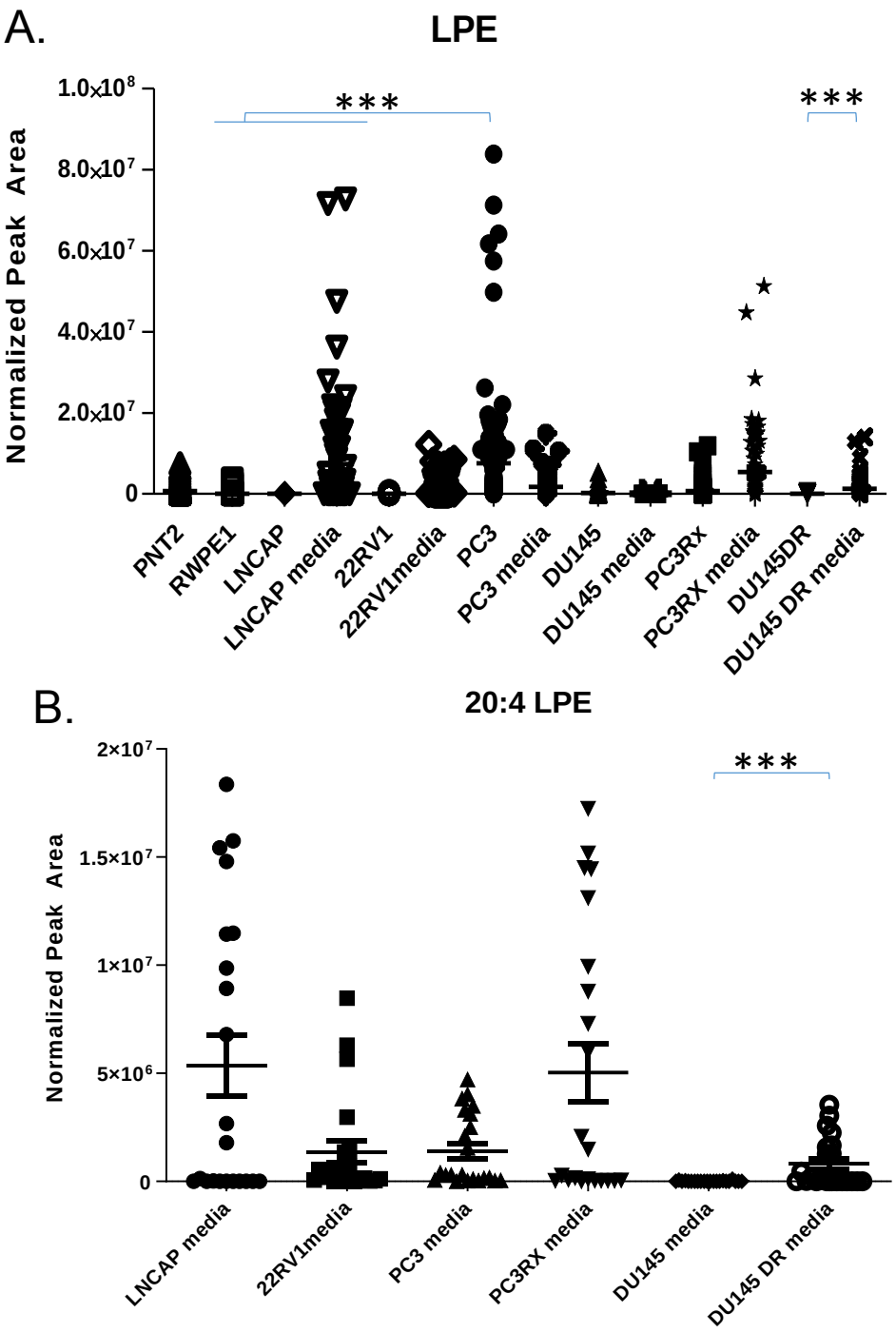
A.
LPE
Normalized Peak Area
1.0x10^8
8.0x10^7
6.0x10^7
4.0x10^7
2.0x10^7
0
***
***
PNT2
RWPE1
LNCAP
LNCAP media
22RV1
22RV1media
PC3
PC3 media
DU145
DU145 media
PC3Rx
PC3RX media
DU145DR
DU145 DR media
B.
20:4 LPE
Normalized Peak Area
2×10^7
1.5×10^7
1×10^7
5×10^6
0
***
LNCAP media
22RV1media
PC3 media
PC3RX media
DU145 media
DU145 DR media

Figure 3.20. Comparison of lysophosphatidylethanolamine (LPE) levels in non-cancerous (PNT2 and RWPE1), hormone-sensitive (LNCaP and 22RV1), castration-resistant (PC-3 and DU-145) and Docetaxel resistant (PC3-Rx and DU145-DR) prostate cell lines and media. Data are indicative of 6 samples per group and are expressed as mean ± SEM (*$p < 0.05$ **$p < 0.01$*** $p < 0.001$). Each symbol represents an individual lipid feature as identified by MS/MS. Normalized peak areas between all cells are shown for **A)** LPE **B)** 20:4 LPE.

A.

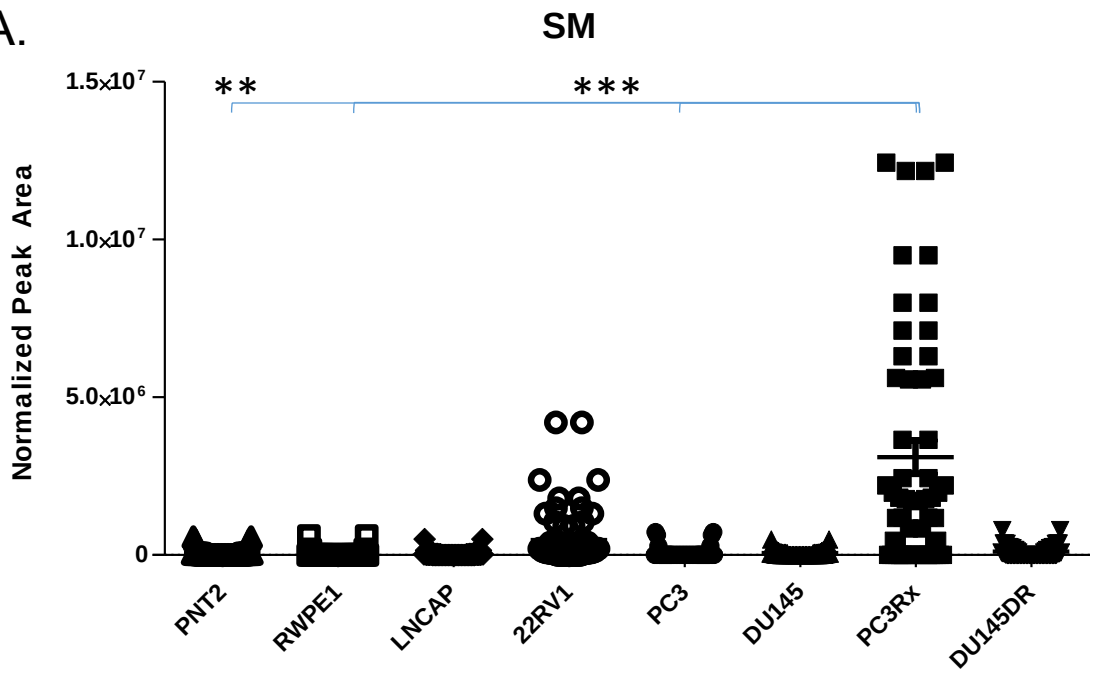
SM
Normalized Peak Area
1.5x10^7
1.0x10^7
5.0x10^6
0
**
***
PNT2
RWPE1
LNCAP
22RV1
PC3
DU145
PC3Rx
DU145DR

B.

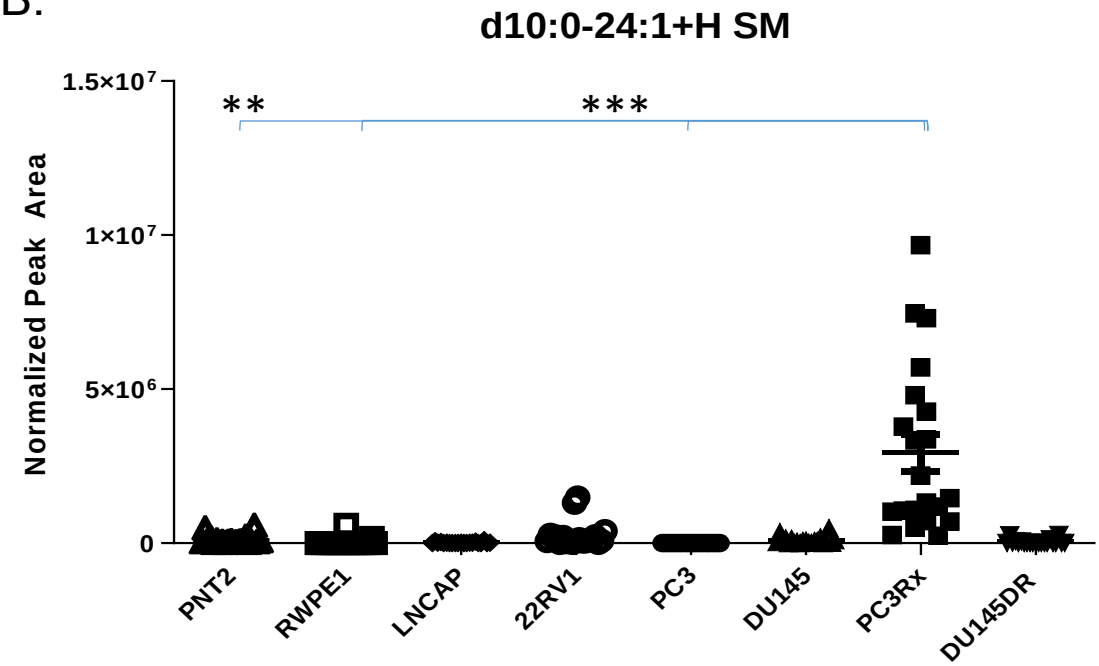
d10:0-24:1+H SM
Normalized Peak Area
1.5×10^7
1×10^7
5×10^6
0
**
***
PNT2
RWPE1
LNCAP
22RV1
PC3
DU145
PC3Rx
DU145DR

Figure 3.21. Comparison of sphingolipid levels in non-cancerous (PNT2 and RWPE1), hormone-sensitive (LNCaP and 22RV1), castration-resistant (PC-3 and DU-145) and Docetaxel resistant (PC3-Rx and DU145-DR) prostate cell lines and media. Data are indicative of 6 samples per group and are expressed as mean ± the SEM (*$p < 0.05$ **$p < 0.01$*** $p < 0.001$). Each symbol represents an individual lipid feature as identified by MS/MS. Normalized peak areas between all cells are shown for **A)** sphingomyelin (SM) and **B)** d10:-20:4+H SM.

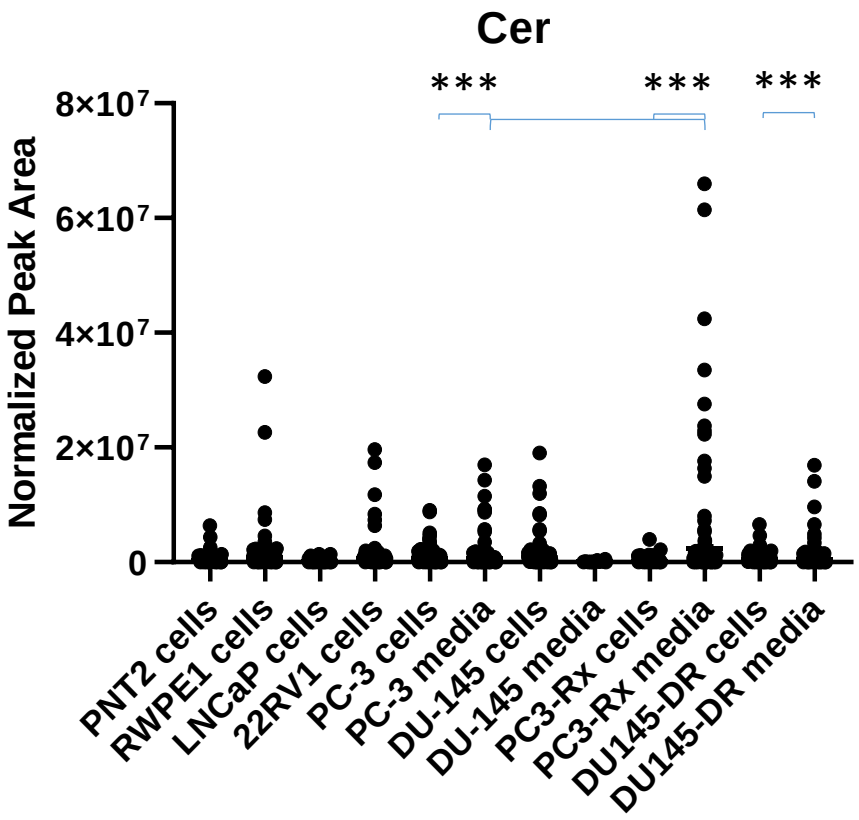

Figure 3.22. Comparison of ceramide levels in non-cancerous (PNT2 and RWPE1), hormone-sensitive (LNCaP and 22RV1), castration-resistant (PC-3 and DU-145) and Docetaxel resistant (PC3-Rx and DU145-DR) prostate cell lines and media. Data are indicative of 6 samples per group and are expressed as mean ± the SEM (*$p < 0.05$ **$p < 0.01$*** $p < 0.001$). Each symbol represents an individual lipid feature as identified by MS/MS. Normalized peak areas between all cells are shown for ceramide.

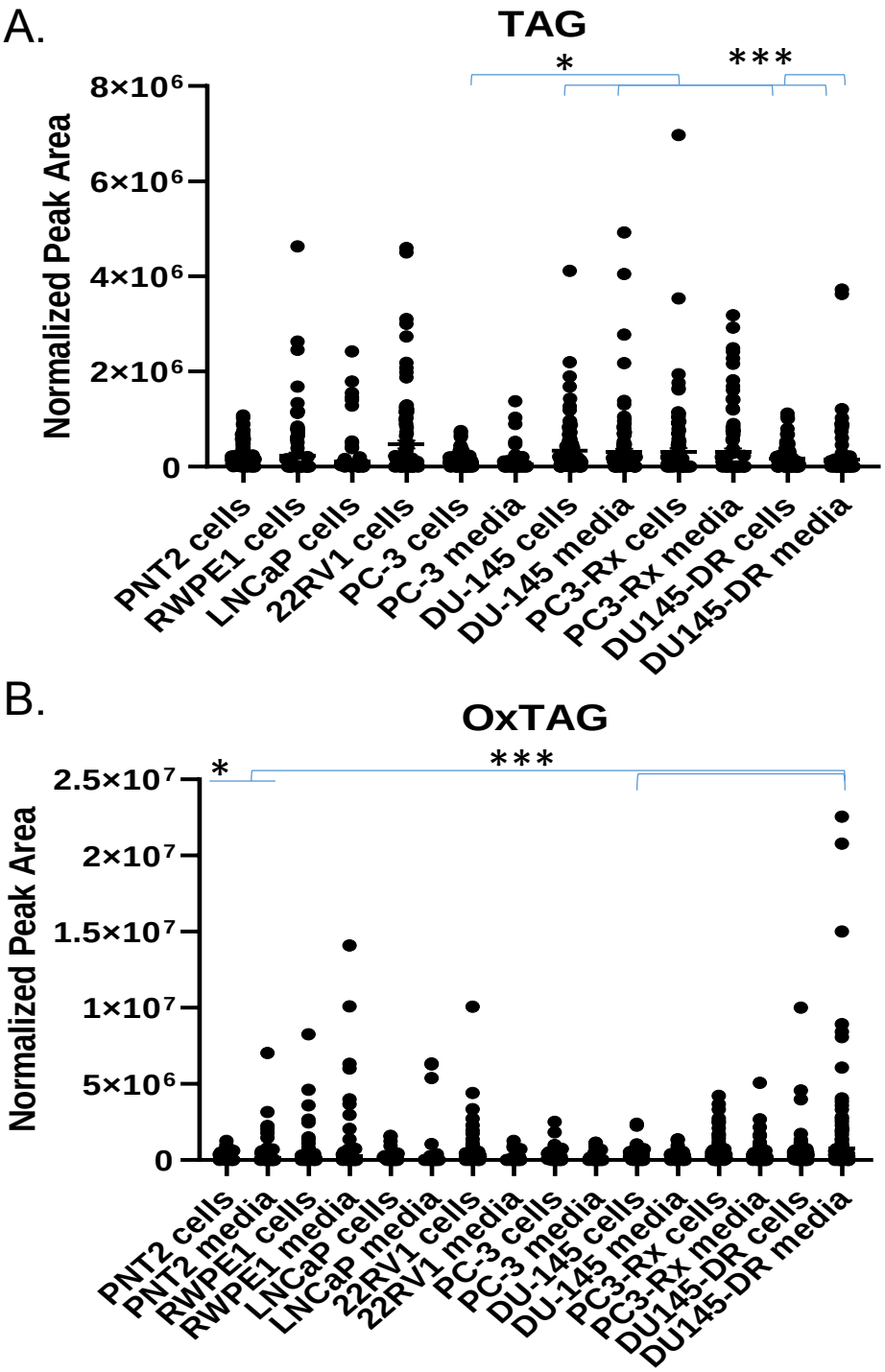
A.
TAG
*
***
Normalized Peak Area
8×10⁶
6×10⁶
4×10⁶
2×10⁶
0
PNT2 cells
RWPE1 cells
LNCaP cells
22RV1 cells
PC-3 cells
PC-3 media
DU-145 cells
DU-145 media
PC3-Rx cells
PC3-Rx media
DU145-DR cells
DU145-DR media
B.
OxTAG
*
***
Normalized Peak Area
2.5×10⁷
2×10⁷
1.5×10⁷
1×10⁷
5×10⁶
0
PNT2 cells
PNT2 media
RWPE1 cells
RWPE1 media
LNCaP cells
LNCaP media
22RV1 cells
22RV1 media
PC-3 cells
PC-3 media
DU-145 cells
DU-145 media
PC3-Rx cells
PC3-Rx media
DU145-DR cells
DU145-DR media

Figure 3.23. Comparison of acylglycerides levels in non-cancerous (PNT2 and RWPE1), hormone-sensitive (LNCaP and 22RV1), castration-resistant (PC-3 and DU-145) and Docetaxel resistant (PC3-Rx and DU145-DR) prostate cell lines and media. Data are indicative of 6 samples per group and are expressed as mean ± the SEM (*$p < 0.05$ **$p < 0.01$*** $p < 0.001$). Each symbol represents an individual lipid feature as identified by MS/MS. Normalized peak areas between all cells are shown for **A)** triacylglycerides (TAG) and **B)** oxidized triacylglycerides (OxTAG).

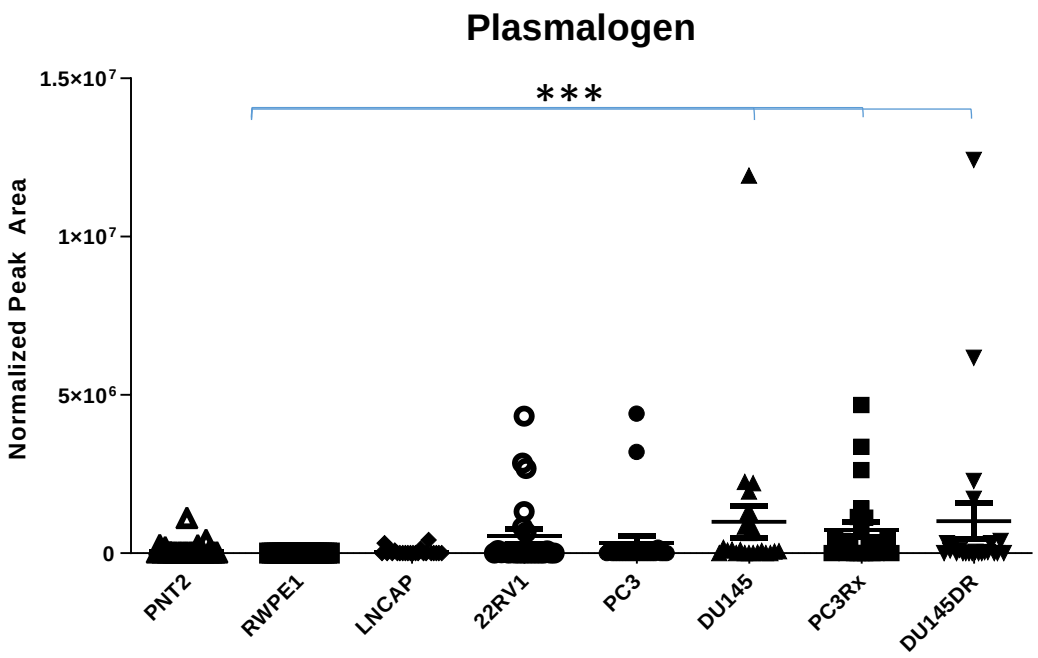

Figure 3.24. Comparison of plasmalogen levels in non-cancerous (PNT2 and RWPE1), hormone-sensitive (LNCaP and 22RV1), castration-resistant (PC-3 and DU-145) and Docetaxel resistant (PC3-Rx and DU145-DR) prostate cell lines and media. Data are indicative of 6 samples per group and are expressed as mean ± SEM (*$p < 0.05$ **$p < 0.01$*** $p < 0.001$). Each symbol represents an individual lipid feature as identified by MS/MS. Data are compared based on normalized peak areas.

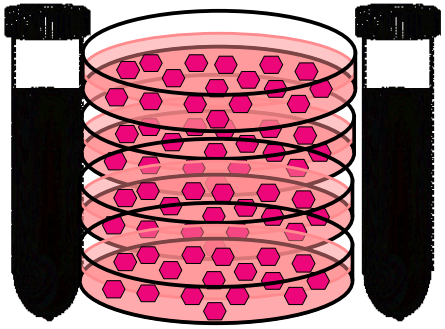

Biological Samples

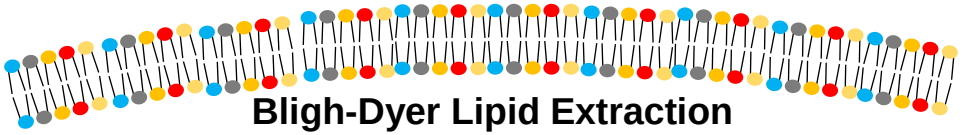

Bligh-Dyer Lipid Extraction

ESI-Mass Spectrometry

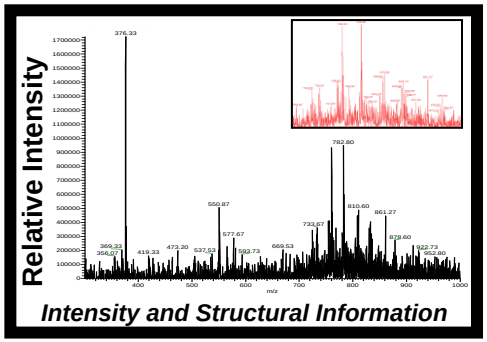

Multivariate and Statistical Analysis

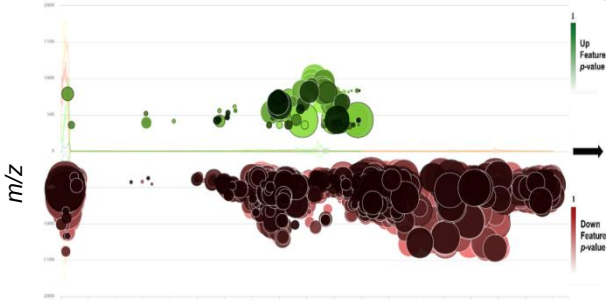

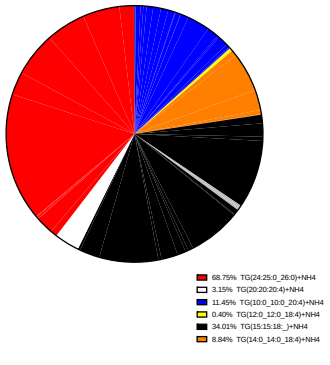

Altered Lipid Composition

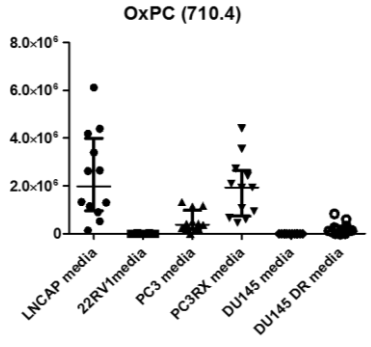

Supplemental Figure 3.1: Lipidomic profiling and data processing approach. This study utilized *in vitro* models that included non-cancerous, hormone sensitive, CRPC and drug-resistant human prostate cell lines combined with both an untargeted shotgun approach (ESI-MS) and quantitative HPLC-ESI-Orbitrap-MS lipidomic analysis. Lipid extracts were obtained by Bligh-Dyer (methanol/chloroform/water) extraction. Shotgun analysis was performed using commercially available standards. For target-based lipidomics, LC separation yielded specific lipid class separation prior to ESI/MS/MS enabling enhanced detection of lipids that are suppressed in the shotgun approach. Reverse-phase LC methods were examined for the class-specific separation of lipids species. Post data acquisition for both shotgun and HPLC-ESI/MS/MS lipidomics were based on multiple methods including isotope, carbon number (to IS) and ionization efficiency-based corrections. Online resources and software's utilized included LipidMatch, LipidNormalizer, Metaboanalyst, LIPID MAPS, XCMS, MZmine, SeeMS and TOPPview

Supplemental Table 3.1: Characteristics of human prostate cell lines.

Cell Line	Cell Type	Androgen Receptor Expression	Disease	Grade	Ethnicity	Age
PNT2	Epithelial	+	Normal	N/A	Caucasian	33-year-old male
RWPE-1	Epithelial	+	Normal	N/A	Caucasian	54-year-old male
22Rv1	Epithelial	+	Carcinoma	N/A	N/A	N/A
LNCaP	Epithelial-like	+	Carcinoma	N/A	Caucasian	50-year-old male
DU-145	Epithelial	-	Adenocarcinoma	II	Caucasian	69-year-old male
PC-3	Epithelial	-	Adenocarcinoma	IV	Caucasian	62-year-old male
DU145-DR	Epithelial	-	(treated with 2nM of Docetaxel to maintain DR)	II	Caucasian	69-year-old male
PC3-Rx	Epithelial	-	(treated with 2nM of Docetaxel to maintain DR)	IV	Caucasian	62-year-old male

A.

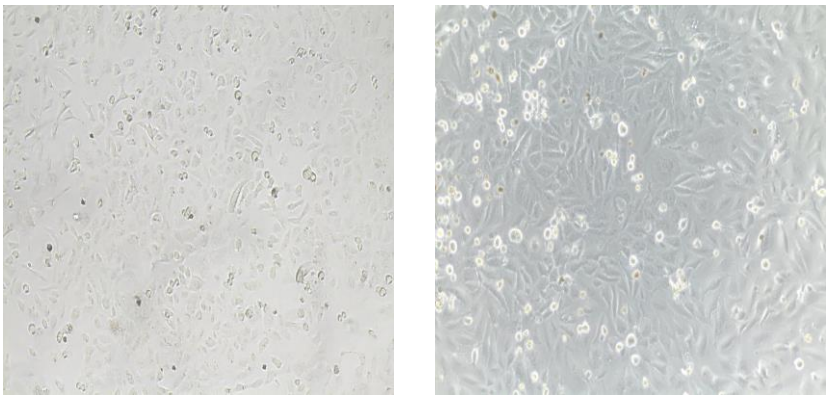

DU145 cells DU145-DR Cells

B.

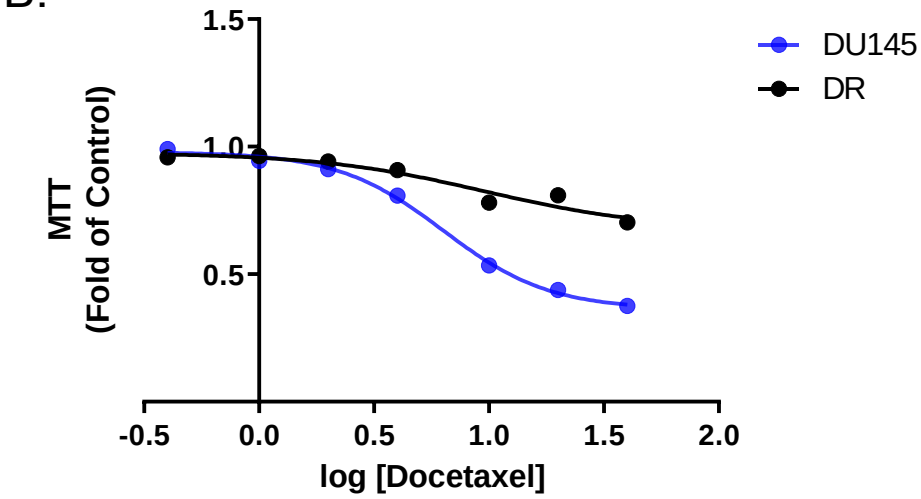

Supplemental Figure 3.2: A) Morphological difference between Docetaxel resistant cells and DU-145 parent control cells **B**) MTT assay shows decrease in MTT staining in parent cell lines as compared to Docetaxel resistant cell lines. This suggests DU145-DR (DR) maintains resistance to Docetaxel as compared to DU145 parent cell

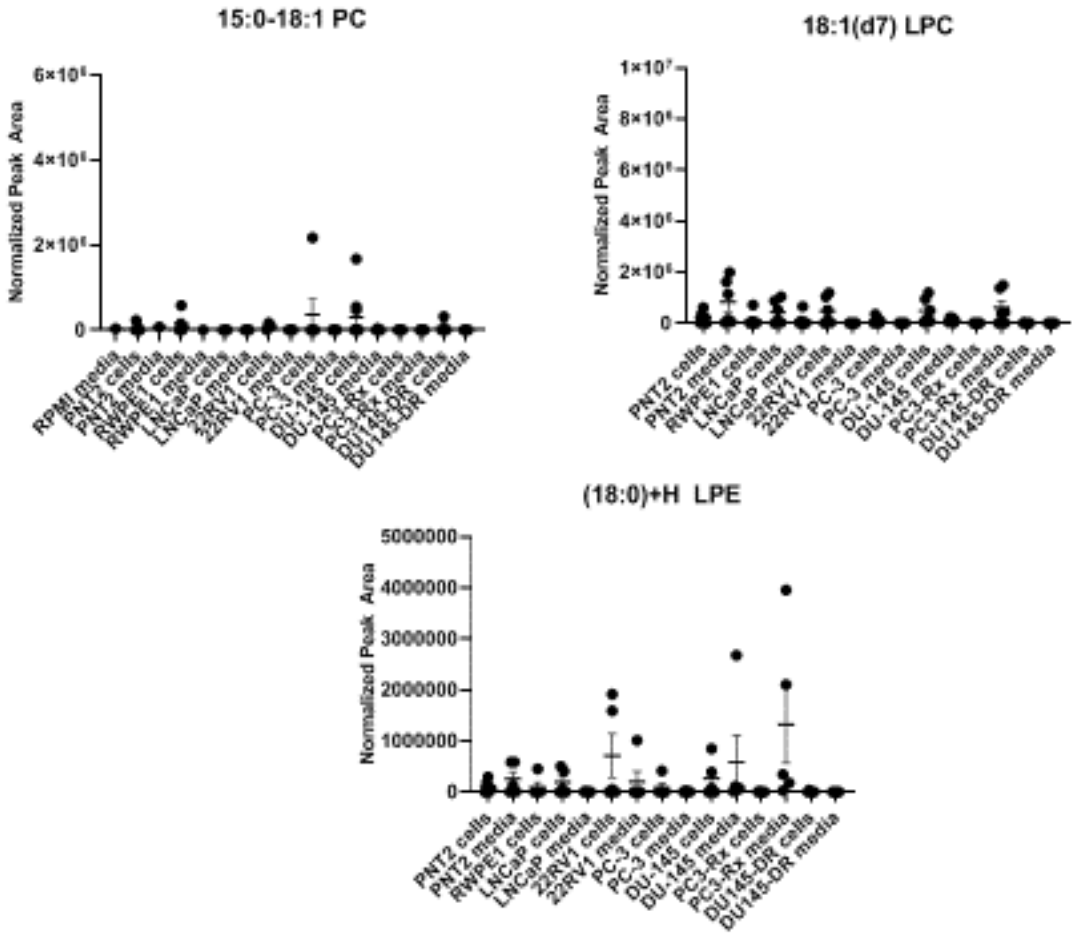

Supplemental Figure 3.3: Splash LipidoMIX Internal Standards. SPLASH (internal standards) are present in all prostate cell lines and media analyzed. Graphical representations are indicative of 6 samples per group. All samples were normalized to IS peak areas for all species.

Supplemental Table 3.2: FDR-corrected significance for Hormone-Sensitive vs. Non-Cancerous Cell Types.

FDR-corrected significant lipids Q value < 0.05

PC

Two-stage linear step-up procedure of Benjamini, Krieger and Yekutieli	Mean rank diff.	Discovery?	q value	Individual P Value
LNCAP vs. RWPE1	308.7	Yes	<0.001	<0.001
22RV1 vs. RWPE1	438.3	Yes	<0.001	<0.001
LNCAP vs. PNT2	50.76	Yes	0.01	0.07
22RV1 vs. PNT2	180.3	Yes	<0.001	<0.001

OxPC

Two-stage linear step-up procedure of Benjamini, Krieger and Yekutieli	Mean rank diff.	Discovery?	q value	Individual P Value
LNCAP vs. RWPE1	-103.4	Yes	<0.001	<0.001
22RV1 vs. RWPE1	-162	Yes	<0.001	<0.001
LNCAP vs. PNT2	-136.2	Yes	<0.001	<0.001
22RV1 vs. PNT2	-194.8	Yes	<0.001	<0.001

Plasmalogen- PC

Two-stage linear step-up procedure of Benjamini, Krieger and Yekutieli	Mean rank diff.	Discovery?	q value	Individual P Value
LNCAP vs. RWPE1	14.28	Yes	0.003	0.002
22RV1 vs. RWPE1	16.33	Yes	0.001	<0.001
LNCAP vs. PNT2	8.889	Yes	0.04	0.06
22RV1 vs. PNT2	10.94	Yes	0.02	0.02

SM

Two-stage linear step-up procedure of Benjamini, Krieger and Yekutieli	Mean rank diff.	Discovery?	q value	Individual P Value
LNCAP vs. RWPE1	32.93	Yes	<0.001	<0.001
22RV1 vs. RWPE1	28.26	Yes	<0.001	<0.001
LNCAP vs. PNT2	-13.88	Yes	0.04	0.09
22RV1 vs. PNT2	-18.55	Yes	0.01	0.02

Cer

Two-stage linear step-up procedure of Benjamini, Krieger and Yekutieli	Mean rank diff.	Discovery?	q value	Individual P Value
LNCAP vs. RWPE1	-37.11	Yes	<0.001	<0.001
22RV1 vs. RWPE1	-27.94	Yes	0.003	0.003
LNCAP vs. PNT2	-5.094	No	0.35	0.58
22RV1 vs. PNT2	4.078	No	0.35	0.66

DAG

Two-stage linear step-up procedure of Benjamini, Krieger and Yekutieli	Mean rank diff.	Discovery?	q value	Individual P Value
LNCAP vs. RWPE1	26.65	Yes	0.006	0.01
22RV1 vs. RWPE1	54.63	Yes	<0.001	<0.001
LNCAP vs. PNT2	20.44	Yes	0.02	0.05
22RV1 vs. PNT2	48.42	Yes	<0.001	<0.001

Supplemental Table 3.3: FDR-corrected significance for Castration-Resistant vs. Non-Cancerous Cell Types.

FDR-corrected significant lipids Q value < 0.05

PC

Two-stage linear step-up procedure of Benjamini, Krieger and Yekutieli	Mean rank diff.	Discovery?	q value	Individual P Value
DU145 vs. PNT2	290.8	Yes	<0.001	<0.001
PC3 vs. RWPE1	315.7	Yes	<0.001	<0.001
DU145 vs. RWPE1	660.5	Yes	<0.001	<0.001

LPC

Two-stage linear step-up procedure of Benjamini, Krieger and Yekutieli	Mean rank diff.	Discovery?	q value	Individual P Value
DU145 vs. PNT2	-120	Yes	<0.001	<0.001
PC3 vs. RWPE1	901	Yes	<0.001	<0.001
DU145 vs. RWPE1	507.9	Yes	<0.001	<0.001

20:4 LPC

Two-stage linear step-up procedure of Benjamini, Krieger and Yekutieli	Mean rank diff.	Discovery?	q value	Individual P Value
PC3 vs. PNT2	14.76	Yes	0.02	0.05
DU145 vs. PNT2	-14.45	Yes	0.02	0.05
PC3 vs. RWPE1	53.45	Yes	<0.001	<0.001
DU145 vs. RWPE1	24.24	Yes	<0.001	0.001

OxPC

Two-stage linear step-up procedure of Benjamini, Krieger and Yekutieli	Mean rank diff.	Discovery?	q value	Individual P Value

PC3 vs. PNT2	637.8	Yes	<0.001	<0.001
PC3 vs. RWPE1	1034	Yes	<0.001	<0.001

OxLPC

Two-stage linear step-up procedure of Benjamini, Krieger and Yekutieli	Mean rank diff.	Discovery?	q value	Individual P Value
PC3 vs. PNT2	343.6	Yes	<0.001	<0.001
PC3 vs. RWPE1	517.8	Yes	<0.001	<0.001

Plasmalogen PC

Two-stage linear step-up procedure of Benjamini, Krieger and Yekutieli	Mean rank diff.	Discovery?	q value	Individual P Value
PC3 vs. PNT2	9.909	Yes	0.04	0.05
DU145 vs. PNT2	17.36	Yes	<0.001	<0.001
PC3 vs. RWPE1	14.82	Yes	0.004	0.003
DU145 vs. RWPE1	22.27	Yes	<0.001	<0.001

PE

Two-stage linear step-up procedure of Benjamini, Krieger and Yekutieli	Mean rank diff.	Discovery?	q value	Individual P Value
DU145 vs. RWPE1	21.16	Yes	0.01	0.002

LPE

Two-stage linear step-up procedure of Benjamini, Krieger and Yekutieli	Mean rank diff.	Discovery?	q value	Individual P Value
PC3 vs. PNT2	176.4	Yes	<0.001	<0.001
DU145 vs. PNT2	-32.66	Yes	0.03	0.16
PC3 vs. RWPE1	434.3	Yes	<0.001	<0.001
DU145 vs. RWPE1	225.2	Yes	<0.001	<0.001

22:6 LPE

Two-stage linear step-up procedure of Benjamini, Krieger and Yekutieli	Mean rank diff.	Discovery?	q value	Individual P Value
PC3 vs. PNT2	10.77	Yes	0.04	0.09
PC3 vs. RWPE1	35.37	Yes	<0.001	<0.001

SM

Two-stage linear step-up procedure of Benjamini, Krieger and Yekutieli	Mean rank diff.	Discovery?	q value	Individual P Value
DU145 vs. PNT2	30	Yes	0.002	0.01
DU145 vs. RWPE1	115.1	Yes	<0.001	<0.001

Cer

Two-stage linear step-up procedure of Benjamini, Krieger and Yekutieli	Mean rank diff.	Discovery?	q value	Individual P Value
PC3 vs. PNT2	-0.5	No	>0.99	0.97
DU145 vs. PNT2	22.13	No	0.17	0.05
PC3 vs. RWPE1	-15.4	No	0.3	0.18
DU145 vs. RWPE1	7.236	No	0.66	0.53

PA

Two-stage linear step-up procedure of Benjamini, Krieger and Yekutieli	Mean rank diff.	Discovery?	q value	Individual P Value
PC3 vs. PNT2	22.42	Yes	0.001	0.004
DU145 vs. PNT2	-6.346	No	0.07	0.42
PC3 vs. RWPE1	45.27	Yes	<0.001	<0.001

PG

Two-stage linear step-up procedure of Benjamini, Krieger and Yekutieli	Mean rank diff.	Discovery?	q value	Individual P Value
PC3 vs. PNT2	6.875	No	0.09	0.21
PC3 vs. RWPE1	27.63	Yes	<0.001	<0.001
DU145 vs. RWPE1	2.792	No	0.21	0.61

DAG

Two-stage linear step-up procedure of Benjamini, Krieger and Yekutieli	Mean rank diff.	Discovery?	q value	Individual P Value
PC3 vs. PNT2	-12.59	No	0.26	0.33
DU145 vs. PNT2	109.1	Yes	<0.001	<0.001
DU145 vs. RWPE1	118.3	Yes	<0.001	<0.001

TAG

Two-stage linear step-up procedure of Benjamini, Krieger and Yekutieli	Mean rank diff.	Discovery?	q value	Individual P Value
PC3 vs. PNT2	-15.48	Yes	0.005	0.02
DU145 vs. PNT2	20.95	Yes	0.001	0.002

Supplemental Table 3.4: FDR-corrected significance for Drug Resistant vs. Non-Cancerous Cell Types.

FDR-corrected significant lipids Q value < 0.05

PC

Two-stage linear step-up procedure of Benjamini, Krieger and Yekutieli	Mean rank diff.	Discovery?	q value	Individual P Value
PC3Rx vs. PC3	765.5	Yes	<0.001	<0.001
RWPE1 vs. PC3	-492.6	Yes	<0.001	<0.001
RWPE1 vs. PC3Rx	-1258	Yes	<0.001	<0.001
PNT2 vs. PC3Rx	-466.4	Yes	<0.001	<0.001
DU145DR vs. DU145	-169.4	Yes	0.001	0.006
RWPE1 vs. DU145DR	-997.2	Yes	<0.001	<0.001
PNT2 vs. DU145DR	-205.6	Yes	<0.001	<0.001

36:1 PC

Two-stage linear step-up procedure of Benjamini, Krieger and Yekutieli	Mean rank diff.	Discovery?	q value	Individual P Value
PC3Rx vs. PC3	111	Yes	<0.001	<0.001
PNT2 vs. PC3Rx	-85.13	Yes	<0.001	<0.001
DU145DR vs. DU145	98.93	Yes	<0.001	<0.001
PNT2 vs. DU145	25.87	Yes	0.04	0.07
RWPE1 vs. DU145DR	-98.93	Yes	<0.001	<0.001
PNT2 vs. DU145DR	-73.07	Yes	<0.001	<0.001

12:0-24:1 PC

Two-stage linear step-up procedure of Benjamini, Krieger and Yekutieli	Mean rank diff.	Discovery?	q value	Individual P Value
PC3Rx vs. PC3	111	Yes	<0.001	<0.001
RWPE1 vs. PC3	0	No	0.41	>0.99
PNT2 vs. PC3	25.87	Yes	0.04	0.07
RWPE1 vs. PC3Rx	-111	Yes	<0.001	<0.001
PNT2 vs. PC3Rx	-85.13	Yes	<0.001	<0.001

DU145DR vs. DU145	98.93	Yes	<0.001	<0.001
RWPE1 vs. DU145DR	-98.93	Yes	<0.001	<0.001
PNT2 vs. DU145DR	-73.07	Yes	<0.001	<0.001

38:4 PC

Two-stage linear step-up procedure of Benjamini, Krieger and Yekutieli	Mean rank diff.	Discovery?	q value	Individual P Value
PC3Rx vs. PC3	46.15	Yes	<0.001	<0.001
RWPE1 vs. PC3Rx	-46.15	Yes	<0.001	<0.001
RWPE1 vs. DU145	-58.15	Yes	<0.001	<0.001
RWPE1 vs. DU145DR	-52.92	Yes	<0.001	<0.001

18:0-22:6 PC

Two-stage linear step-up procedure of Benjamini, Krieger and Yekutieli	Mean rank diff.	Discovery?	q value	Individual P Value
PC3Rx vs. PC3	88.68	Yes	<0.001	<0.001
RWPE1 vs. PC3Rx	-88.68	Yes	<0.001	<0.001
PNT2 vs. PC3Rx	-78.42	Yes	<0.001	<0.001
RWPE1 vs. DU145	-78.05	Yes	<0.001	<0.001
PNT2 vs. DU145	-67.79	Yes	<0.001	<0.001

LPC

Two-stage linear step-up procedure of Benjamini, Krieger and Yekutieli	Mean rank diff.	Discovery?	q value	Individual P Value
RWPE1 vs. PC3	-1693	Yes	<0.001	<0.001
PNT2 vs. PC3	-435.4	Yes	<0.001	<0.001
RWPE1 vs. PC3Rx	-1037	Yes	<0.001	<0.001
PNT2 vs. PC3Rx	221	Yes	<0.001	<0.001

16:0 LPC

Two-stage linear step-up procedure of Benjamini, Krieger and Yekutieli	Mean rank diff.	Discovery?	q value	Individual P Value
RWPE1 cells vs. PC3 cells	-38.67	Yes	0.01	<0.001

18:0 LPC

Two-stage linear step-up procedure of Benjamini, Krieger and Yekutieli	Mean rank diff.	Discovery?	q value	Individual P Value
RWPE1 vs. PC3	-87	Yes	<0.001	<0.001
PNT2 vs. PC3	-45	Yes	0.04	0.02

20:4 LPC

Two-stage linear step-up procedure of Benjamini, Krieger and Yekutieli	Mean rank diff.	Discovery?	q value	Individual P Value
RWPE1 vs. PC3	-166.2	Yes	<0.001	<0.001
22RV1media vs. RWPE1	143.4	Yes	<0.001	<0.001

OxPC

Two-stage linear step-up procedure of Benjamini, Krieger and Yekutieli	Mean rank diff.	Discovery?	q value	Individual P Value
RWPE1 vs. PC3	-1195	Yes	<0.001	<0.001
PNT2 vs. PC3	-425.5	Yes	<0.001	<0.001
RWPE1 vs. PC3Rx	-852	Yes	<0.001	<0.001
DU145 DR media vs. DU145DR	838.8	Yes	<0.001	<0.001
LNCAP media vs. LNCAP	1459	Yes	<0.001	<0.001
PC3 media vs. RWPE1	1000	Yes	<0.001	<0.001
PC3RX media vs. RWPE1	1202	Yes	<0.001	<0.001

DU145 media vs. RWPE1	-257	Yes	<0.001	0.002
PC3RX media vs. PC3 media	201.7	Yes	0.002	0.01
DU145 DR media vs. DU145 media	842.8	Yes	<0.001	<0.001

OxLPC

Two-stage linear step-up procedure of Benjamini, Krieger and Yekutieli	Mean rank diff.	Discovery?	q value	Individual P Value
RWPE1 vs. PC3	-955.7	Yes	<0.001	<0.001
PNT2 vs. PC3	-291.8	Yes	<0.001	<0.001
RWPE1 vs. PC3Rx	-719.8	Yes	<0.001	<0.001
PC3RX media vs. PC3Rx	194.6	Yes	0.006	0.03
DU145DR vs. DU145	-314.4	Yes	<0.001	<0.001
LNCAP media vs. RWPE1	637.2	Yes	<0.001	<0.001
PC3RX media vs. RWPE1	914.3	Yes	<0.001	<0.001
PC3RX media vs. PNT2	250.4	Yes	0.001	0.005
PC3RX media vs. PC3 media	448.7	Yes	<0.001	<0.001
DU145 DR media vs. DU145 media	420.7	Yes	<0.001	<0.001

PE

Two-stage linear step-up procedure of Benjamini, Krieger and Yekutieli	Mean rank diff.	Discovery?	q value	Individual P Value
PC3Rx vs. PC3	75.48	Yes	<0.001	<0.001
RWPE1 vs. PC3Rx	-68.48	Yes	<0.001	<0.001
PNT2 vs. PC3Rx	-66.17	Yes	<0.001	<0.001
RWPE1 vs. DU145	-69.13	Yes	<0.001	<0.001
PNT2 vs. DU145	-66.83	Yes	<0.001	<0.001
RWPE1 vs. DU145DR	-39.48	Yes	0.01	0.01
PNT2 vs. DU145DR	-37.17	Yes	0.01	0.02

RWPE1 vs. 22RV1	-61.96	Yes	<0.001	<0.001
PNT2 vs. 22RV1	-59.65	Yes	<0.001	<0.001

38:4 PE

Two-stage linear step-up procedure of Benjamini, Krieger and Yekutieli	Mean rank diff.	Discovery?	q value	Individual P Value
PC3Rx vs. PC3	31.9	Yes	<0.001	<0.001
RWPE1 vs. PC3Rx	-17.9	Yes	0.04	0.01
PNT2 vs. PC3Rx	-24.8	Yes	0.004	<0.001
PNT2 vs. DU145	-18.6	Yes	0.04	0.01

18:0-20:4 PE

Two-stage linear step-up procedure of Benjamini, Krieger and Yekutieli	Mean rank diff.	Discovery?	q value	Individual P Value
PC3Rx vs. PC3	37.83	Yes	<0.001	<0.001
RWPE1 vs. PC3Rx	-24	Yes	0.009	0.003
PNT2 vs. PC3Rx	-29.33	Yes	0.001	<0.001

18:0-18:4 PE

Two-stage linear step-up procedure of Benjamini, Krieger and Yekutieli	Mean rank diff.	Discovery?	q value	Individual P Value
PC3RX media vs. PC3 media	13.58	No	0.15	0.31
DU145 DR media vs. DU145 media	50.68	Yes	<0.001	<0.001

OxPE

Two-stage linear step-up procedure of Benjamini, Krieger and Yekutieli	Mean rank diff.	Discovery?	q value	Individual P Value
LNCaP vs. PNT2 cells	-764.6	Yes	<0.001	0.002
22RV1 media vs. PNT2 cells	-1498	Yes	<0.001	<0.001
PC-3 cells vs. PNT2 cells	-513	Yes	0.01	0.04
PC3-Rx cells vs. PNT2 cells	-1678	Yes	<0.001	<0.001
LNCaP vs. RWPE1 cells	-1215	Yes	<0.001	<0.001
22RV1 media vs. RWPE1 cells	-1948	Yes	<0.001	<0.001
PC-3 cells vs. RWPE1 cells	-963.1	Yes	<0.001	<0.001
PC3-Rx cells vs. RWPE1 cells	-2129	Yes	<0.001	<0.001
PC3-Rx cells vs. PC-3 cells	-1165	Yes	<0.001	<0.001
DU-145 media vs. DU-145 cells	-742	Yes	<0.001	0.002
DU145-DR cells vs. DU-145 cells	-1695	Yes	<0.001	<0.001

3:0(CHO)-3:0(CHO)+H OxPE

Q	0.05

Two-stage linear step-up procedure of Benjamini, Krieger and Yekutieli	Mean rank diff.	Discovery?	q value	Individual P Value
RWPE1 vs. PC3	-106.4	Yes	<0.001	<0.001
PNT2 vs. PC3	-57.74	Yes	0.01	0.02
RWPE1 vs. PC3Rx	-78.41	Yes	<0.001	0.001
RWPE1 vs. DU145	-152.4	Yes	<0.001	<0.001
PNT2 vs. DU145	-103.7	Yes	<0.001	<0.001
RWPE1 vs. DU145DR	-142.9	Yes	<0.001	<0.001
PNT2 vs. DU145DR	-94.19	Yes	<0.001	<0.001

LPE

Q	0.05

Two-stage linear step-up procedure of Benjamini, Krieger and Yekutieli	Mean rank diff.	Discovery?	q value	Individual P Value
RWPE1 vs. PC3	-944.7	Yes	<0.001	<0.001
PNT2 vs. PC3	-268.9	Yes	<0.001	<0.001
RWPE1 vs. PC3Rx	-609.2	Yes	<0.001	<0.001
LNCAP media vs. RWPE1	485	Yes	<0.001	<0.001
PC3RX media vs. RWPE1	681.4	Yes	<0.001	<0.001
LNCAP media vs. PNT2	-190.8	Yes	<0.001	0.002
DU145 DR media vs. PNT2	-271.9	Yes	<0.001	<0.001
DU145 DR media vs. DU145 media	335.3	Yes	<0.001	<0.001

20:4 LPE

Two-stage linear step-up procedure of Benjamini, Krieger and Yekutieli	Mean rank diff.	Discovery?	q value	Individual P Value
DU145 DR media vs. DU145 media	38.77	Yes	0.002	<0.001

SM

Two-stage linear step-up procedure of Benjamini, Krieger and Yekutieli	Mean rank diff.	Discovery?	q value	Individual P Value
PC3Rx vs. PC3	214.2	Yes	<0.001	<0.001
PNT2 vs. PC3	122.8	Yes	<0.001	<0.001
RWPE1 vs. PC3Rx	-225.8	Yes	<0.001	<0.001
PNT2 vs. PC3Rx	-91.33	Yes	<0.001	<0.001

d10:0-24:1+H SM

Two-stage linear step-up procedure of Benjamini, Krieger and Yekutieli	Mean rank diff.	Discovery?	q value	Individual P Value
PC3Rx vs. PC3	129.2	Yes	<0.001	<0.001
RWPE1 vs. PC3Rx	-118.5	Yes	<0.001	<0.001
PNT2 vs. PC3Rx	-58.33	Yes	<0.001	<0.001

Cer

Two-stage linear step-up procedure of Benjamini, Krieger and Yekutieli	Mean rank diff.	Discovery?	q value	Individual P Value
PC3-Rx media vs. PC-3 media	414.6	Yes	<0.001	<0.001
DU-145 media vs. DU-145 cells	-732.7	Yes	<0.001	<0.001
PC3-Rx media vs. PC3-Rx cells	241.6	Yes	0.002	0.005
DU145-DR media vs. DU145-DR cells	-613.6	Yes	<0.001	<0.001

TAG

Two-stage linear step-up procedure of Benjamini, Krieger and Yekutieli	Mean rank diff.	Discovery?	q value	Individual P Value
PC3-Rx media vs. PC-3 media	155	Yes	0.01	0.01
DU-145 media vs. DU-145 cells	-314.7	Yes	<0.001	<0.001
DU145-DR cells vs. DU-145 cells	-210.8	Yes	0.001	<0.001
DU145-DR media vs. DU-145 media	-233.1	Yes	<0.001	<0.001
DU145-DR media vs. DU145-DR cells	-337	Yes	<0.001	<0.001

Plasmalogen

Two-stage linear step-up procedure of Benjamini, Krieger and Yekutieli	Mean rank diff.	Discovery?	q value	Individual P Value
RWPE1 vs. PC3Rx	-67.33	Yes	<0.001	<0.001
RWPE1 vs. DU145	-70.58	Yes	<0.001	<0.001
RWPE1 vs. DU145DR	-52.13	Yes	0.001	<0.001

OxTAG

Two-stage linear step-up procedure of Benjamini, Krieger and Yekutieli	Mean rank diff.	Discovery?	q value	Individual P Value
DU145-DR cells vs. PNT2 cells	199.5	Yes	0.004	0.005
DU145-DR cells vs. RWPE1 cells	150.4	Yes	0.02	0.04
DU145-DR cells vs. DU-145 cells	-178.4	Yes	0.008	0.01

CHAPTER 4

LIPIDOMIC PATHWAY ENRICHMENTANALYSIS OF PROSTATE CANCER CELL TYPES USING LIPID PATHWAY ANALYSIS (LIPEA) and MS PEAKS to PATHHWAY-METABOANALYST

Lishann M. Ingram and Brian S. Cummings. **To be submitted to Oncogene**

Abstract

The association between lipid metabolism and drug resistance in prostate cancer (PCa) remains poorly understood. The present study aims to identify crucial lipid regulatory networks associated with Docetaxel resistance in PCa using bioinformatics analyses such as Metaboanalyst and Lipid Pathway Enrichment Analysis (LIPEA). A comprehensive lipidomic pathway network was constructed from non-cancerous (PNT2 and RWPE1), hormone-sensitive (LNCaP and 22RV1), castration-resistant (PC-3 and DU-145) and Docetaxel resistant (PC3-Rx and DU145-DR) prostate cell lines and media. Analysis revealed that the lipids associated with glycerophospholipids metabolism, sphingolipid signaling pathways and ferroptosis accounted for a significant portion of the enriched nodes. The present study also identified a number of important lipid pathways within a metabolomic network that may assist with identifying potential targets for either diagnosing advanced PCa, or developing inhibitors of cell progression by targeting the enzyme that mediate the metabolism of these lipids.

Introduction

Drug resistant prostate cancer (PCa) still remains a challenge in the clinic, with no effective treatments being available to inhibit or resolve resistance [262-268]. This is especially true for Docetaxel, a frontline treatment for metastatic PCa. Understanding the precise molecular mechanism associated with development of Docetaxel resistance in PCa is essential for improvement of effective diagnostic and treatment strategies.

Cancer cells regulate their cellular lipids in a multifaceted process. Preclinical cancer studies have suggested a clinical role for lipid metabolism in tumor growth and metastasis in that the level of some lipids, such as phosphatidylcholines, are higher in the serum of patients with Docetaxel resistance [269-271]. Further, other studies have shown an alteration in lipid diversity in the blood and serum. Unfortunately, the consequence of this change in lipid diversity still remains unknown, but the, the current consensus is that changes in lipid composition is associated with altered behavior of cancer cells.

Extensive studies have provided strong evidence for reprogramming of lipid metabolism in cancer [272-274]. Many of these studies are fueled by advanced in mass spectrometry allowing for enhanced analysis of changes in the cellular or blood lipidome. While these studies have identified specific lipids, they have been hampered by the changes in the specific lipids have not been put into context with change in the regulation of overall lipid metabolism. One reason for this gap-in-knowledge is that, unlike genomic and proteomics, analysis tools allowing for assessment of lipid regulation pathways in tandem with lipidomic outcomes are not common. Recent advances from other laboratories have resulted in the development of such tools for the Lipid Pathway Enrichment Analysis, or LIPEA[275]. However, this approach has only seen limited

application. The present study used this tool, in conjunction with data derived from Metaboanalyst to identify the underlying regulatory lipid networks associated with Docetaxel resistance in PCa using bioinformatics analyses. Towards this goal, pathway enrichment analysis was performed in non-cancerous (PNT2 and RWPE1), hormone-sensitive (LNCaP and 22RV1), castration-resistant (PC-3 and DU-145) and Docetaxel resistant (PC3-Rx and DU145-DR) prostate cell lines and corresponding media.

Materials and Methods

Cell Culture

PC-3, LNCaP, 22RV-1, DU-145, RWPE1 and PNT2 cell lines were purchased from ATCC (Manassas, VA). The Docetaxel resistant human DU145-DR cell line was acquired from Dr. Begona Mellado's laboratory in the Medical Oncology Department, Hospital Clinic de Barcelona, Spain. The Docetaxel resistant human PC3-Rx cell line was acquired from Dr. LG Horvath's laboratory in the Garvan Institute of Medical Research in Darlinghurst, Australia. Cell supplements, including antibiotics and primary cell culture media, were purchased from ATCC (Manassas, VA). Standard cell culture media were purchased from Corning Inc. (Corning, NY). Human PCa cells were cultured in 10% FBS (Seradigm, Radnor, PA) and 1% penicillin/streptomycin supplemented RPMI-1640 cell media. All cells were incubated in 95% humidity and 5% CO_2 at 37°C. Docetaxel resistant cell lines maintained resistance by receiving 2 nM concentrations of Docetaxel at every 2nd and 4th passage.

Bligh-Dyer Lipid Extraction

Media from cells were collected followed by centrifugation. Cells were washed twice and harvested in phosphate buffered saline (PBS), followed by centrifugation. Phospholipids from both cells and media were immediately extracted using chloroform and methanol according to the method of Bligh and Dyer [4]. Briefly, cell lines and media were suspended in 3 ml of methanol and 3 ml of chloroform. Tubes were vortexed for 30 s, allowed to sit for 10 min on ice, centrifuged (300 x g; 5 min), and the bottom chloroform

layer was transferred to a new test tube and spiked with a commercial mix of SPLASH Lipidomix internal standards (Avanti Polar Lipids, Inc.). SPLASH Lipidomix Mass Spec standards includes all major lipid classes at ratios similar to that found in human plasma. The extraction procedure was repeated three times and the chloroform layers combined. The collected chloroform layers were dried under nitrogen, reconstituted with 50 µl of methanol: chloroform (3:1 v/v), and stored at 80ºC until analysis.

Liquid Phosphorus Assay

Lipid content was quantified by determining the level of inorganic phosphorus using the Bartlett Assay [5]. Sulfuric acid 400 µl (5M) was added to lipid extracts (10 µL) in a glass test tube, and heated at 180-200ºC for 1 h. H_2O_2 (100 µl of 30 % v/v) was then added while vortexing, and heated at 180-200ºC for 1.5 h. Reagent (4.6 ml of 1.1 g ammonium molybdate tetrahydrate in 12.5 ml sulfuric acid in 500 ml dd$H_2$0) was added followed by vortexing, which was followed by addition of 100 µl of 15% ascorbic acid (v/v), and further vortexing. The solution was heated for 7-10 min at 100ºC, and a 150 µl aliquot was used to measure the absorbance at 830 nm.

NanoHRLC-LTQ-Orbitrap MS

Lipid extracts were also analyzed by using a high resolution LC linear ion trap-Orbitrap Hybrid MS" (nanoHRLC-LTQ-Orbitrap MS, Thermo Scientific, San Jose, CA). Individuals running samples were blinded to sample conditions. Mass spectra were acquired in the positive ion mode. Mass spectrometric parameters for lipid extracts were as follows: spray

voltage: 3.5/2.5 kV, sheath gas: 40/35 AU; auxiliary nitrogen pressure: 15 AU; sweep gas: 1/0 AU; ion transfer tube and vaporizer temperatures: 325 and 300/275°C, respectfully. Full scan, data-dependent MS/MS (top10-ddMS2), and data-independent acquisition were collected at m/z 150–2000, corresponding to the mass range of most expected cellular lipids. External calibration was applied before each run to allow for LC-HRMS analysis at 120,000 resolution (at m/z 200).

Lipids were separated on a nanoC18 column (length, 130 mm; i.d., 100 µm; particle size, 5 µm; pore size, 150 Å; max flow rate, 500 nL/min; packing material, Bruker Micron Magic 18). Mobile phase A was 0.1% formic acid/water; mobile phase B was 0.1% formic acid/acetonitrile. 10 µL of each sample was injected for analysis. A constant flow rate of 500 nL/min was applied to perform a gradient profiling with the following proportional change of solvent A (v/v): 0 to 1.5 min at 98% A, 1.5 to 15.0 min from 98% to 75% A, 15.0 to 20.0 min from 75% to 40% A, 20.0 to 25.0 min from 40% to 5% A, 25.0 to 28.0 min kept at 5% A, and 28.0 to 30.0 min from 5% to 98% A. The washing elution ended with a 4 min re-equilibration. The LTQ-Orbitrap Elite MS was set in the positive full scan mode within range of 50 to 1500 m/z. Settings of the electrospray ionization were: heater temperature of 300°C, sheath gas of 35 arbitrary unit, auxiliary gas of 10 arbitrary unit, capillary temperature of 350°C, and source voltage of +3.0 kV. MS/MS fragmentation was induced using a collision-induced dissociation [10] scan with a Fourier transform resolving power of 120,000 (transient = 192 ms; scan repetition rate = 4 Hz) at 400 m/z over 50–1500 m/z [11]. The autosampler temperature was maintained at 4°C for all experiments. Solvent extraction blanks and samples were jointly analyzed over the course of a batch (10–15 samples).

Pathway Enrichment Analysis

Pathway enrichment analysis of metabolites was performed using LIPEA software [275]. LIPEA is a web tool for over-representation analysis of lipid signatures detection and enriched in biological pathways [275]. Total lipid compounds from all the pathways are extracted and the over-representation analysis (ORA) starts in parallel for each pathway. When all the ORA analysis are completed, the server computes the Benjamini and Bonferroni *p*-values corrections. Once this process is finished, the server returns a list of enriched pathways sorted by *p*-value. Finally, the results are shown in an interactive table. Significance of the pathway fit is calculated with comparison to Fisher's exact test performed on numerous permutations of random features within the total feature list. Hierarchical clustering of this these data identified differentially expressed lipid pathways from the set of lipids identified in our study. The module predicted biological activity directly from mass peak list data, and implements *mummichog* algorithm [276], which was cross referenced with the KEGG database. Biochemical pathways were derived from transformed KEGG IDs, using the internal mapping process (connected to Swiss Lipids, Lipid Maps, HMDB and KEGG databases)[275]. Columns represent individual sample type; rows refer to distinct metabolites, lipids and genes. Shades of green represent low levels and shades of red represent high levels ($p<0.05$).

Results

The development and progression of a cancer may be due, in part, to abnormal changes in lipid pathways rather than individual pathways. To test this hypothesis, we constructed a pathway network using MS Peak to Pathway-Metaboanalyst [277]. **Figure 4.1** demonstrates a lipid pathway network derived from lipid analysis of non-cancerous

(PNT2 and RWPE1), hormone-sensitive (LNCaP and 22RV1), castration-resistant (PC-3 and DU-145) and Docetaxel resistant (PC3-Rx and DU145-DR) prostate cell lines and media. Potential pathways were derived using an algorithm that matched accurate masses of lipid compounds whose level different significantly (e.g., p value < 0.05) between these cells with a minimum specified fold-change (> 1.5). These lipids were than aligned with genes correlating to their metabolism in the KEGG database[276]. (**Figure 4.1**). This analysis essentially identified almost all the regulatory networks involved in glycerophospholipid metabolism. In contrast, specific networks here not identified. The fact that multiple networks were identified may be a result of bias introduced by extraction used, or may suggest that overall glycerophospholipid metabolism is altered. Our initial analysis using MS Peak to Pathway- Metaboanalyst analysis resulted in a broad range of pathways, we attempted to identify possible enriched pathways from metbaoanalyst in **figure 4.1**.

Pathway analysis was also conducted using the MS Peaks to Pathway Activities module from Metaboanalyst, which generated a heat map-specific pathway visualization. This allowed for a convenient overview on associated patterns between non-cancerous (PNT2 and RWPE1), hormone-sensitive (LNCaP and 22RV1), castration-resistant (PC-3 and DU-145) and Docetaxel resistant (PC3-Rx and DU145-DR) prostate cell lines and media (**Figure 4.2A**).Hierarchical clustering of these data identified differential expressed lipid pathways similar to those identified This analysis resulted in several common dysregulated metabolic pathways including glycerophospholipid metabolism (**Figure 4.2B**). These data are supported by the LIPEA analysis that showed that glycerophospholipid metabolism is highly ranked and significantly associated to the set

of lipids identified in our study. The top pathways identified include glycerophospholipid metabolism (53%), sphingolipid metabolism (20%), ferroptosis (20%), and choline metabolism in cancer (20%) (**Table 4.1)[275].** These pathways are important in various cancers[278] and will be a focal point in future PCa research.

Discussion

This study used a pathway enrichment analysis to identify important pathways related to lipid metabolism in prostate cancer cells and media. Our previous studies using both ESI-MS and LC-ESI-MS/MS demonstrated a lipid panel including oxidized lipid species, phosphatidylcholine (PC), phosphatidylethanolamine (PE), sphingolipids (SM & Cer) and plasmalogens whose levels correlated to the various stages of drug resistant PCa. Pathway enrichment was performed to validate these data and to understand how change in this lipid panel may align with changes in the overall regulation of lipid metabolism.

Our initial MS Peak to Pathway- Metaboanalyst tended to identify a large network of multiple pathways. However, none of the individual pathways identified were enriched for one reason or another. This may be due to the number of samples analyzed all-in-one. It's also possible that the data is limited because the extraction method was biased towards glycerophospholipids. Interestingly, there were some KEGG compound IDs which included glycerophospholipid metabolism. Secondary analysis that employs hierarchical clustering using heat map visualization found several nodes which correlated to glycerosphingolipid metabolism. Our analysis of individual lipid shown in chapter 3 identified several sphingolipids that correlated to this analysis. There were some concerns about Metaboanalyst ability to specialize in lipids species. So we used the LIPEA pathway that has recently been identified to mine pathways significantly associated to lipid sets. LIPEA works with compound IDs for lipids found in KEGG Database and finds significantly perturbed pathways and applies statistical tests. Using

this analysis, the number one pathway identified to be significantly enriched was glycerophospholipid metabolism.

Glycerophospholipid metabolism, identified using both analysis employed aligned with lipid moieties are generated from glycerophospholipid metabolism, and molecules such as phosphatidic acid (PA) and diacylglycerol (DAG). These molecules are known for regulating many signaling pathways cells as we well as cell growth [279, 280]. The fact that pathway analysis identified glycerophospholipid metabolism as being altered in prostate cancer cells was expected.

The second was sphingolipid metabolism which agrees with the previous analysis, Metaboanalyst network and hierarchical clustering. Evidence suggest that sphingolipid-mediated gene expression plays a critical role in cancer by several mechanisms [177, 281, 282]. This includes the regulation of lipid-lipid interaction, membrane structure and/or regulation of the interaction of membrane proteins with the membrane bilayer [104].

What was unexpected was the identification of pathways for ferroptosis. This was rather interesting because we did see an increase in oxidized phosphatidylcholine (OxPC). Ferroptosis is a regulated form of iron-dependent, non-apoptotic cell death [283]. Ferroptosis can be driven by extensive lipid peroxidation that alters the physical properties of the membrane or degrade reactive compounds that cross-link DNA or proteins [284-286]. Ferroptosis is linked to numerous diseases of the kidney heart, liver and brain [283, 287]. The increase in ferroptosis aligns with our previous data demonstrating increases in oxidized glycerophospholipids in drug-resistance prostate

cancer cells. As such, ferroptosis may be useful for eliminating cancer cells that have become dependent on its suppression for their survival.

This study presented an innovative method of identifying novel lipid pathways with a metabolic network. Lipid pathways involved in genetic information processing are generally not cohesive and have a high degree of interpathway cross talk. However, new regulatory networks are still associative, and many of the computational method such as LIPEA are considered a hypothesis-generating tool.

Conclusion

This study corroborates that Docetaxel resistance in PCa is highly complex and correlates to alteration in lipid metabolism and regulation. The pathway analysis presented here will assist with improving the understanding of the underlying molecular mechanisms of Docetaxel resistance in PCa and how these mechanisms alter the lipidome. Further functional and validation studies are necessary to confirm the findings presented here. This includes pathways within the entire network interact closely to fulfill various biological functions.

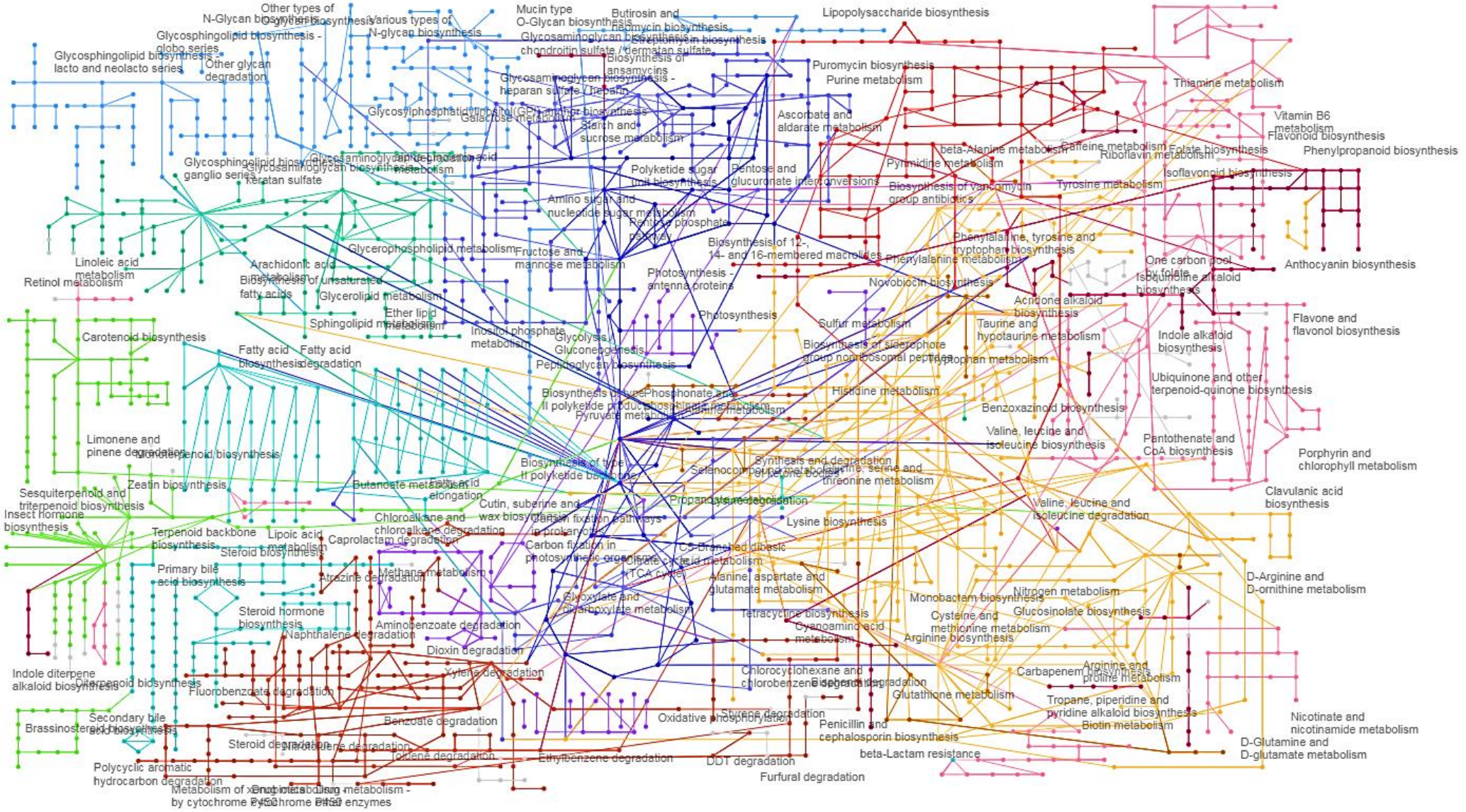

Figure 4.1. Global KEGG metabolic network associated with drug resistant cell types using targeted MS lipid profiles in Metaboanalyst. Each node represents either lipid metabolite, enzyme or other interconnecting metabolism.

A.

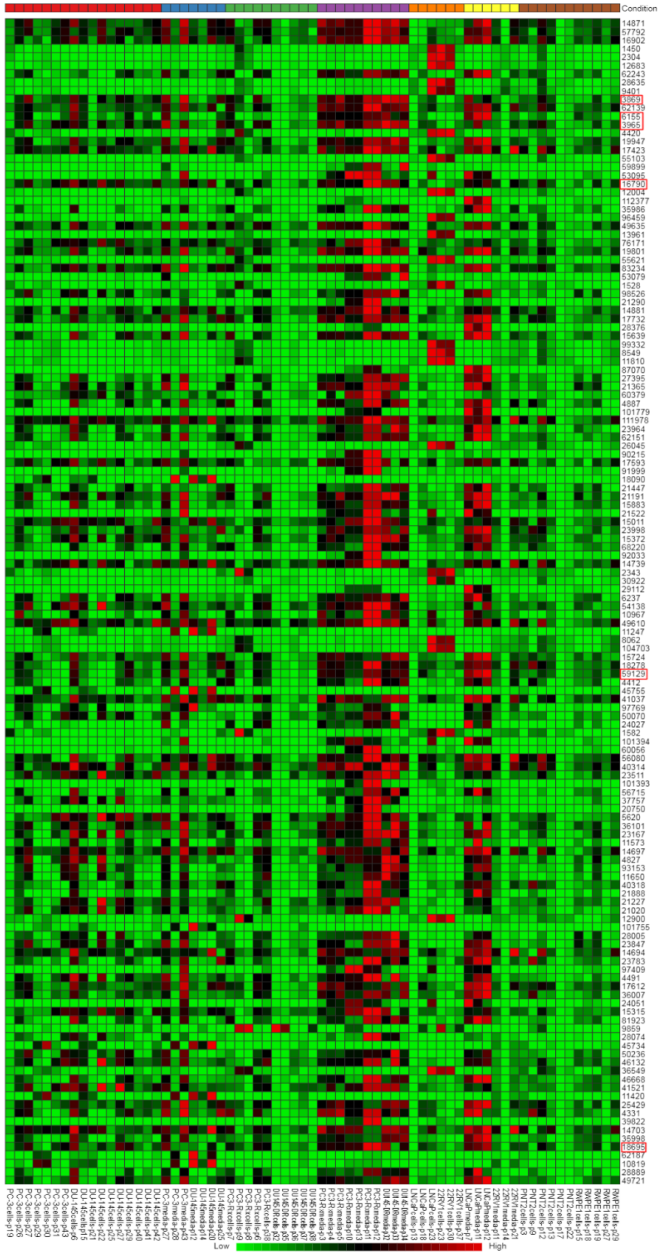
Condition
Low
High

B.

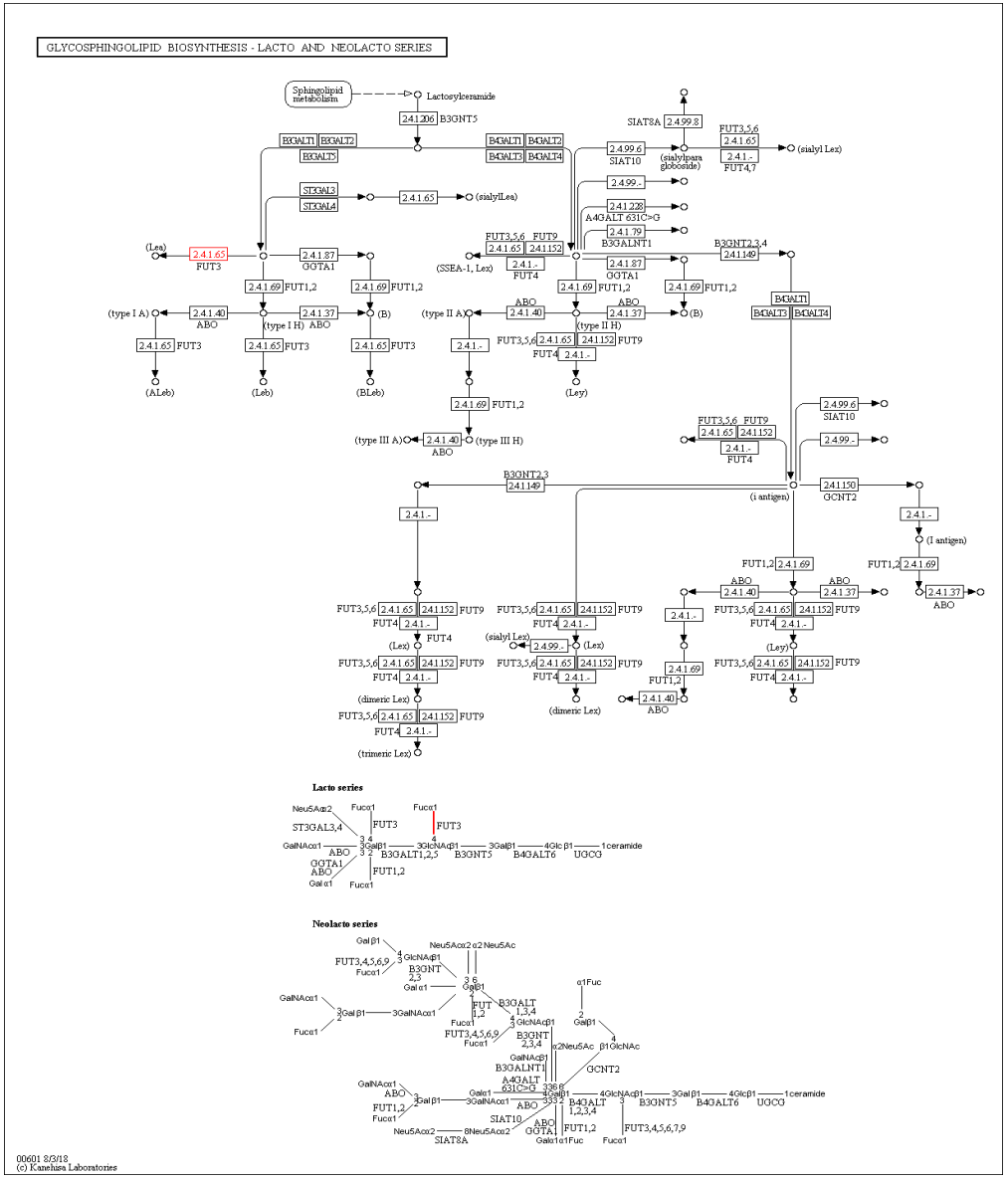
GLYCOSPHINGOLIPID BIOSYNTHESIS - LACTO AND NEOLACTO SERIES
Sphingolipid metabolism
Lactosylceramide
2.4.1.206 B3GNT5
(sialyl Lex)
(sialyl Lea)
(Lea)
(ALeb)
(Leb)
(BLeb)
(type I A)
(type I H)
(B)
(type II A)
(type II H)
(Ley)
(type III A)
(type III H)
(i antigen)
(I antigen)
(Lex)
(dimeric Lex)
(trimeric Lex)
Lacto series
Neolacto series
00601 8/3/18
(c) Kanehisa Laboratories

Figure 4.2. A) Heat map of differentially altered metabolites associated with non-cancerous (PNT2 and RWPE1), hormone-sensitive (LNCaP and 22RV1), castration-resistant (PC-3 and DU-145) and Docetaxel resistant (PC3-Rx and DU145-DR) prostate cell lines and media. **B)** Enriched glycosphingolipid metabolic pathway

Table 4.1 LIPEA pathway analysis. List of results from lipid indicators related to drug resistant cell types.

Pathway name	Pathway lipids	Converted lipids (number)	Converted lipids (percentage)	Converted lipids (list)	*p-value*	Benjamini correction	Bonferroni correction
Glycerophospholipid metabolism	26	8	53%	C02737, C04438, C00416, C04230, C00157, C05973, C04233, C00350	5.20E-08	1.66E-06	1.66E-06
Sphingolipid metabolism	21	3	20%	C00195, C00550, C12126	0.0145	0.0656	0.4069
Ferroptosis	11	3	20%	C21480, C21481, C21484	0.0021	0.0148	0.0591
Sphingolipid signaling pathway	9	3	20%	C00195, C12126, C00550	0.0011	0.0103	0.0310
Necroptosis	4	2	13%	C00195, C00550	0.0001	0.0020	0.0039

Retrograde endocannabinoid signaling	8	2	13%	C00157, C00350	0.0164	0.0656	0.4595
Phospholipase D signaling pathway	7	1	6%	C00416	0.0037	0.0209	0.1046
alpha-Linolenic acid metabolism	23	1	6%	C00157	0.8837	0.8837	1.0000
Glycerolipid metabolism	15	1	6%	C00416	0.4939	0.5122	1.0000
Autophagy - other	3	1	6%	C00350	0.4649	0.5007	1.0000
Autophagy - animal	4	1	6%	C00350	0.3328	0.3727	1.0000
Linoleic acid metabolism	25	1	6%	C00157	0.3328	0.3727	1.0000
Arachidonic acid metabolism	75	1	6%	C00157	0.2559	0.3116	1.0000

Glycine, serine and threonine metabolism	3	1	6%	C02737	0.1013	0.1575	1.0000
Glycosylphosphatidylinositol (GPI)-anchor biosynthesis	3	1	6%	C00350	0.0769	0.1435	1.0000
Neurotrophin signaling pathway	3	1	6%	C00195	0.1709	0.2278	1.0000
cAMP signaling pathway	5	1	6%	C00416	0.0769	0.1435	1.0000
Fc gamma R-mediated phagocytosis	6	1	6%	C00416	0.1251	0.1843	1.0000
GnRH signaling pathway	3	1	6%	C00416	0.0769	0.1435	1.0000
Phosphatidylinositol signaling system	11	1	6%	C00416	0.1483	0.2076	1.0000

AGE-RAGE signaling pathway in diabetic complications	2	1	6%	C00195	0.0769	0.1435	1.0000
Insulin resistance	4	1	6%	C00195	0.0769	0.1435	1.0000
Fat digestion and absorption	8	1	6%	C00416	0.1013	0.1575	1.0000
Adipocytokine signaling pathway	3	1	6%	C00195	0.1013	0.1575	1.0000

References

1. Thadani-Mulero, M., et al., *Androgen receptor splice variants determine taxane sensitivity in prostate cancer.* Cancer research, 2014. **74**(8): p. 2270-2282.

2. Ploussard, G., et al., *Class III β-tubulin expression predicts prostate tumor aggressiveness and patient response to docetaxel-based chemotherapy.* Cancer research, 2010. **70**(22): p. 9253-9264.

3. Zhu, Y., et al., *Inhibition of ABCB1 expression overcomes acquired docetaxel resistance in prostate cancer.* Molecular cancer therapeutics, 2013. **12**(9): p. 1829-1836.

4. Chen, H., H. Li, and Q. Chen, *INPP4B reverses docetaxel resistance and epithelial-to-mesenchymal transition via the PI3K/Akt signaling pathway in prostate cancer.* Biochemical and biophysical research communications, 2016. **477**(3): p. 467-472.

5. de Bessa Garcia, S.A., et al., *Prostate apoptosis response 4 (PAR4) expression modulates WNT signaling pathways in MCF7 breast cancer cells: A possible mechanism underlying PAR4-mediated docetaxel chemosensitivity.* International journal of molecular medicine, 2017. **39**(4): p. 809-818.

6. Codony-Servat, J., et al., *Nuclear factor-kappa B and interleukin-6 related docetaxel resistance in castration-resistant prostate cancer.* The Prostate, 2013. **73**(5): p. 512-521.

7. Marín-Aguilera, M., et al., *Epithelial-to-mesenchymal transition mediates docetaxel resistance and high risk of relapse in prostate cancer.* Molecular cancer therapeutics, 2014. **13**(5): p. 1270-1284.

8. Baenke, F., et al., *Hooked on fat: the role of lipid synthesis in cancer metabolism and tumour development.* Disease models & mechanisms, 2013. **6**(6): p. 1353-1363.

9. Ackerman, D. and M.C. Simon, *Hypoxia, lipids, and cancer: surviving the harsh tumor microenvironment.* Trends in cell biology, 2014. **24**(8): p. 472-478.

10. Cruz, P.M., et al., *The role of cholesterol metabolism and cholesterol transport in carcinogenesis: a review of scientific findings, relevant to future cancer therapeutics.* Frontiers in pharmacology, 2013. **4**: p. 119.

11. Cheng, C., et al., *Glucose-mediated N-glycosylation of SCAP is essential for SREBP-1 activation and tumor growth.* Cancer cell, 2015. **28**(5): p. 569-581.

12. Guo, D., et al., *EGFR signaling through an Akt-SREBP-1–dependent, rapamycin-resistant pathway sensitizes glioblastomas to antilipogenic therapy.* Sci. Signal., 2009. **2**(101): p. ra82-ra82.

13. Guo, D., et al., *An LXR agonist promotes glioblastoma cell death through inhibition of an EGFR/AKT/SREBP-1/LDLR–dependent pathway.* Cancer discovery, 2011. **1**(5): p. 442-456.

14. Acevedo, A., et al., *LIPEA: Lipid Pathway Enrichment Analysis.* bioRxiv, 2018: p. 274969.

15. Li, S., et al., *Predicting network activity from high throughput metabolomics.* PLoS computational biology, 2013. **9**(7): p. e1003123.

16. Chong, J., et al., *MetaboAnalyst 4.0: towards more transparent and integrative metabolomics analysis.* Nucleic Acids Res, 2018. **46**(W1): p. W486-w494.

17. Dolce, V., et al., *Glycerophospholipid synthesis as a novel drug target against cancer.* Curr Mol Pharmacol, 2011. **4**(3): p. 167-75.

18. Tappia, P.S. and T. Singal, *Phospholipid-mediated signaling and heart disease.* Subcell Biochem, 2008. **49**: p. 299-324.

19. Oude Weernink, P.A., et al., *Dynamic phospholipid signaling by G protein-coupled receptors.* Biochim Biophys Acta, 2007. **1768**(4): p. 888-900.

20. Fernandis, A.Z. and M.R. Wenk, *Membrane lipids as signaling molecules.* Curr Opin Lipidol, 2007. **18**(2): p. 121-8.

21. Brzozowski, J.S., et al., *Lipidomic profiling of extracellular vesicles derived from prostate and prostate cancer cell lines.* Lipids Health Dis, 2018. **17**(1): p. 211.

22. Ponnusamy, S., et al., *Sphingolipids and cancer: ceramide and sphingosine-1-phosphate in the regulation of cell death and drug resistance.* Future oncology (London, England), 2010. **6**(10): p. 1603-1624.

23. van Meer, G., D.R. Voelker, and G.W. Feigenson, *Membrane lipids: where they are and how they behave.* Nat Rev Mol Cell Biol, 2008. **9**(2): p. 112-24.

24. Dixon, S.J., et al., *Ferroptosis: an iron-dependent form of nonapoptotic cell death.* Cell, 2012. **149**(5): p. 1060-1072.

25. Latunde-Dada, G.O., *Ferroptosis: Role of lipid peroxidation, iron and ferritinophagy.* Biochim Biophys Acta Gen Subj, 2017. **1861**(8): p. 1893-1900.

26. Agmon, E., et al., *Modeling the effects of lipid peroxidation during ferroptosis on membrane properties.* Sci Rep, 2018. **8**(1): p. 5155.

27. Agmon, E. and B.R. Stockwell, *Lipid homeostasis and regulated cell death.* Curr Opin Chem Biol, 2017. **39**: p. 83-89.

28. Stockwell, B.R., et al., *Ferroptosis: a regulated cell death nexus linking metabolism, redox biology, and disease.* Cell, 2017. **171**(2): p. 273-285.

CHAPTER 5

SUMMARY

Drug resistance is a major obstacle for development of PCa treatments. PCa cells are able to alter and reprogram lipid metabolism to meet increasing energy demands for cell proliferation and the nutrient-deprived tumor microenvironment [288-290]. Hence, a better understanding of lipid metabolic dysregulation could lead to the discovery of novel therapeutic predictors for CRPC. To understand the role of lipid alterations in the development of drug resistance and gain insight into defects in lipid metabolism associated with drug-resistant CRPC progression, we conducted comprehensive, unbiased liquid chromatography-mass spectrometry (LC-MS/MS) based lipidomic profiling of non-cancerous, hormone-sensitive and CRPC and Docetaxel resistant cell lines and media.

Lipidomics has proved to be a useful tool for delineating cellular mechanisms and identifying biomarkers for many diseases, such as obesity, hypertension, diabetes, cystic fibrosis and other cancers [291-301]. A lipidomic approach utilizing whole cell lysates of culture cell lines support the notion that the cellular lipidome is actively remodeled under various physiological conditions [302]. By utilizing open-source date processing tools, we increased the throughput and reproducibility of our lipidomic studies. This expanded coverage helps to characterize a number of species that are often overshadowed, such as oxidized lipids. Furthermore, recent advances in lipidomics have allowed for the

identification of dysregulated lipid signatures that are often a result of complex interactions in metabolism, diet, genetics and lifestyle. Although lipidomics has significant potential for predicting new indicators and understanding health and disease, there is no consensus on proper data processing protocols. For lipidomics to be implemented in a clinical setting, one must account for factors perturbing lipid measurements. With these are numerous sample preparation protocols, and many factors that reduce the accuracy and precision of lipid measurements that are not fully understood. Adaptation of technologies that employ sample processing entirely at cryogenic temperatures or other strategies for preserving sample integrity are needed for robust and accurate lipid measurements.

Without a consensus on the methods, it is difficult to produce annotations and measurements of lipids that are needed for adaptation to the clinical field. The workflows presented in this dissertation utilize community-accepted lipidomics software, such as LipidMatch, XCMS, MZmine, LIPEA and Metaboanalyst. Lipid concentrations measured across labs are often drastically different, and annotations using the most widely accepted software often contain false positives. Furthermore, quantification is problematic due to cost and unavailable lipid standards to cover the diverse species within a given lipidome. Therefore, strategies to select the best internal standards for each lipid class are employed in what is termed relative quantification. However, much work is needed to further improve accuracy of lipid measurements, such as the implementation of better quality controls and certified reference materials.

Owing to the high complexity and diversity among lipid molecules, only a few attempts have been made to identify individual lipid species as biomarkers and

therapeutic agents in various cancers. Earlier reports have shown an association between fatty acids and the progression of breast and ovarian cancer, making it evident that fatty acid synthesis plays a vital role in human cancer development [303, 304]. Plasma lipid biomarkers identified in previous studies had high sensitivity and specificity in the diagnosis of prostate cancer when compared to the prostate specific antigen (PSA) test [305]. However, no such attempts have been made to alleviate drug resistance in prostate cancer treatments. Herein, we present a series of studies that attempt to advance the field of lipid signaling within the context of drug resistance with the overall hypothesis that significant lipidomic alterations in Docetaxel resistant CRPC cell types serve as indicators for drug resistant prostate cancer progression. A novel aspect of these studies is that we capitalized on robust lipidomics techniques, which enables a more precise characterization of lipid classes within given cells. We attempted to understand key aspects of lipid species alteration in the context of drug resistance, which has not been demonstrated in the prostate cancer field. Due to the critical role of lipids in metabolism, and the observed remodeling of the lipidome, monitoring levels of individual lipid classes or lipid species can be used to assess disease progression. Our findings demonstrated a metastatic-dependent shift in individual lipid species that correlate to circulating lipids in patients. Furthermore, clinically relevant indicators recapitulated by our *in vitro* lipidomics studies have the potential to predict patient responses to particular drugs. Findings from these studies could lay the foundation for the development of strategies for detection resistance PCa.

Following lipidomic data processing and identification, data analysis included exploration of lipid species and their putative biological meaning. This was essential to

gain insight into the molecular mechanisms underlying the observed lipid moieties. We derived a set of lipid pathways and compiled integrated lipidomic-transcriptomic signature genes most relevant to prostate cancer. The topmost lipid altered genes found to play a major role in development of drug resistance will be characterized in future work.

Subtle differences in lipid structure can have dramatic influences on the lipid species biology. Currently, biological databases (e.g., Kyoto Encyclopedia of Gene and genomes (KEGG)) are unable to capture the varying lipid structural resolution conferred by mass spectrometry. For example, while there is a general KEGG entry for phosphatidylcholine class (PCs), C00157, there is no KEGG entry for specific PCs. This lack of specificity reduces the scope of biological inference to mechanisms general to all PCs. On the other hand, the Human Metabolome Database (HMDB) contains identifiers for the specific lipid molecule. However, these biological inferences can be too specific and lead to false interpretation of the data.

Drug resistant prostate cancer can be characterized, in part, by the malignant and systemic dysfunction of metabolic processes [306]. In primary cancer cells driven by oncogenic pathways or restrained microenvironments, the lipid metabolic network is deregulated and the balance of lipid uptake/mobilization is disrupted [306]. Consequently, the accumulated signaling lipids may mediate intracellular communication between drug-resistant cancer and non-cancer cells. Lipid homeostasis is crucial to prevent metabolic diseases. Since lipids are not encoded by the genome, targeting lipid enzymes is one of the ways to control lipid homeostasis. For example, lipins are a class of enzymes that catalyze the dephosphorylation of phosphatidic acid to diacylglycerol, which is a precursor

of triacylglycerol and phospholipids [307, 308]. These enzymes also function as co-transcriptional regulators. Thus, they can regulate lipid homeostasis.

Previous studies demonstrated that the lipin-1 knockdown repressed proliferation of prostate and breast cancer cells [309]. However, there is still a gap in knowledge as to how these processes shape the progression of drug-resistant cancer. Recent reports demonstrated that inhibition of lipin with propranolol sensitized cancer cells to rapamycin [309]. Propranolol is also a non-specific inhibitor of lipins. A recent report demonstrated that the non-selective beta adrenergic receptor antagonist (Propranolol) altered late stage breast cancer [310]. Propranolol is widely used and has effects on cellular proliferation and invasion in liver cells [311]. Recent data suggests, propranolol acts on leukemia, breast, melanoma, ovarian, angiosarcoma, prostate, pancreatic and other cancers [312]. Preliminary data from our lab suggests that propranolol sensitized drug resistant DU145-DR cell line to Docetaxel treatment compared to parent control DU-145 cells and HepG2 cells used as a positive control (**Figure 5**). Based on pre-clinical reports, these data suggest that propranolol may be re-purposed as a potential new therapeutic to combat docetaxel resistance.

Moreover, lipid metabolic enzymes and signaling lipids play an important role in the regulation of exosome formation and release from cancer cells. Exosome lipids can modulate their bioactivity in the tumor microenvironment and during distant dissemination. Preliminary studies from our lab demonstrate lipid alterations within the media of cell lines. One consideration is that the drug resistant cancer cells secrete exosomes into the media but the mechanisms are not well studied. The importance of lipids and/or lipid-metabolizing enzymes in the release of exosomes in oligodendroglial, prostate cancer

and breast cancer cell lines has been discussed [313]. A study on PC-3 (metastatic bone prostate cancer cell line) demonstrated major differences in lipid classes and species between the cell lines and their corresponding exosomes. These lipid differences in exosomes might be useful as biomarkers, as similar findings could be found in drug resistant CRPC. Considering exosomes as bioactive lipid drug carriers that could exert specific efforts in recipient cells will facilitate the design of efficient exosome-based cancer therapeutics for drug-resistant PCa.

The overall key findings from this study are the following: (1) identification of a unique lipid signature for drug resistant prostate cancer, and (2) determination aberrant pathways in drug-resistant CRPC progression with an integrated lipidomic/transcriptomic high gene signature score correlated to poor survival. This approach is advantageous because A) bioactive lipids participate in the pathogenesis of multiple cancers via lipid signaling networks, and B) understanding lipidomics, including the underlying molecular machinery of lipid metabolism, would assist in the discovery of novel and potential targets and develop new predictors for personalized cancer treatments. Furthermore, our global lipid pathway analysis suggests glycerophospholipid metabolism is the bottleneck contributor to the tumorigenic lipids that drive drug resistant prostate cancer progression. Thus, the use of lipid profiling in cell culture is critical in assessing the function of various lipid species. An abundance of lipid species can be collected via non-invasive procedures and easily monitored using human biological fluids, which include blood and urine. Our data supports the hypothesis that lipids themselves can be used as therapeutic tools in cells. Our system could potentially provide a translational gateway for understanding lipid-species-mediated drug resistance. Furthermore, abnormalities in lipid metabolism occurs

through a network of multiple signaling pathways which implies that targeting lipid metabolism could be a novel strategy for drug resistance prevention and treatment.

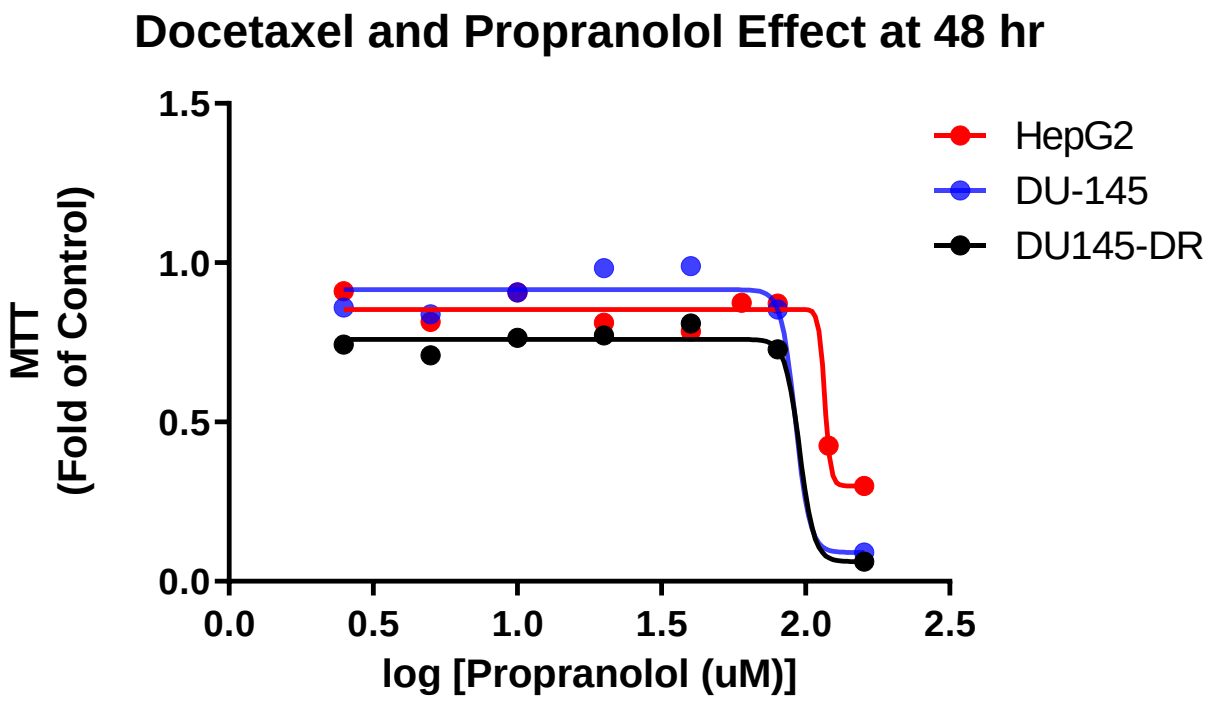

Figure 5: MTT assay shows decrease in MTT staining in Docetaxel resistant cell line as compared to parent cell line (DU-145) and positive control (HepG2). This suggests DU145-DR (black) is sensitized Docetaxel as compared to DU-145 (blue) parent cell and HepG2 (red) positive control.

References

1. Beloribi-Djefaflia, S., S. Vasseur, and F. Guillaumond, *Lipid metabolic reprogramming in cancer cells.* Oncogenesis, 2016. **5**(1): p. e189.

2. DeBerardinis, R.J. and N.S. Chandel, *Fundamentals of cancer metabolism.* Sci Adv, 2016. **2**(5): p. e1600200.

3. DeBerardinis, R.J., et al., *The Biology of Cancer: Metabolic Reprogramming Fuels Cell Growth and Proliferation.* Cell Metabolism, 2008. **7**(1): p. 11-20.

4. Pietilainen, K.H., et al., *Acquired obesity is associated with changes in the serum lipidomic profile independent of genetic effects--a monozygotic twin study.* PLoS One, 2007. **2**(2): p. e218.

5. Ekroos, K., et al., *Lipidomics: a tool for studies of atherosclerosis.* Curr Atheroscler Rep, 2010. **12**(4): p. 273-81.

6. Lankinen, M., et al., *Fatty fish intake decreases lipids related to inflammation and insulin signaling--a lipidomics approach.* PLoS One, 2009. **4**(4): p. e5258.

7. de Mello, V.D., et al., *Link between plasma ceramides, inflammation and insulin resistance: association with serum IL-6 concentration in patients with coronary heart disease.* Diabetologia, 2009. **52**(12): p. 2612-5.

8. Graessler, J., et al., *Top-down lipidomics reveals ether lipid deficiency in blood plasma of hypertensive patients.* PLoS One, 2009. **4**(7): p. e6261.

9. Han, X., et al., *Alterations in myocardial cardiolipin content and composition occur at the very earliest stages of diabetes: a shotgun lipidomics study.* Biochemistry, 2007. **46**(21): p. 6417-28.

10. Ollero, M., et al., *Plasma lipidomics reveals potential prognostic signatures within a cohort of cystic fibrosis patients.* J Lipid Res, 2011. **52**(5): p. 1011-22.

11. Gorke, R., et al., *Determining and interpreting correlations in lipidomic networks found in glioblastoma cells.* BMC Syst Biol, 2010. **4**: p. 126.

12. Balogh, G., et al., *Lipidomics reveals membrane lipid remodelling and release of potential lipid mediators during early stress responses in a murine melanoma cell line.* Biochim Biophys Acta, 2010. **1801**(9): p. 1036-47.

13. Kolak, M., et al., *Adipose tissue inflammation and increased ceramide content characterize subjects with high liver fat content independent of obesity.* Diabetes, 2007. **56**(8): p. 1960-8.

14. Zhao, Y.Y., X.L. Cheng, and R.C. Lin, *Lipidomics applications for discovering biomarkers of diseases in clinical chemistry.* Int Rev Cell Mol Biol, 2014. **313**: p. 1-26.

15. Lydic, T.A. and Y.-H. Goo, *Lipidomics unveils the complexity of the lipidome in metabolic diseases.* Clinical and translational medicine, 2018. **7**(1): p. 4-4.

16. Wu, Q., et al., *Cancer-associated adipocytes: key players in breast cancer progression.* Journal of hematology & oncology, 2019. **12**(1): p. 95-95.

17. Balaban, S., et al., *Obesity and cancer progression: is there a role of fatty acid metabolism?* BioMed research international, 2015. **2015**: p. 274585-274585.

18. Zhou, J. and P. Giannakakou, *Targeting microtubules for cancer chemotherapy.* Curr Med Chem Anticancer Agents, 2005. **5**(1): p. 65-71.

19. Luo, X., et al., *The implications of signaling lipids in cancer metastasis.* Experimental & molecular medicine, 2018. **50**(9): p. 127-127.

20. Zhang, T.Y., et al., *Management of castrate resistant prostate cancer-recent advances and optimal sequence of treatments.* Curr Urol Rep, 2013. **14**(3): p. 174-83.

21. Pascual, F. and G.M. Carman, *Phosphatidate phosphatase, a key regulator of lipid homeostasis.* Biochimica et biophysica acta, 2013. **1831**(3): p. 514-522.

22. Brohée, L., et al., *Lipin-1 regulates cancer cell phenotype and is a potential target to potentiate rapamycin treatment.* Oncotarget, 2015. **6**(13): p. 11264-11280.

23. Montoya, A., et al., *The beta adrenergic receptor antagonist propranolol alters mitogenic and apoptotic signaling in late stage breast cancer.* Biomedical Journal, 2019. **42**(3): p. 155-165.

24. Wang, F., et al., *Propranolol suppresses the proliferation and induces the apoptosis of liver cancer cells.* Molecular medicine reports, 2018. **17**(4): p. 5213-5221.

25. Pantziarka, P., et al., *Repurposing Drugs in Oncology (ReDO)-Propranolol as an anti-cancer agent.* Ecancermedicalscience, 2016. **10**: p. 680-680.

APPENDIX: CHAPTER 1

EFFECT of LOW and HIGH FAT DIET on LIPDOMIC BLOOD CHANGES INDUCED AFTER IN VIVO EXPOSURE of MALE C57BL/6 MICE to PERFLOROOCTANE SULFONIC (PFOS) and PERFLOUROHEXANESULFONIC ACID (PFHxS)

Marisa Pfohl, **Lishann M. Ingram**, Emily Marques, Adam Auclair, Benjamin Barlock, Dwight Anderson, Michael Goedken, Brian S. Cummings and Angela L. Slitt **To be submitted to (Toxicological Sciences)**

Abstract

Millions of people are exposed to per- and polyfluoroalkyl substances (PFASs) every day through diet and it is known that there is an association between exposure to these PFASs and hepatic steatosis. However, there is a significant gap-in-knowledge on the association between changes in blood lipids and exposure to PFASs. There is also a lack of knowledge regarding the effects of low and high fat diet on both hepatotoxicity and blood lipids. We addressed these gaps by exposing C57BL/6 mice to perfluorooctane sulfonic acid (PFOS) and perfluorohexane sulfonic acid (PFHxS) in low-fat diet (LFD (11% kcal from fat)) and high-fat high-carbohydrate diet (HFD (58% kcal from fat)) for 29 weeks. Changes in the blood lipidome were analyzed using both an untargeted shotgun approach (electrospray ionization-mass spectrometry, ESI-MS), and a targeted quantitative approach (HPLC-ESI-Orbitrap-MS/MS). Blood was isolated from C57BL/6 mice that were exposed to either PFOS or PFHxS (~0.3mg/kg/day) via low or high fat diet, and lipids were extracted using the Bligh-Dyer method. The initial untargeted ESI-MS approach demonstrated distinct clustering within the blood lipidome, with the most dramatic shifts occurring between LFD and LFD with PFAS (L-PFOS and L-PFHxS) exposure and HFD and HFD with PFAS (H-PFOS and H-PFHxS) exposure. HPLC-ESI-MS/MS analysis revealed 2,918 discriminatory ion features for lipids isolated from mice exposed to LFD, L-PFOS, L-PFHxS, HFD, H-PFOS, and H-PFHxS. Mice exposed to PFOS and PFHxS in the presence of a LFD had higher levels of phosphatidylcholine (PC), as compared to those exposed to the LFD only. This included 14:0-22:2 PC, which was enriched in the blood of mice exposed to L-PFHxS and L-PFOS as compared to LFD control mice.

Surprisingly, plasmalogens were significantly enriched in mice exposed to H-PFHxS as compared to HFD control mice. These data demonstrate the novel finding that PFAS exposure alters the blood lipidome of mice, and suggests that the effect of PFAS's on the blood lipidome is diet-dependent. These data identify a novel correlation between dietary consumption, PFAS exposure and the blood lipidome that may provide a basis for identification of PFAS related lipid predictors.

Introduction

Poly- and perfluoroalkyl substances (PFASs) are a family of more than 4,000 aliphatic compounds that are used in diverse applications [314]. PFASs are fluorinated aliphatic substances in which the hydrogen substituents of at least one terminal carbon atom are completely replaced by fluorine atoms [315, 316]. The most prevalent PFASs in human samples and the environment are generally perfluorooctanesulfonic acid (PFOS) and perfluorohexanesulfonic (PFHxS) [317, 318]. Their hydrophobic properties result in their use in multiple consumer products such as disposable food packaging, cookware, outdoor gear, furniture and carpet [319, 320].

Foods, and in some cases drinking water, were identified as major exposure sources of PFASs for the general population, with indoor air and dust adding to the total [321, 322]. For examples, fish consumption can lead to high levels of PFOS [319, 323]. Average daily intakes of single PFASs were estimated to be in the range between 0.14 and a few hundred ng/kg body weight (bw)/d for the general adult population [324-326]. In 2012, the European Food Safety Authority (EFSA) assessed the exposure of adults to PFOS and calculated daily intakes of 5-10 and 4-1 ng/kg bd/d respectively [327].

Human exposure to PFASs is a global phenomenon. The Centers for Disease Control and Prevention (CDC) reported that PFASs are detectable in blood of over 98% of the general population [328-330]. However, there is a growing consensus that PFAs pose a threat to human and environmental health. Over 600 studies have evaluated the toxicity of PFAS compounds, with epidemiology studies account for over 400 of the toxicity studies [331]. Evidence from these epidemiology studies suggest links between

PFAS exposure and several health outcomes, including, liver damage, increases in serum lipids, thyroid disease, immune effects, reproductive toxicity, and developmental toxicity [332].

Although there are several human epidemiological studies of PFAS, most toxicity data are based on laboratory animal studies [333, 334]. The most commonly examined end points are liver, body weight, developmental, reproductive and immunological effects with limited studies assessing diet [332]. A few reports have focused more on dietary intake of various PFASs [327]. In 2017 a review focusing on global human dietary exposure to PFASs [335] reported differences in PFAS concentrations in food items from a number of countries. Certain countries that had higher amounts of seafood consumption, had diets that contained higher PFAS concentrations that other food groups analyzed.

Previous studies demonstrate that PFAS exposure has a significant effect on kidney epithelial cells (A6 cells) [336], and human placental chroriocarcinoma (JEG-3) cells [337]. Some of these studies examined the relationship between PFAS and blood lipid levels and found that higher plasma PFAS concentration was associated with higher levels of total cholesterol, triacylglycerides, LDL, and VLDL [338]. PFASs, specifically perfluorononanoic acid (PFNA) and perfluoroundecanoic acid (PFUnDA) were strongly associated with changes in several glycerophosphocholines and fatty acids. Few of these studies assessed the effect of PFAS on overall lipidomic changes, and even fewer assessed the effect of diet on the ability of PFASs to alter the blood lipidome. To address this gap in knowledge, and to fully understand the effect of PFAS on the blood and it's

correlation to liver toxicity we utilized lipidomic approach to identify PFAS-diet interactions on the serum lipidome.

Materials and Methods

Animal conditions

Exposure of animals to PFAS was conducted in the laboratory of Dr. Angela Slitt at the University of Rhode Island in accordance with protocol approved by Institutional Animal Care and Use Committee (IACUC). Male mice, C57BL/6 were acquired from Jackson Labs (Bar Harbor, ME USA) at eight weeks of age. The mice were acclimated for two weeks prior to being weight paired and housed three per cage in a temperature-controlled room. A strict 12-hour dark/light cycle was maintained with access to food and water *ad libitum*. Body weights, water, and food consumption were monitored throughout the study. Following 29 weeks of diet and PFAS administration, mice were anesthetized using isoflurane and sacrificed by cardiac puncture. Trunk blood was acquired via decapitation under isoflurane. Gross liver weight was recorded prior to sectioning in 10% formalin for histology. The remaining tissues were snap frozen in liquid nitrogen for downstream analysis.

Dietary Treatment

The study design was based on a published model of diet-induced non-alcoholic steatohepatitis (NASH) [339]. The mice received either a 11% kcal, low fat diet (LFD) (D12328, Research Diets, New Brunswick), or a 58% kcal, high fat diet (HFD) (D12331, Research Diets, New Brunswick). The mice that received a high fat diet were also administered high carbohydrates diet both through the sucrose content of the high fat diet and through carbohydrates added to drinking water at 42 g/L (55% fructose: 45% sucrose). The mice were assigned to either diet alone, as controls, or to diet containing

0.0003% PFOS or 0.0003% PFHxS. The PFOS and PFHxS chemical stocks were obtained from Sigma-Aldrich (St. Louis, MO, USA). The resulting treatment groups were as follows: low fat diet (LFD), high fat high carbohydrate diet (HFD), LFD + PFOS (L-PFOS), HFD + PFOS (H-PFOS), LFD + PFHxS (L-PFHxS), and HFD+ PFHxS (H-PFHxS) at n = 6 per treatment group. The daily exposure to PFAS via diet was roughly ~0.3mg/kg/day. In the current EPA health advisory document for PFOS, 0.3 mg/kg/day is considered a NOAEL dose for PFOS induced hepatic toxicity [340, 341].

Bligh-Dyer Lipid Extraction of Serum

Serum lipids were isolated for lipidomic analysis according to the method of Bligh and Dyer [227]. Briefly, blood samples designated for lipidomics were suspended in 1.25 ml of methanol and 1.25 ml of chloroform. Tubes were vortexed for 30 s, allowed to sit for 10 min on ice, centrifuged (300 x *g*; 5 min), and the bottom chloroform layer was transferred to a new test tube. The extraction steps were repeated three times and the chloroform layer combined. A commercial mix of SPLASH Lipidomix internal standards (Avanti Polar Lipids, Inc.) were spiked into each sample. SPLASH Lipidomix Mass Spec standards includes all major lipid classes at ratios similar to that found in human plasma. The collected chloroform layers were dried under nitrogen, reconstituted with 50 µl of methanol: chloroform (3:1 v/v), and stored at 80ºC until analysis.

Liquid Phosphorus Assay

Lipid content was quantified by determining the level of inorganic phosphorus using the Bartlett Assay [228]. Sulfuric acid (400 µl, 5M) was added to lipid extracts (10 µL) in a glass test tube, and heated at 180-200ºC for 1 h. H_2O_2 (100 µl of 30 % v/v) was then added while vortexing, and the mixture heated at 180-200ºC for 1.5 h. Reagent (4.6 ml of 1.1 g ammonium molybdate tetrahydrate in 12.5 ml sulfuric acid in 500 ml ddH_2O) was added followed by vortexing, which was followed by addition of 100 µl of 15% ascorbic acid (v/v), and further vortexing. The solution was heated for 7-10 min at 100ºC, and a 150 µl aliquot was used to measure the absorbance at 830 nm (**Supplemental Table 6.1**).

ESI-MS/MS Analysis of Cells and Media

Lipid extracts (500 pmol/µl) were prepared by reconstitution in chloroform: methanol (2:1, v/v). ESI-MS was performed on a 5 µl aliquot of each sample as previously described [229-231] using a LCQ Deca ion-mass spectrometer (LCQ Finnigan mass spectrometer (Thermo Fisher-Fenning Institute, CA)) with nitrogen drying gas flow-rate of 81/min at 350 ºC and a nebulizer pressure of 30 psi. The scanning range was from 200 to 1000 *m/z* in positive and negative mode for 2.5 min. The mobile phase was acetonitrile; methanol; water (2:3:1) in 0.1% ammonium formate. Samples were run in triplicate (n = 3) [232].

NanoHRLC-LTQ-Orbitrap MS

Lipid extracts were also analyzed using a high resolution LC linear ion trap-Orbitrap Hybrid MS" (nanoHRLC-LTQ-Orbitrap MS) (Thermo Scientific, San Jose, CA). Individuals running samples were blinded to sample conditions. Mass spectra were acquired in the positive ion mode. Mass spectrometric parameters for lipid extracts were as follows: spray voltage: 3.5/2.5 kV, sheath gas: 40/35 AU; auxiliary nitrogen pressure: 15 AU; sweep gas: 1/0 AU; ion transfer tube and vaporizer temperatures: 325 and 300/275°C, respectfully. Full scan, data-dependent MS/MS (top10-ddMS2), and data-independent acquisition were collected at *m/z* 150–2000, corresponding to the mass range of most expected cellular lipids. External calibration was applied before each run to allow for LC-HRMS analysis at 120,000 resolution (at *m/z* 200). Lipids were separated on a nanoC18 column (length, 130 mm; i.d, 100 µm; particle size, 5 µm; pore size, 150 Å; max flow rate, 500 nL/min; packing material, Bruker Micron Magic 18). Mobile phase A was 0.1% formic acid/water; mobile phase B was 0.1% formic acid/acetonitrile. 10 µL of each sample was injected for analysis. A constant flow rate of 500 nL/min was applied to perform a gradient profiling with the following proportional change of solvent A (v/v): 0 to 1.5 min at 98% A, 1.5 to 15.0 min from 98% to 75% A, 15.0 to 20.0 min from 75% to 40% A, 20.0 to 25.0 min from 40% to 5% A, 25.0 to 28.0 min kept at 5% A, and 28.0 to 30.0 min from 5% to 98% A. The washing elution ended with a 4 min re-equilibration. The LTQ-Orbitrap Elite MS was set in the positive full scan mode within range of 50 to 1500 m/z. Settings of the electrospray ionization were: heater temperature of 300°C, sheath gas of 35 arbitrary unit, auxiliary gas of 10 arbitrary unit, capillary temperature of 350°C, and source voltage of +3.0 kV. *MS/MS* fragmentation was induced using a collision-

induced dissociation [233] scan with a Fourier transform resolving power of 120,000 (transient = 192 ms; scan repetition rate = 4 Hz) at 400 m/z over 50–1500 m/z [234]. The autosampler temperature was maintained at 4°C for all experiments. Solvent extraction blanks and samples were jointly analyzed over the course of a batch (10–15 samples).

Data Processing

Full scan raw data files were acquired from Xcalibur™ (Thermo Fisher Scientific), centroided and converted to a useable format (mzXML) using MSConvert. Data processing and peak area integration were performed using MZmine [235], and XCMS [236], resulting in a feature intensity table. Feature tables and *MS/MS* data were placed into a directory for each substrate analyzed. Each folder contained each sample type, feature tables end in “pos.csv” for positive mode. LipidMatch developed by Koelmel et al [237] was used to identify features. Peak height were normalized to a mixture of deuterium labeled internal standards for each sample (SPLASH® LIPIDOMIX® Mass Spec standard.

Multivariate Statistical Analysis of Cells and Media

Multivariate principal component analysis (PCA) was performed using MetaboAnalyst 4.0 (http://www.metaboanalyst.ca/). Automatic peak detection and spectrum deconvolution was performed using a peak width set to 0.5. Analysis parameters consisted of interquartile range filtering and sum normalization with no removal of outliers from the dataset. Features were selected based on a one-way ANOVA analysis and were further identified using HPLC-*MS/MS* analysis. Significance for ANOVA plot analysis was

determined based on a fold-change threshold of 2.00, $q \leq 0.05$ and $p \leq 0.05$. Following identification, internal standards were used to normalize each parent lipid level, and the change in the relative abundance of that phospholipid species as compared to its control was determined. This method is standard for lipidomic analysis as reported in our previous studies [231, 238].

Pathway Enrichment Analysis

Pathway enrichment analysis of metabolites was performed using LIPEA software [275]. LIPEA is a web tool for over-representation analysis of lipid signatures detection and enriched in biological pathways [275]. Total lipid compounds from all the pathways are extracted and the over-representation analysis (ORA) starts in parallel for each pathway. When all the ORA analysis are completed, the server computes the Benjamini and Bonferroni *p*-values corrections. Once this process is finished, the server returns a list of enriched pathways sorted by *p*-value. Finally, the results are shown in an interactive table. Significance of the pathway fit is calculated with comparison to Fisher's exact test performed on numerous permutations of random features within the total feature list. Hierarchical clustering of this these data identified differentially expressed lipid pathways from the set of lipids identified in our study. The module predicted biological activity directly from mass peak list data, and implements *mummichog* algorithm [276], which was cross referenced with the KEGG database. Biochemical pathways were derived from transformed KEGG IDs, using the internal mapping process (connected to Swiss Lipids, Lipid Maps, HMDB and KEGG databases)[275]. Columns represent individual sample type; rows refer to distinct metabolites, lipids and genes. Shades of green represent low levels and shades of red represent high levels ($p<0.05$).

Statistical Analyses

All statistical analyses were compiled using GraphPad Prism for windows version 8.2.1 (GraphPad Software, Inc., La Jolla, CA). For all analysis, the experimental unit was individual samples obtained from the 6 groups. For comparative analysis across different features in the XCMS heat map, peak areas were converted to z-scores. The row Z-score or scaled expression value of each feature was calculated as mean abundance subtracted from the abundance and then divided by the standard deviation across all the samples. We controlled for the effect of multiple testing by measuring the statistical significance of each association using both the *p* value and the *q* value. Using a FDR of $q < 0.05$, the *q* value quantifies significance in terms of the false discovery rate (FDR) rather than the false positive rate and forms a measure of how likely a particular *p* value is to represent a genuine association (**Supplemental Table 2**). For all analyses, significance was set at $p \leq 0.05$ where data were expressed as mean ± SEM based on t-test for pairwise analysis and/or ANOVA analysis (with Kruskal-Wallis *post hoc* test).

Results

PFASS exposure causes significant dysregulation of the mouse blood lipidome

Multivariate, unsupervised principal component analysis (PCA) scores plots of spectral data comparing changes in the blood lipidome after exposure to PFASs in the presence of both LFD and HFD showed distinct clustering within the blood lipidome where diet was the major effector (**Supplemental Figure 6.1 and 6.2**)**.** A supervised PLS-DA of the blood lipidome demonstrated separation between the blood lipidome of mice exposed to the LFD and the LFD in the presence of both PFASs (**Supplemental Figure 5.1A**). However, similar results were observed for mice exposed to the HFD and those exposed to the HFD containing both PFASs (**Supplemental Figure 6.2A**). Cross validation values of these PLS-DA models confirmed discrimination between PFASs in the presence of both LFD and HFD, with an accuracy value from 0.35 to 0.8 value of R^2 Model quality, as evaluated using R2Y and Q2 values, which reflect the explained fraction of variance and model predictability (**Supplemental Figure 6.1B, C and 6.2 B, C**)**.** These data suggest that exposure of mice to both PFASs and diet induce differential lipidomic profiles within the blood lipidome. Based on the diet-related comparisons, HPLC-ESI MS/MS was employed to identify the number of features altered between sample types.

Blood from mice exposed to LFD and HFD in the presence and absence of PFASs were analyzed using HPLC-ESI-Orbitrap-MS/MS and the results were analyzed by a cloud plot and a heat map analysis. This identified 2,918 dysregulated ion features, encompassing 28 different lipid species. The cloud plot analysis identified several lipids that had a significant fold-change (**Figure 6.1A**)**.** These lipids were cross-compared to those identified using a heat map analysis (**Figure 6.1B**). The data agree with the above

mentioned ESI-MS analysis supporting the conclusion that PFAS exposure alters the effect of both LFD and HFD on the blood lipidome.

Lipidomic Profiling of Blood Isolated from Mice Exposed to LFD and PFASs

Targeted lipidomics was performed to identify specific changes between the blood lipidome of mice exposed to the LFD and HFD. Diet-related pairwise comparisons identified 146 dysregulated ion features between these two groups**,** as shown by both cloud plot (**Figure 6.2A**) and heat map analysis (**Figure 6.2B**).

LC-ESI-*MS/MS* analysis of the blood lipidome from mice exposed to the LFD, in comparison to those exposed to the LFD and PFOS diet (L-PFOS), identified 1,121 dysregulated ion features between these two groups (**Figure 6.3A** and **B**). A similar analysis was used to compare changes in the lipidome of blood isolated from mice exposed to the LFD and those exposed to the LFD and PFHxS (L-PFHxS). A total of 283 dysregulated ion features were identified between these two groups (**Figure 6.4A** and **B**).

Lipidomic Profiling of Blood Isolated from Mice Exposed to HFD and PFASs

A total of 546 dysregulated ion features were identified in blood isolated from mice exposed to the HFD in comparison to those exposed to the HFD containing PFOS (H-PFOS) (**Figure 6.5A** and **6.5B**). A similar analysis was used to compare changes in the blood lipidome in mice exposed to the HFD as opposed to those exposed to the HFD containing PFHxS (H-PFHxS). This analysis identified 841 dysregulated ion features

dysregulated between the two groups (**Figure 6.6**). These data were used to identify the specific lipids altered in the blood of mice exposed to PFASs and to determine changes in the levels of these lipids.

Identification of Phospholipid Altered by Diet and PFOS

Phosphatidylcholine (PC) lipids were enriched in the blood of mice exposed to HFD and both the L-PFOS and L-PFHxS diets, when compared to mice exposed only to the LFD (**Figure 6.7A**). Amongst the PC lipids, 14:0-22:2 PC was identified as a dominant species in the blood of mice exposed the HFD and to the L-PFOS and L-PFHxS diets (**Figure 6.7B**). Interestingly, oxidized-PC lipids (OxPC) were enriched in the blood mice of exposed the HFD, as compared to mice exposed to the LFD (**Figure 6.7C**). However, there was a significant decrease in OxPC in the blood of mice exposed to the H-PFHxS diet as compared to the HFD alone. Surprisingly, oxidized lysoPC (OxLPC) was significantly enriched in the blood of mice exposed to the HFD and L-PFHxS diet, as compared to the LFD. However, there was a significant decrease of L-PFOS compared to LFD (**Figure 6.7D**).

The levels of phosphatidylethanolamine (PE) decreased in the blood of mice exposed to the L-PFHxS and L-PFOS diets, as compared to those only exposed to the LFD alone (**Figure 6.8A**). Similar results were observed in mice exposed to the H-PFHxS and H-PFOS diets, as compared to those only exposed to the HFD alone (**Figure 6.8A**). LysoPE (LPE) was significantly decreased in the blood of mice exposed to the both L-PFHxS and L-PFOS diets, as compared to the LFD (**Figure 6.8B**). Phosphatidylglycerol (PG) was significantly enriched in the blood of mice exposed to HFD, as compared the other groups analyzed (**Figure 6.9**).

Alterations in Acylglycerol Lipids

Monogalactosyldiacylglycerol (MGDG) levels were significantly enriched in the blood of mice exposed to the HFD, as compared to blood analyzed from mice fed with the LFD. There was a significant decrease in mice exposed to the H-PFHxS diet, as compared to those only exposed to the HFD (**Figure 6.10A**). The levels of oxidized triacylglycerides (OxTAG) decreased in the blood of mice exposed to the L-PFHxS and L-PFOS diets, as compared to those only exposed to the LFD (**Figure 6.10B**).

Alterations in Other Lipids

Sphingomyelin (SM) was significantly decreased in the blood of mice exposed to HFD as well as those exposed to the both L-PFHxS and L-PFOS diets, as compared to the LFD (**Figure 6.11**). Surprisingly, plasmalogen levels were increased in the blood of mice exposed to the L-PFOS and L-PFHxS diets, as compared to the LFD alone (**Figure 6.12**). Plasmalogen levels were also increased in mice exposed to the H-PFHxS diets, as compared to the HFD alone, but were decreased in the blood of mice exposed to the H-PFOS diet (**Figure 6.12**).

Since these results suggest common dysregulated metabolic pathways, we performed lipid pathway enrichment analysis (LIPEA) to further identify the top pathways that may be altered by PFAS and diet. This analysis demonstrated the majority of lipids altered in response to either HFD, of PFAS exposure correlated to that glycerophospholipid metabolism (50%) (**Supplemental Table 6.3**) [275]. Other pathways identified included

those mediating sphingolipids, ferroptosis, choline metabolism in cancer, retrograde endocannabinoid signaling and necroptosis.

Discussion

Although a large number of epidemiology studies have examined the potential for PFASs to induce hepatic steatosis in correlation with other adverse effects, most of the studies do not establish causality. This is especially true for studies demonstrate correlations between hepatic steatosis and change in blood lipids. Further, many studies on blood lipids focus on classical lipid indicators, such as cholesterol, LDL, HDL and others. In contrast, few if any, have studies the ability of PFAs to alter the blood lipidome and correlated these changes to hepatic steatosis, even fewer have examined the effect of diet on either PFAs-induced hepatic steatosis and changes in the blood lipidome. The present study represents a first step toward identifying any such correlation. Data from both untargeted and targeted analysis of the mouse blood lipidome demonstrated diet-dependent shifts in the types and levels of lipids modulated by PFHxS and PFOS exposure. This analysis demonstrated that changes in the lipidome that were dependent on both diet and the presence of PFASs. Subsequent targeted analysis validated these data and identified the specific types of lipids altered. These findings are consistent with the previous literature demonstrating that circulating PC levels were significantly augmented in (non-alcoholic fatty liver (NAFL)) and non-alcoholic steatohepatitis (NASH) patients, as compared to healthy controls [342]. Contrary to PC, the level of PE, as well as lysophosphatidylcholine (LPC, data not shown) and lysophosphatidylethanolamine

(LPE) decreased. This trend was also seen in NAFL and NASH patients in comparison to controls [342].

Oxidized lipids such as those derived from PC, LPC and TAG have not been previously associated with PFAS exposure. It is known that oxidized lipids are not simply by-products formed during lipid peroxidation reactions, but are key mediators in inflammation [131, 133], infection [152], and immune response [153, 154]. Furthermore, oxidized lipids are suggested to be augmented in NASH mediated by increases in BMI levels [343].

Our findings agree with previous studies that demonstrate an increase in plasmalogen levels in steastotic and cirrhotic livers compared to normal livers [344]. Elevated plasmalogens are suggested to indicate increased activity of protective mechanisms against oxidative stress [345]. Furthermore, plasmalogens are enriched in developing lipoproteins secreted by cultured rat hepatocytes where they may serve as endogenous plasma antioxidants [346]. However, there are other reports that demonstrate that serum plasmalogen levels are decreased in patients with NASH and NAFLD as compared to controls [347]. A decrease in plasmalogen levels could be associated with a more severe in NASH patients as opposed to steatosis patients [347].

PFAS exposure has been demonstrated to have strong associations with serum cholesterol [348]. PFAS effects on total cholesterol and triglycerides were measured by our collaborators at the University of Rhode Island (data not shown). These results are in accordance with previous studies showing that PFAS exposure augments in total serum cholesterol compared to HFD control group. These data are in agreement with findings of this studying showing that PFOS caused a significant reduction in total serum

triglycerides compared to both HFD and LFD control groups. Recent reports revealed an absence of many major analytes known to participate in lipid droplet formation in NAFLD progression, including total TAGs and DAGs prominent in steatosis [349]. Associations of PFASs with triacylglycerides and other lipoproteins had generally been inconsistent, and more commonly showed null results [338, 348, 350, 351].

It is important to note that there are considerable differences in the toxicokinetics of PFASs between humans and experimental animals. Adverse health effects in studies in animals have been associated with exposure concentrations or doses that resulted in blood levels of PFASs that were significantly higher than those reported in the general population [352]. For example, the elimination $t_{1/2}$ of these compounds is approximately 4 years in humans compared with days or hours in rodents [353]. These factors, plus issues related to mode of action of PFAS, make it somewhat difficult to determine the true relevance of some effects reported in animal studies to human health.

While this study represents the most comprehensive analysis of the effect of diet and PFAS exposure on the blood lipidome, it is limited as the actual concentrations for lipid species were not provided. This was in part intentional, and these data are meant to springboard further studies focusing on the specific lipids identified are being altered in serum. Furthermore, it is important to point out that many of these lipids are rather novel and do not have a suitable internal standard at this time to allow for quantification. Future studies will focus on quantifying these specific lipids in liver as well as validating their existence in human plasma.

Conclusion

This study demonstrated that exposure of PFAS in the diet alters the effect of LFD and HFD in the blood lipidome of mice after *in vivo* exposure. This supports the hypothesis that the effect of PFAS's on the blood lipidome is diet-dependent. Our findings are consistent with previous literature reports that both diet and PFAS can augment lipid outcomes, and this study provides new evidence that increased oxidative lipid species in serum levels correlate to exposure of PFAS in diet. This study represents the first to characterize diet-PFAS impact on the blood lipidome. The mechanisms by which PFASs may interfere with blood lipids in humans are not well understood. The moderate predictive accuracy of R^2 in **Supplemental Figure 6.1B, C** could be explained by the induced fatty liver due to overconsumption observed in the LFD control groups as well as advanced age (39 weeks) of the male mice. Finally, these findings suggest a correlation between changes in the blood lipidome and PFAS induced hepatic steatosis providing a basis for identification of PFAS related lipid predictors.

References

1. Karantanos, T., P.G. Corn, and T.C. Thompson, *Prostate cancer progression after androgen deprivation therapy: mechanisms of castrate resistance and novel therapeutic approaches.* Oncogene, 2013. **32**(49): p. 5501-5511.

2. Jemal, A., et al., *Cancer statistics, 2008.* CA Cancer J Clin, 2008. **58**(2): p. 71-96.

3. Chambers, S.K., et al., *Defining young in the context of prostate cancer.* Am J Mens Health, 2015. **9**(2): p. 103-14.

4. Siegel, R.L., K.D. Miller, and A. Jemal, *Cancer statistics, 2019.* CA: A Cancer Journal for Clinicians, 2019. **69**(1): p. 7-34.

5. Fontenot, P.A., Jr., et al., *Metastatic prostate cancer in the modern era of PSA screening.* Int Braz J Urol, 2017. **43**(3): p. 416-421.

6. Roobol, M.J., *Screening for prostate cancer: are organized screening programs necessary?* Transl Androl Urol, 2018. **7**(1): p. 4-11.

7. Salinas, C.A., et al., *Prostate cancer in young men: an important clinical entity.* Nat Rev Urol, 2014. **11**(6): p. 317-23.

8. Hiraoka, Y. and M. Akimoto, *Anatomy of the prostate from fetus to adult--origin of benign prostatic hyperplasia.* Urol Res, 1987. **15**(3): p. 177-80.

9. Humphrey, P.A., *Histopathology of Prostate Cancer.* Cold Spring Harb Perspect Med, 2017. **7**(10).

10. Bhavsar, A. and S. Verma, *Anatomic imaging of the prostate.* Biomed Res Int, 2014. **2014**: p. 728539.

11. Garraway, L.A., et al., *Intermediate basal cells of the prostate: in vitro and in vivo characterization.* Prostate, 2003. **55**(3): p. 206-18.

12. van Leenders, G.J. and J.A. Schalken, *Epithelial cell differentiation in the human prostate epithelium: implications for the pathogenesis and therapy of prostate cancer.* Crit Rev Oncol Hematol, 2003. **46 Suppl**: p. S3-10.

13. Man, Y.-G., et al., *Tumor-infiltrating immune cells promoting tumor invasion and metastasis: existing theories.* Journal of Cancer, 2013. **4**(1): p. 84-95.

14. Tchetgen, M.B., et al., *Ejaculation increases the serum prostate-specific antigen concentration.* Urology, 1996. **47**(4): p. 511-6.

15. Liu, A.Y. and L.D. True, *Characterization of prostate cell types by CD cell surface molecules.* Am J Pathol, 2002. **160**(1): p. 37-43.

16. Cary, K.C. and M.R. Cooperberg, *Biomarkers in prostate cancer surveillance and screening: past, present, and future.* Therapeutic advances in urology, 2013. **5**(6): p. 318-329.

17. Petrylak, D.P., et al., *Docetaxel and estramustine compared with mitoxantrone and prednisone for advanced refractory prostate cancer.* New England Journal of Medicine, 2004. **351**(15): p. 1513-1520.

18. Tannock, I.F., et al., *Docetaxel plus prednisone or mitoxantrone plus prednisone for advanced prostate cancer.* New England Journal of Medicine, 2004. **351**(15): p. 1502-1512.

19. de Bono, J.S., et al., *Abiraterone and increased survival in metastatic prostate cancer.* N Engl J Med, 2011. **364**(21): p. 1995-2005.

20. Parker, C., et al., *Alpha emitter radium-223 and survival in metastatic prostate cancer.* New England Journal of Medicine, 2013. **369**(3): p. 213-223.

21. Desouki, M., et al., *hZip2 and hZip3 zinc transporters are down regulated in human prostate adenocarcinomatous glands.* Molecular Cancer, 2007. **6**: p. 37.

22. Logothetis, C., et al., *Current perspectives on bone metastases in castrate-resistant prostate cancer.* Cancer Metastasis Rev, 2018. **37**(1): p. 189-196.

23. Merseburger, A.S., A. Alcaraz, and C.A. von Klot, *Androgen deprivation therapy as backbone therapy in the management of prostate cancer.* Onco Targets Ther, 2016. **9**: p. 7263-7274.

24. Boccon-Gibod, L., E. van der Meulen, and B.-E. Persson, *An update on the use of gonadotropin-releasing hormone antagonists in prostate cancer.* Therapeutic advances in urology, 2011. **3**(3): p. 127-140.

25. Wadosky, K.M. and S. Koochekpour, *Molecular mechanisms underlying resistance to androgen deprivation therapy in prostate cancer.* Oncotarget, 2016. **7**(39): p. 64447-64470.

26. Gamat, M. and D.G. McNeel, *Androgen deprivation and immunotherapy for the treatment of prostate cancer.* Endocrine-related cancer, 2017. **24**(12): p. T297-T310.

27. Montgomery, R.B., et al., *Maintenance of intratumoral androgens in metastatic prostate cancer: a mechanism for castration-resistant tumor growth.* Cancer Res, 2008. **68**(11): p. 4447-54.

28. Heidenreich, A., et al., *[EAU guidelines on prostate cancer. Part I: screening, diagnosis, and treatment of clinically localised disease].* Actas Urol Esp, 2011. **35**(9): p. 501-14.

29. Li, Y., et al., *Androgen receptor splice variants mediate enzalutamide resistance in castration-resistant prostate cancer cell lines.* Cancer Res, 2013. **73**(2): p. 483-9.

30. Crona, D.J. and Y.E. Whang, *Androgen Receptor-Dependent and -Independent Mechanisms Involved in Prostate Cancer Therapy Resistance.* Cancers (Basel), 2017. **9**(6).

31. Thoma, C., *AR-Vs not predictive in mCRPC.* Nature Reviews Urology, 2018. **15**: p. 203.

32. Sharp, A., et al., *Androgen receptor splice variant-7 expression emerges with castration resistance in prostate cancer.* The Journal of Clinical Investigation, 2019. **129**(1): p. 192-208.

33. Chandrasekar, T., et al., *Mechanisms of resistance in castration-resistant prostate cancer (CRPC).* Transl Androl Urol, 2015. **4**(3): p. 365-80.

34. Tilki, D., E.M. Schaeffer, and C.P. Evans, *Understanding Mechanisms of Resistance in Metastatic Castration-resistant Prostate Cancer: The Role of the Androgen Receptor.* European Urology Focus, 2016. **2**(5): p. 499-505.

35. Huang, Y., et al., *Molecular and cellular mechanisms of castration resistant prostate cancer.* Oncol Lett, 2018. **15**(5): p. 6063-6076.

36. Kahn, B., J. Collazo, and N. Kyprianou, *Androgen receptor as a driver of therapeutic resistance in advanced prostate cancer.* Int J Biol Sci, 2014. **10**(6): p. 588-95.

37. Yuan, X. and S.P. Balk, *Mechanisms mediating androgen receptor reactivation after castration.* Urologic oncology, 2009. **27**(1): p. 36-41.

38. Sharifi, N., *Mechanisms of androgen receptor activation in castration-resistant prostate cancer.* Endocrinology, 2013. **154**(11): p. 4010-4017.

39. Tan, M.H.E., et al., *Androgen receptor: structure, role in prostate cancer and drug discovery.* Acta Pharmacologica Sinica, 2014. **36**: p. 3.

40. Prins, G.S. and O. Putz, *Molecular signaling pathways that regulate prostate gland development.* Differentiation; research in biological diversity, 2008. **76**(6): p. 641-659.

41. Di Lorenzo, G., et al., *Expression of Epidermal Growth Factor Receptor Correlates with Disease Relapse and Progression to Androgen-independence in Human Prostate Cancer.* Clinical Cancer Research, 2002. **8**(11): p. 3438-3444.

42. Cai, C., et al., *Intratumoral de novo steroid synthesis activates androgen receptor in castration-resistant prostate cancer and is upregulated by treatment with CYP17A1 inhibitors.* Cancer Res, 2011. **71**(20): p. 6503-13.

43. Kallio, H.M.L., et al., *Constitutively active androgen receptor splice variants AR-V3, AR-V7 and AR-V9 are co-expressed in castration-resistant prostate cancer metastases.* British Journal of Cancer, 2018. **119**(3): p. 347-356.

44. Heinlein, C.A. and C. Chang, *Androgen receptor (AR) coregulators: an overview.* Endocr Rev, 2002. **23**(2): p. 175-200.

45. van der Steen, T., D.J. Tindall, and H. Huang, *Posttranslational modification of the androgen receptor in prostate cancer.* International journal of molecular sciences, 2013. **14**(7): p. 14833-14859.

46. Stein, M.N., et al., *Androgen synthesis inhibitors in the treatment of castration-resistant prostate cancer.* Asian journal of andrology, 2014. **16**(3): p. 387-400.

47. Beer, T.M., et al., *Enzalutamide in metastatic prostate cancer before chemotherapy.* N Engl J Med, 2014. **371**(5): p. 424-33.

48. James, N.D., et al., *Abiraterone for Prostate Cancer Not Previously Treated with Hormone Therapy.* N Engl J Med, 2017. **377**(4): p. 338-351.

49. Armstrong, C.M. and A.C. Gao, *Drug resistance in castration resistant prostate cancer: resistance mechanisms and emerging treatment strategies.* American journal of clinical and experimental urology, 2015. **3**(2): p. 64-76.

50. Schalken, J. and J.M. Fitzpatrick, *Enzalutamide: targeting the androgen signalling pathway in metastatic castration-resistant prostate cancer.* BJU international, 2016. **117**(2): p. 215-225.

51. Rodriguez-Vida, A., et al., *Enzalutamide for the treatment of metastatic castration-resistant prostate cancer.* Drug design, development and therapy, 2015. **9**: p. 3325-3339.

52. Petrylak, D.P., et al., *Docetaxel and estramustine compared with mitoxantrone and prednisone for advanced refractory prostate cancer.* N Engl J Med, 2004. **351**(15): p. 1513-20.

53. Fang, M., et al., *Efficacy of Abiraterone and Enzalutamide in Pre- and Postdocetaxel Castration-Resistant Prostate Cancer: A Trial-Level Meta-Analysis.* Prostate cancer, 2017. **2017**: p. 8560827-8560827.

54. Antonarakis, E.S., *Current understanding of resistance to abiraterone and enzalutamide in advanced prostate cancer.* Clin Adv Hematol Oncol, 2016. **14**(5): p. 316-9.

55. Antonarakis, E.S., et al., *AR-V7 and Resistance to Enzalutamide and Abiraterone in Prostate Cancer.* New England Journal of Medicine, 2014. **371**(11): p. 1028-1038.

56. Hotte, S.J. and F. Saad, *Current management of castrate-resistant prostate cancer.* Current oncology (Toronto, Ont.), 2010. **17 Suppl 2**(Suppl 2): p. S72-S79.

57. Mendiratta, P., A.J. Armstrong, and D.J. George, *Current standard and investigational approaches to the management of hormone-refractory prostate cancer.* Reviews in urology, 2007. **9 Suppl 1**(Suppl 1): p. S9-S19.

58. Berthold, D.R., et al., *Docetaxel plus prednisone or mitoxantrone plus prednisone for advanced prostate cancer: updated survival in the TAX 327 study.* J Clin Oncol, 2008. **26**(2): p. 242-5.

59. Lohiya, V., J.B. Aragon-Ching, and G. Sonpavde, *Role of Chemotherapy and Mechanisms of Resistance to Chemotherapy in Metastatic Castration-Resistant Prostate Cancer.* Clinical Medicine Insights. Oncology, 2016. **10**(Suppl 1): p. 57-66.

60. Dagher, R., et al., *Approval summary: Docetaxel in combination with prednisone for the treatment of androgen-independent hormone-refractory prostate cancer.* Clin Cancer Res, 2004. **10**(24): p. 8147-51.

61. Zhu, M.-L., et al., *Tubulin-targeting chemotherapy impairs androgen receptor activity in prostate cancer.* Cancer research, 2010. **70**(20): p. 7992-8002.

62. Fitzpatrick, J.M. and R. de Wit, *Taxane mechanisms of action: potential implications for treatment sequencing in metastatic castration-resistant prostate cancer.* Eur Urol, 2014. **65**(6): p. 1198-204.

63. Terry, S., et al., *Increased expression of class III β-tubulin in castration-resistant human prostate cancer.* British journal of cancer, 2009. **101**(6): p. 951.

64. Ranganathan, S., et al., *Modulation of endogenous β-tubulin isotype expression as a result of human β III cDNA transfection into prostate carcinoma cells.* British journal of cancer, 2001. **85**(5): p. 735.

65. Oudard, S., *TROPIC: Phase III trial of cabazitaxel for the treatment of metastatic castration-resistant prostate cancer.* Future Oncol, 2011. **7**(4): p. 497-506.

66. Kartner, N., J.R. Riordan, and V. Ling, *Cell surface P-glycoprotein associated with multidrug resistance in mammalian cell lines.* Science, 1983. **221**(4617): p. 1285-8.

67. Assaraf, Y.G., *The role of multidrug resistance efflux transporters in antifolate resistance and folate homeostasis.* Drug Resist Updat, 2006. **9**(4-5): p. 227-46.

68. Wyatt, A.W., et al., *The diverse heterogeneity of molecular alterations in prostate cancer identified through next-generation sequencing.* Asian journal of andrology, 2013. **15**(3): p. 301-308.

69. Hoey, T., *Drug resistance, epigenetics, and tumor cell heterogeneity.* Sci Transl Med, 2010. **2**(28): p. 28ps19.

70. Coyle, K.M., J.E. Boudreau, and P. Marcato, *Genetic Mutations and Epigenetic Modifications: Driving Cancer and Informing Precision Medicine.* BioMed research international, 2017. **2017**: p. 9620870-9620870.

71. Fernandez, E., et al., *Factors and Mechanisms for Pharmacokinetic Differences between Pediatric Population and Adults.* Pharmaceutics, 2011. **3**(1): p. 53-72.

72. Li, M., et al., *Clinical targeting recombinant immunotoxins for cancer therapy.* OncoTargets and therapy, 2017. **10**: p. 3645-3665.

73. Thurber, G.M., M.M. Schmidt, and K.D. Wittrup, *Antibody tumor penetration: transport opposed by systemic and antigen-mediated clearance.* Advanced drug delivery reviews, 2008. **60**(12): p. 1421-1434.

74. Corn, P.G., *The tumor microenvironment in prostate cancer: elucidating molecular pathways for therapy development.* Cancer management and research, 2012. **4**: p. 183-193.

75. Pedraza-Fariña, L.G., *Mechanisms of oncogenic cooperation in cancer initiation and metastasis.* The Yale journal of biology and medicine, 2006. **79**(3-4): p. 95-103.

76. Liu, Y.Y., et al., *Ceramide glycosylation potentiates cellular multidrug resistance.* Faseb j, 2001. **15**(3): p. 719-30.

77. Nguyen, K.T., et al., *Transactivation of the human multidrug resistance (MDR1) gene promoter by p53 mutants.* Oncol Res, 1994. **6**(2): p. 71-7.

78. Smets, L.A., *Programmed cell death (apoptosis) and response to anti-cancer drugs.* Anticancer Drugs, 1994. **5**(1): p. 3-9.

79. Xue, X., et al., *Nanoscale drug delivery platforms overcome platinum-based resistance in cancer cells due to abnormal membrane protein trafficking.* ACS nano, 2013. **7**(12): p. 10452-10464.

80. Glavinas, H., et al., *The role of ABC transporters in drug resistance, metabolism and toxicity.* Curr Drug Deliv, 2004. **1**(1): p. 27-42.

81. Kis, O., et al., *The complexities of antiretroviral drug-drug interactions: role of ABC and SLC transporters.* Trends Pharmacol Sci, 2010. **31**(1): p. 22-35.

82. Goldstein, L.J., et al., *Expression of a multidrug resistance gene in human cancers.* J Natl Cancer Inst, 1989. **81**(2): p. 116-24.

83. Wilkens, S., *Structure and mechanism of ABC transporters.* F1000prime reports, 2015. **7**: p. 14-14.

84. Cunha, G.R., A.A. Donjacour, and Y. Sugimura, *Stromal-epithelial interactions and heterogeneity of proliferative activity within the prostate.* Biochem Cell Biol, 1986. **64**(6): p. 608-14.

85. Filella, X., et al., *Emerging biomarkers in the diagnosis of prostate cancer.* Pharmacogenomics and personalized medicine, 2018. **11**: p. 83-94.

86. Velonas, V.M., et al., *Current status of biomarkers for prostate cancer.* International journal of molecular sciences, 2013. **14**(6): p. 11034-11060.

87. Ross, R.K., et al., *Androgen metabolism and prostate cancer: establishing a model of genetic susceptibility.* Cancer Res, 1998. **58**(20): p. 4497-504.

88. Costello, L.C., R.B. Franklin, and P. Feng, *Mitochondrial function, zinc, and intermediary metabolism relationships in normal prostate and prostate cancer.* Mitochondrion, 2005. **5**(3): p. 143-53.

89. Eidelman, E., et al., *The Metabolic Phenotype of Prostate Cancer.* Frontiers in oncology, 2017. **7**: p. 131-131.

90. Carracedo, A., et al., *Cancer metabolism: fatty acid oxidation in the limelight.* Nature Reviews Cancer, 2013. **13**: p. 227-232.

91. Puchades-Carrasco, L. and A. Pineda-Lucena, *Metabolomics Applications in Precision Medicine: An Oncological Perspective.* Current topics in medicinal chemistry, 2017. **17**(24): p. 2740-2751.

92. Gowda, G.A.N., et al., *Metabolomics-based methods for early disease diagnostics.* Expert review of molecular diagnostics, 2008. **8**(5): p. 617-633.

93. Kelly, R.S., et al., *The role of tumor metabolism as a driver of prostate cancer progression and lethal disease: results from a nested case-control study.* Cancer & metabolism, 2016. **4**: p. 22-22.

94. Mann, T., *The biochemistry of semen and of the male reproductive tract.* The biochemistry of semen and of the male reproductive tract., 1964.

95. De Kretser, D., P. Temple-Smith, and J. Kerr, *Anatomical and functional aspects of the male reproductive organs*, in *Disturbances in Male Fertility*. 1982, Springer. p. 1-131.

96. Everaerts, W. and A.J. Costello, *Applied Anatomy of the Male Pelvis*, in *Prostate Ultrasound: Current Practice and Future Directions*, C.R. Porter and E.M. Wolff, Editors. 2015, Springer New York: New York, NY. p. 11-30.

97. Fine, S.W. and R. Mehra, *Anatomy of the Prostate Revisited: Implications for Prostate Biopsy and Zonal Origins of Prostate Cancer*, in *Genitourinary Pathology: Practical Advances*, C. Magi-Galluzzi and C.G. Przybycin, Editors. 2015, Springer New York: New York, NY. p. 3-12.

98. Rybak, A., R. Bristow, and A. Kapoor, *Prostate cancer stem cells: Deciphering the origins and pathways involved in prostate tumorigenesis and aggression.* Oncotarget, 2014. **6**.

99. Barron, D.A. and D.R. Rowley, *The reactive stroma microenvironment and prostate cancer progression.* 2012. **19**(6): p. R187.

100. Toivanen, R. and M.M. Shen, *Prostate organogenesis: tissue induction, hormonal regulation and cell type specification.* Development, 2017. **144**(8): p. 1382-1398.

101. Obinata, D., et al., *Review of novel therapeutic medicines targeting androgen signaling in castration-resistant prostate cancer.* World Journal of Clinical Urology, 2014. **3**(3): p. 264-271.

102. Turner, B. and L. Drudge-Coates, *New pharmacological treatments for prostate cancer.* Nurse Prescribing, 2012. **10**: p. 498-502.

103. Wenk, M.R., *The emerging field of lipidomics.* Nature Reviews Drug Discovery, 2005. **4**: p. 594.

104. van Meer, G., D.R. Voelker, and G.W. Feigenson, *Membrane lipids: where they are and how they behave.* Nat Rev Mol Cell Biol, 2008. **9**(2): p. 112-24.

105. Gurr, M. and A. James, *Lipid biochemistry: an introduction.(eds.) Chapman & Hall, London.* 1971.

106. Fahy, E., et al., *Update of the LIPID MAPS comprehensive classification system for lipids.* J Lipid Res, 2009. **50 Suppl**: p. S9-14.

107. Kennedy, E.P., *Biosynthesis of complex lipids.* Fed Proc, 1961. **20**: p. 934-40.

108. Rysman, E., et al., *De novo lipogenesis protects cancer cells from free radicals and chemotherapeutics by promoting membrane lipid saturation.* Cancer Research, 2010. **70**: p. 8117-8126.

109. Kent, C., *Regulatory enzymes of phosphatidylcholine biosynthesis: a personal perspective.* Biochim Biophys Acta, 2005. **1733**(1): p. 53-66.

110. Kennedy, E.P. and S.B. Weiss, *The function of cytidine coenzymes in the biosynthesis of phospholipides.* J Biol Chem, 1956. **222**(1): p. 193-214.

111. Lands, W.E., *Metabolism of glycerolipides; a comparison of lecithin and triglyceride synthesis.* J Biol Chem, 1958. **231**(2): p. 883-8.

112. Shimizu, T., T. Ohto, and Y. Kita, *Cytosolic phospholipase A2: biochemical properties and physiological roles.* IUBMB Life, 2006. **58**(5-6): p. 328-33.

113. Schlame, M., D. Rua, and M.L. Greenberg, *The biosynthesis and functional role of cardiolipin.* Prog Lipid Res, 2000. **39**(3): p. 257-88.

114. Lands, W.E., *Stories about acyl chains.* Biochim Biophys Acta, 2000. **1483**(1): p. 1-14.

115. Sergeant, S., et al., *Phosphatidic acid regulates tyrosine phosphorylating activity in human neutrophils enhancement of Fgr activity.* Journal of Biological Chemistry, 2001. **276**(7): p. 4737-4746.

116. Rizzo, M.A., et al., *Phospholipase D and its product, phosphatidic acid, mediate agonist-dependent raf-1 translocation to the plasma membrane and the activation of the mitogen-activated protein kinase pathway.* J Biol Chem, 1999. **274**(2): p. 1131-9.

117. Olivera, A., J. Rosenthal, and S. Spiegel, *Effect of acidic phospholipids on sphingosine kinase.* Journal of cellular biochemistry, 1996. **60**(4): p. 529-537.

118. Lim, H.-K., et al., *Phosphatidic acid regulates systemic inflammatory responses by modulating the Akt-mammalian target of rapamycin-p70 S6 kinase 1 pathway.* Journal of Biological Chemistry, 2003. **278**(46): p. 45117-45127.

119. Daaka, Y., *Mitogenic action of LPA in prostate.* Biochim Biophys Acta, 2002. **1582**(1-3): p. 265-9.

120. Kulkarni, P. and R.H. Getzenberg, *High-fat diet, obesity and prostate disease: the ATX-LPA axis?* Nat Clin Pract Urol, 2009. **6**(3): p. 128-31.

121. Terada, N., et al., *Cyr61 is regulated by cAMP-dependent protein kinase with serum levels correlating with prostate cancer aggressiveness.* Prostate, 2012. **72**(9): p. 966-76.

122. Yui, K., et al., *Eicosanoids Derived From Arachidonic Acid and Their Family Prostaglandins and Cyclooxygenase in Psychiatric Disorders.* Current neuropharmacology, 2015. **13**(6): p. 776-785.

123. MacDonald, J.I. and H. Sprecher, *Phospholipid fatty acid remodeling in mammalian cells.* Biochimica et Biophysica Acta (BBA)-Lipids and Lipid Metabolism, 1991. **1084**(2): p. 105-121.

124. Patel, D. and S.N. Witt, *Ethanolamine and Phosphatidylethanolamine: Partners in Health and Disease.* Oxidative medicine and cellular longevity, 2017. **2017**: p. 4829180-4829180.

125. Chu, Z., et al., *Targeting and cytotoxicity of SapC-DOPS nanovesicles in pancreatic cancer.* PloS one, 2013. **8**(10): p. e75507.

126. Wojton, J., et al., *Systemic delivery of SapC-DOPS has antiangiogenic and antitumor effects against glioblastoma.* Molecular Therapy, 2013. **21**(8): p. 1517-1525.

127. Zhao, S., et al., *SapC–DOPS nanovesicles as targeted therapy for lung cancer.* Molecular cancer therapeutics, 2015. **14**(2): p. 491-498.

128. Murray, N.R. and A.P. Fields, *Phosphatidylglycerol is a physiologic activator of nuclear protein kinase C.* Journal of Biological Chemistry, 1998. **273**(19): p. 11514-11520.

129. Murray, N., L. Thompson, and A. Fields, *Protein Kinase C Molecular Biology Intelligence Unit*. 1997, The role of protein kinase C in cellular proliferation and cell cycle ….

130. Reis, A., *Oxidative Phospholipidomics in health and disease: Achievements, challenges and hopes.* Free Radical Biology and Medicine, 2017. **111**: p. 25-37.

131. Fu, P. and K.G. Birukov, *Oxidized phospholipids in control of inflammation and endothelial barrier.* Translational Research, 2009. **153**(4): p. 166-176.

132. Ashraf, M.Z., N.S. Kar, and E.A. Podrez, *Oxidized phospholipids: Biomarker for cardiovascular diseases.* The International Journal of Biochemistry & Cell Biology, 2009. **41**(6): p. 1241-1244.

133. Maskrey, B.H., et al., *Mechanisms of Resolution of Inflammation.* Arteriosclerosis, Thrombosis, and Vascular Biology, 2011. **31**(5): p. 1001-1006.

134. Salomon, R.G. and A. Bhatnagar, *Structural Identification and Cardiovascular Activities of Oxidized Phospholipids.* Circulation Research, 2012. **111**(7): p. 930-946.

135. Miyazawa, T., et al., *Age-related change of phosphatidylcholine hydroperoxide and phosphatidylethanolamine hydroperoxide levels in normal human red blood cells.* Mechanisms of Ageing and Development, 1996. **86**(3): p. 145-150.

136. Adachi, J., et al., *Plasma phosphatidylcholine hydroperoxide as a new marker of oxidative stress in alcoholic patients.* Journal of Lipid Research, 2004. **45**(5): p. 967-971.

137. Hui, S.-P., et al., *An improved HPLC assay for phosphatidylcholine hydroperoxides (PCOOH) in human plasma with synthetic PCOOH as internal standard.* Journal of Chromatography B, 2007. **857**(1): p. 158-163.

138. Jónasdóttir, H.S., et al., *Detection and Structural Elucidation of Esterified Oxylipids in Human Synovial Fluid by Electrospray Ionization-Fourier Transform Ion-Cyclotron Mass Spectrometry and Liquid Chromatography-Ion Trap-MS3: Detection of Esterified Hydroxylated Docosapentaenoic Acid Containing Phospholipids.* Analytical Chemistry, 2013. **85**(12): p. 6003-6010.

139. Gruber, F., et al., *Photooxidation generates biologically active phospholipids that induce heme oxygenase-1 in skin cells.* Journal of Biological Chemistry, 2007. **282**(23): p. 16934-16941.

140. Birukova, A.A., et al., *Signaling pathways involved in OxPAPC-induced pulmonary endothelial barrier protection.* Microvascular research, 2007. **73**(3): p. 173-181.

141. Stemmer, U., et al., *Toxicity of oxidized phospholipids in cultured macrophages.* Lipids in health and disease, 2012. **11**(1): p. 110.

142. Thimmulappa, R.K., et al., *Oxidized phospholipids impair pulmonary antibacterial defenses: evidence in mice exposed to cigarette smoke.* Biochemical and biophysical research communications, 2012. **426**(2): p. 253-259.

143. Halasiddappa, L.M., et al., *Oxidized phospholipids induce ceramide accumulation in RAW 264.7 macrophages: role of ceramide synthases.* PLoS One, 2013. **8**(7): p. e70002.

144. Koller, D., et al., *Effects of oxidized phospholipids on gene expression in RAW 264.7 macrophages: a microarray study.* PloS one, 2014. **9**(10): p. e110486.

145. Hoff, H.F., et al., *Phospholipid hydroxyalkenals: biological and chemical properties of specific oxidized lipids present in atherosclerotic lesions.* Arteriosclerosis, thrombosis, and vascular biology, 2003. **23**(2): p. 275-282.

146. Kamido, H., et al., *Core aldehydes of alkyl glycerophosphocholines in atheroma induce platelet aggregation and inhibit endothelium-dependent arterial relaxation.* Journal of lipid research, 2002. **43**(1): p. 158-166.

147. Ravandi, A., et al., *Phospholipids and oxophospholipids in atherosclerotic plaques at different stages of plaque development.* Lipids, 2004. **39**(2): p. 97-109.

148. Hammad, L.A., et al., *Elevated levels of hydroxylated phosphocholine lipids in the blood serum of breast cancer patients.* Rapid Communications in Mass

Spectrometry: An International Journal Devoted to the Rapid Dissemination of Up-to-the-Minute Research in Mass Spectrometry, 2009. **23**(6): p. 863-876.

149. Kinoshita, M., et al., *Age-related increases in plasma phosphatidylcholine hydroperoxide concentrations in control subjects and patients with hyperlipidemia.* Clinical chemistry, 2000. **46**(6): p. 822-828.

150. Akasaka, K., et al., *Automatic determination of hydroperoxides of phosphatidylcholine and phosphatidylethanolamine in human plasma.* Journal of Chromatography B: Biomedical Sciences and Applications, 1995. **665**(1): p. 37-43.

151. Rolla, R., et al., *Antibodies against oxidized phospholipids in laboratory tests exploring lupus anti-coagulant activity.* Clinical & Experimental Immunology, 2007. **149**(1): p. 63-69.

152. Matt, U., et al., *Accumulating evidence for a role of oxidized phospholipids in infectious diseases.* Cellular and molecular life sciences, 2015. **72**(6): p. 1059-1071.

153. Cruz, D., et al., *Host-derived oxidized phospholipids and HDL regulate innate immunity in human leprosy.* The Journal of clinical investigation, 2008. **118**(8): p. 2917-2928.

154. O'Donnell, V.B. and R.C. Murphy, *New families of bioactive oxidized phospholipids generated by immune cells: identification and signaling actions.* Blood, 2012. **120**(10): p. 1985-1992.

155. Stübiger, G., et al., *Targeted profiling of atherogenic phospholipids in human plasma and lipoproteins of hyperlipidemic patients using MALDI-QIT-TOF-MS/MS.* Atherosclerosis, 2012. **224**(1): p. 177-186.

156. Frey, B., et al., *Increase in fragmented phosphatidylcholine in blood plasma by oxidative stress.* Journal of lipid research, 2000. **41**(7): p. 1145-1153.

157. Podrez, E.A., et al., *Platelet CD36 links hyperlipidemia, oxidant stress and a prothrombotic phenotype.* Nature medicine, 2007. **13**(9): p. 1086.

158. Korotaeva, A.A., et al., *Oxidized phosphatidylcholine stimulates activity of secretory phospholipase A2 group IIA and abolishes sphingomyelin-induced inhibition of the enzyme.* Prostaglandins & other lipid mediators, 2010. **91**(1-2): p. 38-41.

159. Ramprecht, C., et al., *Toxicity of oxidized phosphatidylcholines in cultured human melanoma cells.* Chemistry and physics of lipids, 2015. **189**: p. 39-47.

160. Bochkov, V., et al., *Oxidized Phospholipids Stimulate Angiogenesis Via Autocrine Mechanisms, Implicating a Novel Role for Lipid Oxidation in the Evolution of Atherosclerotic Lesions*. Vol. 99. 2006. 900-8.

161. T Reddy, S., et al., *Identification of genes induced by oxidized phospholipids in human aortic endothelial cells*. Vol. 38. 2002. 211-8.

162. Oskolkova, O.V., et al., *ATF4-dependent transcription is a key mechanism in VEGF up-regulation by oxidized phospholipids: critical role of oxidized sn-2 residues in activation of unfolded protein response.* Blood, 2008. **112**(2): p. 330-339.

163. Blüml, S., et al., *The Oxidation State of Phospholipids Controls the Oxidative Burst in Neutrophil Granulocytes.* The Journal of Immunology, 2008. **181**(6): p. 4347-4353.

164. Gao, D., et al., *Structural Basis for the Recognition of Oxidized Phospholipids in Oxidized Low Density Lipoproteins by Class B Scavenger Receptors CD36 and SR-BI.* Journal of Biological Chemistry, 2010. **285**(7): p. 4447-4454.

165. Boullier, A., et al., *The Binding of Oxidized Low Density Lipoprotein to Mouse CD36 Is Mediated in Part by Oxidized Phospholipids That Are Associated with Both the Lipid and Protein Moieties of the Lipoprotein.* Journal of Biological Chemistry, 2000. **275**(13): p. 9163-9169.

166. Karupaiah, T. and K. Sundram, *Effects of stereospecific positioning of fatty acids in triacylglycerol structures in native and randomized fats: a review of their nutritional implications.* Nutrition & metabolism, 2007. **4**(1): p. 16.

167. Dircks, L. and H.S. Sul, *Acyltransferases of de novo glycerophospholipid biosynthesis.* Prog Lipid Res, 1999. **38**(5-6): p. 461-79.

168. Weiss, S.B., E.P. Kennedy, and J.Y. Kiyasu, *The enzymatic synthesis of triglycerides.* Journal of Biological Chemistry, 1960. **235**(1): p. 40-44.

169. Coleman, R.A. and D.P. Lee, *Enzymes of triacylglycerol synthesis and their regulation.* Progress in lipid research, 2004. **43**(2): p. 134-176.

170. Wei, L., et al., *A case-control study on the association between serum lipid level and the risk of breast cancer.* Zhonghua yu fang yi xue za zhi [Chinese journal of preventive medicine], 2016. **50**(12): p. 1091-1095.

171. Ogretmen, B. and Y.A. Hannun, *Biologically active sphingolipids in cancer pathogenesis and treatment.* Nature Reviews Cancer, 2004. **4**(8): p. 604.

172. Ogretmen, B., *Sphingolipids in cancer: regulation of pathogenesis and therapy.* FEBS letters, 2006. **580**(23): p. 5467-5476.

173. Ryland, L.K., et al., *Dysregulation of sphingolipid metabolism in cancer.* Cancer biology & therapy, 2011. **11**(2): p. 138-149.

174. Fyrst, H. and J.D. Saba, *An update on sphingosine-1-phosphate and other sphingolipid mediators.* Nat Chem Biol, 2010. **6**(7): p. 489-97.

175. Maula, T., et al., *Importance of the sphingoid base length for the membrane properties of ceramides.* Biophysical journal, 2012. **103**(9): p. 1870-1879.

176. Saddoughi, S.A., P. Song, and B. Ogretmen, *Roles of bioactive sphingolipids in cancer biology and therapeutics.* Sub-cellular biochemistry, 2008. **49**: p. 413-440.

177. Ponnusamy, S., et al., *Sphingolipids and cancer: ceramide and sphingosine-1-phosphate in the regulation of cell death and drug resistance.* Future oncology (London, England), 2010. **6**(10): p. 1603-1624.

178. Taha, T.A., T.D. Mullen, and L.M. Obeid, *A house divided: ceramide, sphingosine, and sphingosine-1-phosphate in programmed cell death.* Biochim Biophys Acta, 2006. **1758**(12): p. 2027-36.

179. Ogretmen, B. and Y.A. Hannun, *Biologically active sphingolipids in cancer pathogenesis and treatment.* Nat Rev Cancer, 2004. **4**(8): p. 604-16.

180. Wang, X.-Z., et al., *Aberrant Sphingolipid Signaling Is Involved in the Resistance of Prostate Cancer Cell Lines to Chemotherapy.* Cancer Research, 1999. **59**(22): p. 5842-5848.

181. García-Barros, M., et al., *Sphingolipids in colon cancer.* Biochimica et biophysica acta, 2014. **1841**(5): p. 773-782.

182. Karahatay, S., et al., *Clinical relevance of ceramide metabolism in the pathogenesis of human head and neck squamous cell carcinoma (HNSCC): attenuation of C(18)-ceramide in HNSCC tumors correlates with lymphovascular invasion and nodal metastasis.* Cancer Lett, 2007. **256**(1): p. 101-11.

183. Schiffmann, S., et al., *Ceramide synthases and ceramide levels are increased in breast cancer tissue.* Carcinogenesis, 2009. **30**(5): p. 745-52.

184. Pralhada Rao, R., et al., *Sphingolipid metabolic pathway: an overview of major roles played in human diseases.* Journal of lipids, 2013. **2013**: p. 178910-178910.

185. Modrak, D.E., D.V. Gold, and D.M. Goldenberg, *Sphingolipid targets in cancer therapy.* Molecular Cancer Therapeutics, 2006. **5**(2): p. 200-208.

186. Lemonnier, L.A., et al., *Sphingomyelin in the suppression of colon tumors: prevention versus intervention.* Arch Biochem Biophys, 2003. **419**(2): p. 129-38.

187. Al Sazzad, M.A., et al., *The Long-Chain Sphingoid Base of Ceramides Determines Their Propensity for Lateral Segregation.* Biophysical journal, 2017. **112**(5): p. 976-983.

188. Dillehay, D.L., et al., *Dietary sphingomyelin inhibits 1,2-dimethylhydrazine-induced colon cancer in CF1 mice.* J Nutr, 1994. **124**(5): p. 615-20.

189. Mehta, S., et al., *Combined cytotoxic action of paclitaxel and ceramide against the human Tu138 head and neck squamous carcinoma cell line.* Cancer Chemother Pharmacol, 2000. **46**(2): p. 85-92.

190. Schmelz, E.M., et al., *Colonic cell proliferation and aberrant crypt foci formation are inhibited by dairy glycosphingolipids in 1, 2-dimethylhydrazine-treated CF1 mice.* J Nutr, 2000. **130**(3): p. 522-7.

191. Onodera, T., et al., *Phosphatidylethanolamine plasmalogen enhances the inhibiting effect of phosphatidylethanolamine on γ-secretase activity.* The Journal of Biochemistry, 2014. **157**(5): p. 301-309.

192. Braverman, N.E. and A.B. Moser, *Functions of plasmalogen lipids in health and disease.* Biochim Biophys Acta, 2012. **1822**(9): p. 1442-52.

193. Hu, C., M. Wang, and X. Han, *Shotgun lipidomics in substantiating lipid peroxidation in redox biology: Methods and applications.* Redox Biol, 2017. **12**: p. 946-955.

194. Wallner, S. and G. Schmitz, *Plasmalogens the neglected regulatory and scavenging lipid species.* Chem Phys Lipids, 2011. **164**(6): p. 573-89.

195. Fuchs, B., *Analytical methods for (oxidized) plasmalogens: Methodological aspects and applications.* Free Radic Res, 2015. **49**(5): p. 599-617.

196. Maeba, R., et al., *Chapter Two - Plasma/Serum Plasmalogens: Methods of Analysis and Clinical Significance*, in *Advances in Clinical Chemistry*, G.S. Makowski, Editor. 2015, Elsevier. p. 31-94.

197. Maeba, R., et al., *Plasma/Serum Plasmalogens: Methods of Analysis and Clinical Significance.* Adv Clin Chem, 2015. **70**: p. 31-94.

198. Han, X., *Lipidomics for studying metabolism.* Nat Rev Endocrinol, 2016. **12**(11): p. 668-679.

199. Mankidy, R., et al., *Membrane plasmalogen composition and cellular cholesterol regulation: a structure activity study.* Lipids Health Dis, 2010. **9**: p. 62.

200. Brites, P., H.R. Waterham, and R.J. Wanders, *Functions and biosynthesis of plasmalogens in health and disease.* Biochim Biophys Acta, 2004. **1636**(2-3): p. 219-31.

201. Fhaner, C.J., et al., *Functional group selective derivatization and gas-phase fragmentation reactions of plasmalogen glycerophospholipids.* Mass Spectrometry, 2013. **2**(Special_Issue): p. S0015-S0015.

202. Gerbig, S., et al., *Analysis of colorectal adenocarcinoma tissue by desorption electrospray ionization mass spectrometric imaging.* Analytical and bioanalytical chemistry, 2012. **403**(8): p. 2315-2325.

203. Lv, J., et al., *Plasma Content Variation and Correlation of Plasmalogen and GIS, TC, and TPL in Gastric Carcinoma Patients: A Comparative Study.* Medical science monitor basic research, 2015. **21**: p. 157-160.

204. Kunkel, G.T., et al., *Targeting the sphingosine-1-phosphate axis in cancer, inflammation and beyond.* Nature reviews. Drug discovery, 2013. **12**(9): p. 688-702.

205. Wang, D. and R.N. Dubois, *Eicosanoids and cancer.* Nature reviews. Cancer, 2010. **10**(3): p. 181-193.

206. Nakanishi, M. and D.W. Rosenberg. *Multifaceted roles of PGE 2 in inflammation and cancer*. in *Seminars in immunopathology*. 2013. Springer.

207. Asgari, Y., et al., *Alterations in cancer cell metabolism: the Warburg effect and metabolic adaptation.* Genomics, 2015. **105**(5-6): p. 275-81.

208. Santos, C., et al., *Lipid metabolism in cancer.* FEBS Journal, 2012. **279**: p. 2610-2623.

209. Dueregger, A., et al., *Differential Utilization of Dietary Fatty Acids in Benign and Malignant Cells of the Prostate.* PLoS One, 2015. **10**(8): p. e0135704.

210. Twum-Ampofo, J., et al., *Metabolic targets for potential prostate cancer therapeutics.* Curr Opin Oncol, 2016. **28**(3): p. 241-7.

211. Ngo, D.C., et al., *Introduction to the molecular basis of cancer metabolism and the Warburg effect.* Mol Biol Rep, 2015. **42**(4): p. 819-23.

212. Medes, G., A. Thomas, and S. Weinhouse, *Metabolism of neoplastic tissue. IV. A study of lipid synthesis in neoplastic tissue slices in vitro.* Cancer Res, 1953. **13**(1): p. 27-9.

213. Ookhtens, M., et al., *Liver and adipose tissue contributions to newly formed fatty acids in an ascites tumor.* Am J Physiol, 1984. **247**(1 Pt 2): p. R146-53.

214. Srihari, S., et al., *Metabolic deregulation in prostate cancer.* Mol Omics, 2018. **14**(5): p. 320-329.

215. Perona, J.S., *Membrane lipid alterations in the metabolic syndrome and the role of dietary oils*. 2017, Elsevier.

216. Hidalgo, A., A. Cruz, and J. Pérez-Gil, *Pulmonary surfactant and nanocarriers: toxicity versus combined nanomedical applications.* Biochimica et Biophysica Acta (BBA)-Biomembranes, 2017. **1859**(9): p. 1740-1748.

217. Echaide, M., et al., *Restoring pulmonary surfactant membranes and films at the respiratory surface.* Biochimica et Biophysica Acta (BBA)-Biomembranes, 2017. **1859**(9): p. 1725-1739.

218. Dumas, F. and E. Haanappel, *Lipids in infectious diseases–the case of AIDS and tuberculosis.* Biochimica et Biophysica Acta (BBA)-Biomembranes, 2017. **1859**(9): p. 1636-1647.

219. Fuentes, N.R., et al., *Emerging role of chemoprotective agents in the dynamic shaping of plasma membrane organization.* Biochimica et Biophysica Acta (BBA)-Biomembranes, 2017. **1859**(9): p. 1668-1678.

220. Ríos-Marco, P., et al., *Alkylphospholipids: An update on molecular mechanisms and clinical relevance*. 2017, Elsevier.

221. Baker, M.J., et al., *FTIR-based spectroscopic analysis in the identification of clinically aggressive prostate cancer.* Br J Cancer, 2008. **99**(11): p. 1859-66.

222. Zhou, X., et al., *Identification of plasma lipid biomarkers for prostate cancer by lipidomics and bioinformatics.* PLoS One, 2012. **7**(11): p. e48889.

223. Sorvina, A., et al., *Lipid profiles of prostate cancer cells.* Oncotarget, 2018. **9**(85): p. 35541-35552.

224. Hultsch, S., et al., *Association of tamoxifen resistance and lipid reprogramming in breast cancer.* BMC Cancer, 2018. **18**(1): p. 850.

225. Lin, H.-M., et al., *A distinct plasma lipid signature associated with poor prognosis in castration-resistant prostate cancer.* International Journal of Cancer, 2017. **141**(10): p. 2112-2120.

226. Horvath, L., et al., *The plasma lipidome in castration-resistant prostate cancer.* Journal of Clinical Oncology, 2017. **35**(15_suppl): p. 5055-5055.

227. Bligh, E.G. and W.J. Dyer, *A rapid method of total lipid extraction and purification.* Canadian journal of biochemistry and physiology, 1959. **37**(8): p. 911-917.

228. Bartlett, G.R., *Phosphorus assay in column chromatography.* J biol chem, 1959. **234**(3): p. 466-468.

229. Kinsey, G.R., et al., *Decreased iPLA2γ expression induces lipid peroxidation and cell death and sensitizes cells to oxidant-induced apoptosis.* Journal of lipid research, 2008. **49**(7): p. 1477-1487.

230. Zhang, L., B.L. Peterson, and B.S. Cummings, *The effect of inhibition of Ca2+-independent phospholipase A2 on chemotherapeutic-induced death and phospholipid profiles in renal cells.* Biochemical pharmacology, 2005. **70**(11): p. 1697-1706.

231. Peterson, B., et al., *Alterations in phospholipid and fatty acid lipid profiles in primary neocortical cells during oxidant-induced cell injury.* Chem Biol Interact, 2008. **174**(3): p. 163-76.

232. Maes, E., et al., *Determination of Variation Parameters as a Crucial Step in Designing TMT-Based Clinical Proteomics Experiments.* PLOS ONE, 2015. **10**(3): p. e0120115.

233. Schaaf, M.J. and J.A. Cidlowski, *Molecular mechanisms of glucocorticoid action and resistance.* J Steroid Biochem Mol Biol, 2002. **83**(1-5): p. 37-48.

234. Kalli, A., et al., *Evaluation and optimization of mass spectrometric settings during data-dependent acquisition mode: focus on LTQ-Orbitrap mass analyzers.* Journal of proteome research, 2013. **12**(7): p. 3071-3086.

235. Pluskal, T., et al., *MZmine 2: modular framework for processing, visualizing, and analyzing mass spectrometry-based molecular profile data.* BMC Bioinformatics, 2010. **11**: p. 395.

236. Tautenhahn, R., et al., *XCMS Online: a web-based platform to process untargeted metabolomic data.* Anal Chem, 2012. **84**(11): p. 5035-9.

237. Koelmel, J.P., et al., *LipidMatch: an automated workflow for rule-based lipid identification using untargeted high-resolution tandem mass spectrometry data.* BMC Bioinformatics, 2017. **18**(1): p. 331.

238. Kinsey, G.R., et al., *Decreased iPLA2gamma expression induces lipid peroxidation and cell death and sensitizes cells to oxidant-induced apoptosis.* J Lipid Res, 2008. **49**(7): p. 1477-87.

239. Trygg, J. and S. Wold, *Orthogonal Projections to Latent Structures (O-PLS).* Journal of Chemometrics, 2002. **16**: p. 119-128.

240. Trygg, J., E. Holmes, and T. Lundstedt, *Chemometrics in Metabonomics.* Journal of proteome research, 2007. **6**: p. 469-79.

241. Worley, B. and R. Powers, *Multivariate Analysis in Metabolomics.* Current Metabolomics, 2013. **1**(1): p. 92-107.

242. Richman, E.L., et al., *Choline intake and risk of lethal prostate cancer: incidence and survival.* The American journal of clinical nutrition, 2012. **96**(4): p. 855-863.

243. Zhou, Y., E.C. Bolton, and J.O. Jones, *Androgens and androgen receptor signaling in prostate tumorigenesis.* 2015. **54**(1): p. R15.

244. Cheng, J.C., et al., *Radiation-induced acid ceramidase confers prostate cancer resistance and tumor relapse.* The Journal of Clinical Investigation, 2013. **123**(10): p. 4344-4358.

245. Merchant, T.E., et al., *Phospholipid profiles of human colon cancer using 31P magnetic resonance spectroscopy.* Int J Colorectal Dis, 1991. **6**(2): p. 121-6.

246. Griner, E.M. and M.G. Kazanietz, *Protein kinase C and other diacylglycerol effectors in cancer.* Nat Rev Cancer, 2007. **7**(4): p. 281-94.

247. Perry, D.K. and Y.A. Hannun, *The role of ceramide in cell signaling.* Biochim Biophys Acta, 1998. **1436**(1-2): p. 233-43.

248. Schneider, G., et al., *Bioactive lipids, LPC and LPA, are novel prometastatic factors and their tissue levels increase in response to radio/chemotherapy.* Molecular cancer research : MCR, 2014. **12**(11): p. 1560-1573.

249. Okita, M., et al., *Elevated levels and altered fatty acid composition of plasma lysophosphatidlycholine (lysoPC) in ovarian cancer patients.* International journal of cancer, 1997. **71**(1): p. 31-34.

250. Phuyal, S., et al., *The ether lipid precursor hexadecylglycerol stimulates the release and changes the composition of exosomes derived from PC-3 cells.* J Biol Chem, 2015. **290**(7): p. 4225-37.

251. Devalapally, H., et al., *Modulation of drug resistance in ovarian adenocarcinoma by enhancing intracellular ceramide using tamoxifen-loaded biodegradable polymeric nanoparticles.* Clin Cancer Res, 2008. **14**(10): p. 3193-203.

252. Park, M.H., et al., *Overexpression of phospholipase D enhances matrix metalloproteinase-2 expression and glioma cell invasion via protein kinase C and protein kinase A/NF-kappaB/Sp1-mediated signaling pathways.* Carcinogenesis, 2009. **30**(2): p. 356-65.

253. Yang, J.S., et al., *Size Dependent Lipidomic Analysis of Urinary Exosomes from Patients with Prostate Cancer by Flow Field-Flow Fractionation and Nanoflow Liquid Chromatography-Tandem Mass Spectrometry.* Analytical Chemistry, 2017. **89**(4): p. 2488-2496.

254. Perry, R.H., et al., *Characterization of MYC-induced tumorigenesis by in situ lipid profiling.* Analytical chemistry, 2013. **85**(9): p. 4259-4262.

255. Shroff, E.H., et al., *MYC oncogene overexpression drives renal cell carcinoma in a mouse model through glutamine metabolism.* Proceedings of the National Academy of Sciences, 2015. **112**(21): p. 6539-6544.

256. Lisec, J., et al., *Cancer cell lipid class homeostasis is altered under nutrient-deprivation but stable under hypoxia.* BMC Cancer, 2019. **19**(1): p. 501.

257. Burch, T.C., et al., *Comparative metabolomic and lipidomic analysis of phenotype stratified prostate cells.* PLoS One, 2015. **10**(8): p. e0134206.

258. Jung, J.H., et al., *Phospholipids of tumor extracellular vesicles stratify gefitinib-resistant nonsmall cell lung cancer cells from gefitinib-sensitive cells.* Proteomics, 2015. **15**(4): p. 824-835.

259. Bevers, E.M., P. Comfurius, and R.F. Zwaal, *Regulatory mechanisms in maintenance and modulation of transmembrane lipid asymmetry: pathophysiological implications.* Lupus, 1996. **5**(5): p. 480-7.

260. Escriba, P.V., et al., *Membranes: a meeting point for lipids, proteins and therapies.* J Cell Mol Med, 2008. **12**(3): p. 829-75.

261. Escriba, P.V., *Membrane-lipid therapy: a new approach in molecular medicine.* Trends Mol Med, 2006. **12**(1): p. 34-43.

262. Thadani-Mulero, M., et al., *Androgen receptor splice variants determine taxane sensitivity in prostate cancer.* Cancer research, 2014. **74**(8): p. 2270-2282.

263. Ploussard, G., et al., *Class III β-tubulin expression predicts prostate tumor aggressiveness and patient response to docetaxel-based chemotherapy.* Cancer research, 2010. **70**(22): p. 9253-9264.

264. Zhu, Y., et al., *Inhibition of ABCB1 expression overcomes acquired docetaxel resistance in prostate cancer.* Molecular cancer therapeutics, 2013. **12**(9): p. 1829-1836.

265. Chen, H., H. Li, and Q. Chen, *INPP4B reverses docetaxel resistance and epithelial-to-mesenchymal transition via the PI3K/Akt signaling pathway in prostate cancer.* Biochemical and biophysical research communications, 2016. **477**(3): p. 467-472.

266. de Bessa Garcia, S.A., et al., *Prostate apoptosis response 4 (PAR4) expression modulates WNT signaling pathways in MCF7 breast cancer cells: A possible mechanism underlying PAR4-mediated docetaxel chemosensitivity.* International journal of molecular medicine, 2017. **39**(4): p. 809-818.

267. Codony-Servat, J., et al., *Nuclear factor-kappa B and interleukin-6 related docetaxel resistance in castration-resistant prostate cancer.* The Prostate, 2013. **73**(5): p. 512-521.

268. Marín-Aguilera, M., et al., *Epithelial-to-mesenchymal transition mediates docetaxel resistance and high risk of relapse in prostate cancer.* Molecular cancer therapeutics, 2014. **13**(5): p. 1270-1284.

269. Baenke, F., et al., *Hooked on fat: the role of lipid synthesis in cancer metabolism and tumour development.* Disease models & mechanisms, 2013. **6**(6): p. 1353-1363.

270. Ackerman, D. and M.C. Simon, *Hypoxia, lipids, and cancer: surviving the harsh tumor microenvironment.* Trends in cell biology, 2014. **24**(8): p. 472-478.

271. Cruz, P.M., et al., *The role of cholesterol metabolism and cholesterol transport in carcinogenesis: a review of scientific findings, relevant to future cancer therapeutics.* Frontiers in pharmacology, 2013. **4**: p. 119.

272. Cheng, C., et al., *Glucose-mediated N-glycosylation of SCAP is essential for SREBP-1 activation and tumor growth.* Cancer cell, 2015. **28**(5): p. 569-581.

273. Guo, D., et al., *EGFR signaling through an Akt-SREBP-1–dependent, rapamycin-resistant pathway sensitizes glioblastomas to antilipogenic therapy.* Sci. Signal., 2009. **2**(101): p. ra82-ra82.

274. Guo, D., et al., *An LXR agonist promotes glioblastoma cell death through inhibition of an EGFR/AKT/SREBP-1/LDLR–dependent pathway.* Cancer discovery, 2011. **1**(5): p. 442-456.

275. Acevedo, A., et al., *LIPEA: Lipid Pathway Enrichment Analysis.* bioRxiv, 2018: p. 274969.

276. Li, S., et al., *Predicting network activity from high throughput metabolomics.* PLoS computational biology, 2013. **9**(7): p. e1003123.

277. Chong, J., et al., *MetaboAnalyst 4.0: towards more transparent and integrative metabolomics analysis.* Nucleic Acids Res, 2018. **46**(W1): p. W486-w494.

278. Dolce, V., et al., *Glycerophospholipid synthesis as a novel drug target against cancer.* Curr Mol Pharmacol, 2011. **4**(3): p. 167-75.

279. Tappia, P.S. and T. Singal, *Phospholipid-mediated signaling and heart disease.* Subcell Biochem, 2008. **49**: p. 299-324.

280. Oude Weernink, P.A., et al., *Dynamic phospholipid signaling by G protein-coupled receptors.* Biochim Biophys Acta, 2007. **1768**(4): p. 888-900.

281. Fernandis, A.Z. and M.R. Wenk, *Membrane lipids as signaling molecules.* Curr Opin Lipidol, 2007. **18**(2): p. 121-8.

282. Brzozowski, J.S., et al., *Lipidomic profiling of extracellular vesicles derived from prostate and prostate cancer cell lines.* Lipids Health Dis, 2018. **17**(1): p. 211.

283. Dixon, S.J., et al., *Ferroptosis: an iron-dependent form of nonapoptotic cell death.* Cell, 2012. **149**(5): p. 1060-1072.

284. Latunde-Dada, G.O., *Ferroptosis: Role of lipid peroxidation, iron and ferritinophagy.* Biochim Biophys Acta Gen Subj, 2017. **1861**(8): p. 1893-1900.

285. Agmon, E., et al., *Modeling the effects of lipid peroxidation during ferroptosis on membrane properties.* Sci Rep, 2018. **8**(1): p. 5155.

286. Agmon, E. and B.R. Stockwell, *Lipid homeostasis and regulated cell death.* Curr Opin Chem Biol, 2017. **39**: p. 83-89.

287. Stockwell, B.R., et al., *Ferroptosis: a regulated cell death nexus linking metabolism, redox biology, and disease.* Cell, 2017. **171**(2): p. 273-285.

288. Co-operation, O.f.E. and Development, *Toward a New Comprehensive Global Database of Per-and Polyfluoroalkyl Substances (PFASs): Summary Report on Updating the OECD 2007 List of per-and Polyfluoroalkyl Substances (PFASs).* 2018.

289. Banks, R.E., B.E. Smart, and J. Tatlow, *Organofluorine chemistry: principles and commercial applications*. 2013: Springer Science & Business Media.

290. Buck, R.C., *Toxicology data for alternative "short-chain" fluorinated substances*, in *Toxicological Effects of Perfluoroalkyl and Polyfluoroalkyl Substances*. 2015, Springer. p. 451-477.

291. Domingo, J.L., *Health risks of dietary exposure to perfluorinated compounds.* Environment international, 2012. **40**: p. 187-195.

292. Suja, F., B.K. Pramanik, and S.M. Zain, *Contamination, bioaccumulation and toxic effects of perfluorinated chemicals (PFCs) in the water environment: a review paper.* Water Science and Technology, 2009. **60**(6): p. 1533-1544.

293. Sunderland, E.M., et al., *A review of the pathways of human exposure to poly- and perfluoroalkyl substances (PFASs) and present understanding of health effects.* J Expo Sci Environ Epidemiol, 2019. **29**(2): p. 131-147.

294. Winkens, K., et al., *Early life exposure to per- and polyfluoroalkyl substances (PFASs): A critical review.* Emerging Contaminants, 2017. **3**(2): p. 55-68.

295. D'Hollander, W., et al., *Perfluorinated substances in human food and other sources of human exposure.* Rev Environ Contam Toxicol, 2010. **208**: p. 179-215.

296. Post, G.B., et al., *Occurrence and potential significance of perfluorooctanoic acid (PFOA) detected in New Jersey public drinking water systems.* Environmental science & technology, 2009. **43**(12): p. 4547-4554.

297. Barbarossa, A., et al., *Assessment of Perfluorooctane Sulfonate and Perfluorooctanoic Acid Exposure Through Fish Consumption in Italy.* Italian journal of food safety, 2016. **5**(4): p. 6055-6055.

298. Shi, Y., et al., *Tissue distribution of perfluorinated compounds in farmed freshwater fish and human exposure by consumption.* Environ Toxicol Chem, 2012. **31**(4): p. 717-23.

299. Eriksson, U., et al., *Perfluoroalkyl substances (PFASs) in food and water from Faroe Islands.* Environ Sci Pollut Res Int, 2013. **20**(11): p. 7940-8.

300. Hlouskova, V., et al., *Occurrence of brominated flame retardants and perfluoroalkyl substances in fish from the Czech aquatic ecosystem.* Sci Total Environ, 2013. **461-462**: p. 88-98.

301. Chain, E.Panel o.C.i.t.F., et al., *Risk to human health related to the presence of perfluorooctane sulfonic acid and perfluorooctanoic acid in food.* EFSA Journal, 2018. **16**(12): p. e05194.

302. Lewis, R.C., L.E. Johns, and J.D. Meeker, *Serum Biomarkers of Exposure to Perfluoroalkyl Substances in Relation to Serum Testosterone and Measures of Thyroid Function among Adults and Adolescents from NHANES 2011-2012.* Int J Environ Res Public Health, 2015. **12**(6): p. 6098-114.

303. Crinnion, W.J., *The CDC fourth national report on human exposure to environmental chemicals: what it tells us about our toxic burden and how it assists environmental medicine physicians.* Alternative medicine review, 2010. **15**(2): p. 101-109.

304. Calafat, A.M., et al., *Polyfluoroalkyl chemicals in the US population: data from the National Health and Nutrition Examination Survey (NHANES) 2003–2004 and comparisons with NHANES 1999–2000.* Environmental health perspectives, 2007. **115**(11): p. 1596-1602.

305. Graber, J.M., et al., *Per and polyfluoroalkyl substances (PFAS) blood levels after contamination of a community water supply and comparison with 2013-2014 NHANES.* Journal of exposure science & environmental epidemiology, 2019. **29**(2): p. 172-182.

306. Borg, D., et al., *Cumulative health risk assessment of 17 perfluoroalkylated and polyfluoroalkylated substances (PFASs) in the Swedish population.* Environment International, 2013. **59**: p. 112-123.

307. Lieder, P.H., et al., *A two-generation oral gavage reproduction study with potassium perfluorobutanesulfonate (K+ PFBS) in Sprague Dawley rats.* Toxicology, 2009. **259**(1-2): p. 33-45.

308. Lieder, P.H., et al., *Toxicological evaluation of potassium perfluorobutanesulfonate in a 90-day oral gavage study with Sprague–Dawley rats.* Toxicology, 2009. **255**(1-2): p. 45-52.

309. Domingo, J.L. and M. Nadal, *Per- and Polyfluoroalkyl Substances (PFASs) in Food and Human Dietary Intake: A Review of the Recent Scientific Literature.* Journal of Agricultural and Food Chemistry, 2017. **65**(3): p. 533-543.

310. Gorrochategui, E., et al., *Perfluoroalkylated Substance Effects in Xenopus laevis A6 Kidney Epithelial Cells Determined by ATR-FTIR Spectroscopy and Chemometric Analysis.* Chemical research in toxicology, 2016. **29**(5): p. 924-932.

311. Gorrochategui, E., et al., *Chemometric strategy for untargeted lipidomics: biomarker detection and identification in stressed human placental cells.* Analytica chimica acta, 2015. **854**: p. 20-33.

312. Lin, P.-I.D., et al., *Per- and polyfluoroalkyl substances and blood lipid levels in pre-diabetic adults—longitudinal analysis of the diabetes prevention program outcomes study.* Environment International, 2019. **129**: p. 343-353.

313. Liu, J., et al., *[Development and evaluation of a high-fat/high-fructose diet-induced nonalcoholic steatohepatitis mouse model].* Zhonghua Gan Zang Bing Za Zhi, 2014. **22**(6): p. 445-50.

314. EPA, U., *Drinking Water Health Advisory for Perfluorooctanoic Acid (PFOA).* EPA Document Number: 822-R-16-005, 2016.

315. PFOS, P.S., *ENVIRONMENTAL CRITERIA PERFLUORINATED ALKYL COMPOUNDS.*

316. Tiwari-Heckler, S., et al., *Circulating Phospholipid Patterns in NAFLD Patients Associated with a Combination of Metabolic Risk Factors.* Nutrients, 2018. **10**(5): p. 649.

317. Ipsen, D.H., J. Lykkesfeldt, and P. Tveden-Nyborg, *Molecular mechanisms of hepatic lipid accumulation in non-alcoholic fatty liver disease.* Cellular and molecular life sciences : CMLS, 2018. **75**(18): p. 3313-3327.

318. Gorden, D.L., et al., *Increased diacylglycerols characterize hepatic lipid changes in progression of human nonalcoholic fatty liver disease; comparison to a murine model.* PloS one, 2011. **6**(8): p. e22775-e22775.

319. Barr, J., et al., *Obesity-dependent metabolic signatures associated with nonalcoholic fatty liver disease progression.* Journal of proteome research, 2012. **11**(4): p. 2521-2532.

320. Vance, J.E., *Lipoproteins secreted by cultured rat hepatocytes contain the antioxidant 1-alk-1-enyl-2-acylglycerophosphoethanolamine.* Biochimica et Biophysica Acta (BBA)-Lipids and Lipid Metabolism, 1990. **1045**(2): p. 128-134.

321. Puri, P., et al., *The plasma lipidomic signature of nonalcoholic steatohepatitis.* Hepatology, 2009. **50**(6): p. 1827-1838.

322. Nelson, J.W., E.E. Hatch, and T.F. Webster, *Exposure to polyfluoroalkyl chemicals and cholesterol, body weight, and insulin resistance in the general US population.* Environmental health perspectives, 2009. **118**(2): p. 197-202.

323. Gorden, D.L., et al., *Biomarkers of NAFLD progression: a lipidomics approach to an epidemic.* Journal of lipid research, 2015. **56**(3): p. 722-736.

324. Fu, Y., et al., *Associations between serum concentrations of perfluoroalkyl acids and serum lipid levels in a Chinese population.* Ecotoxicology and environmental safety, 2014. **106**: p. 246-252.

325. Starling, A.P., et al., *Perfluoroalkyl substances and lipid concentrations in plasma during pregnancy among women in the Norwegian Mother and Child Cohort Study.* Environment international, 2014. **62**: p. 104-112.

326. Liew, Z., H. Goudarzi, and Y. Oulhote, *Developmental Exposures to Perfluoroalkyl Substances (PFASs): An Update of Associated Health Outcomes.* Current environmental health reports, 2018. **5**(1): p. 1-19.

327. Huang, M.C., et al., *Toxicokinetics of perfluorobutane sulfonate (PFBS), perfluorohexane-1-sulphonic acid (PFHxS), and perfluorooctane sulfonic acid (PFOS) in male and female Hsd:Sprague Dawley SD rats after intravenous and gavage administration.* Toxicology reports, 2019. **6**: p. 645-655.

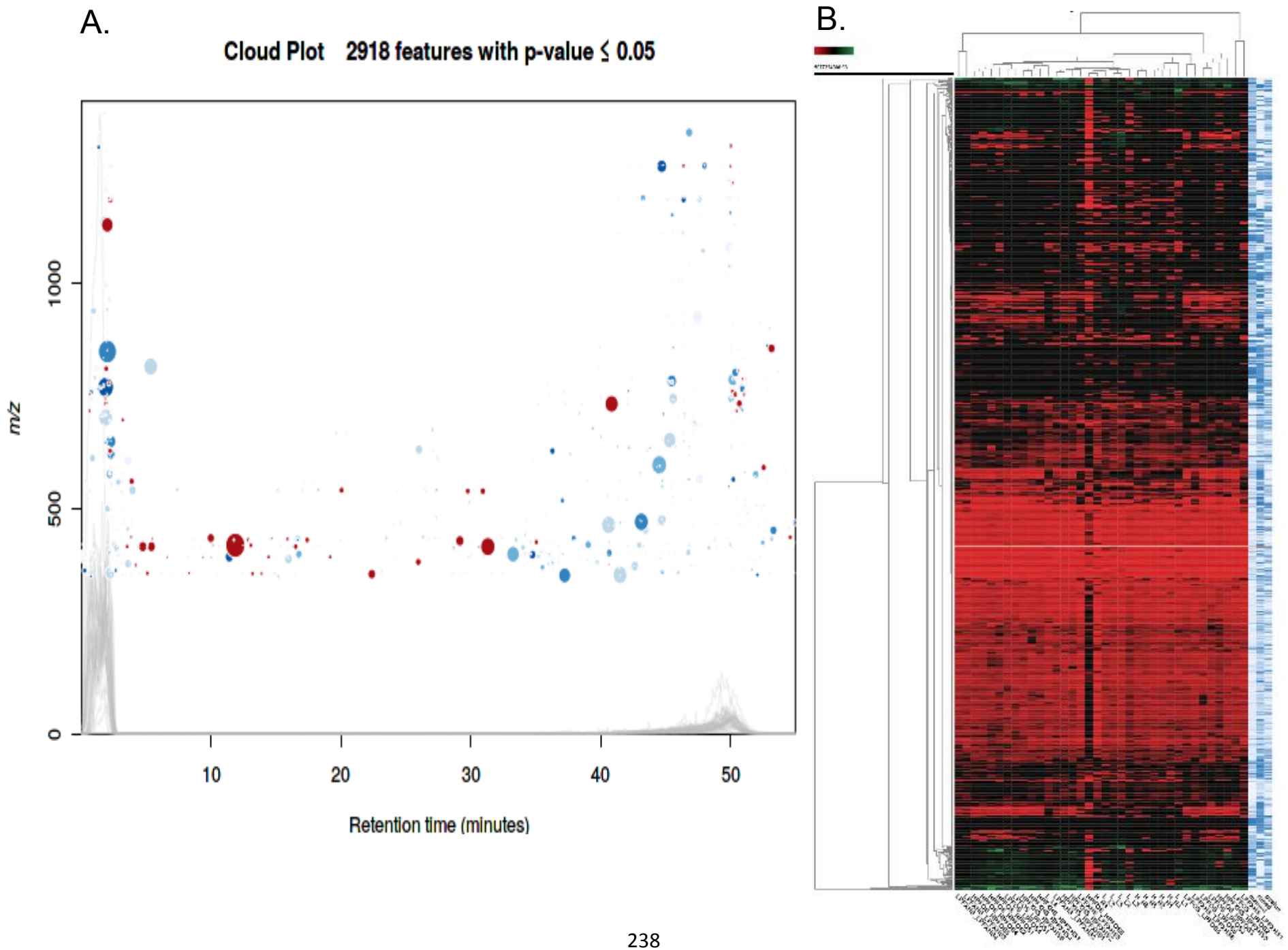
A.
Cloud Plot 2918 features with p-value ≤ 0.05
m/z
0
500
1000
10
20
30
40
50
Retention time (minutes)
B.

Figure 6.1. A) Differential cloud plot demonstrating dysregulated lipid features in the blood of male mice exposed to LFD and LFD containing PFAS (L-PFOS and L-PFHxS) and those exposed to HFD and HFD containing PFAS (H-PFOS and H-PFHxS) ($p < 0.05$ threshold, fold change >= 1.5 threshold). Up-regulated features (features that have a positive fold change) are graphed above the x-axis shown in green while down-regulated features (features that have a negative fold change) are shown in red and are graphed below the x-axis. **B**) Differential expression of lipid features between LFD and LFD with PFAS (L-PFOS and L-PFHxS) exposure and HFD and HFD with PFAS (H-PFOS and H-PFHxS) exposure. Only those features whose levels varied significantly ($p < 0.05$) are projected. Rows represent a metabolite feature and each column representing a sample. Data are indicative of 6 samples per group.

A.

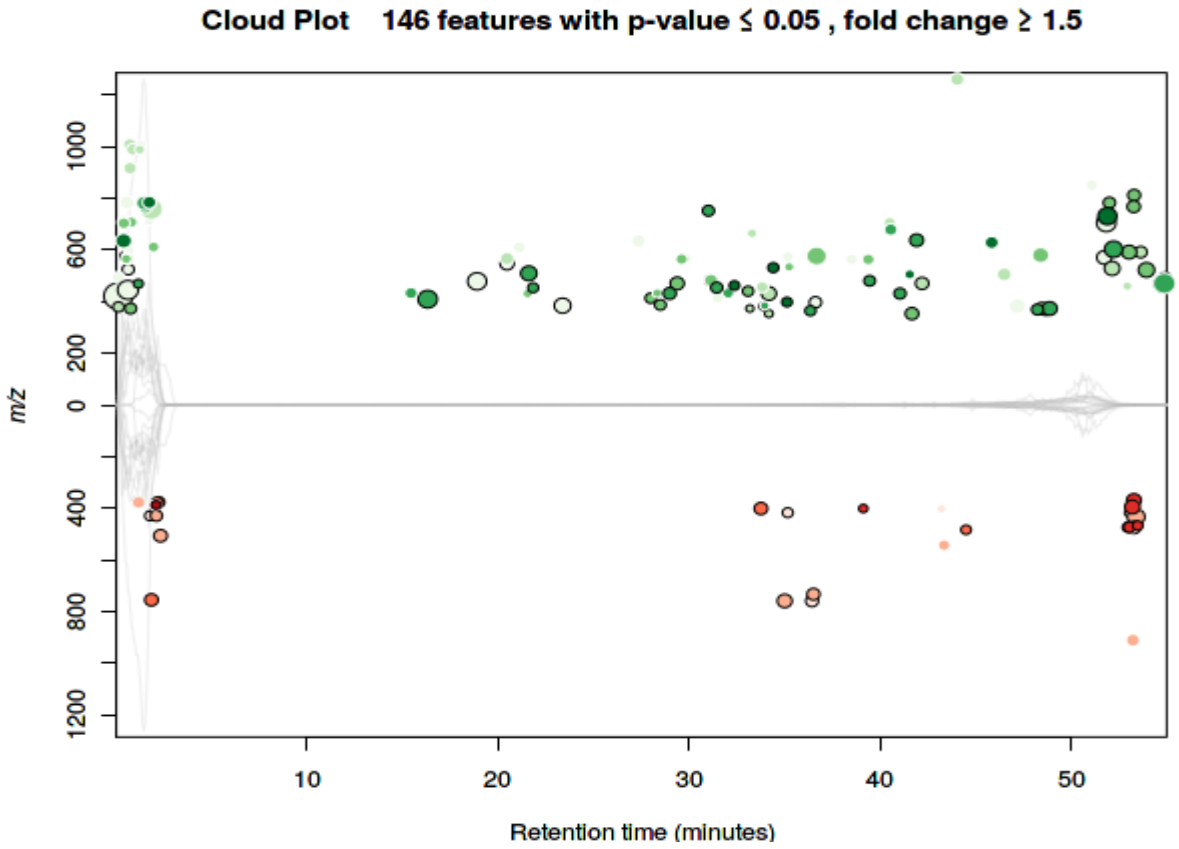
Cloud Plot 146 features with p-value ≤ 0.05 , fold change ≥ 1.5
m/z
1000
600
200
0
400
800
1200
10
20
30
40
50
Retention time (minutes)

B.

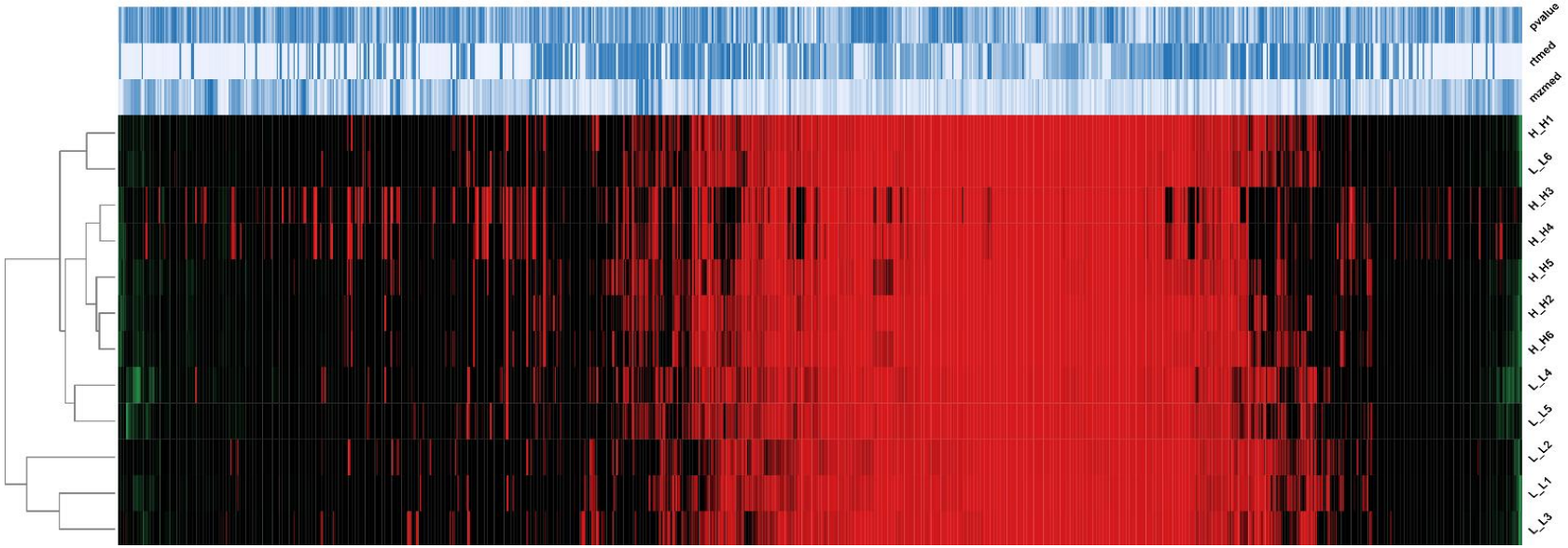
pvalue
rtmed
mzmed
H_H1
L_L6
H_H3
H_H4
H_H5
H_H2
H_H6
L_L4
L_L5
L_L2
L_L1
L_L3

Figure 6.2. A) Differential cloud plot demonstrating dysregulated lipid features in the blood of male mice exposed to a LFD in comparison to those exposed to a HFD ($p < 0.05$ threshold, fold change >= 1.5 threshold). Up-regulated features (features that have a positive fold change) are graphed above the x-axis and are shown in green, while down-regulated features (features that have a negative fold change) are shown in red, and are graphed below the x-axis. **B**) Differential expression of lipid features that differed between mice exposed to LFD and HFD. Only those features whose levels varied significantly ($p < 0.05$) are projected. Rows represents a metabolite feature and each column represents a sample. Data are indicative of 6 samples per group.

A.

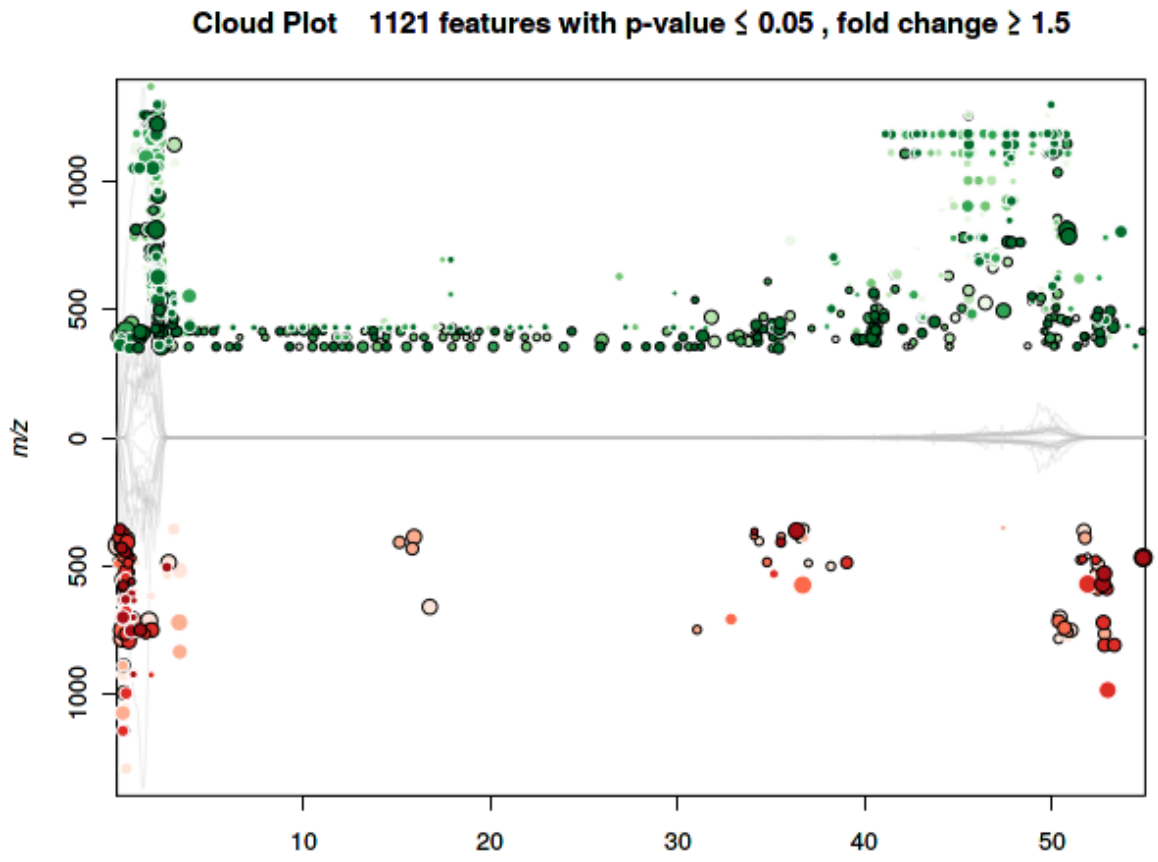
Cloud Plot 1121 features with p-value ≤ 0.05 , fold change ≥ 1.5
m/z
1000
500
0
500
1000
10
20
30
40
50
Retention time (minutes)

B.

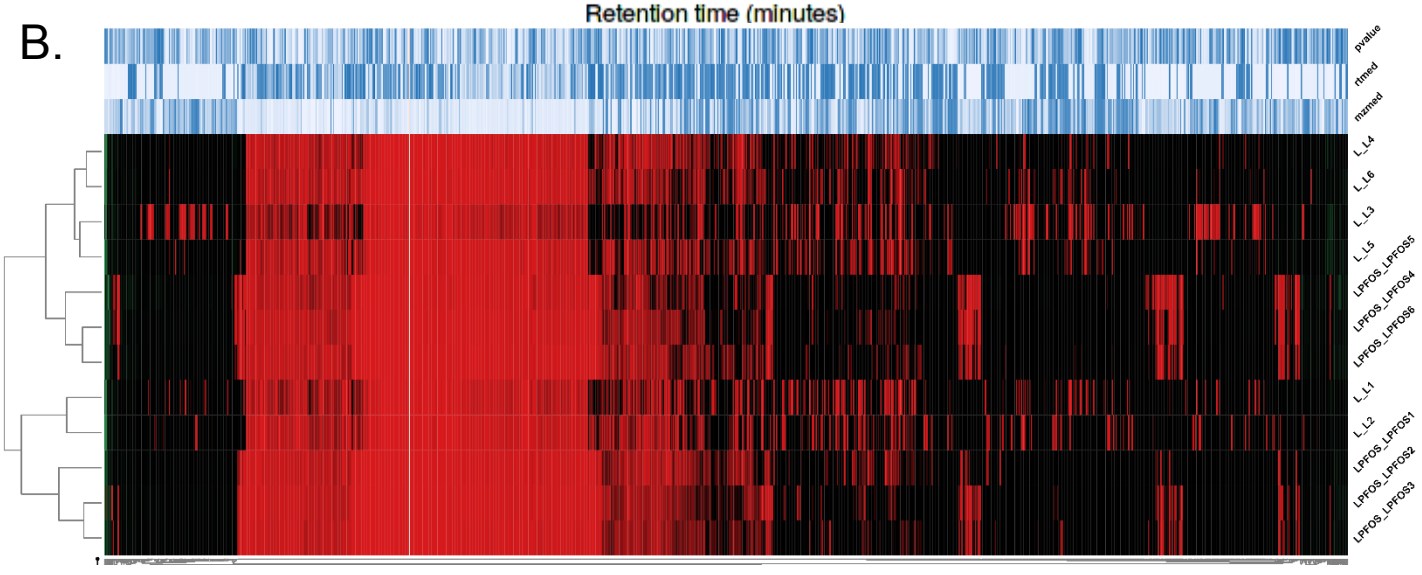
pvalue
rtmed
mzmed
L_L4
L_L6
L_L3
L_L5
LPFOS_LPFOS5
LPFOS_LPFOS4
LPFOS_LPFOS6
L_L1
L_L2
LPFOS_LPFOS1
LPFOS_LPFOS2
LPFOS_LPFOS3

Figure 6.3. A) Differential cloud plot demonstrating dysregulated lipid features in the lipidomic profile of blood isolated from male mice exposed to LFD and LFD containing PFOS (L-PFOS; *p* value < 0.05threshold, fold change >= 1.5 threshold). Up-regulated features (features that have a positive fold change) are graphed above the x-axis shown in green, while down-regulated features (features that have a negative fold change) are shown in red, and are graphed below the x-axis. **B**) Differential expression of lipid features in the blood of mice exposed to LFD in comparison to mice exposed to a LFD containing PFOS (L-PFOS). Only those features whose levels varied significantly ($p < 0.05$) are projected. Rows represents a metabolite feature and each column represents a sample. Data are indicative of 6 samples per group.

A.

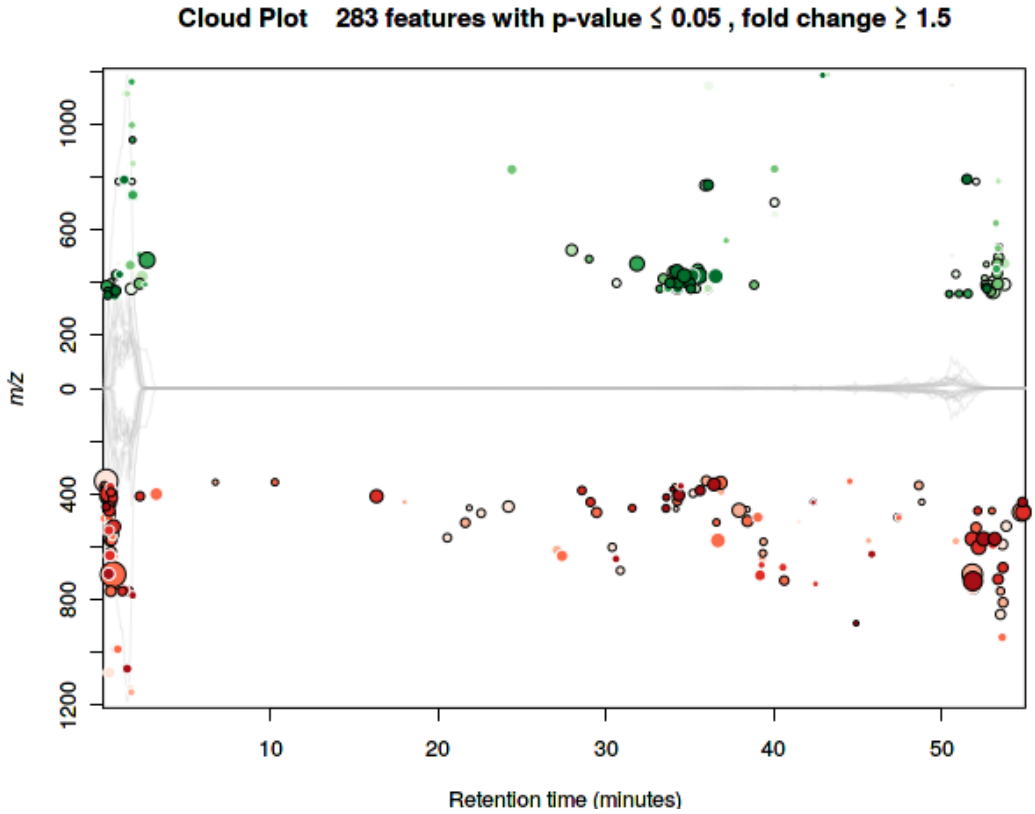
Cloud Plot 283 features with p-value ≤ 0.05 , fold change ≥ 1.5
m/z
1000
600
200
0
400
800
1200
10
20
30
40
50
Retention time (minutes)

B.

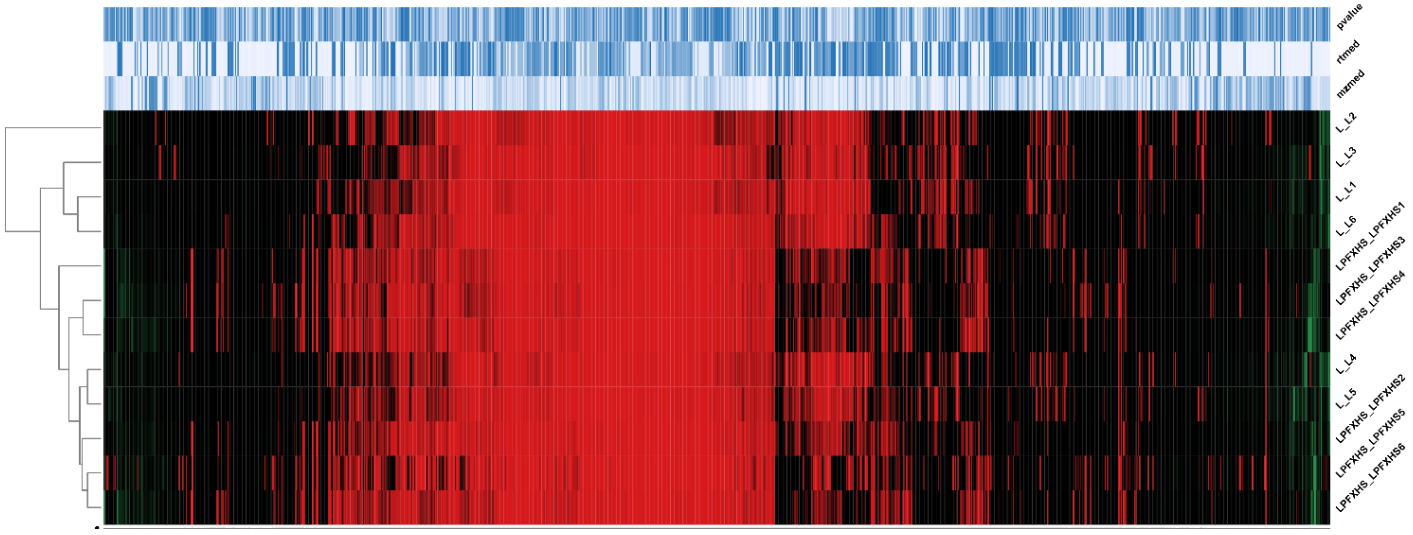
pvalue
rtmed
mzmed
L_L2
L_L3
L_L1
L_L6
LPFXHS_LPFXHS1
LPFXHS_LPFXHS3
LPFXHS_LPFXHS4
L_L4
L_L5
LPFXHS_LPFXHS2
LPFXHS_LPFXHS5
LPFXHS_LPFXHS6

Figure 6.4. A) Differential cloud plot demonstrating dysregulated lipid features in the lipidomic profile of blood isolated from male mice exposed to LFD and LFD containing PFHxS (L- PFHxS; *p* value < 0.05 threshold, fold change >= 1.5 threshold). Up-regulated features (features that have a positive fold change) are graphed above the x-axis shown in green, while down-regulated features (features that have a negative fold change) are shown in red, andare graphed below the x-axis. **B**) Differential expression of lipid features in the blood of mice exposed to LFD in comparison to mice exposed to a LFD containing PFHxS (L- PFHxS). Only those features whose levels varied significantly ($p < 0.05$) are projected. Rows represents a metabolite feature and each column represents a sample.

A.

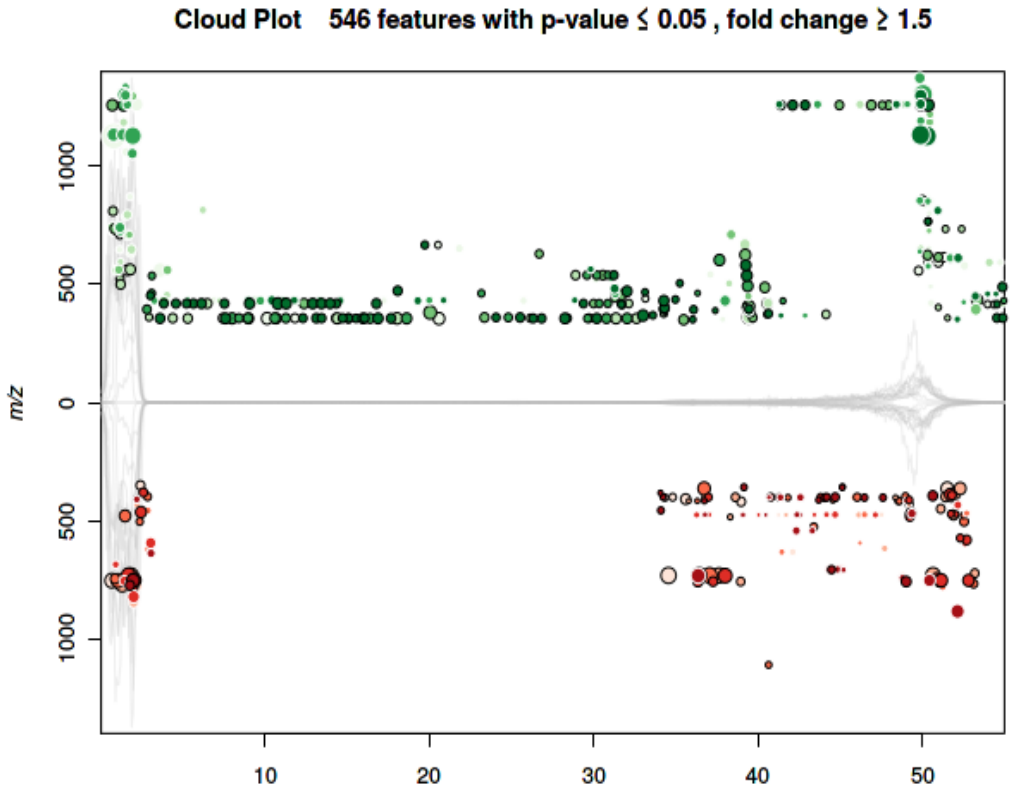
Cloud Plot 546 features with p-value ≤ 0.05 , fold change ≥ 1.5
m/z
1000
500
0
500
1000
10
20
30
40
50
Retention time (minutes)

B.

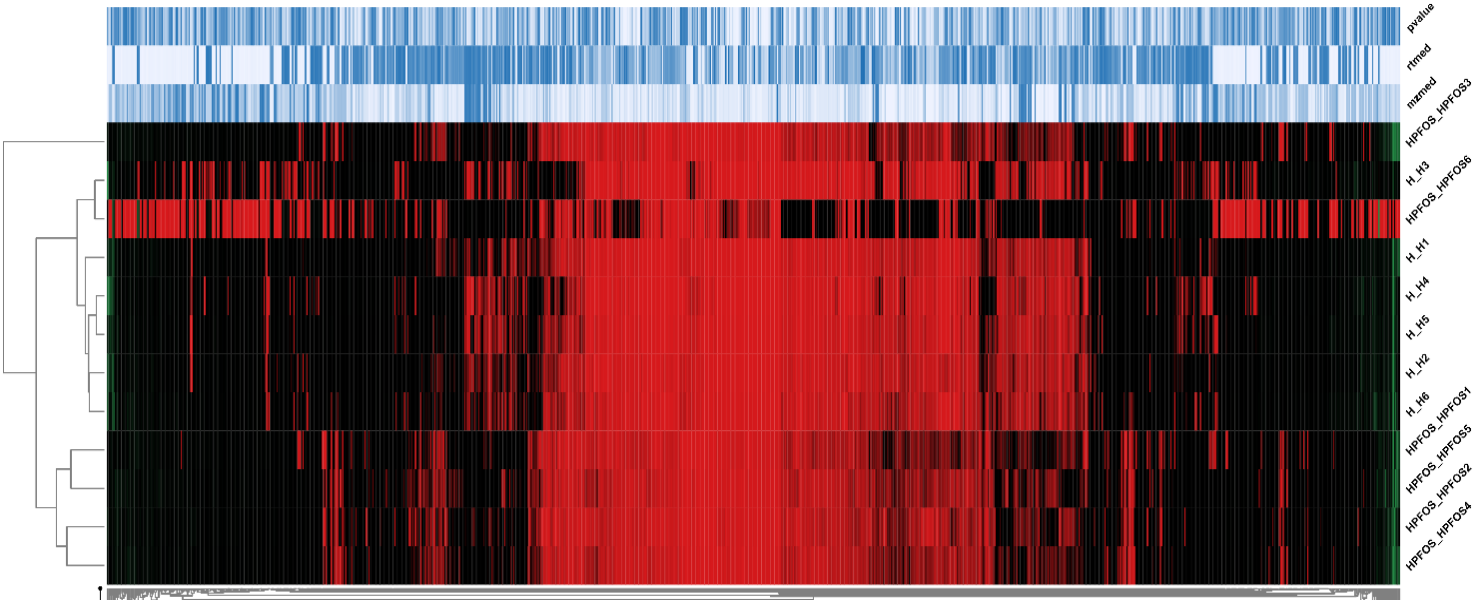
pvalue
rtmed
mzmed
HPFOS_HPFOS3
H_H3
HPFOS_HPFOS6
H_H1
H_H4
H_H5
H_H2
H_H6
HPFOS_HPFOS1
HPFOS_HPFOS5
HPFOS_HPFOS2
HPFOS_HPFOS4

Figure 6.5. A) Differential cloud plot demonstrating dysregulated lipid features in the lipidomic profile of blood isolated from male mice exposed to HFD and HFD containing PFOS (H-PFOS; *p* value < 0.05threshold, fold change >= 1.5 threshold). Up-regulated features (features that have a positive fold change) are graphed above the x-axis shown in green, while down-regulated features (features that have a negative fold change) are shown in red, are graphed below the x-axis. **B**) Differential expression of lipid features in the blood of mice exposed to HFD in comparison to mice exposed to a HFD containing PFOS (H-PFOS). Only those features whose levels varied significantly ($p < 0.05$) are projected. Rows represents a metabolite feature and each column represents a sample.

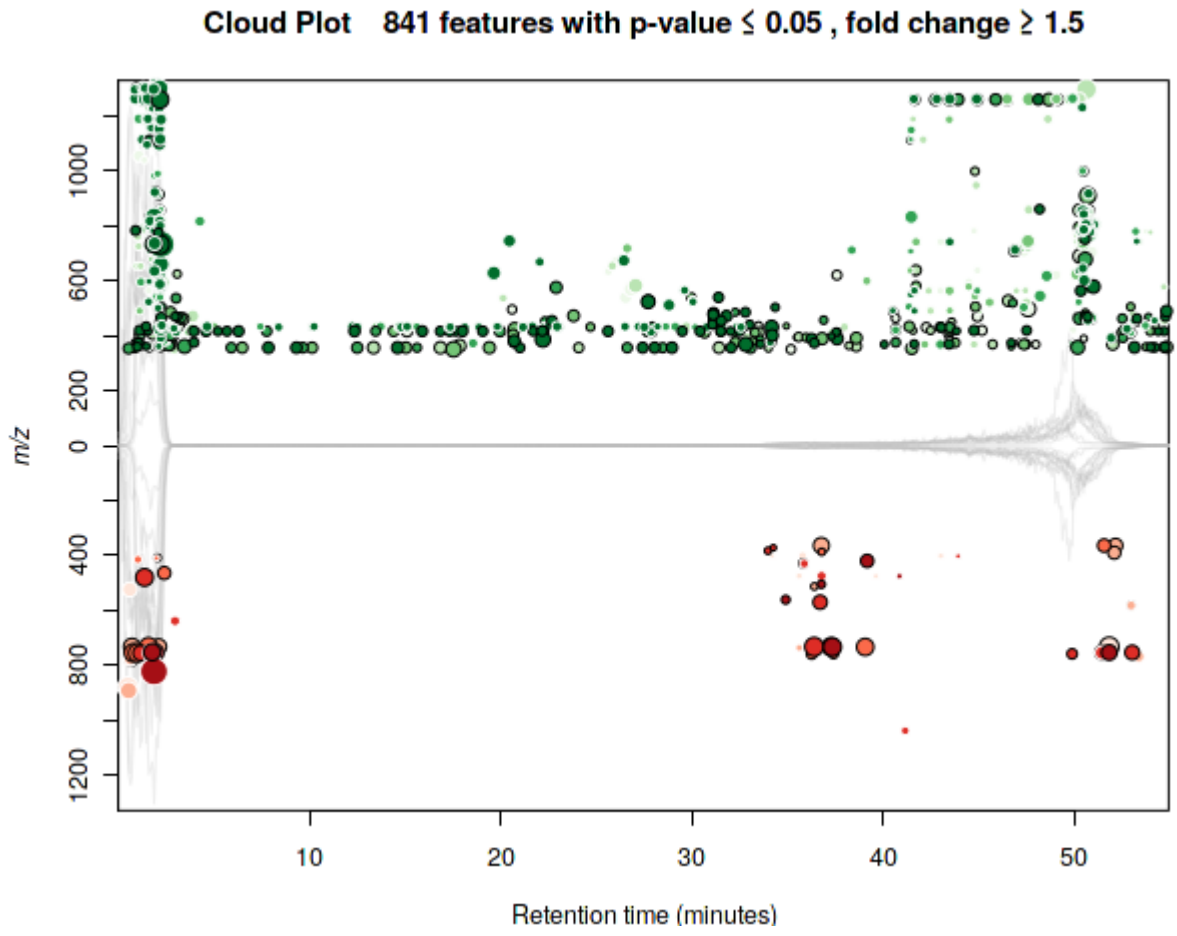

Figure 6.6. A) Differential cloud plot demonstrating dysregulated lipid features between HFD and H-PFHxS (*p* value < 0.05threshold, fold change >= 1.5 threshold). Up-regulated features (features that have a positive fold change) are graphed above the x-axis shown in green, while down-regulated features (features that have a negative fold change) are shown in red, and are graphed below the x-axis.

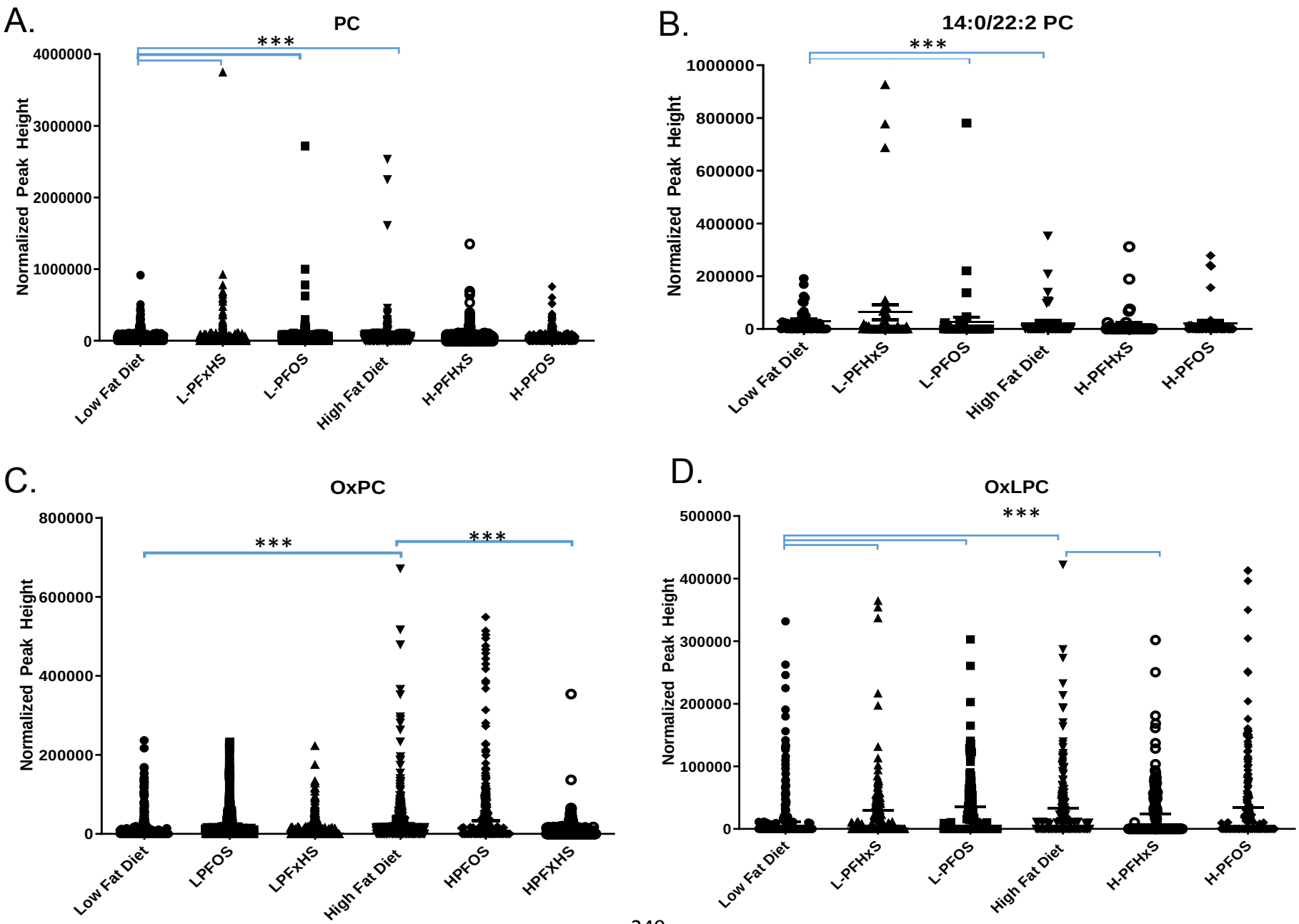
A.
PC
***
Normalized Peak Height
4000000
3000000
2000000
1000000
0
Low Fat Diet
L-PFxHS
L-PFOS
High Fat Diet
H-PFHxS
H-PFOS
B.
14:0/22:2 PC
***
Normalized Peak Height
1000000
800000
600000
400000
200000
0
Low Fat Diet
L-PFHxS
L-PFOS
High Fat Diet
H-PFHxS
H-PFOS
C.
OxPC
***
***
Normalized Peak Height
800000
600000
400000
200000
0
Low Fat Diet
LPFOS
LPFxHS
High Fat Diet
HPFOS
HPFXHS
D.
OxLPC
***
Normalized Peak Height
500000
400000
300000
200000
100000
0
Low Fat Diet
L-PFHxS
L-PFOS
High Fat Diet
H-PFHxS
H-PFOS

Figure 6.7. Comparison of phosphatidylcholine (PC) levels in the blood of male C57BL/6 mice exposed to LFD and LFD with PFAS (L-PFOS and L-PFHxS) or HFD and HFD with PFAS (H-PFOS and H-PFHxS) blood. Data are indicative of 6 samples per group and are expressed as mean ± the SEM (*$p < 0.05$ **$p < 0.01$*** $p < 0.001$). Each symbol represents an individual lipid feature as identified by LC-*MS/MS*. Differences in normalized peak areas between hormone-sensitive and non-cancerous prostate cells are shown for (**A**) phosphatidylcholine (PC), **B**) 14:0-22:2 PC and **C)** oxidized PC (OxPC) and **D)** oxidized LPC (OxLPC).

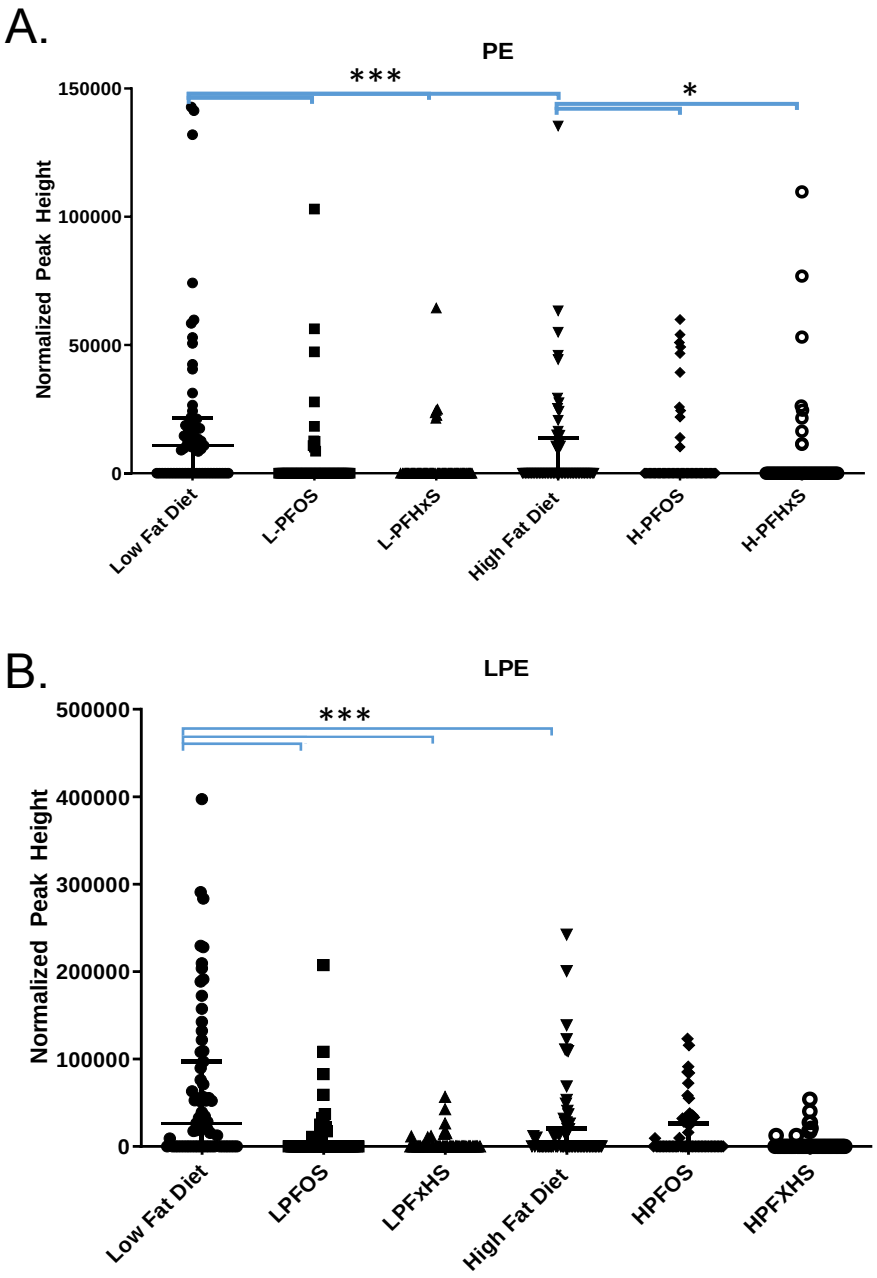

Figure 6.8. Comparison of phosphatidylethanolamine (PE) levels in the blood of male C57BL/6 mice exposed to LFD and LFD with PFAS (L-PFOS and L-PFHxS) or HFD and HFD with PFAS (H-PFOS and H-PFHxS) blood. Data are indicative of 6 samples per group and are expressed as the mean ± the SEM (*$p < 0.05$ **$p < 0.01$*** $p < 0.001$). Each symbol represents an individual lipid feature as identified by LC-*MS/MS*. Normalized peak areas between all cells are shown for **A)** PE and **B)** LPE.

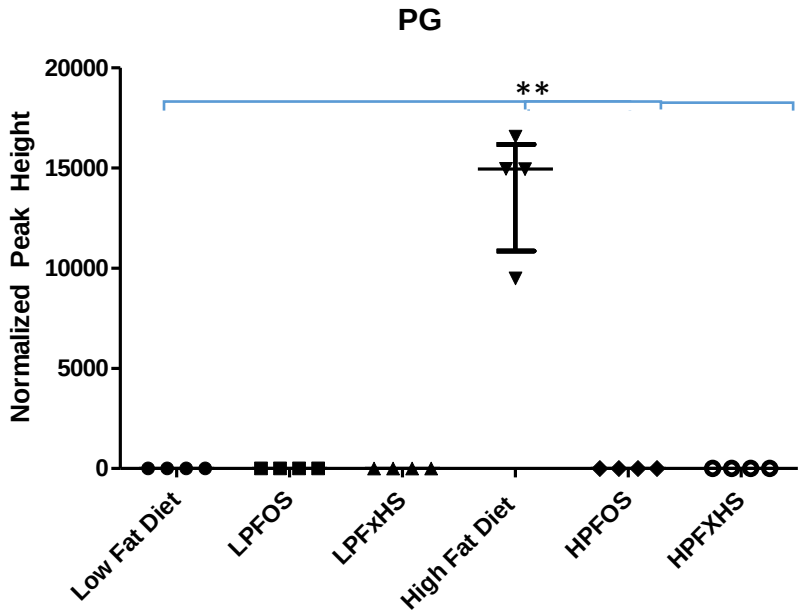

Figure 6.9. Comparison of phosphatidylglycerol (PG) levels in the blood of male C57BL/6 mice exposed to LFD and LFD with PFAS (L-PFOS and L-PFHxS) or HFD and HFD with PFAS (H-PFOS and H-PFHxS) blood. Data are indicative of 6 samples per group and are expressed as the mean ± the SEM (*$p < 0.05$ **$p < 0.01$*** $p < 0.001$). Each symbol represents an individual lipid feature as identified by LC-*MS/MS*. Normalized peak areas between all cells are shown for phosphatidylglycerol.

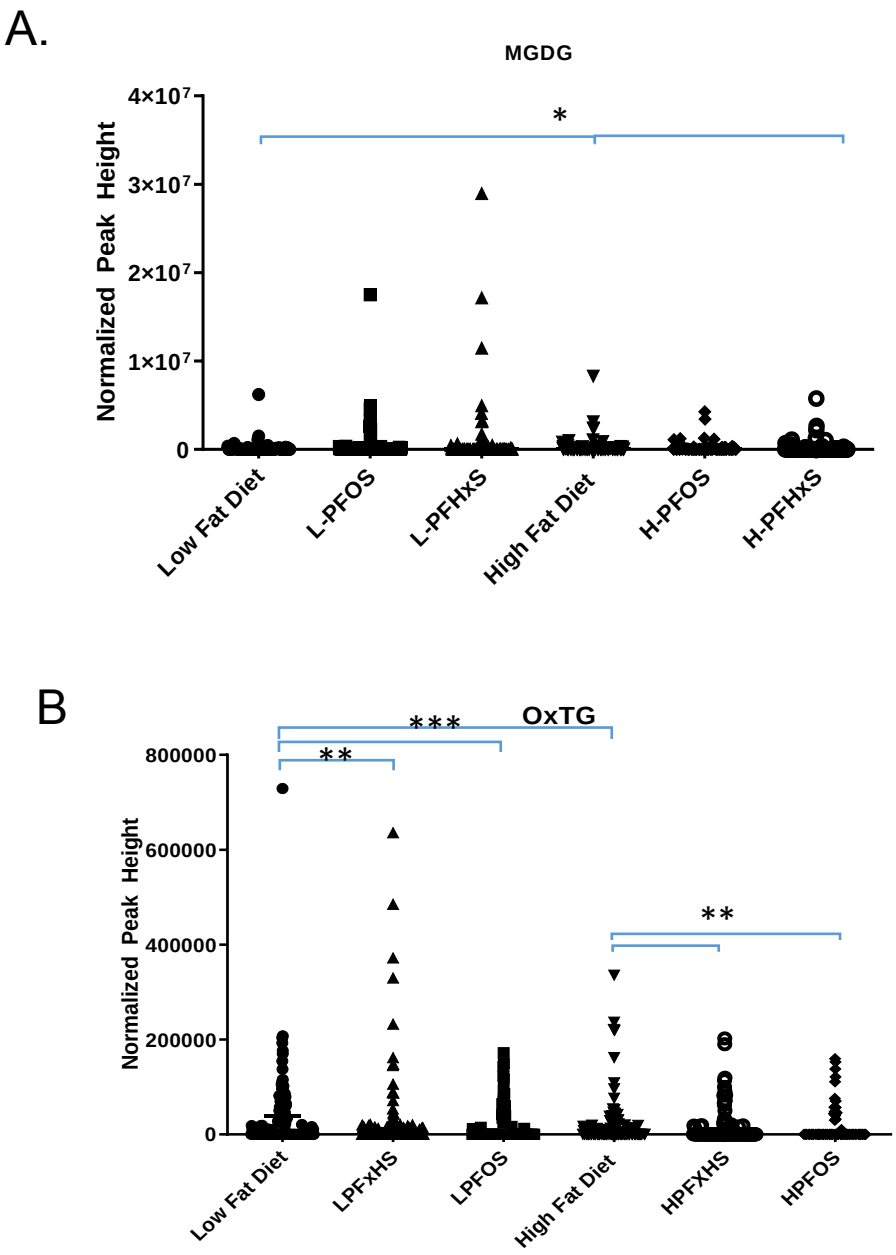

Figure 6.10. Comparison of acylglycerol levels in the blood of male C57BL/6 mice exposed to LFD and LFD with PFAS (L-PFOS and L-PFHxS), or HFD and HFD with PFAS (H-PFOS and H-PFHxS) blood. Data are indicative of 6 samples per group and are expressed as the mean ± the SEM (*$p < 0.05$ **$p < 0.01$*** $p < 0.001$). Each symbol represents an individual lipid feature as identified by LC-*MS/MS*. Normalized peak areas between all cells are shown for **A)** monogalactosyldiacylglycerol (MGDG) and **B)** oxidized triacylglycerol (OxTG).

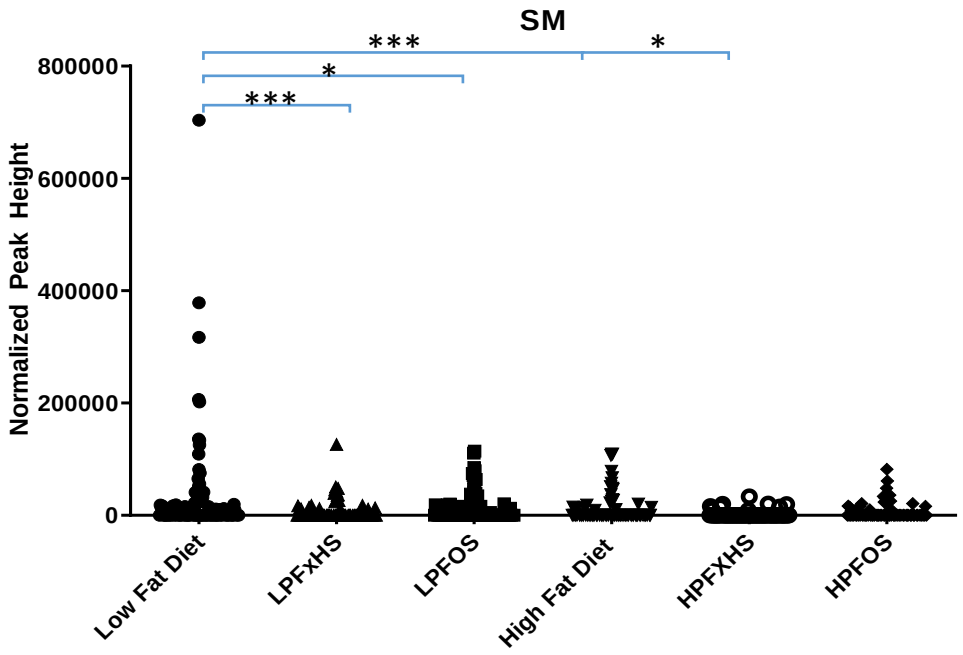

Figure 6.11. Comparison of sphingomyelin levels in the blood of male C57BL/6 mice exposed to LFD and LFD with PFAS (L-PFOS and L-PFHxS), or HFD and HFD with PFAS (H-PFOS and H-PFHxS) blood. Data are indicative of 6 samples per group and are expressed as the mean ± SEM (*$p < 0.05$ **$p < 0.01$*** $p < 0.001$). Each symbol represents an individual lipid feature as identified by LC-*MS/MS*. Data are compared based on normalized peak areas.

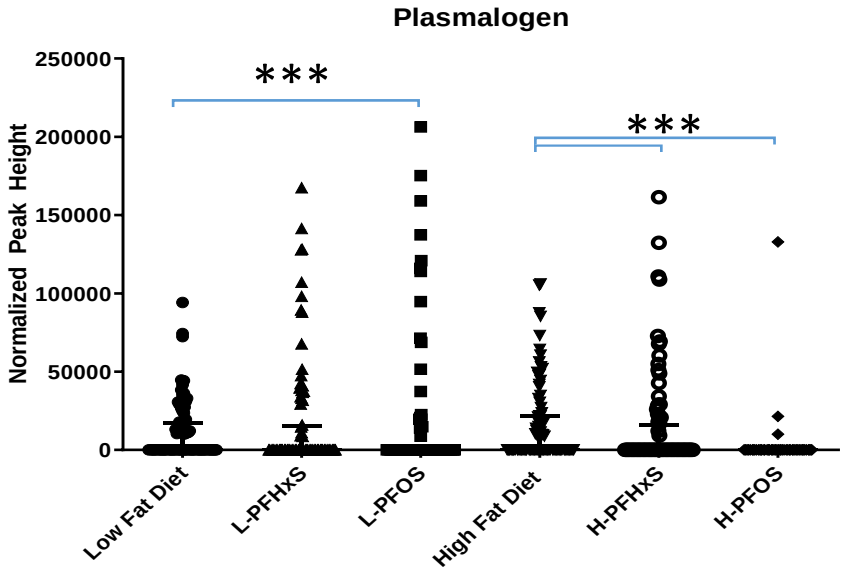

Figure 6.12. Comparison of plasmalogen levels in the blood of male C57BL/6 mice exposed to LFD, LFD with PFAS (L-PFOS and L-PFHxS) or HFD and HFD with PFAS (H-PFOS and H-PFHxS) blood. Data are indicative of 6 samples per group and are expressed as the mean ± SEM (*$p < 0.05$ **$p < 0.01$*** $p < 0.001$). Each symbol represents an individual lipid feature as identified by LC-*MS/MS*. Data are compared based on normalize

A.

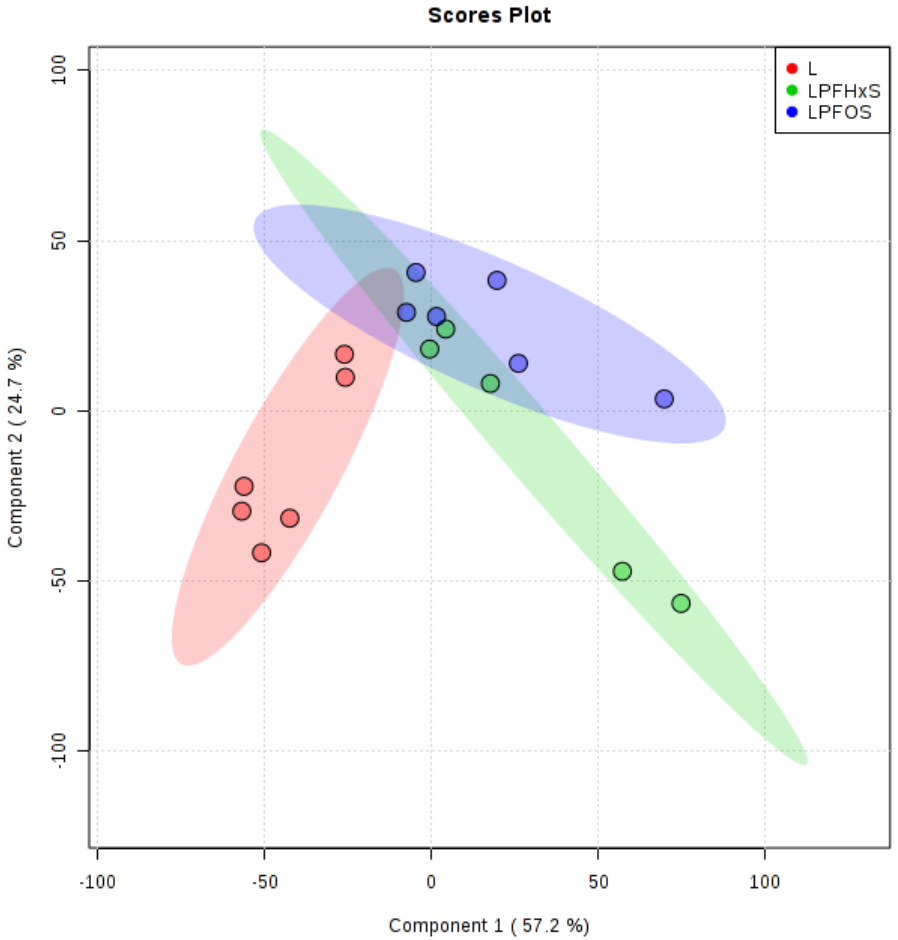

B.

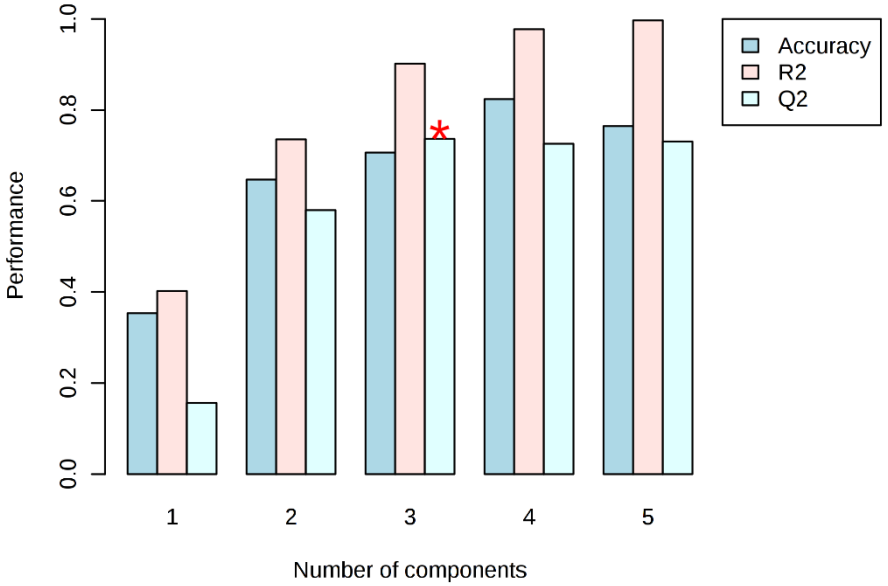

C.

PLS-DA cross validation details:					
Measure	1 comps	2 comps	3 comps	4 comps	5 comps
Accuracy	0.35294	0.64706	0.70588	0.82353	0.76471
R2	0.40194	0.73574	0.90139	0.9776	0.99725
Q2	0.15629	0.57998	0.73675	0.72603	0.73083

Supplemental Figure 6.1. Multivariate statistics revealed a specific lipidomic signature in correlation to PFAS and diet. **A)** Supervised Partial Least Discriminant Analyses indicate discrimination between LFD control and LFD with PFAS compounds based on the lipidome. **B)** PLS-DA classification with different number of components**.** The red asterisk indicates the best classifier. **C)** Cross validation (CV) analyses (10-fold CV method) indicated moderate to high predictive accuracy.

A.

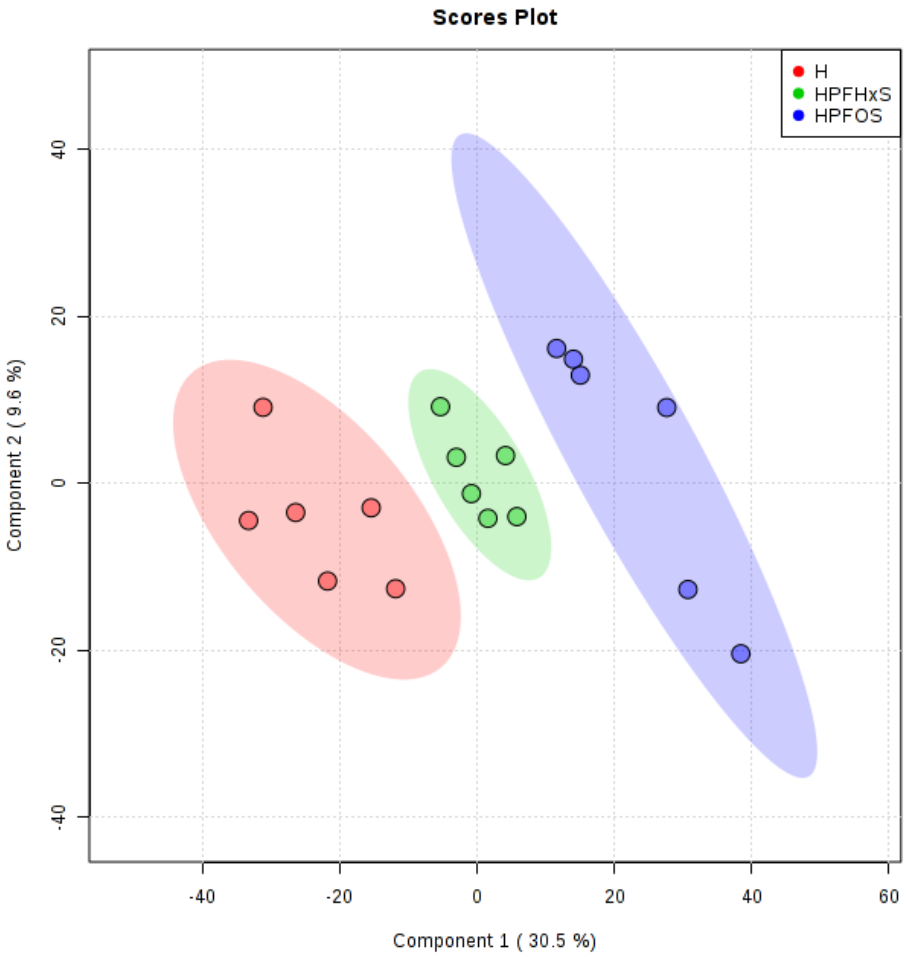

B.

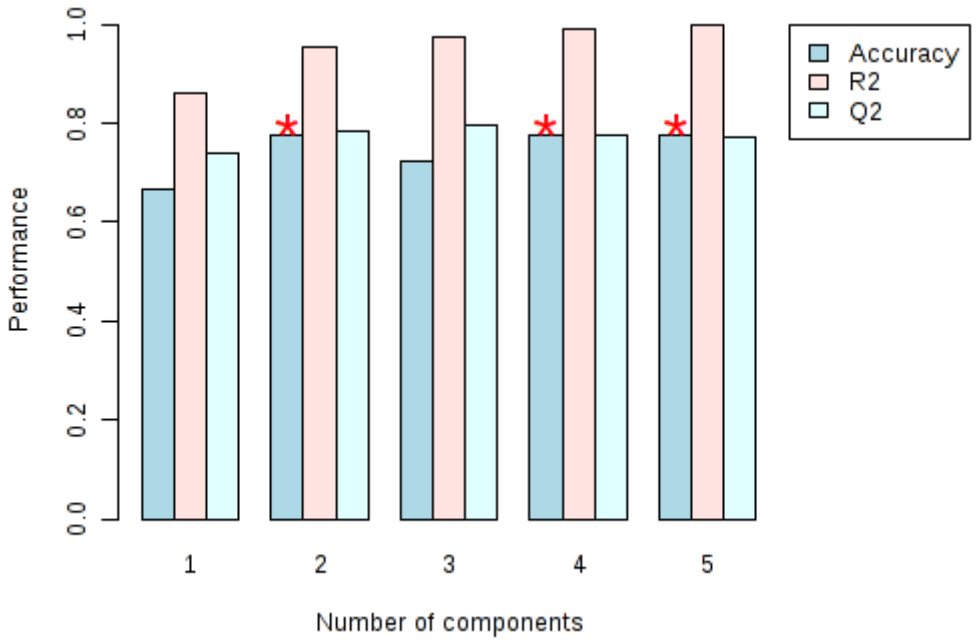

C.

PLS-DA cross validation details:					
Measure	1 comps	2 comps	3 comps	4 comps	5 comps
Accuracy	0.66667	0.77778	0.72222	0.77778	0.77778
R2	0.85914	0.95353	0.97516	0.98994	0.99853
Q2	0.74117	0.78251	0.7955	0.77746	0.77132

Supplemental Figure 6.2. Multivariate statistics revealed a specific lipidomic signature in correlation to PFAS and diet. **A)** Supervised Partial Least Discriminant Analyses indicate that it is possible to discriminate between LFD control and LFD with PFAS compounds based on the lipidome. **B)** PLS-DA classification with different number of components**.** The red asterisk indicates the best classifier. **C)** Cross validation (CV) analyses (10-fold CV method) indicated high predictive accuracy.

Supplemental Table 6.1. Lipid phosphorus assay. Lipids extracted from blood samples were analyzed for inorganic phosphorus content based on analysis of standards ranging from 1 ug to 5 ug at λ=590 nm. Concentrations of samples were diluted to 500 pmol/ul.

Sample	Absorbance (nm)	Concentration (ug)
1	0.5182	2.05
2	0.4911	1.91
3	0.4943	1.93
4	0.476	1.83
5	0.5225	2.07
6	0.4909	1.91
7	0.452	1.71
8	0.4813	1.86
9	0.4554	1.73
10	0.4535	1.72
11	0.4478	1.69
12	0.4879	1.89
13	0.4994	1.95
14	0.4782	1.84
15	0.438	1.64
16	0.4867	1.89
17	0.4868	1.89
18	0.4836	1.87
19	0.5636	2.28
20	0.8733	3.86
21	0.8326	3.65
22	0.8272	3.63
23	0.8338	3.66
24	0.8616	3.80
25	0.8574	3.78
26	0.8514	3.75
27	0.852	3.75
28	0.8602	3.79
29	0.7129	3.04
30	0.8195	3.59
31	0.8458	3.72
32	0.8401	3.69
33	0.8537	3.76

34	0.8586	3.79
35	0.8106	3.54

Supplemental Table 6.2. FDR-corrected significance between LFD and LFD with PFAS (L-PFOS and L-PFHxS) exposure and HFD and HFD with PFAS (H-PFOS and H-PFHxS) exposure.

FDR-Discovery Rate FDR; Q < 0.05

PC

Two-stage linear step-up procedure of Benjamini, Krieger and Yekutieli	Mean rank diff.	Discovery?	q value	Individual P Value
LPFOS vs. Low Fat Diet	-343.3	Yes	<0.001	<0.001
LPFHxS vs. Low Fat Diet	-297.5	Yes	<0.001	<0.001
High Fat Diet vs. Low Fat Diet	-276	Yes	<0.001	<0.001

14:0/22:2 PC

Two-stage linear step-up procedure of Benjamini, Krieger and Yekutieli	Mean rank diff.	Discovery?	q value	Individual P Value
LPFOS vs. Low Fat Diet	-50.18	Yes	0.001	<0.001
High Fat Diet vs. Low Fat Diet	-49.39	Yes	0.001	<0.001

OxPC

Two-stage linear step-up procedure of Benjamini, Krieger and Yekutieli	Mean rank diff.	Discovery?	q value	Individual P Value
High Fat Diet vs. Low Fat Diet	477.8	Yes	<0.001	<0.001
HPFHxS vs. High Fat Diet	-445.8	Yes	<0.001	<0.001

OxLPC

Two-stage linear step-up procedure of Benjamini, Krieger and Yekutieli	Mean rank diff.	Discovery?	q value	Individual P Value
LPFOS vs. Low Fat Diet	95.76	Yes	0.008	0.003
LPFHxS vs. Low Fat Diet	69.81	Yes	0.04	0.03
High Fat Diet vs. Low Fat Diet	104.1	Yes	0.008	0.001
HPFHxS vs. High Fat Diet	-90.5	Yes	0.01	0.004

PE

Two-stage linear step-up procedure of Benjamini, Krieger and Yekutieli	Mean rank diff.	Discovery?	q value	Individual P Value

L-PFOS vs. Low Fat Diet	-90.65	Yes	<0.001	<0.001
L-PFHxS vs. Low Fat Diet	-100.6	Yes	<0.001	<0.001
High Fat Diet vs. Low Fat Diet	-58.71	Yes	<0.001	<0.001
H-PFOS vs. High Fat Diet	-29.88	Yes	0.05	0.05
H-PFHxS vs. High Fat Diet	-36.69	Yes	0.02	0.02

LPE

Two-stage linear step-up procedure of Benjamini, Krieger and Yekutieli	Mean rank diff.	Discovery?	q value	Individual P Value
LPFOS vs. Low Fat Diet	-98.4	Yes	<0.001	<0.001
LPFHxS vs. Low Fat Diet	-115.7	Yes	<0.001	<0.001
High Fat Diet vs. Low Fat Diet	-67.54	Yes	<0.001	<0.001

PG

Two-stage linear step-up procedure of Benjamini, Krieger and Yekutieli	Mean rank diff.	Discovery?	q value	Individual P Value
High Fat Diet vs. Low Fat Diet	12	Yes	<0.001	<0.001
HPFOS vs. High Fat Diet	-12	Yes	<0.001	<0.001
HPFHxS vs. High Fat Diet	-12	Yes	<0.001	<0.001

MGDG

Two-stage linear step-up procedure of Benjamini, Krieger and Yekutieli	Mean rank diff.	Discovery?	q value	Individual P Value
High Fat Diet vs. Low Fat Diet	89.64	Yes	0.01	0.001
HPFHxS vs. High Fat Diet	-83.88	Yes	0.01	0.002

OxTG

Two-stage linear step-up procedure of Benjamini, Krieger and Yekutieli	Mean rank diff.	Discovery?	q value	Individual P Value

LPFOS vs. Low Fat Diet	-119.9	Yes	<0.001	<0.001
LPFHxS vs. Low Fat Diet	-90.89	Yes	<0.001	<0.001
High Fat Diet vs. Low Fat Diet	-74.51	Yes	0.002	0.001
HPFOS vs. High Fat Diet	-74.56	Yes	0.002	0.001
HPFHxS vs. High Fat Diet	-56.38	Yes	0.01	0.01

Plasmalogen

Two-stage linear step-up procedure of Benjamini, Krieger and Yekutieli	Mean rank diff.	Discovery?	q value	Individual P Value
LPFOS vs. Low Fat Diet	-44.59	Yes	0.02	0.02
HPFOS vs. High Fat Diet	-105.3	Yes	<0.001	<0.001
HPFHxS vs. High Fat Diet	-36.65	Yes	0.05	0.05

Supplemental Table 6.3. LIPEA pathway analysis. List of results from lipid indicators LFD and LFD with PFAS (L-PFOS and L-PFHxS) exposure and HFD and HFD with PFAS (H-PFOS and H-PFHxS) exposure.

Pathway name	Pathway lipids	Converted lipids (number)	Converted lipids (percentage)	Converted lipids (list)	*p*-value	Benjamini correction	Bonferroni correction
Glycerophospholipid metabolism	26	7	50%	C04438, C00416, C04230, C00157, C00350, C04233, C05973	7.63199E-07	2.21328E-05	2.21328E-05
Sphingolipid metabolism	21	3	21%	C00195, C00550, C12126	0.0145	0.0656	0.4069
Ferroptosis	11	3	21%	C21480, C21481, C21484	0.0021	0.0148	0.0591
Sphingolipid signaling pathway	9	3	21%	C00195, C12126, C00550	0.0011	0.0103	0.031
Choline metabolism in cancer	5	3	21%	C00416, C04230, C00157	0.0001	0.002	0.0039
Retrograde endocannabinoid signaling	8	2	14%	C00157, C00350	0.0164	0.0656	0.4595

Necroptosis	4	2	14%	C00195, C00550	0.0037	0.0209	0.1046
Arachidonic acid metabolism	75	1	7%	C00157	0.8837	0.8837	1
Linoleic acid metabolism	25	1	7%	C00157	0.4939	0.5122	1
alpha-Linolenic acid metabolism	23	1	7%	C00157	0.4649	0.5007	1
Glycerolipid metabolism	15	1	7%	C00416	0.3328	0.3727	1
Pathways in cancer	15	1	7%	C00416	0.3328	0.3727	1
Phosphatidylinositol signaling system	11	1	7%	C00416	0.2559	0.3116	1
Autophagy - animal	4	1	7%	C00350	0.1013	0.1575	1
Glycosylphosphatidylinositol (GPI)-anchor biosynthesis	3	1	7%	C00350	0.0769	0.1435	1
Phospholipase D signaling pathway	7	1	7%	C00416	0.1709	0.2278	1
Autophagy - other	3	1	7%	C00350	0.0769	0.1435	1
cAMP signaling pathway	5	1	7%	C00416	0.1251	0.1843	1
GnRH signaling pathway	3	1	7%	C00416	0.0769	0.1435	1
Fc gamma R-mediated phagocytosis	6	1	7%	C00416	0.1483	0.2076	1
Neurotrophin signaling pathway	3	1	7%	C00195	0.0769	0.1435	1
Adipocytokine signaling pathway	3	1	7.142857143	C00195	0.0769	0.1435	1
Leishmaniasis	4	1	7.142857143	C00195	0.1013	0.1575	1

Insulin resistance	4	1	7.142857143	C00195	0.1013	0.1575	1
AGE-RAGE signaling pathway in diabetic complications	2	1	7.142857143	C00195	0.0519	0.1435	1
Fat digestion and absorption	8	1	7.142857143	C00416	0.193	0.2456	1
Kaposi's sarcoma-associated herpesvirus infection	3	1	7.142857143	C00350	0.0769	0.1435	1
Pancreatic cancer	2	1	7.142857143	C00416	0.0519	0.1435	1

APPENDIX: CHAPTER 2

PARACRINE FIBROBLAST GROWTH FACTOR INIATES ONCOGENIC SYNERGY with EPITHLIAL FGFR/Src TRANFORMATION in PROSTATE TUMOR PROGRESSION

Qianjin Li, **Lishann Ingram**, Sungjin Kim, Zanna Beharry, Jonathan A. Cooper and Houjian Cai (2018) **Accepted by *Neoplasia*** [354], Reprinted here with permission of publisher

Abstract

Cross talk of stromal-epithelial cells plays an essential role in both normal development and tumor initiation and progression. Fibroblast growth factor (FGF)-FGF receptor (FGFR)-Src kinase axis is one of the major signal transduction pathways to mediate this cross talk. Numerous genomic studies have demonstrated that expression levels of FGFR/Src are dysregulated in prostate cancer; however, the role that paracrine FGF plays in dysregulated expression of epithelial FGFRs/Src and tumor progression *in vivo* is not well evaluated. In this study, we demonstrate that expression of wild-type FGFR1/2 or Src kinase in epithelial cells was not sufficient to initiate prostate tumorigenesis under a normal stromal microenvironment *in vivo*. However, paracrine FGF10 synergized with epithelial FGFR1 or FGFR2 expression induces epithelial-mesenchymal transition. Additionally, paracrine FGF10 sensitized FGFR2-transformed epithelial cells to initiate prostate tumorigenesis. Next, paracrine FGF10 also synergized with overexpression of epithelial Src kinase to high-grade tumors. But loss of the myristoylation site in Src kinase inhibited paracrine FGF10-induced prostate tumorigenesis. Loss of myristoylation alters Src levels in the cell membrane and inhibited FGF-mediated signaling. Our study demonstrates the potential tumor progression by simultaneous dysregulation of FGF/FGFRs/Src signal axis and provides a therapeutic strategy of targeting myristoylation of Src kinase to interfere with the tumorigenic process.

Introduction

Cross talk of stromal-epithelial cells plays an essential role in both physiological development and tumor initiation and progression [84, 355]. A considerable amount of evidence has demonstrated that fibroblast growth factor (FGF)/FGF receptor (FGFR) signaling is highly deregulated in a variety of cancers including prostate cancer [356-360]. Activation of FGFR in epithelial cells initiates prostate adenocarcinoma[361]. Additionally, this signaling axis mediates cross talk of tumorigenic cells with their microenvironment and facilitates tumor progression including prostate bone metastasis [362].

Src family kinases (SFKs) are a group of non-receptor tyrosine kinases. The expression and activity of SFK members are commonly upregulated in advanced prostate cancer [363]. SFKs mediate signaling of a variety of cellular receptors including many receptor tyrosine kinases. Our previous study showed that Src kinase played a role in the tumor microenvironment and autonomous FGFRs and Src are common oncogenic events in advanced prostate tumors [363-365]. However, the synergistic effect of the FGF/FGFRs/Src axis is understudied in prostate cancer progression.

Several mouse models have been utilized to study the deregulation of FGF/FGFR signaling in prostate cancer. A previous study demonstrated that FGFR1 (K656E), a constitutively active FGFR1 mutant with three times more activity than wild-type FGFR1, induces prostate hyperplasia and prostatic intraepithelial neoplasia after mice reached 6 months age [362]. However, genomic studies indicate that no constitutively active mutations, but amplification of FGFR1 or FGFR2, usually occur

in invasive prostate cancer [366, 367]. To study the activation of FGFR1, the juxtaposition of CID and kinases 1 (JOCK1) model was created using a recombinant protein [361, 368]. This model simulates the activation of FGFR1, but it does not allow for studying the interaction of the paracrine natural FGF ligand with epithelial FGFRs in tumor progression. Prostate tissue regeneration in combination with lentiviral delivery of oncogenes provides research approaches for studying the initiation and progression of prostate cancer in vivo. This experimental system has been designed as a model to be used for recapitulating the regeneration of normal prostate tissue, low prostatic intra-epithelial neoplasia (PIN), high grade PIN, as well as invasive human prostate cancer. This model further presents a potential approach for studying synergic oncogenic events, the simulation of prostate cancer responding to castration, and the epithelial tissue in response to paracrine stromal oncogenic stimulation. This model utilizes the combination of prostate primary epithelial cells with embryonic urogenital mesenchymal cells to regenerate prostate tissue[369]. This recombination model makes it possible to study the stromal-epithelial cell interactions. Using this model, it has been shown that ectopic expression of paracrine FGF10 in the urogenital mesenchymal cells initiates prostate adenocarcinoma *in vivo*[370, 371].

Numerous oncogenic signaling pathways and oncogenic events have been identified in prostate tumors including gene translocation of ERG [372], AR-androgen signaling[373], PTEN/PI3K/AKT, Ras/ Raf signaling[374], and many others. The synergy of these oncogenic events, such as Akt and AR [375] and ERG and Akt (or loss of PTEN)[376], significantly promotes cancer progression leading to high-grade

tumors. The synergy of Kras and AR [377]and Src and AR[378] could lead to invasive tumors and epithelial-to-mesenchymal (EMT) transition. In this study, we focus on the FGF/FGFR/Src signal axis in prostate cancer and investigate the oncogenic synergy of paracrine FGF10 with cell autonomous FGFR1, FGFR2, and Src in promoting prostate cancer progression. We demonstrate that elevated expression of wild-type FGFR1 and FGFR2 was not sufficient to induce oncogenic transformation; however, it synergizes with paracrine FGF10 to initiate prostate tumors, promote prostate tumor progression, and induce EMT. We also show that paracrine FGF10 synergized with overexpressed epithelial Src kinase resulting in high-grade tumors but not EMT. The FGF10-Src synergy relied on the myristoylation of Src, suggesting that targeting myristoylation of Src kinase might provide a therapeutic approach for inhibiting paracrine FGF10-induced tumorigenesis.

Materials and Methods

Plasmid Construction

Plasmids containing the coding sequence of mouse FGFR1 [Plasmid #14005, FGFR1 (IIIc) isoform] and FGFR2 [Plasmid #33248, FGFR2 (IIIc) isoform] (with three IgG loops) were obtained from Addgene. The coding sequence of FGFR1 and FGFR2 was sub cloned to the lentiviral vector FUCRW in which RFP is under the control of the CMV promoter and FGFR1/2 is regulated by the human ubiquitin promoter. Similarly, the coding sequence of murine FGF10 was also sub cloned into lentiviral vector FUCGW [379] in which expression of GFP is driven by the CMV promoter, and FGF10 is regulated

by the human ubiquitin promoter. FUCRW-Src (WT) and Src(K298M), a kinase-deficient mutant, were created previously [378]. The Src (G2A) mutant, a loss-of-myristoylation mutation, was created by PCR by introducing a point mutation at Gly2 and subsequently cloned in the FUCRW lentiviral vector. Lentivirus was generated by co-transfecting plasmids expressing the gene of interest and the packaging vectors MDL, VSV, and REV in HEK293T cells. Virus infection was performed as previously described[369]. Lentivirus usage followed the guidelines and regulations of the University of Georgia.

Cell Culture

SYF1 (Src−/−Yes−/−Fyn−/−) and HEK293T were purchased from American Type Culture Collection in September 2013. SYF1 cells were transduced with Src(WT), Src(G2A), or Src(K298M) by lentiviral infection to generate stable cell lines. All cell lines were cultured in American Type Culture Collection–recommended medium and temperature.

Prostate Regeneration Assay

C57BL/6J and CB.17SCID/SCID (SCID) mice were purchased from Taconic (Hudson, NY). Primary prostate cells were isolated from 8- to 12-week-old male C57BL/6J mice. Depending on the experimental settings, freshly isolated prostate primary cells were transduced with FGFR1, FGFR2, Src(WT), or Src(G2A) by lentiviral infection. Urogenital sinus mesenchyme (UGSM) cells were isolated from 16.5-day embryos of C57BL/6J mice and transduced with control vector or FGF10 by lentiviral infection. The transduced prostate primary cells (2 × 105 cells/graft) or freshly isolated prostate cells were combined with FGF10 or control UGSM (4 × 105 cells/graft). The cell mixture was resuspended in

20 µl of collagen type I (pH 7.0) (BD Biosciences). After overnight incubation, grafts were implanted under the kidney capsule of SCID male mice. Grafts were harvested after 8-week incubation.

Real-Time PCR

UGSM cells were infected with lentivirus and cultured for 5 days. Total RNA was isolated using the RNeasy Kit (QIAGEN) following the protocol of the manufacturer. A total of 1.5 µg of total RNA was used for reverse transcription to generate complementary DNA in a 20-µl reaction with a high-capacity cDNA reverse transcription kit (Life Technologies). The RT products were diluted 30 times with distilled H2O, and 2 µl was used as template for each real-time PCR. The reactions were performed using the PerfeCTa SYBR Green FastMix (Quanta Biosciences), and the thermal cycling conditions were an initial denaturation step at 95°C for 1 minute and 40 cycles at 95°C for 10 seconds and 60°C for 50 seconds. The experiments were carried out in triplicate. The relative quantification in fold changes of gene expression was obtained by $2^{-\Delta\Delta Ct}$ method with GAPDH as th internal reference gene. The primers used for RT-PCR were FGF10-F (CAGTGGAAATCGGAGTTGTT) and FGF10-R (CCTTCT TGTTCATGGCTAAGT), and GAPDH-F (AGGTCGGTGT GAACGGATTTG) and GAPDH-R (TGTAGACCATGTAGTT GAGGTCA).

Immunohistochemistry

Formalin-fixed/paraffin-embedded specimens were sectioned at 5-µm thickness and

mounted on positively charged slides. Sections were stained with hematoxylin and eosin (H&E) for histology analysis. Immunohistochemistry was performed using a standard protocol as previously described [28]. For detection of AR and Src expression, primary antibodies for AR (Santa Cruz Biotechnology, SC-816, 1:200) and Src (Cell Signaling, 2109, 1:250) were used and detected with the EnVision+ system (Dako). For immunofluorescent analysis, sections were incubated with primary antibodies against vimentin (Novus Biologicals, NB300-223, 1:250), E-cadherin (Cell Signaling, 3195, 1:250), CK5 (BioLegend, 905501, 1:500), or CK8 (BioLegend, 904801, 1:1000). Expression was detected by Alexa-594– or Alexa-488–conjugated secondary antibodies (Molec- ular Probes; 1:1000) and DAPI (Vector Laboratories) nucleus staining. The images were taken by a fluorescent microscopy with a CCD camera.

Western Blot

Cells were lysed in RIPA buffer [137 mM NaCl, 20 mM Tris-HCl (pH 7.4), 10% glycerol, 1% Triton X-100, 0.5% sodium deoxycholate, 0.1% SDS, 2 mM EDTA protease inhibitor cocktail (Millipore, 539137), phosphatase inhibitor cocktail (Sigma-Aldrich, P0044 and P5726)] for 20 minutes on ice. After short sonication, cell lysates were centrifuged, and the supernatants were collected. Proteins were resolved on 10% SDS-polyacrylamide gels and transferred onto nitrocellulose membranes (Bio-Rad). The membrane was blocked with 5% milk powder (Lab Scientific) in 1× TBS containing 1% Tween-20 (TBST) for 1 hour, washed with TBST, and incubated with the specific antibodies overnight. Antibodies to FGFR1 (Cat# 9740), FGFR2 (Cat# 11835), Src (Cat# 2108), p-Src (Y416) (Cat# 2101), FAK (Cat# 3285), p-FAK (Y925) (Cat# 3284), GAPDH (Cat# 5174), and Caveolin-1 (Cat# 3238) were from Cell Signaling Technology. The antibody to ERK2

(Cat# sc-154) was from Santa Cruz Biotechnology. The antibody to phosphotyrosine (pY) was form Millipore (clone 4G10, Cat#05-321), and the γ-tubulin antibody (Cat# T6557) was from Sigma-Aldrich.

Results

FGFR1 expression in primary prostate epithelial cells is not sufficient to induce prostate tumorigenesis but synergizes with paracrine FGF10 to induce EMT

To examine aberrant expression of FGFR1 in mediation of prostate tumorigenesis *in vivo*, primary prostate epithelia cells were transduced with control vector or FGFR1 by lentiviral infection. First expression levels of FGFR1, FGFR2 (IIIc isoform) (data not shown) and FGF10 (**Figure 7.1A**) were confirmed by western blot or real-time PCR. Urogenital mesenchymal stem cells (UGSM) cells were transduced with FGF10 by lentiviral infection. Prostate epithelia with expression of FGFR1 or control vector were combined with paracrine FGF10 or control vector transduced UGSM cells, and grafts were subjected to the prostate tissue regeneration assay *in vivo* [369](**Figure 7.1B**). As expected, paracrine FGF10 induced adenocarcinoma in the PrECs-Control + FGF10-UGSM group. The transformation was multifocal, likely due to the different amount of FGF10 expression locally [371, 379]. Paracrine FGF10-induced acini showed an expansion of $CK8^+$ luminal cells with no alteration of $CK5^+$ basal cells located at the basal compartment. Tumorigenic cells expressed androgen receptor and E-cadherin, but not vimentin, suggesting epithelial tumorigenic characteristics. However, overexpression of FGFR1 in epithelial cells showed normal regenerated prostate tubules. RFP in prostate tubules indicated successful transduction. Similar to those in the control group, the regenerated tubules were comprised of a single layer of $CK8^+$ luminal cells and $CK5^+$ basal cells. Epithelial cells in the regenerated tubules expressed E-cadherin (**Figure 7.1C**). These data suggested that unlike paracrine FGF10 expression, ectopic expression of the wild-type FGFR1 is not sufficient to induce prostate tumorigenesis. These data

suggested that unlike paracrine FGF10 expression, expression of the FGFR1 is not sufficient to induce prostate tumorigenesis. However, regenerated tissues derived from PrECs-FGFR1 + FGF10-UGSM (RFP^+) showed mild expression of CK8 but not CK5 staining. Some tumorigenic cells co-expressed E-cadherin+ and $vimentin^+$ (**Figure 7.1C**) suggesting that the cells with FGFR1 expression under the induction of FGF10-UGSM underwent EMT.

FGFR2 expression in primary prostate epithelial cells is not sufficient to induce prostate tumorigenesis but synergizes with paracrine FGF10 to induce EMT

The transformation potential of expression of FGFR2 (IIIc isoform) and the synergy with paracrine FGF10 were also examined using the prostate tissue regeneration assay. Normal primary prostate cells or FGFR2 transduced cells were combined with FGF10-UGSM cells in the prostate tissue regeneration assay (**Figure 7.1B**). As expected, while regenerated tissues derived from PrECs-control + GFP-UGSM contained normal tubules, PrECs-control + FGF10-UGSM tissues showed high-grade adenocarcinoma. The FGF10-induced tumors were comprised of disorganized ductal cells expressing CK8 in luminal cells and CK5 at the basal membrane. The normal or transformed epithelial cells were $E\text{-}cadherin^+$ and $vimentin^-$ (**Figure 7.2**)

Expression of FGFR2 Sensitizes Paracrine FGF10- Induced Prostate Tumors

Similar to FGFR1 transformed tubules or PrECs-control + GFP-UGSM, regenerated tissues derived from PrECs-FGFR2 + GFP-UGSM group were comprised of normal tubules including the expression of CK8 luminal marker, CK5 basal marker, and E-cadherin in epithelial cells (**Figure 7.2**) suggesting that ectopic expression of FGFR2 does not sufficiently induce transformation *in vivo*. In contrast, the regenerated tissues from PrECs-FGFR2 + FGF10-UGSM were comprised of sheets of tumorigenic cells (RFP^+). These cells did not express CK8 or CK5 but co-expressed E-cadherin and vimentin (**Figure 7.2**). The data indicate that the synergy of paracrine FGF10 with ectopic expression of FGFR2 in epithelia in the FGF/FGFR signaling axis leads to invasive tumors.

FGFR2 expression sensitizes paracrine FGF10- induced prostate tumors

Although overexpression of wild-type FGFRs alone was not sufficient to induce prostate tumorigenesis, we examined if overexpression of FGFR2 in epithelial cells sensitized the cells to a low dose of paracrine FGF10 to cause tumorigenesis. Primary prostate cells and UGSM cells were transduced with FGFR2 and FGF10 by lentiviral infection, respectively. The FGFR2 transduced cells were combined with 100% GFP-UGSM (control) or a mixture of 25% FGF10-UGSM cells and 75% normal UGSM cells (creating a low dosage of paracrine FGF10 from stromal cells) (Figure 3A). As expected, the regenerated prostate tissues derived from PrECs-control or FGFR2 with 100% GFP-UGSM were comprised of normal tubules with expression of a single layer of CK8+ luminal cells and CK5+ cells in the basal membrane (Figure 3B). While the regenerated tissues from PrECs-control + 25% FGF10-UGSM showed normal tubules with an

increase in branching, the tissues in PrECs-FGFR2 + 25% FGF10-UGSM exhibited low-grade prostatic intraepithelial neoplasia (Figure 3B). The transformed tubules contained stratified CK8+ luminal cells and retained the basal cell layer, and some small acini were visible. Additionally, epithelial cells in normal tubules or in the lesion expressed E-cadherin but not vimentin, indicating the epithelial feature. These results indicate that FGFR2-transduced cells become sensitized to the low dosage of paracrine FGF10 to induce prostate tumorigenesis.

Loss of Src Myristoylation Inhibits Paracrine FGF10-Induced Tumorigenesis In Vivo

Myristoylation is an important lipid modification for Src kinase activity [380-382]. We further examined the role of Src myristoylation in FGF10-induced tumorigenesis in vivo. Overexpression of wild-type Src or the myristoylation defective mutant Src (G2A) was confirmed (**Figure 4A**). Prostate epithelial cells transduced with Src (WT) or Src (G2A) were mixed with FGF10-UGSM or GFP-UGSM cells, and the cell mixtures were used in the prostate regeneration assay. While the weight of regenerated tissues derived from Src(WT) or Src(G2A) + GFP-UGSM had no significant single layer of $CK8^+$ luminal cells and $CK5^+$ basal cell layer [378, 382]. The epithelial cells were E-$cadherin^+$ and $vimentin^-$. Tissues derived from PrECs-Src (WT)+FGF10-UGSM group showed high-grade adenocarci- noma (**Figure 4D**). Transformed regenerated tissues from this group contained an expansion of $CK8^+$ luminal cells without substantial changes in $CK5^+$ basal cells. However, regenerated tissues derived from epithelia-Src (G2A)+FGF10-UGSM were comprised of normal tubules. The tubules contained a single layer of $CK8^+$ luminal cells with $CK5^+$ basal cells as in the PrECs + GFP-UGSM control group (**Figure 4D**).

The data indicate that loss of Src myristoylation inhibits FGF10-induced prostate tumorigenesis, suggesting a potential therapeutic approach of targeting myristoylationm of Src kinase to inhibit FGF/FGFRs-mediated tumorigenic potential.

Discussion

Our study has demonstrated that the FGF/FGFR/Src signaling axis is important in mediating tumor initiation and progression in prostate cancer. Previous prostate cancer models in the study of FGFRs focused on the simulation of activation of FGFRs. Although amplification of FGFR1 or FGFR2 has been well documented, mutations leading to the activation of FGFRs do not often occur in prostate cancer [364]. For example, the translocation of FGFR2 leading to gene fusion of SLC45A3-FGFR2 results in overexpression of FGFR2 [364]. However, our results indicate that ectopic expression of the wild-type FGFR1/2 is not sufficient to induce prostate tumorigenesis under the normal stromal microenvironment. The FGFR2 transformed epithelial cells become sensitized to the amount of paracrine FGF in the microenvironment, leading to transformation. The data emphasize that the dysregulation of the stromal microenvironment is a decisive factor to induce the FGF/FGFR-mediated prostate tumorigenesis. Dysregulated FGF expression plays an essential role in androgen receptor–independent prostate cancer [383]

The activation of FGFR1/2 is an important factor to regulate the EMT in cancer progression. We show that the synergy of paracrine FGF with epithelial wild-type FGFR1/2 in this signaling axis promotes tumor progression and induces EMT in vivo. This is in agreement with the induction of activated FGFR1 in another mouse prostate cancer model [361]. FGFR2-induced EMT occurs when tumorigenic cells undergo the isoform

switch from FGFR2b to FGFR2c during prostate cancer progression [384]. The isoform switch–induced EMT has also been reported in human dermal fibroblasts [385] and rat bladder carcinoma cells [386]. Mechanistically, FGFR2c-induced transformation inhibits the expression of E-cadherin but increases expression levels of vimentin [385]. FGFR2 expression is associated with twist1-induced cancer progression, invasion, and EMT in gastric adenocarcinoma [387]. FGFR2 also mediates N-cadherin–induced EMT to regulate expression levels of snail, twist1, and slug [388].

Paracrine FGF10 also synergizes with epithelial wild-type Src kinase in the FGF/FGFR/Src signaling axis. Ectopic expression of Src kinase in the epithelium synergizes with paracrine FGF10 and leads to high-grade adenocarcinoma. Src kinase is essential in paracrine FGF10-induced prostate tumorigenesis *in vivo* [379]. Pathologically, FGF10-Src (WT) synergy exhibits a much weaker phenotype than FGF10-FGFR2 (WT), suggesting that the participation of other pathways downstream of FGFR also plays important roles for the initiation of EMT. The FGF/FGFR/Src signaling axis is also consistent with numerous in vitro studies showing that Src kinase is associated with FGFRs [389]. However, most of the FGF/FGFR models emphasize FGF/FGFR/FRS2-induced MAPK and PI3K pathways [390]. While some models indicate that Src kinase is associated with PLC-gamma signaling [391], others suggest that Src directly interacts with FGFRs [392]. Further delineation of Src kinase in FGF/FGFR downstream signaling will be helpful for understanding FGF/FGFR signaling in cancer progression.

Our study has shown that expression of the mutant Src (G2A) abolishes FGF10-induced tumorigenesis *in vivo*. Myristoylation has been reported as an important modification for Src kinase to associate with the cytoplasmic membrane [381, 393]. Loss

of Src myristoylation inhibits its kinase activity and increases protein stability [381]. Our data show that loss of Src myristoylation has a significant inhibitory effect on FGF10-induced oncogenic signaling in comparison with the kinase dead mutant. Therefore, targeting N-myristoylation might represent an important chemotherapeutic approach for inhibiting FGF/FGFR/Src-mediated cancer progression [394]. N-myristoyltransferase catalyzes the myristoylation process [395]. Several compounds have been identified that inhibit the catalytic function of NMT including a myristoyl-CoA analog we have recently discovered [382]. Further study of these compounds might provide a therapeutic strategy for inhibiting Src kinase activity, thereby blocking FGF/FGFR/Src mediated cancer.

Conclusion

This study demonstrates that elevated expression of wild-type FGFR1 and FGFR2 was not sufficient to induce oncogenic transformation; however, it synergizes with paracrine FGF10 to initiate prostate tumors, promote prostate tumor progression, and induce EMT. This study also shows that paracrine FGF10 synergized with overexpressed epithelial Src kinase resulting in high-grade tumors but not EMT. The FGF10-Src synergy relied on the myristoylation of Src, suggesting that targeting myristoylation of Src kinase might provide a therapeutic approach for inhibiting paracrine FGF10-induced tumorigenesis.

References

1. Karantanos, T., P.G. Corn, and T.C. Thompson, *Prostate cancer progression after androgen deprivation therapy: mechanisms of castrate resistance and novel therapeutic approaches.* Oncogene, 2013. **32**(49): p. 5501-5511.

2. Jemal, A., et al., *Cancer statistics, 2008.* CA Cancer J Clin, 2008. **58**(2): p. 71-96.

3. Chambers, S.K., et al., *Defining young in the context of prostate cancer.* Am J Mens Health, 2015. **9**(2): p. 103-14.

4. Siegel, R.L., K.D. Miller, and A. Jemal, *Cancer statistics, 2019.* CA: A Cancer Journal for Clinicians, 2019. **69**(1): p. 7-34.

5. Fontenot, P.A., Jr., et al., *Metastatic prostate cancer in the modern era of PSA screening.* Int Braz J Urol, 2017. **43**(3): p. 416-421.

6. Roobol, M.J., *Screening for prostate cancer: are organized screening programs necessary?* Transl Androl Urol, 2018. **7**(1): p. 4-11.

7. Salinas, C.A., et al., *Prostate cancer in young men: an important clinical entity.* Nat Rev Urol, 2014. **11**(6): p. 317-23.

8. Hiraoka, Y. and M. Akimoto, *Anatomy of the prostate from fetus to adult--origin of benign prostatic hyperplasia.* Urol Res, 1987. **15**(3): p. 177-80.

9. Humphrey, P.A., *Histopathology of Prostate Cancer.* Cold Spring Harb Perspect Med, 2017. **7**(10).

10. Bhavsar, A. and S. Verma, *Anatomic imaging of the prostate.* Biomed Res Int, 2014. **2014**: p. 728539.

11. Garraway, L.A., et al., *Intermediate basal cells of the prostate: in vitro and in vivo characterization.* Prostate, 2003. **55**(3): p. 206-18.

12. van Leenders, G.J. and J.A. Schalken, *Epithelial cell differentiation in the human prostate epithelium: implications for the pathogenesis and therapy of prostate cancer.* Crit Rev Oncol Hematol, 2003. **46 Suppl**: p. S3-10.

13. Man, Y.-G., et al., *Tumor-infiltrating immune cells promoting tumor invasion and metastasis: existing theories.* Journal of Cancer, 2013. **4**(1): p. 84-95.

14. Tchetgen, M.B., et al., *Ejaculation increases the serum prostate-specific antigen concentration.* Urology, 1996. **47**(4): p. 511-6.

15. Liu, A.Y. and L.D. True, *Characterization of prostate cell types by CD cell surface molecules.* Am J Pathol, 2002. **160**(1): p. 37-43.

16. Cary, K.C. and M.R. Cooperberg, *Biomarkers in prostate cancer surveillance and screening: past, present, and future.* Therapeutic advances in urology, 2013. **5**(6): p. 318-329.

17. Petrylak, D.P., et al., *Docetaxel and estramustine compared with mitoxantrone and prednisone for advanced refractory prostate cancer.* New England Journal of Medicine, 2004. **351**(15): p. 1513-1520.

18. Tannock, I.F., et al., *Docetaxel plus prednisone or mitoxantrone plus prednisone for advanced prostate cancer.* New England Journal of Medicine, 2004. **351**(15): p. 1502-1512.

19. de Bono, J.S., et al., *Abiraterone and increased survival in metastatic prostate cancer.* N Engl J Med, 2011. **364**(21): p. 1995-2005.

20. Parker, C., et al., *Alpha emitter radium-223 and survival in metastatic prostate cancer.* New England Journal of Medicine, 2013. **369**(3): p. 213-223.

21. Desouki, M., et al., *hZip2 and hZip3 zinc transporters are down regulated in human prostate adenocarcinomatous glands.* Molecular Cancer, 2007. **6**: p. 37.

22. Logothetis, C., et al., *Current perspectives on bone metastases in castrate-resistant prostate cancer.* Cancer Metastasis Rev, 2018. **37**(1): p. 189-196.

23. Merseburger, A.S., A. Alcaraz, and C.A. von Klot, *Androgen deprivation therapy as backbone therapy in the management of prostate cancer.* Onco Targets Ther, 2016. **9**: p. 7263-7274.

24. Boccon-Gibod, L., E. van der Meulen, and B.-E. Persson, *An update on the use of gonadotropin-releasing hormone antagonists in prostate cancer.* Therapeutic advances in urology, 2011. **3**(3): p. 127-140.

25. Wadosky, K.M. and S. Koochekpour, *Molecular mechanisms underlying resistance to androgen deprivation therapy in prostate cancer.* Oncotarget, 2016. **7**(39): p. 64447-64470.

26. Gamat, M. and D.G. McNeel, *Androgen deprivation and immunotherapy for the treatment of prostate cancer.* Endocrine-related cancer, 2017. **24**(12): p. T297-T310.

27. Montgomery, R.B., et al., *Maintenance of intratumoral androgens in metastatic prostate cancer: a mechanism for castration-resistant tumor growth.* Cancer Res, 2008. **68**(11): p. 4447-54.

28. Heidenreich, A., et al., *[EAU guidelines on prostate cancer. Part I: screening, diagnosis, and treatment of clinically localised disease].* Actas Urol Esp, 2011. **35**(9): p. 501-14.

29. Li, Y., et al., *Androgen receptor splice variants mediate enzalutamide resistance in castration-resistant prostate cancer cell lines.* Cancer Res, 2013. **73**(2): p. 483-9.

30. Crona, D.J. and Y.E. Whang, *Androgen Receptor-Dependent and -Independent Mechanisms Involved in Prostate Cancer Therapy Resistance.* Cancers (Basel), 2017. **9**(6).

31. Thoma, C., *AR-Vs not predictive in mCRPC.* Nature Reviews Urology, 2018. **15**: p. 203.

32. Sharp, A., et al., *Androgen receptor splice variant-7 expression emerges with castration resistance in prostate cancer.* The Journal of Clinical Investigation, 2019. **129**(1): p. 192-208.

33. Chandrasekar, T., et al., *Mechanisms of resistance in castration-resistant prostate cancer (CRPC).* Transl Androl Urol, 2015. **4**(3): p. 365-80.

34. Tilki, D., E.M. Schaeffer, and C.P. Evans, *Understanding Mechanisms of Resistance in Metastatic Castration-resistant Prostate Cancer: The Role of the Androgen Receptor.* European Urology Focus, 2016. **2**(5): p. 499-505.

35. Huang, Y., et al., *Molecular and cellular mechanisms of castration resistant prostate cancer.* Oncol Lett, 2018. **15**(5): p. 6063-6076.

36. Kahn, B., J. Collazo, and N. Kyprianou, *Androgen receptor as a driver of therapeutic resistance in advanced prostate cancer.* Int J Biol Sci, 2014. **10**(6): p. 588-95.

37. Yuan, X. and S.P. Balk, *Mechanisms mediating androgen receptor reactivation after castration.* Urologic oncology, 2009. **27**(1): p. 36-41.

38. Sharifi, N., *Mechanisms of androgen receptor activation in castration-resistant prostate cancer.* Endocrinology, 2013. **154**(11): p. 4010-4017.

39. Tan, M.H.E., et al., *Androgen receptor: structure, role in prostate cancer and drug discovery.* Acta Pharmacologica Sinica, 2014. **36**: p. 3.

40. Prins, G.S. and O. Putz, *Molecular signaling pathways that regulate prostate gland development.* Differentiation; research in biological diversity, 2008. **76**(6): p. 641-659.

41. Di Lorenzo, G., et al., *Expression of Epidermal Growth Factor Receptor Correlates with Disease Relapse and Progression to Androgen-independence in Human Prostate Cancer.* Clinical Cancer Research, 2002. **8**(11): p. 3438-3444.

42. Cai, C., et al., *Intratumoral de novo steroid synthesis activates androgen receptor in castration-resistant prostate cancer and is upregulated by treatment with CYP17A1 inhibitors.* Cancer Res, 2011. **71**(20): p. 6503-13.

43. Kallio, H.M.L., et al., *Constitutively active androgen receptor splice variants AR-V3, AR-V7 and AR-V9 are co-expressed in castration-resistant prostate cancer metastases.* British Journal of Cancer, 2018. **119**(3): p. 347-356.

44. Heinlein, C.A. and C. Chang, *Androgen receptor (AR) coregulators: an overview.* Endocr Rev, 2002. **23**(2): p. 175-200.

45. van der Steen, T., D.J. Tindall, and H. Huang, *Posttranslational modification of the androgen receptor in prostate cancer.* International journal of molecular sciences, 2013. **14**(7): p. 14833-14859.

46. Stein, M.N., et al., *Androgen synthesis inhibitors in the treatment of castration-resistant prostate cancer.* Asian journal of andrology, 2014. **16**(3): p. 387-400.

47. Beer, T.M., et al., *Enzalutamide in metastatic prostate cancer before chemotherapy.* N Engl J Med, 2014. **371**(5): p. 424-33.

48. James, N.D., et al., *Abiraterone for Prostate Cancer Not Previously Treated with Hormone Therapy.* N Engl J Med, 2017. **377**(4): p. 338-351.

49. Armstrong, C.M. and A.C. Gao, *Drug resistance in castration resistant prostate cancer: resistance mechanisms and emerging treatment strategies.* American journal of clinical and experimental urology, 2015. **3**(2): p. 64-76.

50. Schalken, J. and J.M. Fitzpatrick, *Enzalutamide: targeting the androgen signalling pathway in metastatic castration-resistant prostate cancer.* BJU international, 2016. **117**(2): p. 215-225.

51. Rodriguez-Vida, A., et al., *Enzalutamide for the treatment of metastatic castration-resistant prostate cancer.* Drug design, development and therapy, 2015. **9**: p. 3325-3339.

52. Petrylak, D.P., et al., *Docetaxel and estramustine compared with mitoxantrone and prednisone for advanced refractory prostate cancer.* N Engl J Med, 2004. **351**(15): p. 1513-20.

53. Fang, M., et al., *Efficacy of Abiraterone and Enzalutamide in Pre- and Postdocetaxel Castration-Resistant Prostate Cancer: A Trial-Level Meta-Analysis.* Prostate cancer, 2017. **2017**: p. 8560827-8560827.

54. Antonarakis, E.S., *Current understanding of resistance to abiraterone and enzalutamide in advanced prostate cancer.* Clin Adv Hematol Oncol, 2016. **14**(5): p. 316-9.

55. Antonarakis, E.S., et al., *AR-V7 and Resistance to Enzalutamide and Abiraterone in Prostate Cancer.* New England Journal of Medicine, 2014. **371**(11): p. 1028-1038.

56. Hotte, S.J. and F. Saad, *Current management of castrate-resistant prostate cancer.* Current oncology (Toronto, Ont.), 2010. **17 Suppl 2**(Suppl 2): p. S72-S79.

57. Mendiratta, P., A.J. Armstrong, and D.J. George, *Current standard and investigational approaches to the management of hormone-refractory prostate cancer.* Reviews in urology, 2007. **9 Suppl 1**(Suppl 1): p. S9-S19.

58. Berthold, D.R., et al., *Docetaxel plus prednisone or mitoxantrone plus prednisone for advanced prostate cancer: updated survival in the TAX 327 study.* J Clin Oncol, 2008. **26**(2): p. 242-5.

59. Lohiya, V., J.B. Aragon-Ching, and G. Sonpavde, *Role of Chemotherapy and Mechanisms of Resistance to Chemotherapy in Metastatic Castration-Resistant Prostate Cancer.* Clinical Medicine Insights. Oncology, 2016. **10**(Suppl 1): p. 57-66.

60. Dagher, R., et al., *Approval summary: Docetaxel in combination with prednisone for the treatment of androgen-independent hormone-refractory prostate cancer.* Clin Cancer Res, 2004. **10**(24): p. 8147-51.

61. Zhu, M.-L., et al., *Tubulin-targeting chemotherapy impairs androgen receptor activity in prostate cancer.* Cancer research, 2010. **70**(20): p. 7992-8002.

62. Fitzpatrick, J.M. and R. de Wit, *Taxane mechanisms of action: potential implications for treatment sequencing in metastatic castration-resistant prostate cancer.* Eur Urol, 2014. **65**(6): p. 1198-204.

63. Terry, S., et al., *Increased expression of class III β-tubulin in castration-resistant human prostate cancer.* British journal of cancer, 2009. **101**(6): p. 951.

64. Ranganathan, S., et al., *Modulation of endogenous β-tubulin isotype expression as a result of human β III cDNA transfection into prostate carcinoma cells.* British journal of cancer, 2001. **85**(5): p. 735.

65. Oudard, S., *TROPIC: Phase III trial of cabazitaxel for the treatment of metastatic castration-resistant prostate cancer.* Future Oncol, 2011. **7**(4): p. 497-506.

66. Kartner, N., J.R. Riordan, and V. Ling, *Cell surface P-glycoprotein associated with multidrug resistance in mammalian cell lines.* Science, 1983. **221**(4617): p. 1285-8.

67. Assaraf, Y.G., *The role of multidrug resistance efflux transporters in antifolate resistance and folate homeostasis.* Drug Resist Updat, 2006. **9**(4-5): p. 227-46.

68. Wyatt, A.W., et al., *The diverse heterogeneity of molecular alterations in prostate cancer identified through next-generation sequencing.* Asian journal of andrology, 2013. **15**(3): p. 301-308.

69. Hoey, T., *Drug resistance, epigenetics, and tumor cell heterogeneity.* Sci Transl Med, 2010. **2**(28): p. 28ps19.

70. Coyle, K.M., J.E. Boudreau, and P. Marcato, *Genetic Mutations and Epigenetic Modifications: Driving Cancer and Informing Precision Medicine.* BioMed research international, 2017. **2017**: p. 9620870-9620870.

71. Fernandez, E., et al., *Factors and Mechanisms for Pharmacokinetic Differences between Pediatric Population and Adults.* Pharmaceutics, 2011. **3**(1): p. 53-72.

72. Li, M., et al., *Clinical targeting recombinant immunotoxins for cancer therapy.* OncoTargets and therapy, 2017. **10**: p. 3645-3665.

73. Thurber, G.M., M.M. Schmidt, and K.D. Wittrup, *Antibody tumor penetration: transport opposed by systemic and antigen-mediated clearance.* Advanced drug delivery reviews, 2008. **60**(12): p. 1421-1434.

74. Corn, P.G., *The tumor microenvironment in prostate cancer: elucidating molecular pathways for therapy development.* Cancer management and research, 2012. **4**: p. 183-193.

75. Pedraza-Fariña, L.G., *Mechanisms of oncogenic cooperation in cancer initiation and metastasis.* The Yale journal of biology and medicine, 2006. **79**(3-4): p. 95-103.

76. Liu, Y.Y., et al., *Ceramide glycosylation potentiates cellular multidrug resistance.* Faseb j, 2001. **15**(3): p. 719-30.

77. Nguyen, K.T., et al., *Transactivation of the human multidrug resistance (MDR1) gene promoter by p53 mutants.* Oncol Res, 1994. **6**(2): p. 71-7.

78. Smets, L.A., *Programmed cell death (apoptosis) and response to anti-cancer drugs.* Anticancer Drugs, 1994. **5**(1): p. 3-9.

79. Xue, X., et al., *Nanoscale drug delivery platforms overcome platinum-based resistance in cancer cells due to abnormal membrane protein trafficking.* ACS nano, 2013. **7**(12): p. 10452-10464.

80. Glavinas, H., et al., *The role of ABC transporters in drug resistance, metabolism and toxicity.* Curr Drug Deliv, 2004. **1**(1): p. 27-42.

81. Kis, O., et al., *The complexities of antiretroviral drug-drug interactions: role of ABC and SLC transporters.* Trends Pharmacol Sci, 2010. **31**(1): p. 22-35.

82. Goldstein, L.J., et al., *Expression of a multidrug resistance gene in human cancers.* J Natl Cancer Inst, 1989. **81**(2): p. 116-24.

83. Wilkens, S., *Structure and mechanism of ABC transporters.* F1000prime reports, 2015. **7**: p. 14-14.

84. Cunha, G.R., A.A. Donjacour, and Y. Sugimura, *Stromal-epithelial interactions and heterogeneity of proliferative activity within the prostate.* Biochem Cell Biol, 1986. **64**(6): p. 608-14.

85. Filella, X., et al., *Emerging biomarkers in the diagnosis of prostate cancer.* Pharmacogenomics and personalized medicine, 2018. **11**: p. 83-94.

86. Velonas, V.M., et al., *Current status of biomarkers for prostate cancer.* International journal of molecular sciences, 2013. **14**(6): p. 11034-11060.

87. Ross, R.K., et al., *Androgen metabolism and prostate cancer: establishing a model of genetic susceptibility.* Cancer Res, 1998. **58**(20): p. 4497-504.

88. Costello, L.C., R.B. Franklin, and P. Feng, *Mitochondrial function, zinc, and intermediary metabolism relationships in normal prostate and prostate cancer.* Mitochondrion, 2005. **5**(3): p. 143-53.

89. Eidelman, E., et al., *The Metabolic Phenotype of Prostate Cancer.* Frontiers in oncology, 2017. **7**: p. 131-131.

90. Carracedo, A., et al., *Cancer metabolism: fatty acid oxidation in the limelight.* Nature Reviews Cancer, 2013. **13**: p. 227-232.

91. Puchades-Carrasco, L. and A. Pineda-Lucena, *Metabolomics Applications in Precision Medicine: An Oncological Perspective.* Current topics in medicinal chemistry, 2017. **17**(24): p. 2740-2751.

92. Gowda, G.A.N., et al., *Metabolomics-based methods for early disease diagnostics.* Expert review of molecular diagnostics, 2008. **8**(5): p. 617-633.

93. Kelly, R.S., et al., *The role of tumor metabolism as a driver of prostate cancer progression and lethal disease: results from a nested case-control study.* Cancer & metabolism, 2016. **4**: p. 22-22.

94. Mann, T., *The biochemistry of semen and of the male reproductive tract.* The biochemistry of semen and of the male reproductive tract., 1964.

95. De Kretser, D., P. Temple-Smith, and J. Kerr, *Anatomical and functional aspects of the male reproductive organs*, in *Disturbances in Male Fertility*. 1982, Springer. p. 1-131.

96. Everaerts, W. and A.J. Costello, *Applied Anatomy of the Male Pelvis*, in *Prostate Ultrasound: Current Practice and Future Directions*, C.R. Porter and E.M. Wolff, Editors. 2015, Springer New York: New York, NY. p. 11-30.

97. Fine, S.W. and R. Mehra, *Anatomy of the Prostate Revisited: Implications for Prostate Biopsy and Zonal Origins of Prostate Cancer*, in *Genitourinary Pathology: Practical Advances*, C. Magi-Galluzzi and C.G. Przybycin, Editors. 2015, Springer New York: New York, NY. p. 3-12.

98. Rybak, A., R. Bristow, and A. Kapoor, *Prostate cancer stem cells: Deciphering the origins and pathways involved in prostate tumorigenesis and aggression.* Oncotarget, 2014. **6**.

99. Barron, D.A. and D.R. Rowley, *The reactive stroma microenvironment and prostate cancer progression.* 2012. **19**(6): p. R187.

100. Toivanen, R. and M.M. Shen, *Prostate organogenesis: tissue induction, hormonal regulation and cell type specification.* Development, 2017. **144**(8): p. 1382-1398.

101. Obinata, D., et al., *Review of novel therapeutic medicines targeting androgen signaling in castration-resistant prostate cancer.* World Journal of Clinical Urology, 2014. **3**(3): p. 264-271.

102. Turner, B. and L. Drudge-Coates, *New pharmacological treatments for prostate cancer.* Nurse Prescribing, 2012. **10**: p. 498-502.

103. Wenk, M.R., *The emerging field of lipidomics.* Nature Reviews Drug Discovery, 2005. **4**: p. 594.

104. van Meer, G., D.R. Voelker, and G.W. Feigenson, *Membrane lipids: where they are and how they behave.* Nat Rev Mol Cell Biol, 2008. **9**(2): p. 112-24.

105. Gurr, M. and A. James, *Lipid biochemistry: an introduction.(eds.) Chapman & Hall, London.* 1971.

106. Fahy, E., et al., *Update of the LIPID MAPS comprehensive classification system for lipids.* J Lipid Res, 2009. **50 Suppl**: p. S9-14.

107. Kennedy, E.P., *Biosynthesis of complex lipids.* Fed Proc, 1961. **20**: p. 934-40.

108. Rysman, E., et al., *De novo lipogenesis protects cancer cells from free radicals and chemotherapeutics by promoting membrane lipid saturation.* Cancer Research, 2010. **70**: p. 8117-8126.

109. Kent, C., *Regulatory enzymes of phosphatidylcholine biosynthesis: a personal perspective.* Biochim Biophys Acta, 2005. **1733**(1): p. 53-66.

110. Kennedy, E.P. and S.B. Weiss, *The function of cytidine coenzymes in the biosynthesis of phospholipides.* J Biol Chem, 1956. **222**(1): p. 193-214.

111. Lands, W.E., *Metabolism of glycerolipides; a comparison of lecithin and triglyceride synthesis.* J Biol Chem, 1958. **231**(2): p. 883-8.

112. Shimizu, T., T. Ohto, and Y. Kita, *Cytosolic phospholipase A2: biochemical properties and physiological roles.* IUBMB Life, 2006. **58**(5-6): p. 328-33.

113. Schlame, M., D. Rua, and M.L. Greenberg, *The biosynthesis and functional role of cardiolipin.* Prog Lipid Res, 2000. **39**(3): p. 257-88.

114. Lands, W.E., *Stories about acyl chains.* Biochim Biophys Acta, 2000. **1483**(1): p. 1-14.

115. Sergeant, S., et al., *Phosphatidic acid regulates tyrosine phosphorylating activity in human neutrophils enhancement of Fgr activity.* Journal of Biological Chemistry, 2001. **276**(7): p. 4737-4746.

116. Rizzo, M.A., et al., *Phospholipase D and its product, phosphatidic acid, mediate agonist-dependent raf-1 translocation to the plasma membrane and the activation of the mitogen-activated protein kinase pathway.* J Biol Chem, 1999. **274**(2): p. 1131-9.

117. Olivera, A., J. Rosenthal, and S. Spiegel, *Effect of acidic phospholipids on sphingosine kinase.* Journal of cellular biochemistry, 1996. **60**(4): p. 529-537.

118. Lim, H.-K., et al., *Phosphatidic acid regulates systemic inflammatory responses by modulating the Akt-mammalian target of rapamycin-p70 S6 kinase 1 pathway.* Journal of Biological Chemistry, 2003. **278**(46): p. 45117-45127.

119. Daaka, Y., *Mitogenic action of LPA in prostate.* Biochim Biophys Acta, 2002. **1582**(1-3): p. 265-9.

120. Kulkarni, P. and R.H. Getzenberg, *High-fat diet, obesity and prostate disease: the ATX-LPA axis?* Nat Clin Pract Urol, 2009. **6**(3): p. 128-31.

121. Terada, N., et al., *Cyr61 is regulated by cAMP-dependent protein kinase with serum levels correlating with prostate cancer aggressiveness.* Prostate, 2012. **72**(9): p. 966-76.

122. Yui, K., et al., *Eicosanoids Derived From Arachidonic Acid and Their Family Prostaglandins and Cyclooxygenase in Psychiatric Disorders.* Current neuropharmacology, 2015. **13**(6): p. 776-785.

123. MacDonald, J.I. and H. Sprecher, *Phospholipid fatty acid remodeling in mammalian cells.* Biochimica et Biophysica Acta (BBA)-Lipids and Lipid Metabolism, 1991. **1084**(2): p. 105-121.

124. Patel, D. and S.N. Witt, *Ethanolamine and Phosphatidylethanolamine: Partners in Health and Disease.* Oxidative medicine and cellular longevity, 2017. **2017**: p. 4829180-4829180.

125. Chu, Z., et al., *Targeting and cytotoxicity of SapC-DOPS nanovesicles in pancreatic cancer.* PloS one, 2013. **8**(10): p. e75507.

126. Wojton, J., et al., *Systemic delivery of SapC-DOPS has antiangiogenic and antitumor effects against glioblastoma.* Molecular Therapy, 2013. **21**(8): p. 1517-1525.

127. Zhao, S., et al., *SapC–DOPS nanovesicles as targeted therapy for lung cancer.* Molecular cancer therapeutics, 2015. **14**(2): p. 491-498.

128. Murray, N.R. and A.P. Fields, *Phosphatidylglycerol is a physiologic activator of nuclear protein kinase C.* Journal of Biological Chemistry, 1998. **273**(19): p. 11514-11520.

129. Murray, N., L. Thompson, and A. Fields, *Protein Kinase C Molecular Biology Intelligence Unit*. 1997, The role of protein kinase C in cellular proliferation and cell cycle ….

130. Reis, A., *Oxidative Phospholipidomics in health and disease: Achievements, challenges and hopes.* Free Radical Biology and Medicine, 2017. **111**: p. 25-37.

131. Fu, P. and K.G. Birukov, *Oxidized phospholipids in control of inflammation and endothelial barrier.* Translational Research, 2009. **153**(4): p. 166-176.

132. Ashraf, M.Z., N.S. Kar, and E.A. Podrez, *Oxidized phospholipids: Biomarker for cardiovascular diseases.* The International Journal of Biochemistry & Cell Biology, 2009. **41**(6): p. 1241-1244.

133. Maskrey, B.H., et al., *Mechanisms of Resolution of Inflammation.* Arteriosclerosis, Thrombosis, and Vascular Biology, 2011. **31**(5): p. 1001-1006.

134. Salomon, R.G. and A. Bhatnagar, *Structural Identification and Cardiovascular Activities of Oxidized Phospholipids.* Circulation Research, 2012. **111**(7): p. 930-946.

135. Miyazawa, T., et al., *Age-related change of phosphatidylcholine hydroperoxide and phosphatidylethanolamine hydroperoxide levels in normal human red blood cells.* Mechanisms of Ageing and Development, 1996. **86**(3): p. 145-150.

136. Adachi, J., et al., *Plasma phosphatidylcholine hydroperoxide as a new marker of oxidative stress in alcoholic patients.* Journal of Lipid Research, 2004. **45**(5): p. 967-971.

137. Hui, S.-P., et al., *An improved HPLC assay for phosphatidylcholine hydroperoxides (PCOOH) in human plasma with synthetic PCOOH as internal standard.* Journal of Chromatography B, 2007. **857**(1): p. 158-163.

138. Jónasdóttir, H.S., et al., *Detection and Structural Elucidation of Esterified Oxylipids in Human Synovial Fluid by Electrospray Ionization-Fourier Transform Ion-Cyclotron Mass Spectrometry and Liquid Chromatography-Ion Trap-MS3: Detection of Esterified Hydroxylated Docosapentaenoic Acid Containing Phospholipids.* Analytical Chemistry, 2013. **85**(12): p. 6003-6010.

139. Gruber, F., et al., *Photooxidation generates biologically active phospholipids that induce heme oxygenase-1 in skin cells.* Journal of Biological Chemistry, 2007. **282**(23): p. 16934-16941.

140. Birukova, A.A., et al., *Signaling pathways involved in OxPAPC-induced pulmonary endothelial barrier protection.* Microvascular research, 2007. **73**(3): p. 173-181.

141. Stemmer, U., et al., *Toxicity of oxidized phospholipids in cultured macrophages.* Lipids in health and disease, 2012. **11**(1): p. 110.

142. Thimmulappa, R.K., et al., *Oxidized phospholipids impair pulmonary antibacterial defenses: evidence in mice exposed to cigarette smoke.* Biochemical and biophysical research communications, 2012. **426**(2): p. 253-259.

143. Halasiddappa, L.M., et al., *Oxidized phospholipids induce ceramide accumulation in RAW 264.7 macrophages: role of ceramide synthases.* PLoS One, 2013. **8**(7): p. e70002.

144. Koller, D., et al., *Effects of oxidized phospholipids on gene expression in RAW 264.7 macrophages: a microarray study.* PloS one, 2014. **9**(10): p. e110486.

145. Hoff, H.F., et al., *Phospholipid hydroxyalkenals: biological and chemical properties of specific oxidized lipids present in atherosclerotic lesions.* Arteriosclerosis, thrombosis, and vascular biology, 2003. **23**(2): p. 275-282.

146. Kamido, H., et al., *Core aldehydes of alkyl glycerophosphocholines in atheroma induce platelet aggregation and inhibit endothelium-dependent arterial relaxation.* Journal of lipid research, 2002. **43**(1): p. 158-166.

147. Ravandi, A., et al., *Phospholipids and oxophospholipids in atherosclerotic plaques at different stages of plaque development.* Lipids, 2004. **39**(2): p. 97-109.

148. Hammad, L.A., et al., *Elevated levels of hydroxylated phosphocholine lipids in the blood serum of breast cancer patients.* Rapid Communications in Mass

Spectrometry: An International Journal Devoted to the Rapid Dissemination of Up‐to‐the‐Minute Research in Mass Spectrometry, 2009. **23**(6): p. 863-876.

149. Kinoshita, M., et al., *Age-related increases in plasma phosphatidylcholine hydroperoxide concentrations in control subjects and patients with hyperlipidemia.* Clinical chemistry, 2000. **46**(6): p. 822-828.

150. Akasaka, K., et al., *Automatic determination of hydroperoxides of phosphatidylcholine and phosphatidylethanolamine in human plasma.* Journal of Chromatography B: Biomedical Sciences and Applications, 1995. **665**(1): p. 37-43.

151. Rolla, R., et al., *Antibodies against oxidized phospholipids in laboratory tests exploring lupus anti‐coagulant activity.* Clinical & Experimental Immunology, 2007. **149**(1): p. 63-69.

152. Matt, U., et al., *Accumulating evidence for a role of oxidized phospholipids in infectious diseases.* Cellular and molecular life sciences, 2015. **72**(6): p. 1059-1071.

153. Cruz, D., et al., *Host-derived oxidized phospholipids and HDL regulate innate immunity in human leprosy.* The Journal of clinical investigation, 2008. **118**(8): p. 2917-2928.

154. O'Donnell, V.B. and R.C. Murphy, *New families of bioactive oxidized phospholipids generated by immune cells: identification and signaling actions.* Blood, 2012. **120**(10): p. 1985-1992.

155. Stübiger, G., et al., *Targeted profiling of atherogenic phospholipids in human plasma and lipoproteins of hyperlipidemic patients using MALDI-QIT-TOF-MS/MS.* Atherosclerosis, 2012. **224**(1): p. 177-186.

156. Frey, B., et al., *Increase in fragmented phosphatidylcholine in blood plasma by oxidative stress.* Journal of lipid research, 2000. **41**(7): p. 1145-1153.

157. Podrez, E.A., et al., *Platelet CD36 links hyperlipidemia, oxidant stress and a prothrombotic phenotype.* Nature medicine, 2007. **13**(9): p. 1086.

158. Korotaeva, A.A., et al., *Oxidized phosphatidylcholine stimulates activity of secretory phospholipase A2 group IIA and abolishes sphingomyelin-induced inhibition of the enzyme.* Prostaglandins & other lipid mediators, 2010. **91**(1-2): p. 38-41.

159. Ramprecht, C., et al., *Toxicity of oxidized phosphatidylcholines in cultured human melanoma cells.* Chemistry and physics of lipids, 2015. **189**: p. 39-47.

160. Bochkov, V., et al., *Oxidized Phospholipids Stimulate Angiogenesis Via Autocrine Mechanisms, Implicating a Novel Role for Lipid Oxidation in the Evolution of Atherosclerotic Lesions*. Vol. 99. 2006. 900-8.

161. T Reddy, S., et al., *Identification of genes induced by oxidized phospholipids in human aortic endothelial cells*. Vol. 38. 2002. 211-8.

162. Oskolkova, O.V., et al., *ATF4-dependent transcription is a key mechanism in VEGF up-regulation by oxidized phospholipids: critical role of oxidized sn-2 residues in activation of unfolded protein response.* Blood, 2008. **112**(2): p. 330-339.

163. Blüml, S., et al., *The Oxidation State of Phospholipids Controls the Oxidative Burst in Neutrophil Granulocytes.* The Journal of Immunology, 2008. **181**(6): p. 4347-4353.

164. Gao, D., et al., *Structural Basis for the Recognition of Oxidized Phospholipids in Oxidized Low Density Lipoproteins by Class B Scavenger Receptors CD36 and SR-BI.* Journal of Biological Chemistry, 2010. **285**(7): p. 4447-4454.

165. Boullier, A., et al., *The Binding of Oxidized Low Density Lipoprotein to Mouse CD36 Is Mediated in Part by Oxidized Phospholipids That Are Associated with Both the Lipid and Protein Moieties of the Lipoprotein.* Journal of Biological Chemistry, 2000. **275**(13): p. 9163-9169.

166. Karupaiah, T. and K. Sundram, *Effects of stereospecific positioning of fatty acids in triacylglycerol structures in native and randomized fats: a review of their nutritional implications.* Nutrition & metabolism, 2007. **4**(1): p. 16.

167. Dircks, L. and H.S. Sul, *Acyltransferases of de novo glycerophospholipid biosynthesis.* Prog Lipid Res, 1999. **38**(5-6): p. 461-79.

168. Weiss, S.B., E.P. Kennedy, and J.Y. Kiyasu, *The enzymatic synthesis of triglycerides.* Journal of Biological Chemistry, 1960. **235**(1): p. 40-44.

169. Coleman, R.A. and D.P. Lee, *Enzymes of triacylglycerol synthesis and their regulation.* Progress in lipid research, 2004. **43**(2): p. 134-176.

170. Wei, L., et al., *A case-control study on the association between serum lipid level and the risk of breast cancer.* Zhonghua yu fang yi xue za zhi [Chinese journal of preventive medicine], 2016. **50**(12): p. 1091-1095.

171. Ogretmen, B. and Y.A. Hannun, *Biologically active sphingolipids in cancer pathogenesis and treatment.* Nature Reviews Cancer, 2004. **4**(8): p. 604.

172. Ogretmen, B., *Sphingolipids in cancer: regulation of pathogenesis and therapy.* FEBS letters, 2006. **580**(23): p. 5467-5476.

173. Ryland, L.K., et al., *Dysregulation of sphingolipid metabolism in cancer.* Cancer biology & therapy, 2011. **11**(2): p. 138-149.

174. Fyrst, H. and J.D. Saba, *An update on sphingosine-1-phosphate and other sphingolipid mediators.* Nat Chem Biol, 2010. **6**(7): p. 489-97.

175. Maula, T., et al., *Importance of the sphingoid base length for the membrane properties of ceramides.* Biophysical journal, 2012. **103**(9): p. 1870-1879.

176. Saddoughi, S.A., P. Song, and B. Ogretmen, *Roles of bioactive sphingolipids in cancer biology and therapeutics.* Sub-cellular biochemistry, 2008. **49**: p. 413-440.

177. Ponnusamy, S., et al., *Sphingolipids and cancer: ceramide and sphingosine-1-phosphate in the regulation of cell death and drug resistance.* Future oncology (London, England), 2010. **6**(10): p. 1603-1624.

178. Taha, T.A., T.D. Mullen, and L.M. Obeid, *A house divided: ceramide, sphingosine, and sphingosine-1-phosphate in programmed cell death.* Biochim Biophys Acta, 2006. **1758**(12): p. 2027-36.

179. Ogretmen, B. and Y.A. Hannun, *Biologically active sphingolipids in cancer pathogenesis and treatment.* Nat Rev Cancer, 2004. **4**(8): p. 604-16.

180. Wang, X.-Z., et al., *Aberrant Sphingolipid Signaling Is Involved in the Resistance of Prostate Cancer Cell Lines to Chemotherapy.* Cancer Research, 1999. **59**(22): p. 5842-5848.

181. García-Barros, M., et al., *Sphingolipids in colon cancer.* Biochimica et biophysica acta, 2014. **1841**(5): p. 773-782.

182. Karahatay, S., et al., *Clinical relevance of ceramide metabolism in the pathogenesis of human head and neck squamous cell carcinoma (HNSCC): attenuation of C(18)-ceramide in HNSCC tumors correlates with lymphovascular invasion and nodal metastasis.* Cancer Lett, 2007. **256**(1): p. 101-11.

183. Schiffmann, S., et al., *Ceramide synthases and ceramide levels are increased in breast cancer tissue.* Carcinogenesis, 2009. **30**(5): p. 745-52.

184. Pralhada Rao, R., et al., *Sphingolipid metabolic pathway: an overview of major roles played in human diseases.* Journal of lipids, 2013. **2013**: p. 178910-178910.

185. Modrak, D.E., D.V. Gold, and D.M. Goldenberg, *Sphingolipid targets in cancer therapy.* Molecular Cancer Therapeutics, 2006. **5**(2): p. 200-208.

186. Lemonnier, L.A., et al., *Sphingomyelin in the suppression of colon tumors: prevention versus intervention.* Arch Biochem Biophys, 2003. **419**(2): p. 129-38.

187. Al Sazzad, M.A., et al., *The Long-Chain Sphingoid Base of Ceramides Determines Their Propensity for Lateral Segregation.* Biophysical journal, 2017. **112**(5): p. 976-983.

188. Dillehay, D.L., et al., *Dietary sphingomyelin inhibits 1,2-dimethylhydrazine-induced colon cancer in CF1 mice.* J Nutr, 1994. **124**(5): p. 615-20.

189. Mehta, S., et al., *Combined cytotoxic action of paclitaxel and ceramide against the human Tu138 head and neck squamous carcinoma cell line.* Cancer Chemother Pharmacol, 2000. **46**(2): p. 85-92.

190. Schmelz, E.M., et al., *Colonic cell proliferation and aberrant crypt foci formation are inhibited by dairy glycosphingolipids in 1, 2-dimethylhydrazine-treated CF1 mice.* J Nutr, 2000. **130**(3): p. 522-7.

191. Onodera, T., et al., *Phosphatidylethanolamine plasmalogen enhances the inhibiting effect of phosphatidylethanolamine on γ-secretase activity.* The Journal of Biochemistry, 2014. **157**(5): p. 301-309.

192. Braverman, N.E. and A.B. Moser, *Functions of plasmalogen lipids in health and disease.* Biochim Biophys Acta, 2012. **1822**(9): p. 1442-52.

193. Hu, C., M. Wang, and X. Han, *Shotgun lipidomics in substantiating lipid peroxidation in redox biology: Methods and applications.* Redox Biol, 2017. **12**: p. 946-955.

194. Wallner, S. and G. Schmitz, *Plasmalogens the neglected regulatory and scavenging lipid species.* Chem Phys Lipids, 2011. **164**(6): p. 573-89.

195. Fuchs, B., *Analytical methods for (oxidized) plasmalogens: Methodological aspects and applications.* Free Radic Res, 2015. **49**(5): p. 599-617.

196. Maeba, R., et al., *Chapter Two - Plasma/Serum Plasmalogens: Methods of Analysis and Clinical Significance*, in *Advances in Clinical Chemistry*, G.S. Makowski, Editor. 2015, Elsevier. p. 31-94.

197. Maeba, R., et al., *Plasma/Serum Plasmalogens: Methods of Analysis and Clinical Significance.* Adv Clin Chem, 2015. **70**: p. 31-94.

198. Han, X., *Lipidomics for studying metabolism.* Nat Rev Endocrinol, 2016. **12**(11): p. 668-679.

199. Mankidy, R., et al., *Membrane plasmalogen composition and cellular cholesterol regulation: a structure activity study.* Lipids Health Dis, 2010. **9**: p. 62.

200. Brites, P., H.R. Waterham, and R.J. Wanders, *Functions and biosynthesis of plasmalogens in health and disease.* Biochim Biophys Acta, 2004. **1636**(2-3): p. 219-31.

201. Fhaner, C.J., et al., *Functional group selective derivatization and gas-phase fragmentation reactions of plasmalogen glycerophospholipids.* Mass Spectrometry, 2013. **2**(Special_Issue): p. S0015-S0015.

202. Gerbig, S., et al., *Analysis of colorectal adenocarcinoma tissue by desorption electrospray ionization mass spectrometric imaging.* Analytical and bioanalytical chemistry, 2012. **403**(8): p. 2315-2325.

203. Lv, J., et al., *Plasma Content Variation and Correlation of Plasmalogen and GIS, TC, and TPL in Gastric Carcinoma Patients: A Comparative Study.* Medical science monitor basic research, 2015. **21**: p. 157-160.

204. Kunkel, G.T., et al., *Targeting the sphingosine-1-phosphate axis in cancer, inflammation and beyond.* Nature reviews. Drug discovery, 2013. **12**(9): p. 688-702.

205. Wang, D. and R.N. Dubois, *Eicosanoids and cancer.* Nature reviews. Cancer, 2010. **10**(3): p. 181-193.

206. Nakanishi, M. and D.W. Rosenberg. *Multifaceted roles of PGE 2 in inflammation and cancer*. in *Seminars in immunopathology*. 2013. Springer.

207. Asgari, Y., et al., *Alterations in cancer cell metabolism: the Warburg effect and metabolic adaptation.* Genomics, 2015. **105**(5-6): p. 275-81.

208. Santos, C., et al., *Lipid metabolism in cancer.* FEBS Journal, 2012. **279**: p. 2610-2623.

209. Dueregger, A., et al., *Differential Utilization of Dietary Fatty Acids in Benign and Malignant Cells of the Prostate.* PLoS One, 2015. **10**(8): p. e0135704.

210. Twum-Ampofo, J., et al., *Metabolic targets for potential prostate cancer therapeutics.* Curr Opin Oncol, 2016. **28**(3): p. 241-7.

211. Ngo, D.C., et al., *Introduction to the molecular basis of cancer metabolism and the Warburg effect.* Mol Biol Rep, 2015. **42**(4): p. 819-23.

212. Medes, G., A. Thomas, and S. Weinhouse, *Metabolism of neoplastic tissue. IV. A study of lipid synthesis in neoplastic tissue slices in vitro.* Cancer Res, 1953. **13**(1): p. 27-9.

213. Ookhtens, M., et al., *Liver and adipose tissue contributions to newly formed fatty acids in an ascites tumor.* Am J Physiol, 1984. **247**(1 Pt 2): p. R146-53.

214. Srihari, S., et al., *Metabolic deregulation in prostate cancer.* Mol Omics, 2018. **14**(5): p. 320-329.

215. Perona, J.S., *Membrane lipid alterations in the metabolic syndrome and the role of dietary oils*. 2017, Elsevier.

216. Hidalgo, A., A. Cruz, and J. Pérez-Gil, *Pulmonary surfactant and nanocarriers: toxicity versus combined nanomedical applications.* Biochimica et Biophysica Acta (BBA)-Biomembranes, 2017. **1859**(9): p. 1740-1748.

217. Echaide, M., et al., *Restoring pulmonary surfactant membranes and films at the respiratory surface.* Biochimica et Biophysica Acta (BBA)-Biomembranes, 2017. **1859**(9): p. 1725-1739.

218. Dumas, F. and E. Haanappel, *Lipids in infectious diseases–the case of AIDS and tuberculosis.* Biochimica et Biophysica Acta (BBA)-Biomembranes, 2017. **1859**(9): p. 1636-1647.

219. Fuentes, N.R., et al., *Emerging role of chemoprotective agents in the dynamic shaping of plasma membrane organization.* Biochimica et Biophysica Acta (BBA)-Biomembranes, 2017. **1859**(9): p. 1668-1678.

220. Ríos-Marco, P., et al., *Alkylphospholipids: An update on molecular mechanisms and clinical relevance*. 2017, Elsevier.

221. Baker, M.J., et al., *FTIR-based spectroscopic analysis in the identification of clinically aggressive prostate cancer.* Br J Cancer, 2008. **99**(11): p. 1859-66.

222. Zhou, X., et al., *Identification of plasma lipid biomarkers for prostate cancer by lipidomics and bioinformatics.* PLoS One, 2012. **7**(11): p. e48889.

223. Sorvina, A., et al., *Lipid profiles of prostate cancer cells.* Oncotarget, 2018. **9**(85): p. 35541-35552.

224. Hultsch, S., et al., *Association of tamoxifen resistance and lipid reprogramming in breast cancer.* BMC Cancer, 2018. **18**(1): p. 850.

225. Lin, H.-M., et al., *A distinct plasma lipid signature associated with poor prognosis in castration-resistant prostate cancer.* International Journal of Cancer, 2017. **141**(10): p. 2112-2120.

226. Horvath, L., et al., *The plasma lipidome in castration-resistant prostate cancer.* Journal of Clinical Oncology, 2017. **35**(15_suppl): p. 5055-5055.

227. Bligh, E.G. and W.J. Dyer, *A rapid method of total lipid extraction and purification.* Canadian journal of biochemistry and physiology, 1959. **37**(8): p. 911-917.

228. Bartlett, G.R., *Phosphorus assay in column chromatography.* J biol chem, 1959. **234**(3): p. 466-468.

229. Kinsey, G.R., et al., *Decreased iPLA2γ expression induces lipid peroxidation and cell death and sensitizes cells to oxidant-induced apoptosis.* Journal of lipid research, 2008. **49**(7): p. 1477-1487.

230. Zhang, L., B.L. Peterson, and B.S. Cummings, *The effect of inhibition of Ca2+-independent phospholipase A2 on chemotherapeutic-induced death and phospholipid profiles in renal cells.* Biochemical pharmacology, 2005. **70**(11): p. 1697-1706.

231. Peterson, B., et al., *Alterations in phospholipid and fatty acid lipid profiles in primary neocortical cells during oxidant-induced cell injury.* Chem Biol Interact, 2008. **174**(3): p. 163-76.

232. Maes, E., et al., *Determination of Variation Parameters as a Crucial Step in Designing TMT-Based Clinical Proteomics Experiments.* PLOS ONE, 2015. **10**(3): p. e0120115.

233. Schaaf, M.J. and J.A. Cidlowski, *Molecular mechanisms of glucocorticoid action and resistance.* J Steroid Biochem Mol Biol, 2002. **83**(1-5): p. 37-48.

234. Kalli, A., et al., *Evaluation and optimization of mass spectrometric settings during data-dependent acquisition mode: focus on LTQ-Orbitrap mass analyzers.* Journal of proteome research, 2013. **12**(7): p. 3071-3086.

235. Pluskal, T., et al., *MZmine 2: modular framework for processing, visualizing, and analyzing mass spectrometry-based molecular profile data.* BMC Bioinformatics, 2010. **11**: p. 395.

236. Tautenhahn, R., et al., *XCMS Online: a web-based platform to process untargeted metabolomic data.* Anal Chem, 2012. **84**(11): p. 5035-9.

237. Koelmel, J.P., et al., *LipidMatch: an automated workflow for rule-based lipid identification using untargeted high-resolution tandem mass spectrometry data.* BMC Bioinformatics, 2017. **18**(1): p. 331.

238. Kinsey, G.R., et al., *Decreased iPLA2gamma expression induces lipid peroxidation and cell death and sensitizes cells to oxidant-induced apoptosis.* J Lipid Res, 2008. **49**(7): p. 1477-87.

239. Trygg, J. and S. Wold, *Orthogonal Projections to Latent Structures (O-PLS).* Journal of Chemometrics, 2002. **16**: p. 119-128.

240. Trygg, J., E. Holmes, and T. Lundstedt, *Chemometrics in Metabonomics.* Journal of proteome research, 2007. **6**: p. 469-79.

241. Worley, B. and R. Powers, *Multivariate Analysis in Metabolomics.* Current Metabolomics, 2013. **1**(1): p. 92-107.

242. Richman, E.L., et al., *Choline intake and risk of lethal prostate cancer: incidence and survival.* The American journal of clinical nutrition, 2012. **96**(4): p. 855-863.

243. Zhou, Y., E.C. Bolton, and J.O. Jones, *Androgens and androgen receptor signaling in prostate tumorigenesis.* 2015. **54**(1): p. R15.

244. Cheng, J.C., et al., *Radiation-induced acid ceramidase confers prostate cancer resistance and tumor relapse.* The Journal of Clinical Investigation, 2013. **123**(10): p. 4344-4358.

245. Merchant, T.E., et al., *Phospholipid profiles of human colon cancer using 31P magnetic resonance spectroscopy.* Int J Colorectal Dis, 1991. **6**(2): p. 121-6.

246. Griner, E.M. and M.G. Kazanietz, *Protein kinase C and other diacylglycerol effectors in cancer.* Nat Rev Cancer, 2007. **7**(4): p. 281-94.

247. Perry, D.K. and Y.A. Hannun, *The role of ceramide in cell signaling.* Biochim Biophys Acta, 1998. **1436**(1-2): p. 233-43.

248. Schneider, G., et al., *Bioactive lipids, LPC and LPA, are novel prometastatic factors and their tissue levels increase in response to radio/chemotherapy.* Molecular cancer research : MCR, 2014. **12**(11): p. 1560-1573.

249. Okita, M., et al., *Elevated levels and altered fatty acid composition of plasma lysophosphatidlycholine (lysoPC) in ovarian cancer patients.* International journal of cancer, 1997. **71**(1): p. 31-34.

250. Phuyal, S., et al., *The ether lipid precursor hexadecylglycerol stimulates the release and changes the composition of exosomes derived from PC-3 cells.* J Biol Chem, 2015. **290**(7): p. 4225-37.

251. Devalapally, H., et al., *Modulation of drug resistance in ovarian adenocarcinoma by enhancing intracellular ceramide using tamoxifen-loaded biodegradable polymeric nanoparticles.* Clin Cancer Res, 2008. **14**(10): p. 3193-203.

252. Park, M.H., et al., *Overexpression of phospholipase D enhances matrix metalloproteinase-2 expression and glioma cell invasion via protein kinase C and protein kinase A/NF-kappaB/Sp1-mediated signaling pathways.* Carcinogenesis, 2009. **30**(2): p. 356-65.

253. Yang, J.S., et al., *Size Dependent Lipidomic Analysis of Urinary Exosomes from Patients with Prostate Cancer by Flow Field-Flow Fractionation and Nanoflow Liquid Chromatography-Tandem Mass Spectrometry.* Analytical Chemistry, 2017. **89**(4): p. 2488-2496.

254. Perry, R.H., et al., *Characterization of MYC-induced tumorigenesis by in situ lipid profiling.* Analytical chemistry, 2013. **85**(9): p. 4259-4262.

255. Shroff, E.H., et al., *MYC oncogene overexpression drives renal cell carcinoma in a mouse model through glutamine metabolism.* Proceedings of the National Academy of Sciences, 2015. **112**(21): p. 6539-6544.

256. Lisec, J., et al., *Cancer cell lipid class homeostasis is altered under nutrient-deprivation but stable under hypoxia.* BMC Cancer, 2019. **19**(1): p. 501.

257. Burch, T.C., et al., *Comparative metabolomic and lipidomic analysis of phenotype stratified prostate cells.* PLoS One, 2015. **10**(8): p. e0134206.

258. Jung, J.H., et al., *Phospholipids of tumor extracellular vesicles stratify gefitinib-resistant nonsmall cell lung cancer cells from gefitinib-sensitive cells.* Proteomics, 2015. **15**(4): p. 824-835.

259. Bevers, E.M., P. Comfurius, and R.F. Zwaal, *Regulatory mechanisms in maintenance and modulation of transmembrane lipid asymmetry: pathophysiological implications.* Lupus, 1996. **5**(5): p. 480-7.

260. Escriba, P.V., et al., *Membranes: a meeting point for lipids, proteins and therapies.* J Cell Mol Med, 2008. **12**(3): p. 829-75.

261. Escriba, P.V., *Membrane-lipid therapy: a new approach in molecular medicine.* Trends Mol Med, 2006. **12**(1): p. 34-43.

262. Thadani-Mulero, M., et al., *Androgen receptor splice variants determine taxane sensitivity in prostate cancer.* Cancer research, 2014. **74**(8): p. 2270-2282.

263. Ploussard, G., et al., *Class III β-tubulin expression predicts prostate tumor aggressiveness and patient response to docetaxel-based chemotherapy.* Cancer research, 2010. **70**(22): p. 9253-9264.

264. Zhu, Y., et al., *Inhibition of ABCB1 expression overcomes acquired docetaxel resistance in prostate cancer.* Molecular cancer therapeutics, 2013. **12**(9): p. 1829-1836.

265. Chen, H., H. Li, and Q. Chen, *INPP4B reverses docetaxel resistance and epithelial-to-mesenchymal transition via the PI3K/Akt signaling pathway in prostate cancer.* Biochemical and biophysical research communications, 2016. **477**(3): p. 467-472.

266. de Bessa Garcia, S.A., et al., *Prostate apoptosis response 4 (PAR4) expression modulates WNT signaling pathways in MCF7 breast cancer cells: A possible mechanism underlying PAR4-mediated docetaxel chemosensitivity.* International journal of molecular medicine, 2017. **39**(4): p. 809-818.

267. Codony‐Servat, J., et al., *Nuclear factor‐kappa B and interleukin‐6 related docetaxel resistance in castration‐resistant prostate cancer.* The Prostate, 2013. **73**(5): p. 512-521.

268. Marín-Aguilera, M., et al., *Epithelial-to-mesenchymal transition mediates docetaxel resistance and high risk of relapse in prostate cancer.* Molecular cancer therapeutics, 2014. **13**(5): p. 1270-1284.

269. Baenke, F., et al., *Hooked on fat: the role of lipid synthesis in cancer metabolism and tumour development.* Disease models & mechanisms, 2013. **6**(6): p. 1353-1363.

270. Ackerman, D. and M.C. Simon, *Hypoxia, lipids, and cancer: surviving the harsh tumor microenvironment.* Trends in cell biology, 2014. **24**(8): p. 472-478.

271. Cruz, P.M., et al., *The role of cholesterol metabolism and cholesterol transport in carcinogenesis: a review of scientific findings, relevant to future cancer therapeutics.* Frontiers in pharmacology, 2013. **4**: p. 119.

272. Cheng, C., et al., *Glucose-mediated N-glycosylation of SCAP is essential for SREBP-1 activation and tumor growth.* Cancer cell, 2015. **28**(5): p. 569-581.

273. Guo, D., et al., *EGFR signaling through an Akt-SREBP-1–dependent, rapamycin-resistant pathway sensitizes glioblastomas to antilipogenic therapy.* Sci. Signal., 2009. **2**(101): p. ra82-ra82.

274. Guo, D., et al., *An LXR agonist promotes glioblastoma cell death through inhibition of an EGFR/AKT/SREBP-1/LDLR–dependent pathway.* Cancer discovery, 2011. **1**(5): p. 442-456.

275. Acevedo, A., et al., *LIPEA: Lipid Pathway Enrichment Analysis.* bioRxiv, 2018: p. 274969.

276. Li, S., et al., *Predicting network activity from high throughput metabolomics.* PLoS computational biology, 2013. **9**(7): p. e1003123.

277. Chong, J., et al., *MetaboAnalyst 4.0: towards more transparent and integrative metabolomics analysis.* Nucleic Acids Res, 2018. **46**(W1): p. W486-w494.

278. Dolce, V., et al., *Glycerophospholipid synthesis as a novel drug target against cancer.* Curr Mol Pharmacol, 2011. **4**(3): p. 167-75.

279. Tappia, P.S. and T. Singal, *Phospholipid-mediated signaling and heart disease.* Subcell Biochem, 2008. **49**: p. 299-324.

280. Oude Weernink, P.A., et al., *Dynamic phospholipid signaling by G protein-coupled receptors.* Biochim Biophys Acta, 2007. **1768**(4): p. 888-900.

281. Fernandis, A.Z. and M.R. Wenk, *Membrane lipids as signaling molecules.* Curr Opin Lipidol, 2007. **18**(2): p. 121-8.

282. Brzozowski, J.S., et al., *Lipidomic profiling of extracellular vesicles derived from prostate and prostate cancer cell lines.* Lipids Health Dis, 2018. **17**(1): p. 211.

283. Dixon, S.J., et al., *Ferroptosis: an iron-dependent form of nonapoptotic cell death.* Cell, 2012. **149**(5): p. 1060-1072.

284. Latunde-Dada, G.O., *Ferroptosis: Role of lipid peroxidation, iron and ferritinophagy.* Biochim Biophys Acta Gen Subj, 2017. **1861**(8): p. 1893-1900.

285. Agmon, E., et al., *Modeling the effects of lipid peroxidation during ferroptosis on membrane properties.* Sci Rep, 2018. **8**(1): p. 5155.

286. Agmon, E. and B.R. Stockwell, *Lipid homeostasis and regulated cell death.* Curr Opin Chem Biol, 2017. **39**: p. 83-89.

287. Stockwell, B.R., et al., *Ferroptosis: a regulated cell death nexus linking metabolism, redox biology, and disease.* Cell, 2017. **171**(2): p. 273-285.

288. Beloribi-Djefaflia, S., S. Vasseur, and F. Guillaumond, *Lipid metabolic reprogramming in cancer cells.* Oncogenesis, 2016. **5**(1): p. e189.

289. DeBerardinis, R.J. and N.S. Chandel, *Fundamentals of cancer metabolism.* Sci Adv, 2016. **2**(5): p. e1600200.

290. DeBerardinis, R.J., et al., *The Biology of Cancer: Metabolic Reprogramming Fuels Cell Growth and Proliferation.* Cell Metabolism, 2008. **7**(1): p. 11-20.

291. Pietilainen, K.H., et al., *Acquired obesity is associated with changes in the serum lipidomic profile independent of genetic effects--a monozygotic twin study.* PLoS One, 2007. **2**(2): p. e218.

292. Ekroos, K., et al., *Lipidomics: a tool for studies of atherosclerosis.* Curr Atheroscler Rep, 2010. **12**(4): p. 273-81.

293. Lankinen, M., et al., *Fatty fish intake decreases lipids related to inflammation and insulin signaling--a lipidomics approach.* PLoS One, 2009. **4**(4): p. e5258.

294. de Mello, V.D., et al., *Link between plasma ceramides, inflammation and insulin resistance: association with serum IL-6 concentration in patients with coronary heart disease.* Diabetologia, 2009. **52**(12): p. 2612-5.

295. Graessler, J., et al., *Top-down lipidomics reveals ether lipid deficiency in blood plasma of hypertensive patients.* PLoS One, 2009. **4**(7): p. e6261.

296. Han, X., et al., *Alterations in myocardial cardiolipin content and composition occur at the very earliest stages of diabetes: a shotgun lipidomics study.* Biochemistry, 2007. **46**(21): p. 6417-28.

297. Ollero, M., et al., *Plasma lipidomics reveals potential prognostic signatures within a cohort of cystic fibrosis patients.* J Lipid Res, 2011. **52**(5): p. 1011-22.

298. Gorke, R., et al., *Determining and interpreting correlations in lipidomic networks found in glioblastoma cells.* BMC Syst Biol, 2010. **4**: p. 126.

299. Balogh, G., et al., *Lipidomics reveals membrane lipid remodelling and release of potential lipid mediators during early stress responses in a murine melanoma cell line.* Biochim Biophys Acta, 2010. **1801**(9): p. 1036-47.

300. Kolak, M., et al., *Adipose tissue inflammation and increased ceramide content characterize subjects with high liver fat content independent of obesity.* Diabetes, 2007. **56**(8): p. 1960-8.

301. Zhao, Y.Y., X.L. Cheng, and R.C. Lin, *Lipidomics applications for discovering biomarkers of diseases in clinical chemistry.* Int Rev Cell Mol Biol, 2014. **313**: p. 1-26.

302. Lydic, T.A. and Y.-H. Goo, *Lipidomics unveils the complexity of the lipidome in metabolic diseases.* Clinical and translational medicine, 2018. **7**(1): p. 4-4.

303. Wu, Q., et al., *Cancer-associated adipocytes: key players in breast cancer progression.* Journal of hematology & oncology, 2019. **12**(1): p. 95-95.

304. Balaban, S., et al., *Obesity and cancer progression: is there a role of fatty acid metabolism?* BioMed research international, 2015. **2015**: p. 274585-274585.

305. Zhou, J. and P. Giannakakou, *Targeting microtubules for cancer chemotherapy.* Curr Med Chem Anticancer Agents, 2005. **5**(1): p. 65-71.

306. Luo, X., et al., *The implications of signaling lipids in cancer metastasis.* Experimental & molecular medicine, 2018. **50**(9): p. 127-127.

307. Zhang, T.Y., et al., *Management of castrate resistant prostate cancer-recent advances and optimal sequence of treatments.* Curr Urol Rep, 2013. **14**(3): p. 174-83.

308. Pascual, F. and G.M. Carman, *Phosphatidate phosphatase, a key regulator of lipid homeostasis.* Biochimica et biophysica acta, 2013. **1831**(3): p. 514-522.

309. Brohée, L., et al., *Lipin-1 regulates cancer cell phenotype and is a potential target to potentiate rapamycin treatment.* Oncotarget, 2015. **6**(13): p. 11264-11280.

310. Montoya, A., et al., *The beta adrenergic receptor antagonist propranolol alters mitogenic and apoptotic signaling in late stage breast cancer.* Biomedical Journal, 2019. **42**(3): p. 155-165.

311. Wang, F., et al., *Propranolol suppresses the proliferation and induces the apoptosis of liver cancer cells.* Molecular medicine reports, 2018. **17**(4): p. 5213-5221.

312. Pantziarka, P., et al., *Repurposing Drugs in Oncology (ReDO)-Propranolol as an anti-cancer agent.* Ecancermedicalscience, 2016. **10**: p. 680-680.

313. Hessvik, N.P. and A. Llorente, *Current knowledge on exosome biogenesis and release.* Cellular and molecular life sciences : CMLS, 2018. **75**(2): p. 193-208.

314. Co-operation, O.f.E. and Development, *Toward a New Comprehensive Global Database of Per-and Polyfluoroalkyl Substances (PFASs): Summary Report on Updating the OECD 2007 List of per-and Polyfluoroalkyl Substances (PFASs).* 2018.

315. Banks, R.E., B.E. Smart, and J. Tatlow, *Organofluorine chemistry: principles and commercial applications*. 2013: Springer Science & Business Media.

316. Buck, R.C., *Toxicology data for alternative "short-chain" fluorinated substances*, in *Toxicological Effects of Perfluoroalkyl and Polyfluoroalkyl Substances*. 2015, Springer. p. 451-477.

317. Domingo, J.L., *Health risks of dietary exposure to perfluorinated compounds.* Environment international, 2012. **40**: p. 187-195.

318. Suja, F., B.K. Pramanik, and S.M. Zain, *Contamination, bioaccumulation and toxic effects of perfluorinated chemicals (PFCs) in the water environment: a review paper.* Water Science and Technology, 2009. **60**(6): p. 1533-1544.

319. Sunderland, E.M., et al., *A review of the pathways of human exposure to poly- and perfluoroalkyl substances (PFASs) and present understanding of health effects.* J Expo Sci Environ Epidemiol, 2019. **29**(2): p. 131-147.

320. Winkens, K., et al., *Early life exposure to per- and polyfluoroalkyl substances (PFASs): A critical review.* Emerging Contaminants, 2017. **3**(2): p. 55-68.

321. D'Hollander, W., et al., *Perfluorinated substances in human food and other sources of human exposure.* Rev Environ Contam Toxicol, 2010. **208**: p. 179-215.

322. Post, G.B., et al., *Occurrence and potential significance of perfluorooctanoic acid (PFOA) detected in New Jersey public drinking water systems.* Environmental science & technology, 2009. **43**(12): p. 4547-4554.

323. Barbarossa, A., et al., *Assessment of Perfluorooctane Sulfonate and Perfluorooctanoic Acid Exposure Through Fish Consumption in Italy.* Italian journal of food safety, 2016. **5**(4): p. 6055-6055.

324. Shi, Y., et al., *Tissue distribution of perfluorinated compounds in farmed freshwater fish and human exposure by consumption.* Environ Toxicol Chem, 2012. **31**(4): p. 717-23.

325. Eriksson, U., et al., *Perfluoroalkyl substances (PFASs) in food and water from Faroe Islands.* Environ Sci Pollut Res Int, 2013. **20**(11): p. 7940-8.

326. Hlouskova, V., et al., *Occurrence of brominated flame retardants and perfluoroalkyl substances in fish from the Czech aquatic ecosystem.* Sci Total Environ, 2013. **461-462**: p. 88-98.

327. Chain, E.Panel o.C.i.t.F., et al., *Risk to human health related to the presence of perfluorooctane sulfonic acid and perfluorooctanoic acid in food.* EFSA Journal, 2018. **16**(12): p. e05194.

328. Lewis, R.C., L.E. Johns, and J.D. Meeker, *Serum Biomarkers of Exposure to Perfluoroalkyl Substances in Relation to Serum Testosterone and Measures of Thyroid Function among Adults and Adolescents from NHANES 2011-2012.* Int J Environ Res Public Health, 2015. **12**(6): p. 6098-114.

329. Crinnion, W.J., *The CDC fourth national report on human exposure to environmental chemicals: what it tells us about our toxic burden and how it assists environmental medicine physicians.* Alternative medicine review, 2010. **15**(2): p. 101-109.

330. Calafat, A.M., et al., *Polyfluoroalkyl chemicals in the US population: data from the National Health and Nutrition Examination Survey (NHANES) 2003–2004 and comparisons with NHANES 1999–2000.* Environmental health perspectives, 2007. **115**(11): p. 1596-1602.

331. Graber, J.M., et al., *Per and polyfluoroalkyl substances (PFAS) blood levels after contamination of a community water supply and comparison with 2013-2014 NHANES.* Journal of exposure science & environmental epidemiology, 2019. **29**(2): p. 172-182.

332. Borg, D., et al., *Cumulative health risk assessment of 17 perfluoroalkylated and polyfluoroalkylated substances (PFASs) in the Swedish population.* Environment International, 2013. **59**: p. 112-123.

333. Lieder, P.H., et al., *A two-generation oral gavage reproduction study with potassium perfluorobutanesulfonate (K+ PFBS) in Sprague Dawley rats.* Toxicology, 2009. **259**(1-2): p. 33-45.

334. Lieder, P.H., et al., *Toxicological evaluation of potassium perfluorobutanesulfonate in a 90-day oral gavage study with Sprague–Dawley rats.* Toxicology, 2009. **255**(1-2): p. 45-52.

335. Domingo, J.L. and M. Nadal, *Per- and Polyfluoroalkyl Substances (PFASs) in Food and Human Dietary Intake: A Review of the Recent Scientific Literature.* Journal of Agricultural and Food Chemistry, 2017. **65**(3): p. 533-543.

336. Gorrochategui, E., et al., *Perfluoroalkylated Substance Effects in Xenopus laevis A6 Kidney Epithelial Cells Determined by ATR-FTIR Spectroscopy and Chemometric Analysis.* Chemical research in toxicology, 2016. **29**(5): p. 924-932.

337. Gorrochategui, E., et al., *Chemometric strategy for untargeted lipidomics: biomarker detection and identification in stressed human placental cells.* Analytica chimica acta, 2015. **854**: p. 20-33.

338. Lin, P.-I.D., et al., *Per- and polyfluoroalkyl substances and blood lipid levels in pre-diabetic adults—longitudinal analysis of the diabetes prevention program outcomes study.* Environment International, 2019. **129**: p. 343-353.

339. Liu, J., et al., *[Development and evaluation of a high-fat/high-fructose diet-induced nonalcoholic steatohepatitis mouse model].* Zhonghua Gan Zang Bing Za Zhi, 2014. **22**(6): p. 445-50.

340. EPA, U., *Drinking Water Health Advisory for Perfluorooctanoic Acid (PFOA).* EPA Document Number: 822-R-16-005, 2016.

341. PFOS, P.S., *ENVIRONMENTAL CRITERIA PERFLUORINATED ALKYL COMPOUNDS.*

342. Tiwari-Heckler, S., et al., *Circulating Phospholipid Patterns in NAFLD Patients Associated with a Combination of Metabolic Risk Factors.* Nutrients, 2018. **10**(5): p. 649.

343. Ipsen, D.H., J. Lykkesfeldt, and P. Tveden-Nyborg, *Molecular mechanisms of hepatic lipid accumulation in non-alcoholic fatty liver disease.* Cellular and molecular life sciences : CMLS, 2018. **75**(18): p. 3313-3327.

344. Gorden, D.L., et al., *Increased diacylglycerols characterize hepatic lipid changes in progression of human nonalcoholic fatty liver disease; comparison to a murine model.* PloS one, 2011. **6**(8): p. e22775-e22775.

345. Barr, J., et al., *Obesity-dependent metabolic signatures associated with nonalcoholic fatty liver disease progression.* Journal of proteome research, 2012. **11**(4): p. 2521-2532.

346. Vance, J.E., *Lipoproteins secreted by cultured rat hepatocytes contain the antioxidant 1-alk-1-enyl-2-acylglycerophosphoethanolamine.* Biochimica et Biophysica Acta (BBA)-Lipids and Lipid Metabolism, 1990. **1045**(2): p. 128-134.

347. Puri, P., et al., *The plasma lipidomic signature of nonalcoholic steatohepatitis.* Hepatology, 2009. **50**(6): p. 1827-1838.

348. Nelson, J.W., E.E. Hatch, and T.F. Webster, *Exposure to polyfluoroalkyl chemicals and cholesterol, body weight, and insulin resistance in the general US population.* Environmental health perspectives, 2009. **118**(2): p. 197-202.

349. Gorden, D.L., et al., *Biomarkers of NAFLD progression: a lipidomics approach to an epidemic.* Journal of lipid research, 2015. **56**(3): p. 722-736.

350. Fu, Y., et al., *Associations between serum concentrations of perfluoroalkyl acids and serum lipid levels in a Chinese population.* Ecotoxicology and environmental safety, 2014. **106**: p. 246-252.

351. Starling, A.P., et al., *Perfluoroalkyl substances and lipid concentrations in plasma during pregnancy among women in the Norwegian Mother and Child Cohort Study.* Environment international, 2014. **62**: p. 104-112.

352. Liew, Z., H. Goudarzi, and Y. Oulhote, *Developmental Exposures to Perfluoroalkyl Substances (PFASs): An Update of Associated Health Outcomes.* Current environmental health reports, 2018. **5**(1): p. 1-19.

353. Huang, M.C., et al., *Toxicokinetics of perfluorobutane sulfonate (PFBS), perfluorohexane-1-sulphonic acid (PFHxS), and perfluorooctane sulfonic acid (PFOS) in male and female Hsd:Sprague Dawley SD rats after intravenous and gavage administration.* Toxicology reports, 2019. **6**: p. 645-655.

354. Li, Q., et al., *Paracrine Fibroblast Growth Factor Initiates Oncogenic Synergy with Epithelial FGFR/Src Transformation in Prostate Tumor Progression.* Neoplasia, 2018. **20**(3): p. 233-243.

355. Hayward, S.W., et al., *Malignant transformation in a nontumorigenic human prostatic epithelial cell line.* Cancer research, 2001. **61**(22): p. 8135-8142.

356. Katoh, M. and H. Nakagama, *FGF receptors: cancer biology and therapeutics.* Medicinal research reviews, 2014. **34**(2): p. 280-300.

357. Feng, S., et al., *FGF23 promotes prostate cancer progression.* Oncotarget, 2015. **6**(19): p. 17291.

358. Corn, P.G., et al., *Targeting fibroblast growth factor pathways in prostate cancer.* Clinical cancer research, 2013. **19**(21): p. 5856-5866.

359. Nagamatsu, H., et al., *FGF19 promotes progression of prostate cancer.* The Prostate, 2015. **75**(10): p. 1092-1101.

360. Dieci, M.V., et al., *Fibroblast growth factor receptor inhibitors as a cancer treatment: from a biologic rationale to medical perspectives.* Cancer discovery, 2013. **3**(3): p. 264-279.

361. Acevedo, V.D., et al., *Inducible FGFR-1 activation leads to irreversible prostate adenocarcinoma and an epithelial-to-mesenchymal transition.* Cancer cell, 2007. **12**(6): p. 559-571.

362. Wan, X., et al., *Prostate cancer cell-stromal cell crosstalk via FGFR1 mediates antitumor activity of dovitinib in bone metastases.* Sci Transl Med, 2014. **6**(252): p. 252ra122.

363. Guo, Z., et al., *Regulation of androgen receptor activity by tyrosine phosphorylation.* Cancer cell, 2006. **10**(4): p. 309-319.

364. Wu, Y.-M., et al., *Identification of targetable FGFR gene fusions in diverse cancers.* Cancer discovery, 2013. **3**(6): p. 636-647.

365. Kwabi-Addo, B., M. Ozen, and M. Ittmann, *The role of fibroblast growth factors and their receptors in prostate cancer.* Endocrine-related cancer, 2004. **11**(4): p. 709-724.

366. Bova, G.S., et al., *Integrated clinical, whole-genome, and transcriptome analysis of multisampled lethal metastatic prostate cancer.* Molecular Case Studies, 2016. **2**(3): p. a000752.

367. Mehta, P., et al., *Fibroblast growth factor receptor‐2 mutation analysis in human prostate cancer.* BJU international, 2000. **86**(6): p. 681-685.

368. Freeman, K.W., et al., *Inducible prostate intraepithelial neoplasia with reversible hyperplasia in conditional FGFR1-expressing mice.* Cancer research, 2003. **63**(23): p. 8256-8263.

369. Xin, L., et al., *In vivo regeneration of murine prostate from dissociated cell populations of postnatal epithelia and urogenital sinus mesenchyme.* Proceedings of the National Academy of Sciences, 2003. **100**(suppl 1): p. 11896-11903.

370. Memarzadeh, S., et al., *Enhanced paracrine FGF10 expression promotes formation of multifocal prostate adenocarcinoma and an increase in epithelial androgen receptor.* Cancer cell, 2007. **12**(6): p. 572-585.

371. Memarzadeh, S., et al., *Role of autonomous androgen receptor signaling in prostate cancer initiation is dichotomous and depends on the oncogenic signal.* Proceedings of the National Academy of Sciences, 2011. **108**(19): p. 7962-7967.

372. Tomlins, S.A., et al., *Role of the TMPRSS2-ERG gene fusion in prostate cancer.* Neoplasia (New York, NY), 2008. **10**(2): p. 177.

373. Sadar, M.D., *Small molecule inhibitors targeting the "achilles' heel" of androgen receptor activity.* Cancer research, 2011. **71**(4): p. 1208-1213.

374. Taylor, B.S., et al., *Integrative genomic profiling of human prostate cancer.* Cancer cell, 2010. **18**(1): p. 11-22.

375. Xin, L., et al., *Progression of prostate cancer by synergy of AKT with genotropic and nongenotropic actions of the androgen receptor.* Proceedings of the National Academy of Sciences, 2006. **103**(20): p. 7789-7794.

376. Zong, Y., et al., *ETS family transcription factors collaborate with alternative signaling pathways to induce carcinoma from adult murine prostate cells.* Proc Natl Acad Sci U S A, 2009. **106**(30): p. 12465-70.

377. Cai, H., et al., *Collaboration of Kras and androgen receptor signaling stimulates EZH2 expression and tumor-propagating cells in prostate cancer.* Cancer Res, 2012. **72**(18): p. 4672-81.

378. Cai, H., et al., *Invasive prostate carcinoma driven by c-Src and androgen receptor synergy.* Cancer research, 2011. **71**(3): p. 862-872.

379. Cai, H., et al., *Differential transformation capacity of Src family kinases during the initiation of prostate cancer.* Proceedings of the National Academy of Sciences, 2011. **108**(16): p. 6579-6584.

380. Lacal, P., C. Pennington, and J. Lacal, *Transforming activity of ras proteins translocated to the plasma membrane by a myristoylation sequence from the src gene product.* Oncogene, 1988. **2**(6): p. 533-537.

381. Patwardhan, P. and M.D. Resh, *Myristoylation and membrane binding regulate c-Src stability and kinase activity.* Molecular and cellular biology, 2010. **30**(17): p. 4094-4107.

382. Kim, S., et al., *Blocking myristoylation of Src inhibits its kinase activity and suppresses prostate cancer progression.* Cancer research, 2017. **77**(24): p. 6950-6962.

383. Bluemn, E.G., et al., *Androgen receptor pathway-independent prostate cancer is sustained through FGF signaling.* Cancer cell, 2017. **32**(4): p. 474-489. e6.

384. Katoh, Y. and M. Katoh, *FGFR2-related pathogenesis and FGFR2-targeted therapeutics.* International journal of molecular medicine, 2009. **23**(3): p. 307-311.

385. Ranieri, D., et al., *Expression of the FGFR2 mesenchymal splicing variant in epithelial cells drives epithelial-mesenchymal transition.* Oncotarget, 2016. **7**(5): p. 5440.

386. Savagner, P., et al., *Alternative splicing in fibroblast growth factor receptor 2 is associated with induced epithelial-mesenchymal transition in rat bladder carcinoma cells.* Molecular biology of the cell, 1994. **5**(8): p. 851-862.

387. Zhu, D.-Y., et al., *Twist1 correlates with poor differentiation and progression in gastric adenocarcinoma via elevation of FGFR2 expression.* World Journal of Gastroenterology: WJG, 2014. **20**(48): p. 18306.

388. Qian, X., et al., *N-cadherin/FGFR promotes metastasis through epithelial-to-mesenchymal transition and stem/progenitor cell-like properties.* Oncogene, 2014. **33**(26): p. 3411.

389. Sandilands, E., et al., *Src kinase modulates the activation, transport and signalling dynamics of fibroblast growth factor receptors.* EMBO reports, 2007. **8**(12): p. 1162-1169.

390. Brooks, A.N., E. Kilgour, and P.D. Smith, *Molecular pathways: fibroblast growth factor signaling: a new therapeutic opportunity in cancer.* Clinical cancer research, 2012. **18**(7): p. 1855-1862.

391. Ridyard, M.S. and S.M. Robbins, *Fibroblast growth factor-2-induced signaling through lipid raft-associated fibroblast growth factor receptor substrate 2 (FRS2).* J Biol Chem, 2003. **278**(16): p. 13803-9.

392. Su, N., M. Jin, and L. Chen, *Role of FGF/FGFR signaling in skeletal development and homeostasis: learning from mouse models.* Bone Res, 2014. **2**: p. 14003.

393. Kim, S., et al., *Myristoylation of Src kinase mediates Src-induced and high-fat diet–accelerated prostate tumor progression in mice.* Journal of Biological Chemistry, 2017. **292**(45): p. 18422-18433.

394. Felsted, R.L., C.J. Glover, and K. Hartman, *Protein N-myristoylation as a chemotherapeutic target for cancer.* J Natl Cancer Inst, 1995. **87**(21): p. 1571-3.

395. Ducker, C.E., et al., *Two N-myristoyltransferase isozymes play unique roles in protein myristoylation, proliferation, and apoptosis.* Mol Cancer Res, 2005. **3**(8): p. 463-76.

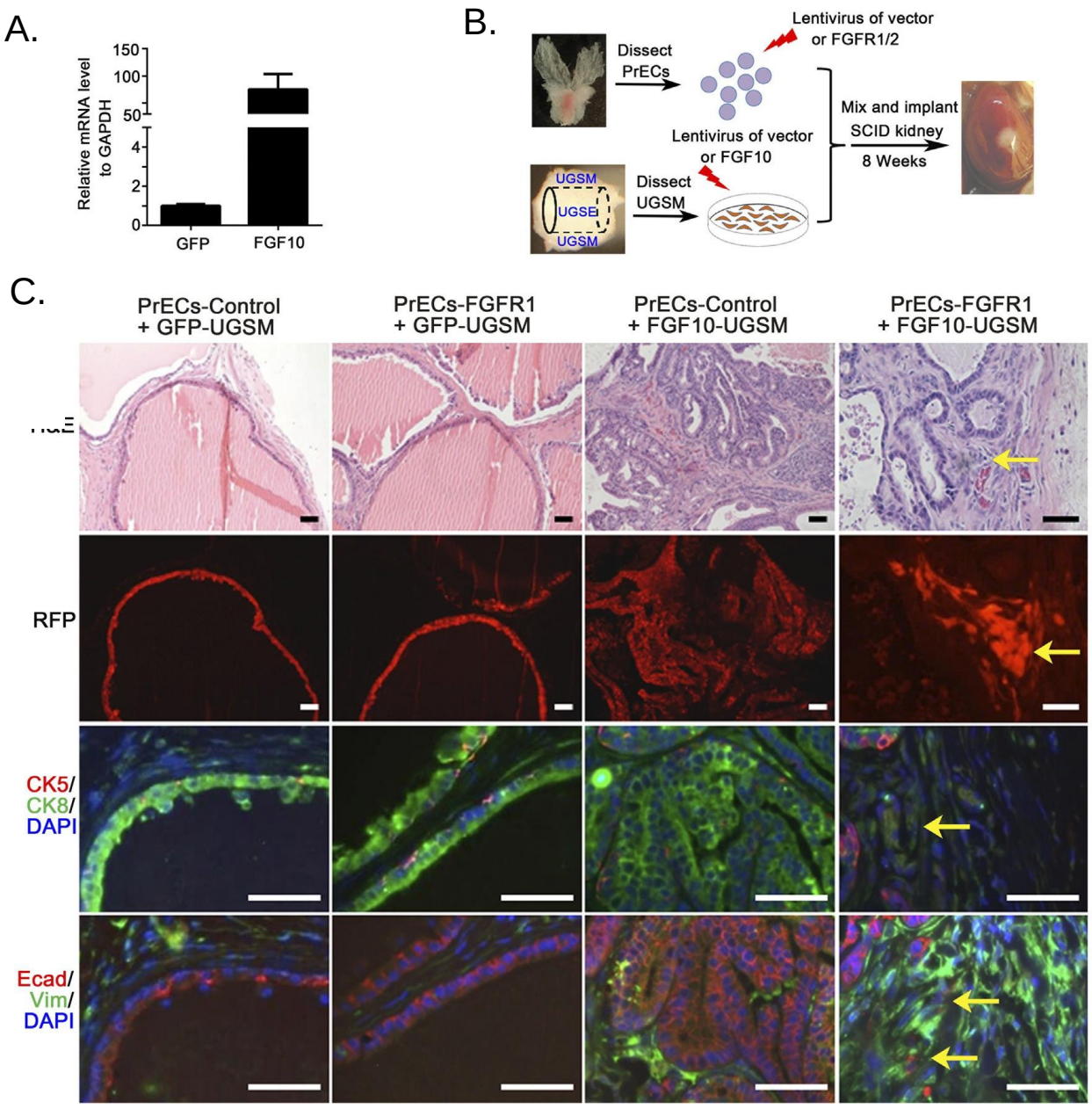
A.
Relative mRNA level to GAPDH
150
100
50
4
2
0
GFP
FGF10
B.
Dissect PrECs
Lentivirus of vector or FGFR1/2
Lentivirus of vector or FGF10
Dissect UGSM
UGSM
UGSE
UGSM
Mix and implant
SCID kidney
8 Weeks
C.
PrECs-Control + GFP-UGSM
PrECs-FGFR1 + GFP-UGSM
PrECs-Control + FGF10-UGSM
PrECs-FGFR1 + FGF10-UGSM
RFP
CK5/
CK8/
DAPI
Ecad/
Vim/
DAPI

Figure 7.1. Overexpression of epithelial wild-type FGFR1 synergizes with paracrine FGF10 to induce EMT. A) UGSM cells were transduced with control vector or FGF10 by lentiviral infection. Total mRNA was extracted for the analysis of FGF10 expression by RT-PCR. FGF10 was highly expressed in FGF10-UGSM cells. B) Diagram for evaluation of FGFR1/2 overexpression in epithelium and aberrant paracrine FGF10-induced tumorigenesis by the prostate tissue regeneration assay *in vivo*. Freshly isolated prostate epithelial cells were transduced with control vector (FUCRW), FGFR1, or FGFR2 by lentiviral infection. UGSM cells were isolated from 16.5-day-old mouse embryos. UGSM cells were transduced with GFP (control) or FGF10 by lentiviral infection. The FGFR1/2-transduced prostate epithelial cells were combined with GFP- or FGF10-UGSM. The combined cells were mixed with collagen and implanted under SCID mouse kidney capsule. The regenerated prostate tissues were harvested after 8-week incubation. C) The regenerated prostate tissues derived from the experimental groups including PrECs-control + GFP-UGSM, PrECs-FGFR1 + GFP-UGSM, PrECs-control + FGF10-UGSM, and PrECs-FGFR1 + FGF10-UGSM were analyzed for H&E, RFP signal, and IHC staining of CK5 (red)/CK8 (green)/DAPI (blue), and E-Cadherin (red)/vimentin (green)/DAPI (blue). Scale bar, 100 μm.

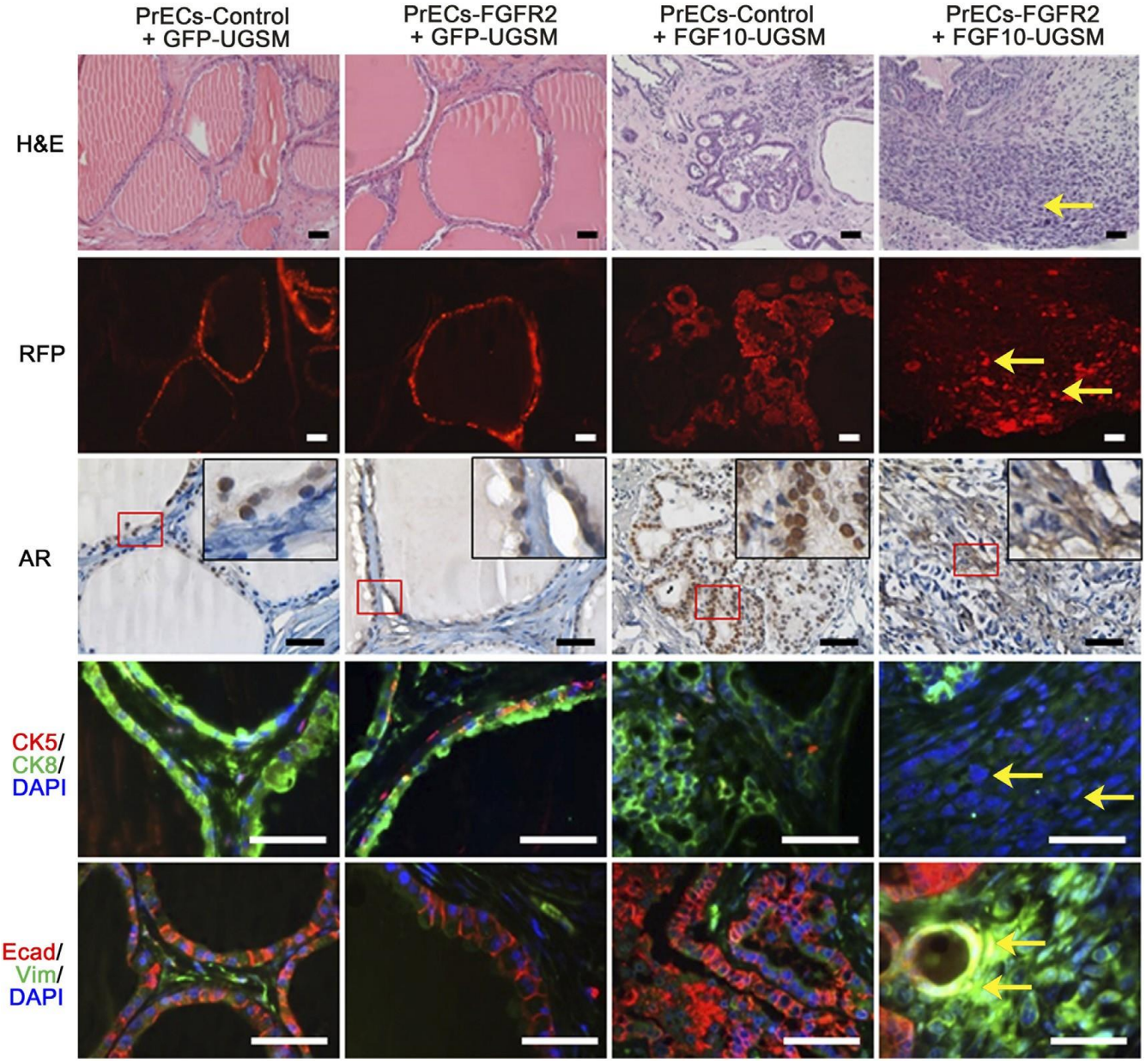
PrECs-Control
+ GFP-UGSM
PrECs-FGFR2
+ GFP-UGSM
PrECs-Control
+ FGF10-UGSM
PrECs-FGFR2
+ FGF10-UGSM
H&E
RFP
AR
CK5/
CK8/
DAPI
Ecad/
Vim/
DAPI

Figure 7.2. Overexpression of epithelial wild-type FGFR2 synergizes with paracrine FGF10 to induce EMT. Freshly isolated prostate cells were transduced with control vector or FGFR2 by lentiviral infection as shown in the diagram of Figure 1B. The transduced epithelial cells were mixed with GFP-UGSM or FGF10-UGSM. The regenerated prostate tissues derived from PrECs-control + GFP-UGSM, PrECs-FGFR2 + GFP-UGSM, PrECs-control + FGF10-UGSM, and PrECs-FGFR2 + FGF10-UGSM were analyzed for H&E staining, RFP signal, and IHC staining of AR, CK5 (red)/CK8 (green)/DAPI (blue), and E-Cadherin (red)/vimentin (green)/DAPI (blue). Yellow arrow indicates FGFR2 transformed tissue. Scale bar, 100 μm.

A.

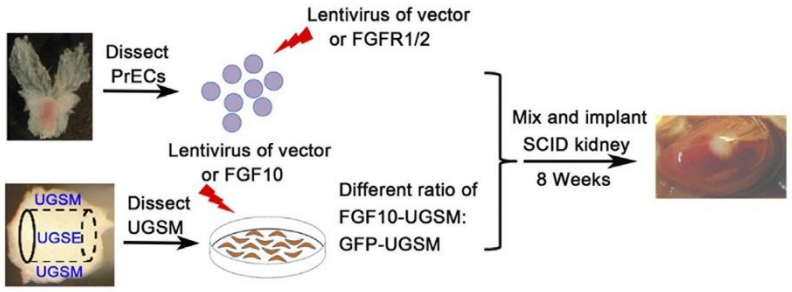

B.

Epithelia ($2x10^5$ cells)	Control	FGFR2	Control	FGFR2
UGSM ($4x10^5$ cells)	100% GFP	100% GFP	25% FGF10 +75% GFP	25% FGF10 +75% GFP

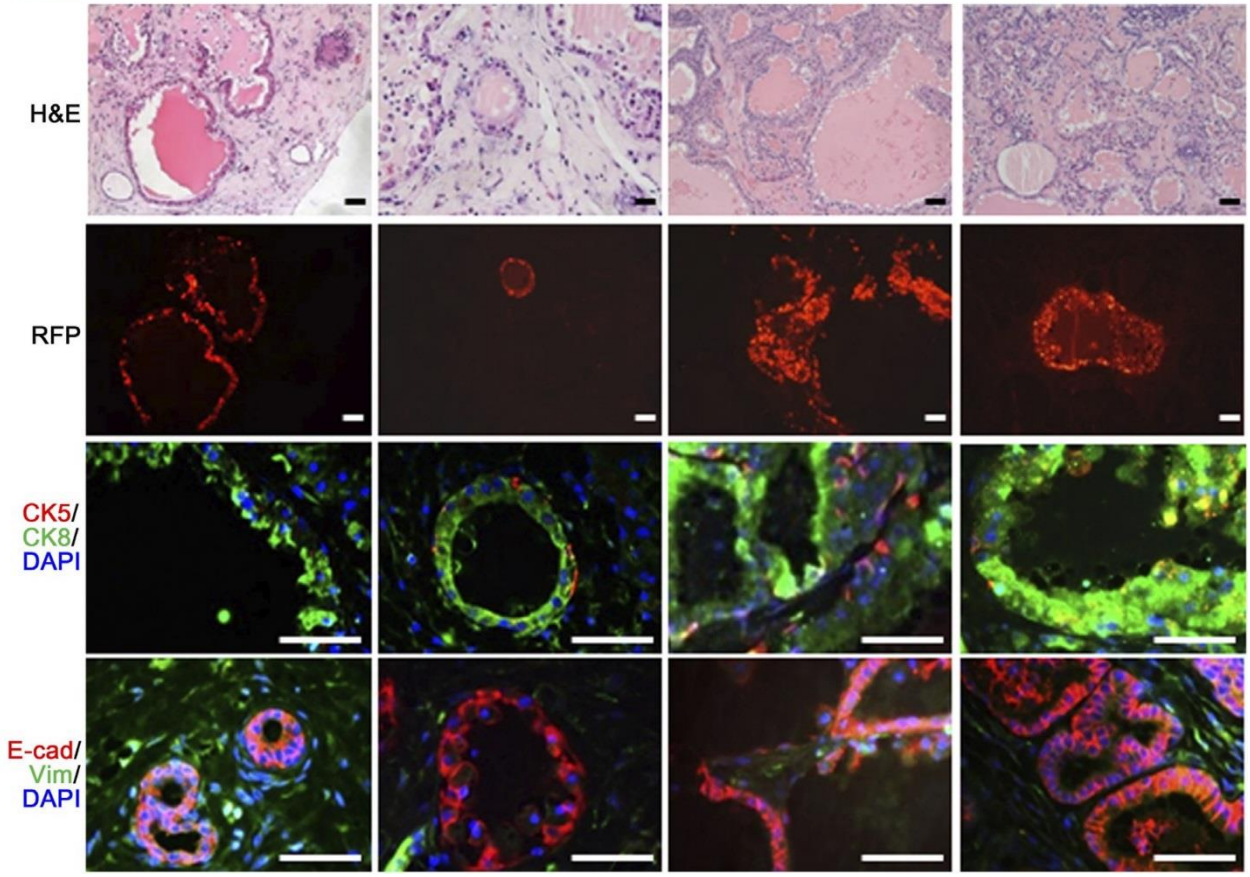

Figure 7.3. Overexpression of wild-type FGFR2 sensitizes epithelial cells to low-dose paracrine FGF10 for initiation of prostate tumorigenesis. A) Experimental setup for studying the synergy of a low dosage of paracrine FGF10-induced tumorigenesis with the transformation of FGFR2 (FGFR2c isoform) in epithelia. Freshly isolated prostate cells were transduced with control vector or FGFR2 by lentiviral infection. UGSM cells were transduced with FGF10 or control vector by lentiviral infection. The transduced epithelial cells were mixed with 100% GFP-UGSM (normal UGSM as a control) or 75% control-UGSM + 25% FGF10-UGSM. B) The regenerated prostate tissues derived from the experimental groups [PrECs-control + GFP-UGSM, PrECs-FGFR2 + GFP-UGSM, PrECs-control + (25% FGF10-UGSM + 75% GFP-UGSM), and PrECs-FGFR2 + (25% FGF10-UGSM + 75% GFP-UGSM)] were analyzed for H&E staining, RFP signal, and IHC staining of CK5 (red)/CK8 (green)/DAPI (blue) and E-Cadherin (red)/vimentin (green)/DAPI (blue). Scale bar, 100 μm.

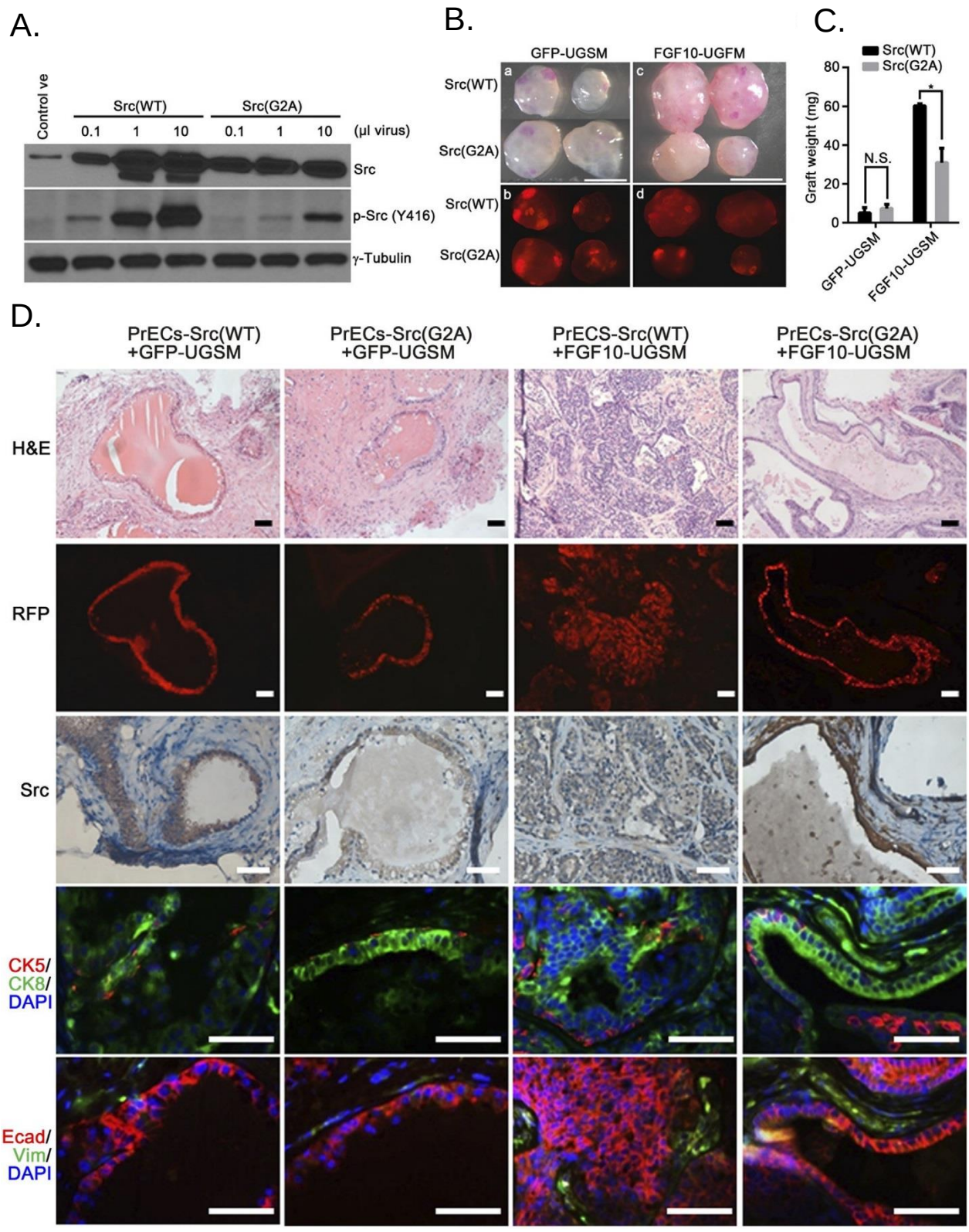
A.
Control ve
Src(WT)
Src(G2A)
0.1
1
10
0.1
1
10
(μl virus)
Src
p-Src (Y416)
γ-Tubulin
B.
GFP-UGSM
FGF10-UGFM
Src(WT)
Src(G2A)
Src(WT)
Src(G2A)
a
c
b
d
C.
Src(WT)
Src(G2A)
Graft weight (mg)
80
60
40
20
0
N.S.
*
GFP-UGSM
FGF10-UGSM
D.
PrECs-Src(WT)
+GFP-UGSM
PrECs-Src(G2A)
+GFP-UGSM
PrECS-Src(WT)
+FGF10-UGSM
PrECs-Src(G2A)
+FGF10-UGSM
H&E
RFP
Src
CK5/
CK8/
DAPI
Ecad/
Vim/
DAPI

Figure 7.4. Loss of Src myristoylation inhibits paracrine FGF10-induced tumorigenesis. A) 293 T cells were transduced with control vector, 0.1, 1, and 10 μL of Src (WT) or Src (G2A) lentivirus. The transduced cells were harvested, and protein lysates were analyzed for the expression levels of Src, phospho-Src and γ-tubulin. B) Phase and RFP fluorescence images and C) weight of the regenerated prostate tissues derived from PrECs-Src (WT) + GFP-UGSM, PrECs-Src (G2A) + GFP-UGSM, PrECs-Src (WT) + FGF10-UGSM, and PrECs-Src (G2A) + FGF10-UGSM groups. Scale bar, 0.5 mm. Values are mean ± SD. *: pb0.05. D) The regenerated tissues derived from PrECs-Src(WT) + GFP-UGSM, PrECs-Src(G2A) + GFP-UGSM, PrECs-Src(WT) + FGF10-UGSM, and PrECs-Src(G2A) + FGF10-UGSM groups were analyzed for H&E staining, RFP signal, and IHC staining of Src, CK5 (red)/CK8 (green)/DAPI (blue), and E-Cadherin (red)/ vimentin (green)/DAPI (blue). Scale bar, 100 μm